BMJ Open is committed to open peer review. As part of this commitment we make the peer review history of every article we publish publicly available.

When an article is published we post the peer reviewers' comments and the authors' responses online. We also post the versions of the paper that were used during peer review. These are the versions that the peer review comments apply to.

The versions of the paper that follow are the versions that were submitted during the peer review process. They are not the versions of record or the final published versions. They should not be cited or distributed as the published version of this manuscript.

BMJ Open is an open access journal and the full, final, typeset and author-corrected version of record of the manuscript is available on our site with no access controls, subscription charges or pay-per-view fees (http://bmjopen.bmj.com).

If you have any questions on BMJ Open's open peer review process please email info.bmjopen@bmj.com

BMJ Open: first published as 10.1136/bmjopen-2022-063051 on 8 November 2022. Downloaded from http://bmjopen.bmj.com/ on June 10, 2025 at Agence Bibliographique de l Enseignement Superieur (ABES) .
Protected by copyright, including for uses related to text and data mining, AI training, and similar technologies.

BMJ Open

Geometric uncertainty in intracranial aneurysm rupture status discrimination: a two-site retrospective study.

Journal:	*BMJ Open*
Manuscript ID	bmjopen-2022-063051
Article Type:	Original research
Date Submitted by the Author:	23-Mar-2022
Complete List of Authors:	Hellmeier, Florian; Charité – Universitätsmedizin Berlin, Institute for Computer-Assisted Cardiovascular Medicine Brüning, Jan; Charité Universitätsmedizin Berlin, Insitute for Computer-Assisted Cardiovascular Medicine Berg, Philipp; University of Magdeburg, Fluid Dynamics and Technical Flows Saalfeld, Sylvia; University of Magdeburg 'Otto von Guericke', Department of Simulation and Graphics Spuler, Andreas; Helios Klinikum Berlin-Buch Sandalcioglu, I. Erol; Otto von Guericke Universitat Magdeburg, Department of Neurosurgery Beuing, Oliver; AMEOS Hospital Bernburg, Deparment of Radiology Larsen, Naomi; University Medical Center Schleswig-Holstein, Department of Radiology and Neuroradiology Schaller, Jens; Charité – Universitätsmedizin Berlin Goubergrits, Leonid ; Charite Universitatsmedizin Berlin, Institute for Computer-Assisted Cardiovascular Medicine
Keywords:	Neurology < INTERNAL MEDICINE, Neuroradiology < RADIOLOGY & IMAGING, Neurosurgery < SURGERY

SCHOLARONE™
Manuscripts

BMJ Open: first published as 10.1136/bmjopen-2022-063051 on 8 November 2022. Downloaded from http://bmjopen.bmj.com/ on June 10, 2025 at Agence Bibliographique de l Enseignement Superieur (ABES) .
Protected by copyright, including for uses related to text and data mining, AI training, and similar technologies.

I, the Submitting Author has the right to grant and does grant on behalf of all authors of the Work (as defined in the below author licence), an exclusive licence and/or a non-exclusive licence for contributions from authors who are: i) UK Crown employees; ii) where BMJ has agreed a CC-BY licence shall apply, and/or iii) in accordance with the terms applicable for US Federal Government officers or employees acting as part of their official duties; on a worldwide, perpetual, irrevocable, royalty-free basis to BMJ Publishing Group Ltd ("BMJ") its licensees and where the relevant Journal is co-owned by BMJ to the co-owners of the Journal, to publish the Work in this journal and any other BMJ products and to exploit all rights, as set out in our licence.

The Submitting Author accepts and understands that any supply made under these terms is made by BMJ to the Submitting Author unless you are acting as an employee on behalf of your employer or a postgraduate student of an affiliated institution which is paying any applicable article publishing charge ("APC") for Open Access articles. Where the Submitting Author wishes to make the Work available on an Open Access basis (and intends to pay the relevant APC), the terms of reuse of such Open Access shall be governed by a Creative Commons licence – details of these licences and which Creative Commons licence will apply to this Work are set out in our licence referred to above.

Other than as permitted in any relevant BMJ Author's Self Archiving Policies, I confirm this Work has not been accepted for publication elsewhere, is not being considered for publication elsewhere and does not duplicate material already published. I confirm all authors consent to publication of this Work and authorise the granting of this licence.

For peer review only

Enseignement Superieur (ABES) .
Protected by copyright, including for uses related to text and data mining, AI training, and similar technologies.

BMJ Open: first published as 10.1136/bmjopen-2022-063051 on 8 November 2022. Downloaded from http://bmjopen.bmj.com/ on June 10, 2025 at Agence Bibliographique de l Enseignement Superieur (ABES) . Protected by copyright, including for uses related to text and data mining, AI training, and similar technologies.

Geometric uncertainty in intracranial aneurysm rupture status discrimination: a two-site retrospective study.

Florian Hellmeier[1], Jan Brüning[1], Philipp Berg[2,3], Sylvia Saalfeld[3,4], Andreas Spuler[5], I. Erol Sandalcioglu[6], Oliver Beuing[7], Naomi Larsen[8], Jens Schaller[1], Leonid Goubergrits[1,9]

[1] Institute of Computer-assisted Cardiovascular Medicine, Charité – Universitätsmedizin Berlin, Berlin, Germany

[2] Laboratory of Fluid Dynamics and Technical Flows, University of Magdeburg, Magdeburg, Germany

[3] Research Campus *STIMULATE*, University of Magdeburg, Magdeburg, Germany

[4] Department of Simulation and Graphics, University of Magdeburg, Magdeburg, Germany

[5] Helios Klinikum Berlin-Buch, Berlin, Germany

[6] Department of Neurosurgery, University Hospital Magdeburg, Magdeburg, Germany

[7] Department of Radiology, AMEOS Hospital, Bernburg, Germany

[8] Department of Radiology and Neuroradiology, University Medical Center Schleswig-Holstein (UKSH), Kiel, Germany

[9] Einstein Center Digital Future, Berlin, Germany

Correspondence:

Jan Brüning

Email: jan.bruening@charite.de

Telephone: +49 30 450 553 879

Telefax: +49 30 450 553 838

Charité – Universitätsmedizin Berlin
Institute of Computer-assisted Cardiovascular Medicine
Augustenburger Platz 1
13353 Berlin
Germany

Keywords: intracranial aneurysms; uncertainty analysis; rupture risk assessment;

Word count: 3328

For peer review only

For peer review only

BMJ Open: first published as 10.1136/bmjopen-2022-063051 on 8 November 2022. Downloaded from http://bmjopen.bmj.com/ on June 10, 2025 at Agence Bibliographique de l Enseignement Superieur (ABES) .
Protected by copyright, including for uses related to text and data mining, AI training, and similar technologies.

Abstract

Objectives: Assessing the risk associated with unruptured intracranial aneurysms (IA) is essential in clinical decision making. Several geometric risk parameters have been proposed for this purpose. However, performance of these parameters has been inconsistent. This study evaluates the performance and robustness of geometric risk parameters on two datasets and compare it to the uncertainty inherent in assessing these parameters and quantifies inter-parameter correlations.

Methods: Two datasets containing 244 IA geometries from 178 patients were retrospectively analyzed. IAs were stratified by anatomical region, based on the PHASES score locations. 37 geometric risk parameters representing four groups (size, neck, non-dimensional, and curvature parameters) were assessed. Analysis included standardized absolute differences (SAD) between ruptured and unruptured IAs, ratios of SAD to median relative uncertainty (MRU) associated with the parameters, and inter-parameter correlation.

Results: The ratio of SAD to MRU was lower for higher-dimensional size parameters (i.e., areas and volumes) than for one-dimensional size parameters. Non-dimensional size parameters performed comparatively well with regard to SAD and MRU. SAD was higher in the posterior anatomical region. Correlation of parameters was strongest within parameter (sub)groups and between size and curvature parameters, while anatomical region did not strongly affect correlation patterns.

Conclusion: Non-dimensional parameters and few parameters from other groups were comparatively robust, suggesting that they might generalize better to other datasets. The data on discriminative performance and inter-parameter correlations presented in this study may aid in developing and choosing robust geometric risk parameters for use in rupture risk models.

For peer review only

BMJ Open: first published as 10.1136/bmjopen-2022-063051 on 8 November 2022. Downloaded from http://bmjopen.bmj.com/ on June 10, 2025 at Agence Bibliographique de l Enseignement Superieur (ABES) . Protected by copyright, including for uses related to text and data mining, AI training, and similar technologies.

Introduction

A relevant part of the general population harbors one or more unruptured intracranial aneurysms (IAs), with the overall prevalence estimated around 3% [1]. While most IAs do not rupture [2], the question of whether and when to treat them remains relevant due to the poor prognosis of ruptured IAs [3, 4] as well as the risk of intervention [3, 5]. Current American Heart Association/American Stroke Association guidelines list several modifiable and non-modifiable risk factors for IA growth and/or rupture, including IA location, growth rate, morphology, smoking status, alcohol consumption, hypertension, age, sex, previous IA, and family history [6]. Attempts have been made to develop scoring systems to quantify rupture risk, growth risk, and/or support treatment decisions, these include the PHASES score by Greving et al. [7], the UIATS by Etminan et al. [8] and the ELAPSS score by Backes et al. [9]. All three of these scores are based on clinically available data and all include geometric rupture risk parameters: IA size in case of the PHASES score [7], surface irregularity, size ratio, as well as aspect ratio in case of the UIATS [8], and IA size as well as surface irregularity for the ELAPSS score [9]. While these metrics were designed to support clinical decision making, performance on clinical data has been mixed [10-12] and improvements, particularly for patients harboring multiple IAs, are desired by clinicians [13].

The aim of this paper is to assess the ability of a broad number of proposed geometric risk parameters to differentiate between unruptured and ruptured IAs while also comparing their discriminative ability relative to the uncertainty encountered in determining them. Any acquisition of patient-specific IA geometries and subsequent use of these geometries to derive geometric risk parameters is affected by a number of uncertainty-introducing factors. Starting with the medical imaging acquisition itself, which is followed by image data pre-processing, segmentation, geometry reconstruction including post-processing (e.g., smoothing, checking of topology), and finally calculation of the geometric risk parameters. All these processing steps are associated with some errors, resulting in uncertainty, which negatively affects the ability of parameters to discriminate IA rupture status. Discrimination of rupture status on an individual IA level is, however, necessary if these parameters are to support the clinical decision-making process, including any decisions regarding treatment modalities. Previous studies found high variability in the uncertainty of different geometric risk parameters as well as differences in their ability to differentiate between ruptured and unruptured IAs [14-16]. Furthermore, for geometric risk parameters with multiple alternative definitions, the specific implementation can affect the discriminative performance of the parameter itself and any derived parameters, as demonstrated by Lauric et al. for parameters incorporating IA and neck size [17].

The current study was performed to facilitate optimal selection of geometric rupture risk parameters by identifying geometric parameters, which are good discriminators while also exhibiting low uncertainty. The analysis is performed on two datasets processed by different research groups and is differentiated by

BMJ Open: first published as 10.1136/bmjopen-2022-063051 on 8 November 2022. Downloaded from http://bmjopen.bmj.com/ on June 10, 2025 at Agence Bibliographique de l Enseignement Superieur (ABES) . Protected by copyright, including for uses related to text and data mining, AI training, and similar technologies.

For peer review only

anatomical region, in order to assess how the predictive suitability of the geometric risk parameters is affected by geometry processing as well as anatomical location. Additionally, correlation of the geometric risk parameters with each other is assessed.

For peer review only

BMJ Open: first published as 10.1136/bmjopen-2022-063051 on 8 November 2022. Downloaded from http://bmjopen.bmj.com/ on June 10, 2025 at Agence Bibliographique de l Enseignement Superieur (ABES) .
Protected by copyright, including for uses related to text and data mining, AI training, and similar technologies.

Methods

Medical imaging data

IA geometries were retrospectively reconstructed and segmented from 3D rotational angiography data acquired for routine clinical indications. 142 IAs were acquired in the Helios Klinikum Berlin-Buch (Berlin, Germany), 38 in KRH Klinikum Nordstadt (Hanover, Germany), 23 in the University Medical Center Schleswig-Holstein (UKSH) (Kiel, Germany), and 41 in the University Hospital Magdeburg (Magdeburg, Germany). Processing of the imaging data, including segmentation, was performed at two sites: Berlin, which processed 142 IAs from Helios Klinikum Berlin-Buch (dataset 1), and Magdeburg, which processed 102 IAs from KRH Klinikum Nordstadt, UKSH, and University Hospital Magdeburg (dataset 2). Overall, 244 IAs from 178 patients were included, from which geometric risk parameters were subsequently calculated. Based on the PHASES score [7], aneurysm location was classified into four anatomical regions: internal carotid artery (ICA), middle cerebral artery (MCA), anterior region (all vessels anterior of the ICA/MCA), and posterior region (all vessels posterior of the ICA/MCA). The distribution of the individual IA locations and their assignment to the four anatomical regions are shown in Table 1.

Table 1: Frequency and rupture status of individual IA locations by dataset. ACA: anterior cerebral artery, AComA: anterior communicating artery, AChA: anterior choroidal artery, ICA: internal carotid artery, MCA: middle cerebral artery, PComA: posterior communicating artery, PCA: posterior cerebral artery, SCA: superior cerebellar artery, BA: basilar artery, PICA: posterior inferior cerebellar artery, VA: vertebral artery.

Anatomical region	Vessel	Dataset 1 unruptured	Dataset 1 ruptured	Dataset 2 unruptured	Dataset 2 ruptured
Anterior	ACA	3	1	2	2
	AComA	10	22	11	5
ICA	AChA	0	1	1	2
	ICA	29	8	19	4
MCA	MCA	28	10	31	8
Posterior	PComA	8	10	2	4
	PCA	0	1	0	0
	SCA	0	0	1	1
	BA	4	3	3	4
	PICA	0	4	1	0
	VA	0	0	0	1

Geometric risk parameters

Historically, a large number of geometric parameters for IA rupture risk assessment have been proposed. In order to have access to information on parameter uncertainty, the parameters chosen for this study were limited to a subset of the parameters reported in Goubergrits et al. [14], a parameter uncertainty study

BMJ Open: first published as 10.1136/bmjopen-2022-063051 on 8 November 2022. Downloaded from http://bmjopen.bmj.com/ on June 10, 2025 at Agence Bibliographique de l Enseignement Superieur (ABES) . Protected by copyright, including for uses related to text and data mining, AI training, and similar technologies.

performed on segmentation data obtained during the Multiple Aneurysms AnaTomy Challenge (MATCH) 2018 [18]. For a detailed description of the parameters and the rationale for choosing the parameters, the interested reader is referred to Goubergrits et al. [14]. Table 2 lists the geometric parameters and their abbreviations.

Table 2: List of the investigated geometric parameters, their descriptions, and median relative uncertainties (MRU). Note that terminology and implementation in the references might differ subtly. Derived and modified from tables 1-5 from Goubergrits et al. [14], used under Creative Commons Attribution License (CC BY 4.0). The CC BY 4.0 license text is available at https://creativecommons.org/licenses/by/4.0/.

Parameter group	Parameter name, unit [exemplary reference]	Parameter abbreviation	Short description	MRU
Size	Height, mm [19]	H	Maximum perpendicular distance from the neck plane to the aneurysm surface	0.140
	Maximum dimension, mm [20]	L_{max}	Maximum distance between two points on the aneurysm surface	0.157
	Maximum height, mm [15]	H_{max}	Maximum distance between the centroid of the neck and the aneurysm surface	0.123
	Maximum diameter, mm [17]	D_{max}	Maximum neck plane-parallel distance between two points on the aneurysm surface	0.16[illegible]
	Bulge height, mm [19]	H_b	Distance between the neck plane and the maximum diameter	0.37[illegible]
	Surface area, mm² [15]	A	Surface area of the aneurysm	0.21[illegible]
	Convex hull surface area, mm² [15]	A_{CH}	Surface area of the aneurysm's convex hull	0.2[illegible]7
	Minimal bounding sphere surface area, mm² [21]	A_{MBS}	Surface area of the aneurysm's minimal bounding sphere	0.305
	Closed surface area, mm²	A_{closed}	Surface area of the neck-closed aneurysm	0.283
	Volume, mm³ [15]	V	Volume of the neck-closed aneurysm	0.392
	Convex hull volume, mm³ [15]	V_{CH}	Volume of the aneurysm's convex hull	0.399
	Minimal bounding sphere volume, mm³ [21]	V_{MBS}	Volume of the aneurysm's minimal bounding sphere	0.451
Neck	Minimum neck diameter, mm [17]	$D_{neck,min}$	Minimum distance between two opposite points on the neck perimeter	0.306
	Maximum neck diameter, mm [22]	$D_{neck,max}$	Maximum distance between two points on the neck perimeter	0.348
	Neck perimeter, mm [19]	P_{neck}	Perimeter of the aneurysm neck	0.374
	Equivalent neck diameter, mm [19]	$D_{neck,equiv}$	Hydraulic diameter of the aneurysm neck	0.276
	Neck area, mm² [19]	A_{neck}	Area of the aneurysm neck	0.593

BMJ Open: first published as 10.1136/bmjopen-2022-063051 on 8 November 2022. Downloaded from http://bmjopen.bmj.com/ on June 10, 2025 at Agence Bibliographique de l Enseignement Superieur (ABES) . Protected by copyright, including for uses related to text and data mining, AI training, and similar technologies.

	Elliptical neck area, mm^2	$A_{neck,elliptical}$	Neck area calculated as the product of the minimum and maximum neck diameter	0.650
Non-dimensional	Aspect ratio [22]	AR	Ratio of height to maximum neck diameter	0.293
	Equivalent aspect ratio [19]	eAR	Ratio of height to equivalent neck diameter	0.326
	Bottleneck factor [19]	BF	Ratio of maximum diameter to maximum neck diameter	0.201
	Bulge location [19]	BL	Ratio of bulge height to height	0.301
	Nonsphericity index [15]	NSI	Normalized ratio of volume to surface area relative to a hemisphere	0.108
	Aneurysm volume to bounding sphere volume [21]	AVSV	Ratio of volume to minimal bounding sphere volume	0.173
	Aneurysm surface area to bounding sphere area [21]	AASA	Ratio of surface area to minimal bounding sphere surface area	0.695
	Undulation index [15]	UI	1 minus the ratio of volume to convex hull volume	0.709
	Ellipticity index [15]	EI	Normalized ratio of convex hull volume to convex hull surface area relative to a hemisphere	0.651
Curvature	Mean of mean curvature, mm^{-1} [19]	MAA	Surface average of local mean curvature	0.[illegible]
	Mean of absolute mean curvature, mm^{-1}	absMAA	Surface average of the magnitude of the local mean curvature	0.131
	Standard deviation of mean curvature, mm^{-1}	MSD	Standard deviation of the local mean curvature	1.011
	High mean curvature, % [21]	HMC	Relative increase of the mean of absolute mean curvature over the mean curvature of the minimal bounding sphere	0.390
	L2-norm of mean curvature [19]	MLN	Scale invariant measure of surface irregularity, uses mean curvature	0.150
	Mean of Gaussian curvature, mm^{-2} [19]	GAA	Surface average of local Gaussian curvature	0.344
	Mean of absolute Gaussian curvature, mm^{-2}	absGAA	Surface average of the magnitude of the local Gaussian curvature	0.485
	Standard deviation of Gaussian curvature, mm^{-2}	GSD	Standard deviation of the local Gaussian curvature	1.798
	High Gaussian curvature, % [21]	HGC	Relative increase of the mean of absolute Gaussian curvature over the Gaussian curvature of the minimal bounding sphere	0.822
	L2-norm of Gaussian curvature [19]	GLN	Scale invariant measure of surface irregularity, uses Gaussian curvature	0.545

BMJ Open: first published as 10.1136/bmjopen-2022-063051 on 8 November 2022. Downloaded from http://bmjopen.bmj.com/ on June 10, 2025 at Agence Bibliographique de l Enseignement Superieur (ABES) . Protected by copyright, including for uses related to text and data mining, AI training, and similar technologies.

BMJ Open: first published as 10.1136/bmjopen-2022-063051 on 8 November 2022. Downloaded from http://bmjopen.bmj.com/ on June 10, 2025 at Agence Bibliographique de l Enseignement Superieur (ABES) . Protected by copyright, including for uses related to text and data mining, AI training, and similar technologies.

Since the diameter of the parent vessel was not available for all IAs studied, size ratio could not be calculated and was excluded. Furthermore, UI and CR as well as NSI and NPR are directly related through $CR = 1 - UI$ and $IPR = \frac{\sqrt[3]{18\pi}}{1 - NSI}$, respectively. CR and IPR were therefore not included in the analysis, in order to avoid redundancy. Geometric risk parameters were calculated from the IA geometries using MATLAB (version R2017b, MathWorks, Natick, USA), Python (version 3.7.1, Python Software Foundation, Delaware, USA), and ZIBAmira (version 2015.28, Zuse Institute Berlin, Germany). The individual parameter values, IA location, and rupture status for each IA in this study, as well as the exact values of the inter-parameter correlation coefficients are provided as supplemental material 1 and 2 respectively.

Statistical analysis

Since most of the geometric risk parameters were non-normally distributed, as assessed by Q-Q plots and Shapiro-Wilk tests, the median was used to quantify central tendency and the interquartile range was used to quantify dispersion. Correlations were quantified using Pearson's r with correlations $|r| \geq 0.75$ referred to as strong, while those with $0.75 > |r| \geq 0.25$ and $|r| < 0.25$ referred to as moderate and weak, respectively. Statistical analysis was performed using SPSS (version 28.0.0.0, IBM, Armonk, USA) and MATLAB.

The discriminative ability of the individual parameters was assessed by standardizing the absolute difference between the medians of the ruptured and unruptured IAs with the weighted arithmetic mean of the IQRs of the two groups. This measure of effect size will be referred to as the standardized absolute group difference (SAD). Furthermore, the ratio of the SAD to the relative uncertainty, a measure of the uncertainty associated with parameter calculation, from Goubergrits et al. [14] was calculated for all parameters and will be referred to as the group difference-uncertainty ratio (DUR). The equations for SAD and DUR are thus $SAD = \frac{(n_r + n_u) \cdot |m_r - m_u|}{n_r IQR_r + n_u IQR_u}$ and $DUR = \frac{SAD}{MRU}$, where n_i, m_i, and IQR_i are the sample sizes, median values, and interquartile ranges of the ruptured (subscript r) and unruptured (subscript u) samples, while MRU is the median relative uncertainty from Goubergrits et al. [14], which is also listed in Table 2. SAD and DUR may take any value ≥0 with higher values indicating stronger discriminative ability and a better ratio of discriminative ability to uncertainty, respectively. SAD and DUR values of zero would indicate no discriminative ability and the worst possible ratio of discriminative ability to uncertainty, respectively. Additionally, the correlation coefficients between the parameters were calculated. Analysis of SAD and DUR as well as the correlation coefficients was performed individually for each anatomical region and each dataset.

Patient and public involvement

Due to the purely retrospective manner of this study, no involvement of patients or the general public was considered.

For peer review only

BMJ Open: first published as 10.1136/bmjopen-2022-063051 on 8 November 2022. Downloaded from http://bmjopen.bmj.com/ on June 10, 2025 at Agence Bibliographique de l Enseignement Superieur (ABES) .
Protected by copyright, including for uses related to text and data mining, AI training, and similar technologies.

BMJ Open: first published as 10.1136/bmjopen-2022-063051 on 8 November 2022. Downloaded from http://bmjopen.bmj.com/ on June 10, 2025 at Agence Bibliographique de l Enseignement Superieur (ABES) . Protected by copyright, including for uses related to text and data mining, AI training, and similar technologies.

Results

Error! Reference source not found. shows SAD for all geometric risk parameters by anatomical region and dataset. Considering both datasets, the following parameters achieved the comparatively highest SAD for each anatomical region: curvature (HMC, MLN, HGC, GLN) and non-dimensional (AR, eAR, AVSV, AASA) parameters in the anterior region, curvature (HMC, HGC) and non-dimensional (NSI, AASA, EI) parameters in the ICA, non-dimensional (AR, eAR, BL, AVSV, AASA) parameters in the MCA, and size (H, L_{max}, A, A_{MBS}) and curvature (MSD, absGAA, GSD) parameters in the posterior region. Compared to the other anatomical regions, SAD was higher in the posterior region and more parameters exhibited relatively high SAD. Looking at all anatomical regions combined, curvature (HMC, MLN, absGAA, HGC, GLN) and non-dimensional (AR, eAR, AVSV, AASA) parameters as well as one neck ($D_{neck,min}$) and one size (H_b) parameter show comparatively high SAD in both datasets. Furthermore, the differences between the two datasets become less pronounced when combining all anatomical regions.

Error! Reference source not found. shows DUR for all geometric risk parameters by anatomical region and dataset. Considering both datasets, the following parameters achieved the comparatively highest DUR for each anatomical region: non-dimensional (AASA, EI) and one curvature (MLN) parameter in the anterior region, non-dimensional (EI, AASA, NSI) parameters in the ICA, non-dimensional (AASA, EI) parameters in the MCA, and size parameters (H, L_{max}, H_{max}, A), curvature (MAA, absMAA), and one non-dimensional (EI) parameter in the posterior region. Similar to SAD, DUR in the posterior region was overall higher and more parameters exhibited relatively high DUR, compared to the other anatomical regions. Looking at all anatomical regions combined, non-dimensional (NSI, AVSV, AASA, EI) and curvature (absMAA, MLN) parameters show comparatively high DUR in both datasets. As for SAD, the differences between the two datasets are less pronounced when looking at all anatomical regions combined.

Figures **Error! Reference source not found.** and **Error! Reference source not found.** show correlation coefficients between the geometric risk parameters by anatomical region for both datasets. The following general features are present in most data correlation plots: The size parameters (H, L_{max}, H_{max}, D_{max}, H_b, A, A_{CH}, A_{MBS}, A_{closed}, V, V_{CH}, V_{MBS}) are generally strongly correlated with each other. Similarly, the neck parameters ($D_{neck,min}$, $D_{neck,max}$, P_{neck}, $D_{neck,equiv}$, A_{neck}, $A_{neck,elliptical}$) are also generally strongly correlated with each other.

Within the non-dimensional parameter group, there are two distinct subgroups in most plots: one formed by AR, eAR, BF, and BL and one formed by NSI, AVSV, AASA, UI, and EI. Within the latter subgroup, several of the correlations are negative but their magnitude is overall moderate to strong. The curvature parameters also form two subgroups, one formed by dimensional curvature parameters (MAA, absMAA, MDS, GAA, absGAA, GSD) and one by non-dimensional curvature parameters (HMC, MLN, HGC, GLN).

With regard to correlations between parameter groups, there is generally moderate to strong correlation between the size and neck parameters. Additionally, the size and neck parameters are generally moderately correlated with the curvature parameters, the direction of the correlation being positive for the non-dimensional curvature parameters and negative for the dimensional curvature parameters.

For peer review only

BMJ Open: first published as 10.1136/bmjopen-2022-063051 on 8 November 2022. Downloaded from http://bmjopen.bmj.com/ on June 10, 2025 at Agence Bibliographique de l Enseignement Superieur (ABES) .
Protected by copyright, including for uses related to text and data mining, AI training, and similar technologies.

BMJ Open: first published as 10.1136/bmjopen-2022-063051 on 8 November 2022. Downloaded from http://bmjopen.bmj.com/ on June 10, 2025 at Agence Bibliographique de l Enseignement Superieur (ABES) . Protected by copyright, including for uses related to text and data mining, AI training, and similar technologies.

Discussion

Previous research has assessed the impact of uncertainty on geometric risk parameters in a limited fashion. Ma et al. examined the influence of random noise on the calculation of 14 geometric risk parameters, finding curvature parameters more susceptible to random noise than size, neck, and non-dimensional parameters [19]. Others have examined the influence of imaging modality [23] and CT angiography reconstruction kernel [24] on geometric risk parameters. Regarding image acquisition, Ramachandran et al. have examined the influence of imaging modality [23], while O'Meara et al. [24] and Berg et al. [25] have focused on the reconstruction kernel's effect on geometric and hemodynamic risk parameters, respectively. Other sensitivity and uncertainty aspects of computational fluid dynamics approaches to IAs have been explored, e.g., by Cebral et al. [26], Sarrami-Foroushani et al. [27], and Schneiders et al. [28]. To the authors' knowledge there is, however, no comprehensive publication relating discriminative performance and uncertainty of geometric risk parameters, while also providing detailed data on their correlation with each other.

Looking at the parameter groups examined in this study, the following findings can be made: the size and neck parameters measuring areas (A, A_{CH}, A_{MBS}, A_{closed}, A_{neck}, $A_{neck,elliptical}$) and volumes (V, V_{CH}, V_{MBS}) generally do not achieve high DUR, despite having SAD similar to the size and neck parameters measuring length (H, L_{max}, H_{max}, D_{max}, H_b, $D_{neck,min}$, $D_{neck,max}$, P_{neck}, $D_{neck,equiv}$). The cause is the higher uncertainty encountered in determining the higher-dimensional parameters when compared to the one-dimensional parameters [14]. This suggests that higher-dimensional size parameters tend to be less robust and thus less suitable for use in practical risk models than one-dimensional size parameters. Similar to Lauric et al. [17], there are instances of noticeable differences in the discriminative performance of parameters capturing the same aspect of IA geometry, e.g. for the neck size parameters. The non-dimensional parameters exhibit comparatively high SAD and DUR, with the exception of BL and UI, which exhibit lower discriminative ability and/or higher uncertainty in their calculation. The curvature parameters show substantial variability in SAD and DUR depending on the anatomical region and the particular parameter, with MLN performing comparatively well overall. It is notable that the posterior region tends to exhibit higher SAD and DUR than the other regions, indicating more pronounced geometric differences between ruptured and unruptured IAs in this region. Regarding the differences in SAD and DUR between datasets 1 and 2, it is likely that differences in the patient collectives, subsample sizes, and reconstruction techniques are the main causes. The latter could in the future be tackled through the use of machine learning-based segmentation methods, which can reduce operator-induced uncertainty. Examples of such methods have previously been presented, e.g., in the context of the CADA challenge [29].

Regarding the correlation patterns, there is substantial similarity between all analyzed anatomical regions and datasets. Parameters tend to be most strongly correlated with other parameters from the same parameter group, with the exception of the non-dimensional and curvature parameters, which form two subgroups each. This is reasonable, given that the parameters within each parameter group capture similar aspects of IA geometry. For the size and neck parameter groups this is fairly obvious, since they both capture aspects of IA and neck size, respectively. The two distinct correlation subgroups within the non-dimensional parameter group are likely caused by the underlying parameter subgroups capturing different aspects of aneurysm shape. While the parameters of the first subgroup (AR, eAR, BF, BL) are simply ratios of one-dimensional size parameters, the second subgroup (NSI, AVSV, AASA, UI, EI) is formed by parameters relating aneurysm area and/or volume to geometric reference objects, e.g., the minimal bounding sphere or convex hull. The negative correlation between AVSV and AASA with the other parameters from the second subgroup is due to the parameter definitions, which cause AVSV and AASA to increase with increasing sphericity, while the other parameters tend to decrease with increasing sphericity. The curvature parameters also form two subgroups, with the first subgroup consisting of the dimensional parameters quantifying the mean or dispersion of IA surface curvature (MAA, absMAA, MSD, GAA, absGAA, GSD) and the second subgroup consisting of non-dimensional, scale invariant curvature parameters (HMC, MLN, HGC, GLN). Since the former parameters intrinsically decrease with IA size, while the latter parameters increase with IA size, the negative correlation of the two subgroups with each other makes sense. It should be noted that the positive correlation of the non-dimensional curvature parameters with IA size is not an intrinsic property of the non-dimensional parameters themselves, since they are designed to be scale invariant. It rather indicates that curvature and irregularities of the IA surface increase in larger IAs.

For a geometric risk parameter to be a good candidate for rupture risk prediction, it should generally have a high SAD, in order to be able to differentiate between ruptured and unruptured IAs. Additionally, DUR should be high, indicating low sensitivity of the parameter to the particular imaging, segmentation, and calculation workflow, by which it is calculated. This is desirable because it allows models including such parameters to generalize well to other datasets. Finally, when choosing a set of parameters, data from the correlation analysis can be used to identify parameters that are not strongly correlated. Neyazi et al. have previously used this method to derive a two-parameter rupture status prediction model from a set of 49 geometric and hemodynamic rupture risk parameters, identifying AR and the maximal relative residence time as the most suitable model parameters [13]. Other attempts to identify suitable rupture status prediction models based on geometric risk parameters have been attempted, e.g., Dhar et al. [15] and Zhang et al. [30], but results have generally been inconsistent. Possible reasons for the discrepant findings regarding optimal parameter choice are the sample sizes used and the uncertainty inherent in the workflow by which the parameters are calculated. This may lead to the selection of less robust parameters that perform well on a given dataset but generalize less well to others. Based on the results of this study and considering SAD,

BMJ Open: first published as 10.1136/bmjopen-2022-063051 on 8 November 2022. Downloaded from http://bmjopen.bmj.com/ on June 10, 2025 at Agence Bibliographique de l Enseignement Superieur (ABES) .
Protected by copyright, including for uses related to text and data mining, AI training, and similar technologies.

For peer review only

BMJ Open: first published as 10.1136/bmjopen-2022-063051 on 8 November 2022. Downloaded from http://bmjopen.bmj.com/ on June 10, 2025 at Agence Bibliographique de l Enseignement Superieur (ABES) . Protected by copyright, including for uses related to text and data mining, AI training, and similar technologies.

DUR, as well as the correlation between geometric risk parameters, examples of more robust parameter choices could look as follows:

- H_{max}, $D_{neck,min}$, AR, AASA, and MLN for the anterior region.
- L_{max}, P_{neck}, AR, AASA, and HGC for the ICA.
- D_{max}, $D_{neck,min}$, eAR, AASA, and HMC for the MCA.
- L_{max}, $D_{neck,min}$, BL, EI, and absMAA for the posterior region.
- H_b, $D_{neck,min}$, AR, AASA, and MLN if looking at all anatomical regions combined.

Overall, while individual size, neck, and curvature parameters achieved good discriminative performance and robustness, the non-dimensional parameters tended to perform well as a group. This suggests that non-dimensional geometric risk parameters can provide comparatively good discriminative performance, while the nondimensionalization itself mitigates some of the uncertainty introduced through the workflow by which the parameters are calculated [14].

Limitations

IAs were grouped by anatomical region because IA location is an important determinant of rupture risk, as demonstrated by its weight in current risk scores [7-9]. However, by analyzing the datasets by anatomical region, some subsamples become quite small. Small sample size might affect the accuracy of the median and interquartile range estimates derived from these groups. This limitation is, however, partially mitigated by also analyzing all anatomical regions combined and using two datasets, in order to get a more comprehensive picture of the risk parameters' performance. Another potential limitation are the uncertainty values from Goubergrits et al. [14], which were used to calculate DUR. These values were calculated on a sample containing MCA and posterior region IAs [14]. While it does not seem particularly probable, it is possible that IA location might affect the uncertainty inherent in calculating the geometric risk parameters in a relevant manner, which in turn could influence DUR results. A more fundamental limitations is the focus on geometric risk parameters. These parameters serve as proxies for the pathophysiological processes leading to IA rupture through the latter's influence on the geometry of the IA surface. Due to their nature, geometric risk parameters cannot directly capture the hemodynamic, mechanical, or biochemical aspects of IA rupture. Nevertheless, they are among the most intensely researched types of IA rupture risk parameters, due to the comparative ease with which they can be calculated from clinical data.

Conclusion

Based on datasets from two research groups, the present study provides location-specific estimates of the discriminative ability of a large set of geometric risk parameters for IA rupture risk assessment, while also considering uncertainty. Additionally, correlation patterns between the parameters are identified. The presented data is potentially useful in evaluating geometric risk parameters for use in rupture risk models or when choosing input parameters for machine learning approaches to rupture risk prediction. It may also be helpful when designing future geometric risk parameters for clinical use.

For peer review only

BMJ Open: first published as 10.1136/bmjopen-2022-063051 on 8 November 2022. Downloaded from http://bmjopen.bmj.com/ on June 10, 2025 at Agence Bibliographique de l Enseignement Superieur (ABES) . Protected by copyright, including for uses related to text and data mining, AI training, and similar technologies.

Conflict of interest statement

The authors declare that there is no conflict of interest.

Acknowledgments

The authors kindly acknowledge PD Dr. Belal Neyazi (Department of Neurosurgery, University Hospital Magdeburg) for his assistance during data acquisition as well as Adriano Schlief (Institute of Computer-assisted Cardiovascular Medicine, Charité – Universitätsmedizin Berlin) for his help in checking the topology and scaling of the IA geometries.

Data Availability Statement

All individual parameter values as well as the correlation coefficients are made available as supplemental material.

- supplemental material 1: individual parameter values, IA location, and rupture status for each IA
- supplemental material 2: exact values of the inter-parameter correlation coefficients

Ethical approval statements

In this study, patient-specific 3D reconstructions of intracranial aneurysms based on routine information were evaluated retrospectively. Use of retrospective data was approved by the local ethics committees (Ethikkommission der Charité - Universitätsmedizin Berlin: EA2/222/19; Ethikkommission der Med. Hochschule Hannover: NOVA Nr. 68/20).

Funding

This study was partly funded by the Federal Ministry of Education and Research in Germany within the Forschungscampus *STIMULATE* (grant number 13GW0473A) and the German Research Foundation (grant number SA 3461/2-1, BE 6230/2-1).

Author contributions

All roles according to CRediT (contributor roles taxonomy). Conceptualization: LG, JS, FH, JB, and PB. Methodology: FH, JS, and LG. Resources: AS, IES, OB, NL, SS, and PB. Investigation: JB, FH, and JS. Formal Analysis: FH. Funding acquisition: LG, PB, and SS. Supervision: LG. Writing – original draft: FH, LG, and JB. Writing – review & editing: PB, SS, AS, IES, OB, NL, and JS.

For peer review only

BMJ Open: first published as 10.1136/bmjopen-2022-063051 on 8 November 2022. Downloaded from http://bmjopen.bmj.com/ on June 10, 2025 at Agence Bibliographique de l Enseignement Superieur (ABES) .
Protected by copyright, including for uses related to text and data mining, AI training, and similar technologies.

BMJ Open: first published as 10.1136/bmjopen-2022-063051 on 8 November 2022. Downloaded from http://bmjopen.bmj.com/ on June 10, 2025 at Agence Bibliographique de l Enseignement Superieur (ABES) . Protected by copyright, including for uses related to text and data mining, AI training, and similar technologies.

References

1. Vlak, M.H., A. Algra, R. Brandenburg, and G.J. Rinkel, *Prevalence of unruptured intracranial aneurysms, with emphasis on sex, age, comorbidity, country, and time period: a systematic review and meta-analysis.* Lancet Neurol, 2011. **10**(7): p. 626-36.
2. Brown, R.D., Jr. and J.P. Broderick, *Unruptured intracranial aneurysms: epidemiology, natural history, management options, and familial screening.* Lancet Neurol, 2014. **13**(4): p. 393-404.
3. Wiebers, D.O., J.P. Whisnant, J. Huston, 3rd, I. Meissner, R.D. Brown, Jr., D.G. Piepgras, G.S. Forbes, K. Thielen, D. Nichols, W.M. O'Fallon, J. Peacock, L. Jaeger, N.F. Kassell, G.L. Kongable-Beckman, J.C. Torner, and I. International Study of Unruptured Intracranial Aneurysms, *Unruptured intracranial aneurysms: natural history, clinical outcome, and risks of surgical and endovascular treatment.* Lancet, 2003. **362**(9378): p. 103-10.
4. Rackauskaite, D., E. Svanborg, E. Andersson, K. Lowhagen, L. Csajbok, and B. Nellgard, *Prospective study: Long-term outcome at 12-15 years after aneurysmal subarachnoid hemorrhage.* Acta Neurol Scand, 2018. **138**(5): p. 400-407.
5. Pontes, F.G.B., E.M. da Silva, J.C. Baptista-Silva, and V. Vasconcelos, *Treatments for unruptured intracranial aneurysms.* Cochrane Database Syst Rev, 2021. **5**: p. CD013312.
6. Thompson, B.G., et al., *Guidelines for the Management of Patients With Unruptured Intracranial Aneurysms: A Guideline for Healthcare Professionals From the American Heart Association/American Stroke Association.* Stroke, 2015. **46**(8): p. 2368-400.
7. Greving, J.P., M.J. Wermer, R.D. Brown, Jr., A. Morita, S. Juvela, M. Yonekura, T. Ishibashi, J.C. Torner, T. Nakayama, G.J. Rinkel, and A. Algra, *Development of the PHASES score for prediction of risk of rupture of intracranial aneurysms: a pooled analysis of six prospective cohort studies.* Lancet Neurol, 2014. **13**(1): p. 59-66.
8. Etminan, N., et al., *The unruptured intracranial aneurysm treatment score: a multidisciplinary consensus.* Neurology, 2015. **85**(10): p. 881-9.
9. Backes, D., et al., *ELAPSS score for prediction of risk of growth of unruptured intracranial aneurysms.* Neurology, 2017. **88**(17): p. 1600-1606.
10. Juvela, S., *PHASES score and treatment scoring with cigarette smoking in the long-term prediction of rupturing of unruptured intracranial aneurysms.* J Neurosurg, 2022. **136**(1): p. 156-162.
11. Molenberg, R., M.W. Aalbers, A. Mazuri, G.J. Luijckx, J.D.M. Metzemaekers, R.J.M. Groen, M. Uyttenboogaart, and J.M.C. van Dijk, *The Unruptured Intracranial Aneurysm Treatment Score as a predictor of aneurysm growth or rupture.* Eur J Neurol, 2021. **28**(3): p. 837-843.
12. Hernandez-Duran, S., D. Mielke, V. Rohde, and V. Malinova, *Is the unruptured intracranial aneurysm treatment score (UIATS) sensitive enough to detect aneurysms at risk of rupture?* Neurosurg Rev, 2021. **44**(2): p. 987-993.
13. Neyazi, B., V.M. Swiatek, M. Skalej, O. Beuing, K.P. Stein, J. Hattingen, B. Preim, P. Berg, S. Saalfeld, and I.E. Sandalcioglu, *Rupture risk assessment for multiple intracranial aneurysms: why there is no need for dozens of clinical, morphological and hemodynamic parameters.* Ther Adv Neurol Disord, 2020. **13**: p. 1756286420966159.
14. Goubergrits, L., F. Hellmeier, J. Bruening, A. Spuler, H.C. Hege, S. Voss, G. Janiga, S. Saalfeld, O. Beuing, and P. Berg, *Multiple Aneurysms AnaTomy CHallenge 2018 (MATCH): uncertainty quantification of geometric rupture risk parameters.* Biomed Eng Online, 2019. **18**(1): p. 35.
15. Dhar, S., M. Tremmel, J. Mocco, M. Kim, J. Yamamoto, A.H. Siddiqui, L.N. Hopkins, and H. Meng, *Morphology parameters for intracranial aneurysm rupture risk assessment.* Neurosurgery, 2008. **63**(2): p. 185-96; discussion 196-7.
16. Detmer, F.J., B.J. Chung, F. Mut, M. Slawski, F. Hamzei-Sichani, C. Putman, C. Jimenez, and J.R. Cebral, *Development and internal validation of an aneurysm rupture probability model based on patient characteristics and aneurysm location, morphology, and hemodynamics.* Int J Comput Assist Radiol Surg, 2018. **13**(11): p. 1767-1779.

17. Lauric, A., M.I. Baharoglu, and A.M. Malek, *Ruptured status discrimination performance of aspect ratio, height/width, and bottleneck factor is highly dependent on aneurysm sizing methodology.* Neurosurgery, 2012. **71**(1): p. 38-45.
18. Berg, P., et al., *Multiple Aneurysms AnaTomy CHallenge 2018 (MATCH): Phase I: Segmentation.* Cardiovasc Eng Technol, 2018. **9**(4): p. 565-581.
19. Ma, B., R.E. Harbaugh, and M.L. Raghavan, *Three-dimensional geometrical characterization of cerebral aneurysms.* Ann Biomed Eng, 2004. **32**(2): p. 264-73.
20. Lauric, A., E.L. Miller, M.I. Baharoglu, and A.M. Malek, *3D shape analysis of intracranial aneurysms using the writhe number as a discriminant for rupture.* Ann Biomed Eng, 2011. **39**(5): p. 1457-69.
21. Chien, A., J. Sayre, and F. Vinuela, *Comparative morphological analysis of the geometry of ruptured and unruptured aneurysms.* Neurosurgery, 2011. **69**(2): p. 349-56.
22. Ujiie, H., Y. Tamano, K. Sasaki, and T. Hori, *Is the aspect ratio a reliable index for predicting the rupture of a saccular aneurysm?* Neurosurgery, 2001. **48**(3): p. 495-502; discussion 502-3.
23. Ramachandran, M., R. Retarekar, R.E. Harbaugh, D. Hasan, B. Policeni, R. Rosenwasser, C. Ogilvy, and M.L. Raghavan, *Sensitivity of Quantified Intracranial Aneurysm Geometry to Imaging Modality.* Cardiovasc Eng Technol, 2013. **4**(1): p. 75-86.
24. O'Meara, B., J.P. Rahal, A. Lauric, and A.M. Malek, *Benefit of a sharp computed tomography angiography reconstruction kernel for improved characterization of intracranial aneurysms.* Neurosurgery, 2014. **10 Suppl 1**: p. 97-105; discussion 105.
25. Berg, P., S. Saalfeld, S. Voss, T. Redel, B. Preim, G. Janiga, and O. Beuing, *Does the DSA reconstruction kernel affect hemodynamic predictions in intracranial aneurysms? An analysis of geometry and blood flow variations.* J Neurointerv Surg, 2018. **10**(3): p. 290-296.
26. Cebral, J.R., M.A. Castro, S. Appanaboyina, C.M. Putman, D. Millan, and A.F. Frangi, *Efficient pipeline for image-based patient-specific analysis of cerebral aneurysm hemodynamics: technique and sensitivity.* IEEE Trans Med Imaging, 2005. **24**(4): p. 457-67.
27. Sarrami-Foroushani, A., T. Lassila, and A.F. Frangi, *Virtual endovascular treatment of intracranial aneurysms: models and uncertainty.* Wiley Interdiscip Rev Syst Biol Med, 2017. **9**(4).
28. Schneiders, J.J., H.A. Marquering, L. Antiga, R. van den Berg, E. VanBavel, and C.B. Majoie, *Intracranial aneurysm neck size overestimation with 3D rotational angiography: the impact on intra-aneurysmal hemodynamics simulated with computational fluid dynamics.* AJNR Am J Neuroradiol, 2013. **34**(1): p. 121-8.
29. Ivantsits, M., et al., *Detection and analysis of cerebral aneurysms based on X-ray rotational angiography - the CADA 2020 challenge.* Med Image Anal, 2021. **77**: p. 102333.
30. Zheng, Y., F. Xu, J. Ren, Q. Xu, Y. Liu, Y. Tian, and B. Leng, *Assessment of intracranial aneurysm rupture based on morphology parameters and anatomical locations.* J Neurointerv Surg, 2016. **8**(12): p. 1240-1246.

For peer review only

BMJ Open: first published as 10.1136/bmjopen-2022-063051 on 8 November 2022. Downloaded from http://bmjopen.bmj.com/ on June 10, 2025 at Agence Bibliographique de l Enseignement Superieur (ABES) . Protected by copyright, including for uses related to text and data mining, AI training, and similar technologies.

Figures

Figure 1: Standardized absolute group difference (SAD) for each anatomical region and dataset.

Figure 2: Group difference-uncertainty ratio (DUR) for each anatomical region and dataset.

Figure 3: Pearson's r for correlation between geometric risk parameters by anatomical region for dataset 1.

Figure 4: Pearson's r for correlation between geometric risk parameters by anatomical region for dataset 4.

For peer review only

BMJ Open: first published as 10.1136/bmjopen-2022-063051 on 8 November 2022. Downloaded from http://bmjopen.bmj.com/ on June 10, 2025 at Agence Bibliographique de l Enseignement Superieur (ABES) .
Protected by copyright, including for uses related to text and data mining, AI training, and similar technologies.

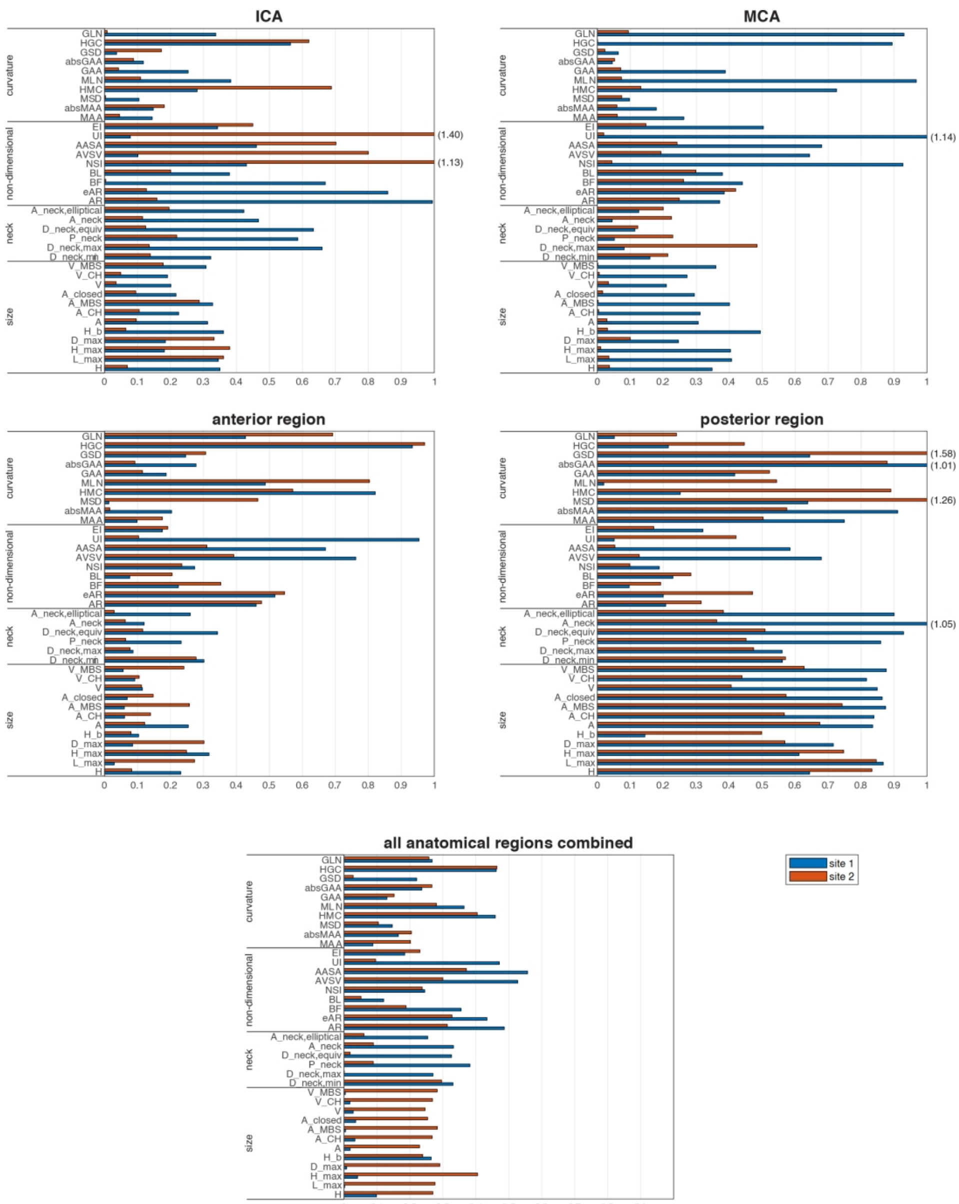

196x248mm (300 x 300 DPI)

BMJ Open: first published as 10.1136/bmjopen-2022-063051 on 8 November 2022. Downloaded from http://bmjopen.bmj.com/ on June 10, 2025 at Agence Bibliographique de l Enseignement Superieur (ABES) .
Protected by copyright, including for uses related to text and data mining, AI training, and similar technologies.

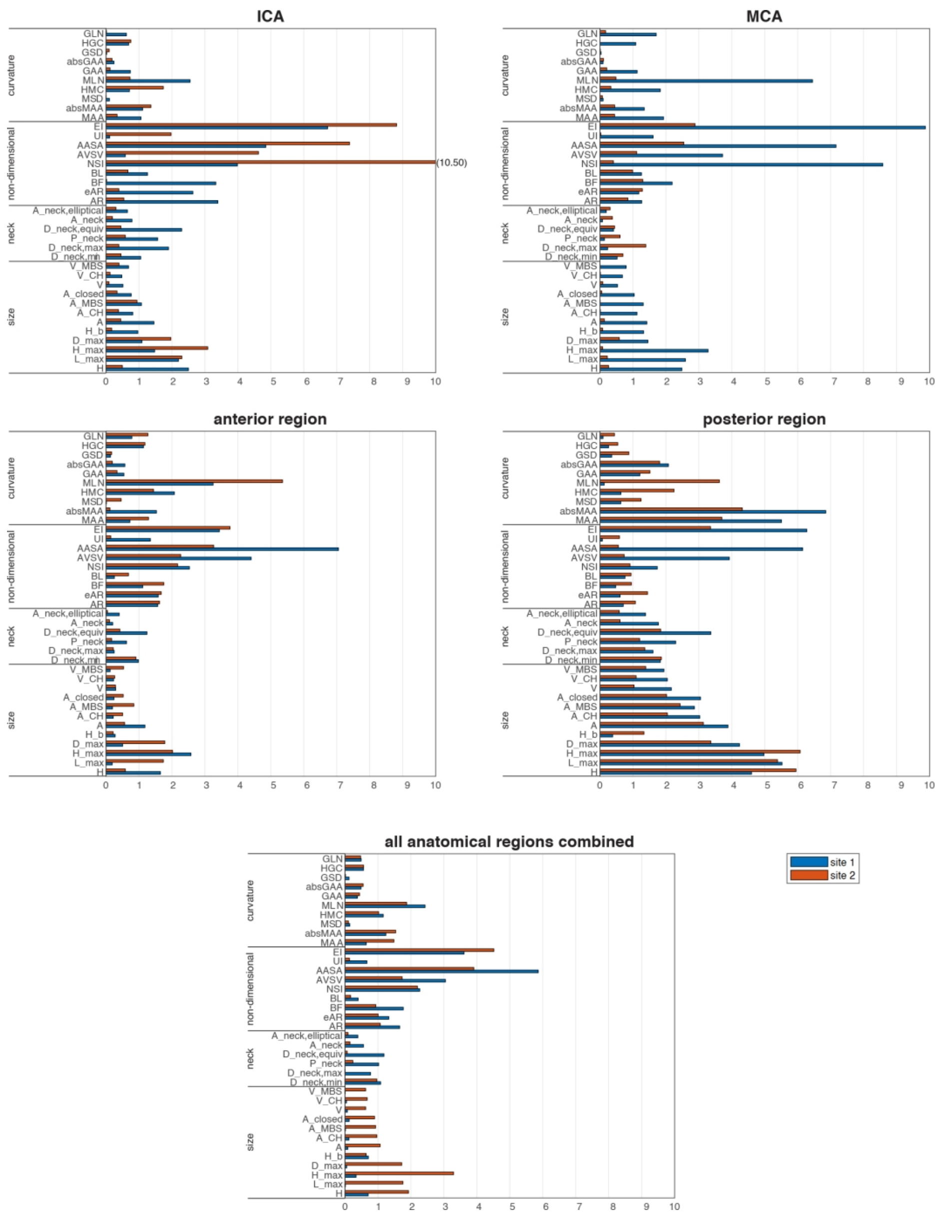

192x248mm (300 x 300 DPI)

BMJ Open: first published as 10.1136/bmjopen-2022-063051 on 8 November 2022. Downloaded from http://bmjopen.bmj.com/ on June 10, 2025 at Agence Bibliographique de l Enseignement Superieur (ABES) . Protected by copyright, including for uses related to text and data mining, AI training, and similar technologies.

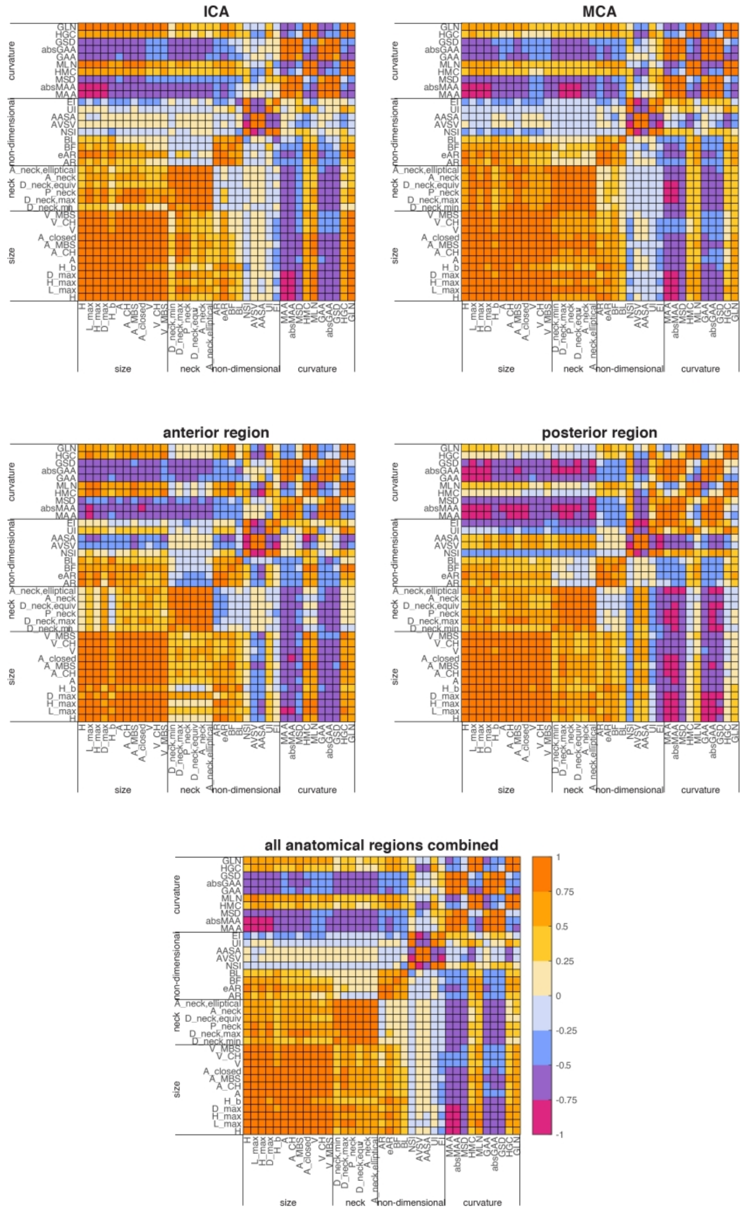

198x325mm (300 x 300 DPI)

BMJ Open: first published as 10.1136/bmjopen-2022-063051 on 8 November 2022. Downloaded from http://bmjopen.bmj.com/ on June 10, 2025 at Agence Bibliographique de l Enseignement Superieur (ABES) . Protected by copyright, including for uses related to text and data mining, AI training, and similar technologies.

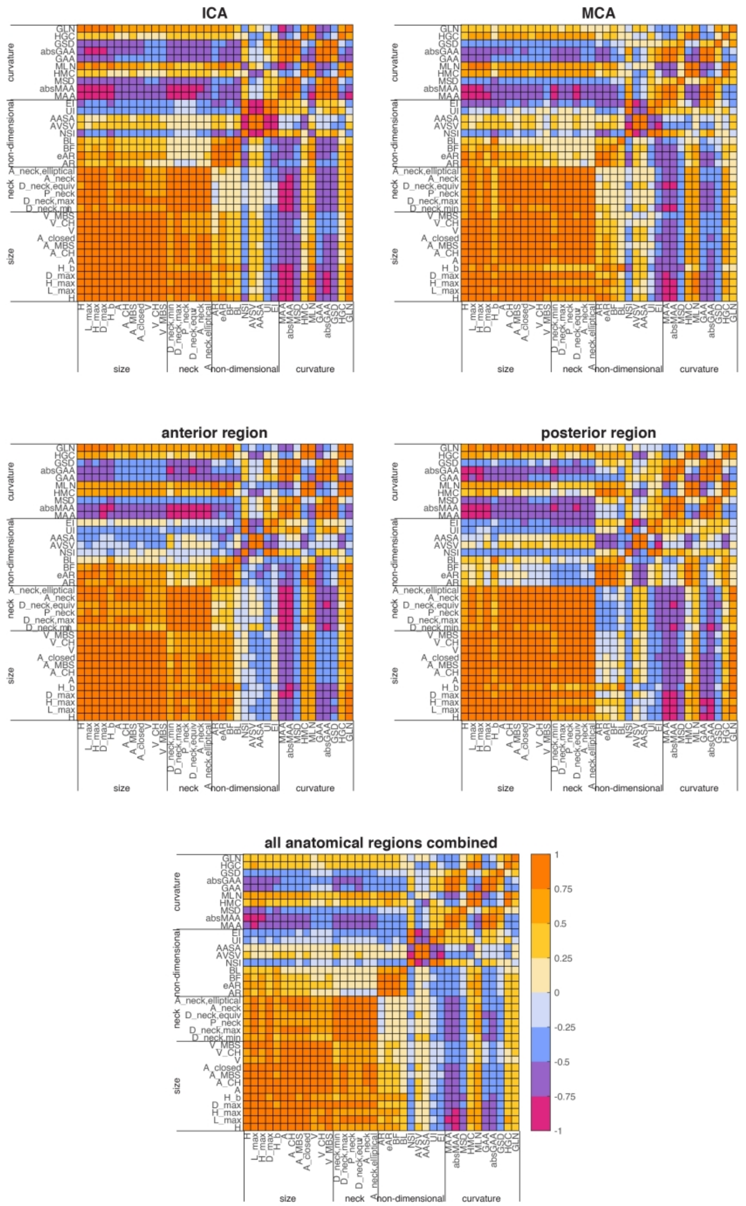

BMJ Open: first published as 10.1136/bmjopen-2022-063051 on 8 November 2022. Downloaded from http://bmjopen.bmj.com/ on June 10, 2025 at Agence Bibliographique de l Enseignement Superieur (ABES) . Protected by copyright, including for uses related to text and data mining, AI training, and similar technologies.

Pearson's r	H	L_max	H_max	D_max	H_b	A	A_CH
H	1.000	0.872	0.968	0.610	0.836	0.867	0.830
L_max	0.872	1.000	0.950	0.884	0.648	0.962	0.960
H_max	0.968	0.950	1.000	0.728	0.783	0.922	0.894
D_max	0.610	0.884	0.728	1.000	0.349	0.873	0.900
H_b	0.836	0.648	0.783	0.349	1.000	0.653	0.605
A	0.867	0.962	0.922	0.873	0.653	1.000	0.993
A_CH	0.830	0.960	0.894	0.900	0.605	0.993	1.000
A_MBS	0.835	0.973	0.919	0.863	0.596	0.967	0.957
A_closed	0.827	0.957	0.890	0.899	0.606	0.992	1.000
V	0.779	0.917	0.842	0.869	0.565	0.980	0.988
V_CH	0.778	0.924	0.846	0.880	0.548	0.982	0.988
V_MBS	0.769	0.918	0.857	0.822	0.522	0.934	0.919
D_neck,mi	0.220	0.402	0.246	0.535	0.125	0.415	0.484
D_neck,ma	0.153	0.466	0.248	0.642	-0.049	0.426	0.520
P_neck	0.059	0.376	0.158	0.554	-0.075	0.353	0.454
D_neck,eq	0.159	0.428	0.224	0.609	-0.014	0.417	0.508
A_neck	0.089	0.392	0.170	0.583	-0.064	0.390	0.491
A_neck,elli	0.179	0.448	0.240	0.630	0.028	0.450	0.541
AR	0.867	0.582	0.784	0.236	0.849	0.579	0.503
eAR	0.879	0.639	0.819	0.304	0.801	0.608	0.536
BF	0.701	0.727	0.749	0.684	0.595	0.735	0.682
BL	0.627	0.461	0.580	0.273	0.884	0.464	0.423
NSI	0.173	0.275	0.235	0.216	-0.021	0.142	0.129
AVSV	-0.393	-0.491	-0.481	-0.331	-0.275	-0.315	-0.287
AASA	-0.455	-0.558	-0.551	-0.378	-0.337	-0.380	-0.350
UI	0.405	0.494	0.463	0.437	0.137	0.365	0.356
EI	0.012	0.091	0.067	0.013	-0.075	-0.034	-0.050
MAA	-0.661	-0.763	-0.698	-0.727	-0.481	-0.702	-0.740
absMAA	-0.692	-0.755	-0.711	-0.701	-0.547	-0.710	-0.747
MSD	-0.504	-0.453	-0.465	-0.370	-0.517	-0.489	-0.513
HMC	0.672	0.801	0.776	0.698	0.434	0.706	0.672
MLN	0.727	0.775	0.790	0.706	0.500	0.745	0.704
GAA	-0.627	-0.693	-0.655	-0.632	-0.443	-0.590	-0.621
absGAA	-0.647	-0.688	-0.659	-0.626	-0.534	-0.639	-0.672
GSD	-0.547	-0.567	-0.541	-0.507	-0.511	-0.550	-0.584
HGC	0.618	0.783	0.727	0.735	0.322	0.710	0.685
GLN	0.614	0.729	0.698	0.731	0.300	0.711	0.681

For peer review only

BMJ Open: first published as 10.1136/bmjopen-2022-063051 on 8 November 2022. Downloaded from http://bmjopen.bmj.com/ on June 10, 2025 at Agence Bibliographique de l Enseignement Superieur (ABES) . Protected by copyright, including for uses related to text and data mining, AI training, and similar technologies.

A_MBS	A_closed	V	V_CH	V_MBS	D_neck,min	D_neck,max	P_neck
0.835	0.827	0.779	0.778	0.769	0.220	0.153	0.059
0.973	0.957	0.917	0.924	0.918	0.402	0.466	0.376
0.919	0.890	0.842	0.846	0.857	0.246	0.248	0.158
0.863	0.899	0.869	0.880	0.822	0.535	0.642	0.554
0.596	0.606	0.565	0.548	0.522	0.125	-0.049	-0.075
0.967	0.992	0.980	0.982	0.934	0.415	0.426	0.353
0.957	1.000	0.988	0.988	0.919	0.484	0.520	0.454
1.000	0.952	0.939	0.953	0.984	0.346	0.375	0.290
0.952	1.000	0.989	0.988	0.913	0.494	0.526	0.462
0.939	0.989	1.000	0.998	0.920	0.486	0.503	0.457
0.953	0.988	0.998	1.000	0.940	0.460	0.485	0.430
0.984	0.913	0.920	0.940	1.000	0.298	0.302	0.223
0.346	0.494	0.486	0.460	0.298	1.000	0.685	0.681
0.375	0.526	0.503	0.485	0.302	0.685	1.000	0.952
0.290	0.462	0.457	0.430	0.223	0.681	0.952	1.000
0.361	0.516	0.504	0.485	0.310	0.907	0.870	0.857
0.321	0.500	0.503	0.477	0.263	0.780	0.944	0.974
0.377	0.550	0.543	0.517	0.316	0.909	0.909	0.886
0.568	0.498	0.454	0.459	0.527	-0.127	-0.328	-0.375
0.610	0.529	0.473	0.480	0.553	-0.208	-0.214	-0.304
0.753	0.675	0.643	0.668	0.743	0.043	-0.096	-0.153
0.362	0.427	0.370	0.348	0.268	0.087	-0.061	-0.064
0.334	0.113	0.080	0.131	0.361	-0.197	-0.061	-0.176
-0.501	-0.273	-0.225	-0.261	-0.486	0.179	0.068	0.160
-0.558	-0.337	-0.288	-0.320	-0.535	0.160	0.041	0.130
0.494	0.340	0.273	0.321	0.477	-0.152	0.134	-0.008
0.166	-0.065	-0.072	-0.032	0.209	-0.227	-0.193	-0.269
-0.636	-0.743	-0.667	-0.654	-0.529	-0.582	-0.679	-0.648
-0.627	-0.752	-0.683	-0.661	-0.516	-0.646	-0.664	-0.637
-0.379	-0.521	-0.510	-0.474	-0.310	-0.620	-0.396	-0.402
0.801	0.661	0.604	0.639	0.770	-0.028	0.133	-0.011
0.753	0.697	0.631	0.658	0.708	-0.009	0.127	-0.014
-0.547	-0.622	-0.527	-0.520	-0.433	-0.446	-0.584	-0.543
-0.551	-0.678	-0.607	-0.582	-0.440	-0.652	-0.603	-0.580
-0.453	-0.592	-0.545	-0.515	-0.360	-0.695	-0.549	-0.547
0.811	0.672	0.627	0.670	0.805	-0.029	0.180	0.038
0.748	0.672	0.626	0.664	0.737	-0.038	0.158	0.024

For peer review only

BMJ Open: first published as 10.1136/bmjopen-2022-063051 on 8 November 2022. Downloaded from http://bmjopen.bmj.com/ on June 10, 2025 at Agence Bibliographique de l Enseignement Superieur (ABES) . Protected by copyright, including for uses related to text and data mining, AI training, and similar technologies.

D_neck,equi	A_neck	A_neck,ellipt	AR	eAR	BF	BL	NSI
0.159	0.089	0.179	0.867	0.879	0.701	0.627	0.173
0.428	0.392	0.448	0.582	0.639	0.727	0.461	0.275
0.224	0.170	0.240	0.784	0.819	0.749	0.580	0.235
0.609	0.583	0.630	0.236	0.304	0.684	0.273	0.216
-0.014	-0.064	0.028	0.849	0.801	0.595	0.884	-0.021
0.417	0.390	0.450	0.579	0.608	0.735	0.464	0.142
0.508	0.491	0.541	0.503	0.536	0.682	0.423	0.129
0.361	0.321	0.377	0.568	0.610	0.753	0.362	0.334
0.516	0.500	0.550	0.498	0.529	0.675	0.427	0.113
0.504	0.503	0.543	0.454	0.473	0.643	0.370	0.080
0.485	0.477	0.517	0.459	0.480	0.668	0.348	0.131
0.310	0.263	0.316	0.527	0.553	0.743	0.268	0.361
0.907	0.780	0.909	-0.127	-0.208	0.043	0.087	-0.197
0.870	0.944	0.909	-0.328	-0.214	-0.096	-0.061	-0.061
0.857	0.974	0.886	-0.375	-0.304	-0.153	-0.064	-0.176
1.000	0.927	0.953	-0.267	-0.298	-0.034	-0.040	-0.113
0.927	1.000	0.949	-0.353	-0.317	-0.119	-0.074	-0.157
0.953	0.949	1.000	-0.266	-0.247	-0.036	0.004	-0.155
-0.267	-0.353	-0.266	1.000	0.946	0.687	0.672	0.175
-0.298	-0.317	-0.247	0.946	1.000	0.669	0.627	0.253
-0.034	-0.119	-0.036	0.687	0.669	1.000	0.525	0.300
-0.040	-0.074	0.004	0.672	0.627	0.525	1.000	-0.267
-0.113	-0.157	-0.155	0.175	0.253	0.300	-0.267	1.000
0.141	0.175	0.161	-0.403	-0.468	-0.491	-0.075	-0.823
0.129	0.153	0.138	-0.450	-0.524	-0.532	-0.148	-0.751
0.019	-0.021	-0.047	0.320	0.427	0.442	-0.027	0.824
-0.219	-0.243	-0.226	0.085	0.141	0.157	-0.325	0.922
-0.656	-0.622	-0.632	-0.337	-0.379	-0.384	-0.446	0.044
-0.678	-0.632	-0.667	-0.377	-0.393	-0.371	-0.492	0.103
-0.516	-0.461	-0.553	-0.319	-0.252	-0.158	-0.456	0.370
0.017	-0.024	0.030	0.536	0.649	0.764	0.318	0.542
0.022	-0.028	0.035	0.591	0.685	0.804	0.463	0.314
-0.543	-0.499	-0.495	-0.365	-0.417	-0.365	-0.436	-0.045
-0.634	-0.575	-0.635	-0.368	-0.375	-0.327	-0.513	0.183
-0.631	-0.563	-0.640	-0.296	-0.265	-0.203	-0.488	0.303
0.077	0.033	0.055	0.449	0.560	0.753	0.186	0.602
0.064	0.022	0.042	0.453	0.551	0.779	0.234	0.427

For peer review only

BMJ Open: first published as 10.1136/bmjopen-2022-063051 on 8 November 2022. Downloaded from http://bmjopen.bmj.com/ on June 10, 2025 at Agence Bibliographique de l Enseignement Superieur (ABES) .
Protected by copyright, including for uses related to text and data mining, AI training, and similar technologies.

AVSV	AASA	UI	EI	MAA	absMAA	MSD	HMC
-0.393	-0.455	0.405	0.012	-0.661	-0.692	-0.504	0.672
-0.491	-0.558	0.494	0.091	-0.763	-0.755	-0.453	0.801
-0.481	-0.551	0.463	0.067	-0.698	-0.711	-0.465	0.776
-0.331	-0.378	0.437	0.013	-0.727	-0.701	-0.370	0.698
-0.275	-0.337	0.137	-0.075	-0.481	-0.547	-0.517	0.434
-0.315	-0.380	0.365	-0.034	-0.702	-0.710	-0.489	0.706
-0.287	-0.350	0.356	-0.050	-0.740	-0.747	-0.513	0.672
-0.501	-0.558	0.494	0.166	-0.636	-0.627	-0.379	0.801
-0.273	-0.337	0.340	-0.065	-0.743	-0.752	-0.521	0.661
-0.225	-0.288	0.273	-0.072	-0.667	-0.683	-0.510	0.604
-0.261	-0.320	0.321	-0.032	-0.654	-0.661	-0.474	0.639
-0.486	-0.535	0.477	0.209	-0.529	-0.516	-0.310	0.770
0.179	0.160	-0.152	-0.227	-0.582	-0.646	-0.620	-0.028
0.068	0.041	0.134	-0.193	-0.679	-0.664	-0.396	0.133
0.160	0.130	-0.008	-0.269	-0.648	-0.637	-0.402	-0.011
0.141	0.129	0.019	-0.219	-0.656	-0.678	-0.516	0.017
0.175	0.153	-0.021	-0.243	-0.622	-0.632	-0.461	-0.024
0.161	0.138	-0.047	-0.226	-0.632	-0.667	-0.553	0.030
-0.403	-0.450	0.320	0.085	-0.337	-0.377	-0.319	0.536
-0.468	-0.524	0.427	0.141	-0.379	-0.393	-0.252	0.649
-0.491	-0.532	0.442	0.157	-0.384	-0.371	-0.158	0.764
-0.075	-0.148	-0.027	-0.325	-0.446	-0.492	-0.456	0.318
-0.823	-0.751	0.824	0.922	0.044	0.103	0.370	0.542
1.000	0.988	-0.699	-0.776	0.120	0.070	-0.205	-0.736
0.988	1.000	-0.667	-0.702	0.177	0.129	-0.138	-0.785
-0.699	-0.667	1.000	0.556	-0.297	-0.203	0.211	0.706
-0.776	-0.702	0.556	1.000	0.257	0.273	0.377	0.341
0.120	0.177	-0.297	0.257	1.000	0.974	0.558	-0.424
0.070	0.129	-0.203	0.273	0.974	1.000	0.709	-0.339
-0.205	-0.138	0.211	0.377	0.558	0.709	1.000	0.032
-0.736	-0.785	0.706	0.341	-0.424	-0.339	0.032	1.000
-0.488	-0.536	0.586	0.075	-0.511	-0.427	0.009	0.912
0.207	0.254	-0.399	0.184	0.968	0.923	0.460	-0.446
0.021	0.088	-0.094	0.314	0.933	0.973	0.764	-0.290
-0.118	-0.050	0.060	0.393	0.798	0.880	0.904	-0.119
-0.689	-0.718	0.778	0.366	-0.422	-0.320	0.097	0.961
-0.487	-0.516	0.661	0.173	-0.452	-0.345	0.122	0.881

BMJ Open: first published as 10.1136/bmjopen-2022-063051 on 8 November 2022. Downloaded from http://bmjopen.bmj.com/ on June 10, 2025 at Agence Bibliographique de l Enseignement Superieur (ABES) . Protected by copyright, including for uses related to text and data mining, AI training, and similar technologies.

MLN	GAA	absGAA	GSD	HGC	GLN
0.727	-0.627	-0.647	-0.547	0.618	0.614
0.775	-0.693	-0.688	-0.567	0.783	0.729
0.790	-0.655	-0.659	-0.541	0.727	0.698
0.706	-0.632	-0.626	-0.507	0.735	0.731
0.500	-0.443	-0.534	-0.511	0.322	0.300
0.745	-0.590	-0.639	-0.550	0.710	0.711
0.704	-0.621	-0.672	-0.584	0.685	0.681
0.753	-0.547	-0.551	-0.453	0.811	0.748
0.697	-0.622	-0.678	-0.592	0.672	0.672
0.631	-0.527	-0.607	-0.545	0.627	0.626
0.658	-0.520	-0.582	-0.515	0.670	0.664
0.708	-0.433	-0.440	-0.360	0.805	0.737
-0.009	-0.446	-0.652	-0.695	-0.029	-0.038
0.127	-0.584	-0.603	-0.549	0.180	0.158
-0.014	-0.543	-0.580	-0.547	0.038	0.024
0.022	-0.543	-0.634	-0.631	0.077	0.064
-0.028	-0.499	-0.575	-0.563	0.033	0.022
0.035	-0.495	-0.635	-0.640	0.055	0.042
0.591	-0.365	-0.368	-0.296	0.449	0.453
0.685	-0.417	-0.375	-0.265	0.560	0.551
0.804	-0.365	-0.327	-0.203	0.753	0.779
0.463	-0.436	-0.513	-0.488	0.186	0.234
0.314	-0.045	0.183	0.303	0.602	0.427
-0.488	0.207	0.021	-0.118	-0.689	-0.487
-0.536	0.254	0.088	-0.050	-0.718	-0.516
0.586	-0.399	-0.094	0.060	0.778	0.661
0.075	0.184	0.314	0.393	0.366	0.173
-0.511	0.968	0.933	0.798	-0.422	-0.452
-0.427	0.923	0.973	0.880	-0.320	-0.345
0.009	0.460	0.764	0.904	0.097	0.122
0.912	-0.446	-0.290	-0.119	0.961	0.881
1.000	-0.519	-0.372	-0.166	0.886	0.941
-0.519	1.000	0.888	0.724	-0.438	-0.459
-0.372	0.888	1.000	0.937	-0.231	-0.256
-0.166	0.724	0.937	1.000	-0.051	-0.034
0.886	-0.438	-0.231	-0.051	1.000	0.939
0.941	-0.459	-0.256	-0.034	0.939	1.000

For peer review only

BMJ Open: first published as 10.1136/bmjopen-2022-063051 on 8 November 2022. Downloaded from http://bmjopen.bmj.com/ on June 10, 2025 at Agence Bibliographique de l Enseignement Superieur (ABES) .
Protected by copyright, including for uses related to text and data mining, AI training, and similar technologies.

parameter name	patient and ane	site supplyin	site processi	IA location	IA anatomi	rupture sta	height
abbreviation	-	-	-	-	-	-	H
unit	-	-	-	-	-	1=ruptured	mm
	1	Berlin	Berlin	AComA	anterior	1	5.748
	2	Berlin	Berlin	PComA	posterior	0	8.261
	3	Berlin	Berlin	PICA	posterior	1	6.023
	4	Berlin	Berlin	AComA	anterior	1	5.698
	5	Berlin	Berlin	ACA	anterior	0	5.667
	6	Berlin	Berlin	MCA	MCA	0	2.849
	7	Berlin	Berlin	ICA	ICA	0	19.575
	8	Berlin	Berlin	MCA	MCA	0	4.199
	9	Berlin	Berlin	MCA	MCA	0	3.795
	10	Berlin	Berlin	AComA	anterior	1	5.051
	11	Berlin	Berlin	MCA	MCA	0	6.789
	12	Berlin	Berlin	ICA	ICA	1	7.610
	13	Berlin	Berlin	MCA	MCA	0	8.157
	14	Berlin	Berlin	AComA	anterior	1	2.542
	15	Berlin	Berlin	PComA	posterior	1	3.196
	16A	Berlin	Berlin	ICA	ICA	1	9.587
	16B	Berlin	Berlin	ACA	anterior	0	1.879
	17A	Berlin	Berlin	ICA	ICA	0	12.261
	17B	Berlin	Berlin	ICA	ICA	0	2.791
	17C	Berlin	Berlin	AComA	anterior	0	4.530
	18	Berlin	Berlin	MCA	MCA	1	5.597
	19	Berlin	Berlin	AComA	anterior	1	5.177
	20	Berlin	Berlin	PComA	posterior	1	10.569
	21	Berlin	Berlin	ICA	ICA	0	4.966
	22	Berlin	Berlin	ICA	ICA	0	7.908
	23	Berlin	Berlin	MCA	MCA	1	4.598
	24	Berlin	Berlin	ICA	ICA	0	2.906
	25	Berlin	Berlin	BA	posterior	0	8.473
	26	Berlin	Berlin	MCA	MCA	1	4.210
	27	Berlin	Berlin	AComA	anterior	1	4.597
	28	Berlin	Berlin	MCA	MCA	1	5.480
	29	Berlin	Berlin	ICA	ICA	0	12.780
	30A	Berlin	Berlin	ICA	ICA	0	4.078
	30B	Berlin	Berlin	AComA	anterior	0	3.135
	30C	Berlin	Berlin	AComA	anterior	1	5.085
	30D	Berlin	Berlin	MCA	MCA	0	2.715
	30E	Berlin	Berlin	PICA	posterior	1	4.983
	31	Berlin	Berlin	MCA	MCA	0	4.542
	32	Berlin	Berlin	ICA	ICA	0	9.475
	33	Berlin	Berlin	AComA	anterior	1	6.212
	34	Berlin	Berlin	AComA	anterior	0	3.383
	35	Berlin	Berlin	ICA	ICA	1	11.690
	36	Berlin	Berlin	BA	posterior	0	20.748
	37	Berlin	Berlin	AComA	anterior	1	5.543
	38	Berlin	Berlin	AComA	anterior	0	8.400
	39	Berlin	Berlin	ICA	ICA	1	4.290
	40	Berlin	Berlin	PComA	posterior	1	13.786

For peer review only

BMJ Open: first published as 10.1136/bmjopen-2022-063051 on 8 November 2022. Downloaded from http://bmjopen.bmj.com/ on June 10, 2025 at Agence Bibliographique de l Enseignement Superieur (ABES) .
Protected by copyright, including for uses related to text and data mining, AI training, and similar technologies.

41	Berlin	Berlin	AComA	anterior	1	4.301
42	Berlin	Berlin	PComA	posterior	0	5.891
43	Berlin	Berlin	ICA	ICA	0	6.872
44	Berlin	Berlin	PICA	posterior	1	4.213
45A	Berlin	Berlin	ICA	ICA	0	2.414
45B	Berlin	Berlin	ICA	ICA	1	3.501
45C	Berlin	Berlin	ICA	ICA	0	2.297
46	Berlin	Berlin	BA	posterior	0	11.175
47	Berlin	Berlin	ICA	ICA	0	4.636
48	Berlin	Berlin	MCA	MCA	0	2.204
49	Berlin	Berlin	MCA	MCA	1	16.986
50	Berlin	Berlin	PComA	posterior	1	7.588
51	Berlin	Berlin	AComA	anterior	0	5.047
52	Berlin	Berlin	ACA	anterior	1	2.779
53	Berlin	Berlin	AChA	ICA	1	6.830
54	Berlin	Berlin	PComA	posterior	1	4.857
55	Berlin	Berlin	AComA	anterior	0	3.330
56	Berlin	Berlin	MCA	MCA	1	2.092
57A	Berlin	Berlin	ICA	ICA	0	2.831
57B	Berlin	Berlin	ICA	ICA	0	4.277
57C	Berlin	Berlin	ICA	ICA	0	4.910
57D	Berlin	Berlin	AComA	anterior	1	2.565
57E	Berlin	Berlin	MCA	MCA	0	6.612
57F	Berlin	Berlin	MCA	MCA	0	1.536
57G	Berlin	Berlin	MCA	MCA	0	3.139
58	Berlin	Berlin	PComA	posterior	1	3.998
59	Berlin	Berlin	ICA	ICA	0	4.875
60A	Berlin	Berlin	MCA	MCA	0	8.547
60B	Berlin	Berlin	MCA	MCA	0	3.172
61	Berlin	Berlin	AComA	anterior	1	10.866
62	Berlin	Berlin	ICA	ICA	1	4.541
63	Berlin	Berlin	AComA	anterior	1	5.524
64	Berlin	Berlin	ICA	ICA	1	13.839
65	Berlin	Berlin	ICA	ICA	0	7.768
66	Berlin	Berlin	AComA	anterior	1	3.652
67	Berlin	Berlin	MCA	MCA	1	4.031
68	Berlin	Berlin	AComA	anterior	1	2.672
69	Berlin	Berlin	ICA	ICA	0	11.746
70	Berlin	Berlin	AComA	anterior	1	2.739
71	Berlin	Berlin	PComA	posterior	0	3.684
72A	Berlin	Berlin	PComA	posterior	0	9.969
72B	Berlin	Berlin	AComA	anterior	0	3.769
73	Berlin	Berlin	AComA	anterior	1	7.640
74	Berlin	Berlin	ICA	ICA	0	2.422
75A	Berlin	Berlin	PComA	posterior	0	2.277
75B	Berlin	Berlin	BA	posterior	1	4.556
76	Berlin	Berlin	PComA	posterior	1	4.974
77	Berlin	Berlin	MCA	MCA	0	10.165
78	Berlin	Berlin	MCA	MCA	0	5.020
79	Berlin	Berlin	ICA	ICA	0	9.202

For peer review only

BMJ Open: first published as 10.1136/bmjopen-2022-063051 on 8 November 2022. Downloaded from http://bmjopen.bmj.com/ on June 10, 2025 at Agence Bibliographique de l Enseignement Superieur (ABES) . Protected by copyright, including for uses related to text and data mining, AI training, and similar technologies.

80	Berlin	Berlin	AComA	anterior	1	8.132
81	Berlin	Berlin	ICA	ICA	0	21.514
82A	Berlin	Berlin	ICA	ICA	0	2.039
82B	Berlin	Berlin	MCA	MCA	0	3.698
82C	Berlin	Berlin	ACA	anterior	0	1.486
83	Berlin	Berlin	PComA	posterior	0	10.503
84A	Berlin	Berlin	ICA	ICA	0	6.331
84B	Berlin	Berlin	MCA	MCA	0	3.509
85	Berlin	Berlin	MCA	MCA	0	2.996
86	Berlin	Berlin	MCA	MCA	0	2.575
87	Berlin	Berlin	AComA	anterior	1	3.971
88A	Berlin	Berlin	MCA	MCA	0	1.489
88B	Berlin	Berlin	MCA	MCA	0	2.304
89	Berlin	Berlin	ICA	ICA	0	5.728
90	Berlin	Berlin	MCA	MCA	0	4.016
91	Berlin	Berlin	AComA	anterior	0	6.147
92	Berlin	Berlin	PComA	posterior	0	7.023
93	Berlin	Berlin	PComA	posterior	1	10.373
94	Berlin	Berlin	MCA	MCA	0	19.183
95	Berlin	Berlin	AComA	anterior	1	6.261
96	Berlin	Berlin	ICA	ICA	0	5.202
97A	Berlin	Berlin	ICA	ICA	0	1.702
97B	Berlin	Berlin	AComA	anterior	0	5.381
98	Berlin	Berlin	PICA	posterior	1	4.524
99	Berlin	Berlin	PComA	posterior	0	6.067
100A	Berlin	Berlin	MCA	MCA	1	6.738
100B	Berlin	Berlin	ICA	ICA	0	2.364
100C	Berlin	Berlin	ICA	ICA	0	8.467
100D	Berlin	Berlin	MCA	MCA	0	2.488
100E	Berlin	Berlin	MCA	MCA	0	1.914
101	Berlin	Berlin	PComA	posterior	1	5.048
102	Berlin	Berlin	AComA	anterior	1	5.931
103	Berlin	Berlin	PCA	posterior	1	5.602
104	Berlin	Berlin	MCA	MCA	0	4.629
105	Berlin	Berlin	ICA	ICA	1	7.092
106	Berlin	Berlin	MCA	MCA	1	8.177
107	Berlin	Berlin	PComA	posterior	1	8.598
108	Berlin	Berlin	AComA	anterior	1	3.886
109	Berlin	Berlin	BA	posterior	1	13.918
110	Berlin	Berlin	BA	posterior	0	12.591
111	Berlin	Berlin	AComA	anterior	0	6.025
112	Berlin	Berlin	BA	posterior	1	7.000
113A	Berlin	Berlin	MCA	MCA	0	9.488
113B	Berlin	Berlin	MCA	MCA	0	6.242
114	Berlin	Berlin	MCA	MCA	1	3.622
115A	Hanover	Magdeburg	MCA	MCA	1	4.340
115B	Hanover	Magdeburg	MCA	MCA	0	1.149
116A	Hanover	Magdeburg	AComA	anterior	1	4.055
116B	Hanover	Magdeburg	AComA	anterior	0	1.031
117A	Hanover	Magdeburg	BA	posterior	1	8.476

BMJ Open: first published as 10.1136/bmjopen-2022-063051 on 8 November 2022. Downloaded from http://bmjopen.bmj.com/ on June 10, 2025 at Agence Bibliographique de l Enseignement Superieur (ABES) .
Protected by copyright, including for uses related to text and data mining, AI training, and similar technologies.

117B	Hanover	Magdeburg	AComA	anterior	0	4.088
118A	Hanover	Magdeburg	AComA	anterior	0	5.039
118B	Hanover	Magdeburg	PComA	posterior	1	4.528
119	Hanover	Magdeburg	MCA	MCA	1	1.132
120A	Hanover	Magdeburg	MCA	MCA	1	4.881
120B	Hanover	Magdeburg	ICA	ICA	1	2.325
121	Hanover	Magdeburg	ICA	ICA	1	18.704
122	Hanover	Magdeburg	ICA	ICA	0	6.667
123A	Hanover	Magdeburg	PComA	posterior	1	5.230
123B	Hanover	Magdeburg	MCA	MCA	0	2.984
124A	Hanover	Magdeburg	ACA	anterior	1	2.914
124B	Hanover	Magdeburg	AComA	anterior	0	1.201
124C	Hanover	Magdeburg	AComA	anterior	0	2.671
125	Hanover	Magdeburg	ICA	ICA	0	7.204
126A	Hanover	Magdeburg	MCA	MCA	1	8.466
126B	Hanover	Magdeburg	MCA	MCA	0	5.410
127A	Hanover	Magdeburg	AComA	anterior	1	2.663
127B	Hanover	Magdeburg	MCA	MCA	0	2.098
128A	Hanover	Magdeburg	ICA	ICA	1	1.429
128B	Hanover	Magdeburg	ICA	ICA	0	1.275
129A	Hanover	Magdeburg	BA	posterior	1	2.818
129B	Hanover	Magdeburg	SCA	posterior	0	1.293
130A	Hanover	Magdeburg	MCA	MCA	1	7.171
130B	Hanover	Magdeburg	AComA	anterior	0	4.247
131A	Hanover	Magdeburg	BA	posterior	0	4.863
131B	Hanover	Magdeburg	BA	posterior	1	3.992
132A	Hanover	Magdeburg	PComA	posterior	0	4.359
132B	Hanover	Magdeburg	AComA	anterior	1	16.578
133A	Hanover	Magdeburg	BA	posterior	1	6.042
133B	Hanover	Magdeburg	AComA	anterior	0	3.105
134A	Hanover	Magdeburg	MCA	MCA	1	6.298
134B	Hanover	Magdeburg	MCA	MCA	0	3.067
135	Hanover	Magdeburg	ICA	ICA	0	2.406
136A	Kiel	Magdeburg	MCA	MCA	0	1.108
136B	Kiel	Magdeburg	MCA	MCA	0	6.352
137	Kiel	Magdeburg	MCA	MCA	0	3.274
138	Kiel	Magdeburg	MCA	MCA	0	4.033
139	Kiel	Magdeburg	MCA	MCA	0	6.259
140	Kiel	Magdeburg	MCA	MCA	0	10.513
141	Kiel	Magdeburg	MCA	MCA	0	8.471
142	Kiel	Magdeburg	MCA	MCA	0	6.008
143	Kiel	Magdeburg	MCA	MCA	0	5.184
144	Kiel	Magdeburg	MCA	MCA	0	10.421
145	Kiel	Magdeburg	MCA	MCA	0	8.720
146A	Kiel	Magdeburg	MCA	MCA	0	6.242
146B	Kiel	Magdeburg	ACA	anterior	0	2.012
147A	Kiel	Magdeburg	MCA	MCA	0	5.580
147B	Kiel	Magdeburg	MCA	MCA	0	0.684
147C	Kiel	Magdeburg	MCA	MCA	0	0.573
147D	Kiel	Magdeburg	ACA	anterior	0	3.651

For peer review only

BMJ Open: first published as 10.1136/bmjopen-2022-063051 on 8 November 2022. Downloaded from http://bmjopen.bmj.com/ on June 10, 2025 at Agence Bibliographique de l Enseignement Superieur (ABES) .
Protected by copyright, including for uses related to text and data mining, AI training, and similar technologies.

147E	Kiel	Magdeburg	AComA	anterior	0	1.213
147F	Kiel	Magdeburg	AComA	anterior	0	1.384
148	Kiel	Magdeburg	MCA	MCA	0	4.650
149	Kiel	Magdeburg	MCA	MCA	0	6.489
150	Kiel	Magdeburg	MCA	MCA	0	4.962
151	Kiel	Magdeburg	MCA	MCA	0	3.962
152	Magdeburg	Magdeburg	MCA	MCA	0	5.866
153	Magdeburg	Magdeburg	ACA	anterior	1	3.594
154	Magdeburg	Magdeburg	PComA	posterior	1	9.941
155A	Magdeburg	Magdeburg	AComA	anterior	1	2.543
155B	Magdeburg	Magdeburg	AComA	anterior	0	3.589
155C	Magdeburg	Magdeburg	MCA	MCA	0	5.120
156A	Magdeburg	Magdeburg	ICA	ICA	0	7.048
156B	Magdeburg	Magdeburg	ICA	ICA	0	1.214
156C	Magdeburg	Magdeburg	ICA	ICA	0	1.765
156D	Magdeburg	Magdeburg	ICA	ICA	0	2.037
157	Magdeburg	Magdeburg	VA	posterior	1	5.194
158	Magdeburg	Magdeburg	AChA	ICA	0	3.248
159	Magdeburg	Magdeburg	MCA	MCA	0	5.645
160A	Magdeburg	Magdeburg	AChA	ICA	1	2.988
160B	Magdeburg	Magdeburg	ICA	ICA	0	2.842
161A	Magdeburg	Magdeburg	ICA	ICA	1	5.684
161B	Magdeburg	Magdeburg	ICA	ICA	0	2.089
161C	Magdeburg	Magdeburg	PICA	posterior	0	2.497
162	Magdeburg	Magdeburg	AChA	ICA	1	4.811
163	Magdeburg	Magdeburg	ICA	ICA	0	4.981
164	Magdeburg	Magdeburg	MCA	MCA	0	3.817
165A	Magdeburg	Magdeburg	MCA	MCA	0	3.419
165B	Magdeburg	Magdeburg	PComA	posterior	0	5.533
165C	Magdeburg	Magdeburg	BA	posterior	0	2.856
165D	Magdeburg	Magdeburg	SCA	posterior	1	4.595
166	Magdeburg	Magdeburg	ICA	ICA	0	3.638
167	Magdeburg	Magdeburg	ICA	ICA	0	3.481
168	Magdeburg	Magdeburg	ICA	ICA	0	6.061
169	Magdeburg	Magdeburg	ICA	ICA	0	7.142
170	Magdeburg	Magdeburg	ICA	ICA	0	5.557
171	Magdeburg	Magdeburg	ICA	ICA	0	11.276
172A	Magdeburg	Magdeburg	AComA	anterior	1	3.283
172B	Magdeburg	Magdeburg	MCA	MCA	0	2.319
173A	Magdeburg	Magdeburg	MCA	MCA	1	4.176
173B	Magdeburg	Magdeburg	ICA	ICA	0	3.188
174	Magdeburg	Magdeburg	ICA	ICA	0	3.711
175	Magdeburg	Magdeburg	MCA	MCA	0	4.156
176	Magdeburg	Magdeburg	AComA	anterior	0	3.397
177A	Magdeburg	Magdeburg	PComA	posterior	1	6.322
177B	Magdeburg	Magdeburg	BA	posterior	0	1.516
178	Magdeburg	Magdeburg	MCA	MCA	1	5.269

For peer review only

BMJ Open: first published as 10.1136/bmjopen-2022-063051 on 8 November 2022. Downloaded from http://bmjopen.bmj.com/ on June 10, 2025 at Agence Bibliographique de l Enseignement Superieur (ABES) .
Protected by copyright, including for uses related to text and data mining, AI training, and similar technologies.

maximum c	maximum h	maximum c	bulge heigh	surface area	convex hull	minimal bo	closed aneu	volume
L_max	H_max	D_max	H_b	A	A_CH	A_MBS	A_closed	V
mm	mm	mm	mm	cm^2	cm^2	cm^2	cm^2	ml
6.629	5.790	5.713	0.877	0.887	1.018	1.495	1.003	0.083
11.888	8.544	10.931	3.003	2.391	2.722	4.652	2.537	0.269
7.306	6.133	4.862	0.313	0.742	0.914	1.677	0.888	0.064
7.867	6.544	7.165	3.567	1.018	1.146	1.979	1.122	0.097
7.336	6.315	6.104	1.929	0.888	1.022	1.749	1.014	0.085
6.275	4.482	5.783	0.575	0.693	0.906	1.269	0.900	0.074
23.888	20.508	23.475	9.621	12.495	13.243	18.371	13.239	4.106
6.597	4.534	6.403	1.473	0.746	0.934	1.422	0.924	0.076
5.837	3.939	5.183	0.070	0.568	0.802	1.099	0.795	0.060
6.518	5.449	5.861	2.398	0.713	0.822	1.338	0.809	0.059
8.495	6.902	7.441	3.391	1.540	1.813	2.341	1.803	0.215
11.246	9.797	10.200	3.153	1.755	1.899	3.981	1.853	0.195
11.394	8.611	10.972	4.429	2.218	2.475	4.079	2.459	0.334
7.308	4.479	7.292	0.287	0.574	0.844	1.684	0.826	0.059
4.672	3.411	4.157	0.033	0.354	0.489	0.729	0.486	0.027
13.627	11.834	11.081	4.341	3.153	3.480	5.839	3.381	0.526
2.875	1.899	2.875	0.057	0.126	0.180	0.276	0.178	0.006
14.303	12.591	12.333	6.473	3.921	4.285	6.591	4.242	0.730
3.763	2.874	3.382	1.302	0.281	0.342	0.445	0.341	0.018
5.669	4.725	4.473	2.104	0.553	0.648	1.015	0.643	0.044
7.910	6.289	6.673	3.770	1.024	1.175	1.970	1.151	0.101
6.439	5.233	5.830	1.474	0.815	0.991	1.327	0.978	0.081
12.632	11.229	10.859	3.425	3.001	3.307	5.029	3.293	0.523
8.453	6.020	7.820	1.936	0.987	1.244	2.245	1.236	0.112
9.521	8.035	9.229	3.504	2.125	2.439	2.878	2.433	0.344
8.530	5.733	7.294	1.949	1.050	1.420	2.328	1.397	0.132
4.793	3.005	4.741	0.075	0.310	0.479	0.797	0.470	0.025
14.667	10.280	13.848	1.293	4.122	5.440	6.782	5.419	1.129
7.677	4.990	6.526	2.190	0.873	1.094	1.890	1.060	0.085
8.500	5.691	8.412	2.083	1.088	1.325	2.270	1.310	0.124
10.420	6.548	10.246	2.938	1.204	1.480	3.411	1.377	0.112
15.754	13.711	11.401	3.704	3.516	3.937	7.802	3.868	0.564
6.137	4.508	5.343	2.007	0.663	0.820	1.184	0.817	0.063
6.677	3.854	6.460	1.201	0.590	0.769	1.402	0.757	0.054
6.751	5.481	4.736	1.330	0.577	0.716	1.432	0.696	0.045
3.661	2.760	3.246	1.172	0.232	0.303	0.424	0.301	0.014
6.655	5.163	5.034	1.727	0.691	0.832	1.391	0.823	0.062
8.135	5.839	7.993	1.423	1.186	1.438	2.167	1.417	0.142
16.986	10.740	15.845	2.213	5.926	6.882	9.209	6.869	1.564
7.950	6.713	6.080	1.989	1.030	1.244	2.022	1.224	0.108
5.212	3.563	5.005	0.689	0.483	0.669	0.895	0.665	0.046
12.891	11.777	8.932	5.558	2.584	2.875	5.260	2.844	0.398
24.926	21.090	22.734	9.915	14.654	15.321	19.652	15.279	5.424
8.946	6.977	8.075	2.268	1.298	1.555	2.541	1.527	0.157
14.786	10.742	14.206	1.633	2.875	3.216	6.868	3.132	0.407
6.715	5.085	5.948	1.913	0.712	0.843	1.420	0.839	0.066
15.827	13.957	14.042	6.937	5.487	5.906	7.992	5.870	1.249

For peer review only

BMJ Open: first published as 10.1136/bmjopen-2022-063051 on 8 November 2022. Downloaded from http://bmjopen.bmj.com/ on June 10, 2025 at Agence Bibliographique de l Enseignement Superieur (ABES) .
Protected by copyright, including for uses related to text and data mining, AI training, and similar technologies.

6.419	4.551	6.134	0.624	0.618	0.839	1.316	0.813	0.058
8.062	6.217	6.768	2.455	1.126	1.368	2.042	1.365	0.137
17.188	10.658	16.238	2.250	3.236	4.445	9.425	4.430	0.696
7.303	4.996	6.301	1.470	0.688	0.925	1.676	0.910	0.072
4.605	2.692	4.603	0.037	0.296	0.466	0.713	0.462	0.023
4.605	3.619	3.564	1.963	0.355	0.438	0.677	0.430	0.023
4.653	2.599	4.537	0.354	0.303	0.480	0.698	0.475	0.025
13.326	11.629	11.342	5.799	3.546	3.816	5.596	3.800	0.658
7.105	4.947	6.019	0.113	0.678	0.891	1.586	0.882	0.061
4.777	2.888	4.516	0.482	0.282	0.439	0.727	0.433	0.023
18.334	17.219	14.463	8.226	5.638	6.064	10.560	5.978	1.232
11.513	9.974	11.050	4.580	2.241	2.481	4.240	2.396	0.285
6.880	5.489	6.061	2.068	0.829	0.999	1.492	0.993	0.086
4.149	2.840	3.778	0.926	0.297	0.384	0.541	0.382	0.021
11.234	7.779	10.623	2.600	2.129	2.279	3.965	2.254	0.282
6.535	5.085	5.126	0.262	0.507	0.706	1.400	0.685	0.041
6.195	3.881	6.006	0.616	0.577	0.840	1.210	0.829	0.061
4.282	2.759	3.841	0.151	0.216	0.331	0.590	0.325	0.013
5.968	3.703	5.938	1.423	0.517	0.678	1.119	0.668	0.043
4.773	4.310	4.200	2.368	0.467	0.513	0.771	0.506	0.031
9.479	6.686	9.469	2.116	1.305	1.446	2.823	1.429	0.139
4.362	2.739	4.165	0.197	0.326	0.447	0.600	0.445	0.025
7.928	6.831	6.578	2.903	1.256	1.465	2.026	1.456	0.154
2.798	1.593	2.792	0.014	0.105	0.170	0.266	0.167	0.005
6.330	3.703	6.047	0.954	0.580	0.806	1.259	0.803	0.058
7.668	6.509	6.943	1.249	0.852	1.054	1.873	0.999	0.070
8.038	5.767	7.357	1.708	0.972	1.152	2.030	1.143	0.103
13.384	9.880	12.864	3.835	3.174	3.751	5.854	3.690	0.603
4.583	3.361	4.077	0.084	0.364	0.502	0.704	0.498	0.030
13.573	12.129	7.940	6.398	2.411	2.619	5.788	2.564	0.328
6.253	4.782	5.560	2.596	0.679	0.785	1.232	0.782	0.060
6.774	5.738	4.776	1.687	0.752	0.882	1.467	0.876	0.070
19.580	14.862	19.183	7.524	7.554	7.889	12.044	7.851	1.917
10.702	7.977	8.927	2.139	2.019	2.495	3.606	2.481	0.325
6.698	4.629	5.540	0.489	0.576	0.764	1.410	0.757	0.055
6.354	4.692	5.177	1.312	0.626	0.795	1.289	0.776	0.053
6.204	3.207	6.016	0.114	0.413	0.706	1.215	0.694	0.044
14.376	13.009	10.934	6.325	2.638	2.994	6.492	2.830	0.343
6.016	4.460	5.142	0.926	0.678	0.873	1.149	0.866	0.071
5.832	3.890	5.511	0.286	0.536	0.691	1.071	0.684	0.046
14.708	12.119	12.964	4.615	3.419	3.829	6.796	3.791	0.609
5.100	3.825	4.479	0.525	0.452	0.611	0.840	0.603	0.038
10.529	8.923	7.517	2.011	1.266	1.421	3.483	1.355	0.113
6.886	3.607	6.764	0.185	0.510	0.851	1.490	0.837	0.060
4.974	3.155	4.670	0.739	0.312	0.487	0.792	0.479	0.026
6.182	5.235	3.884	2.072	0.422	0.503	1.203	0.487	0.025
8.405	5.927	8.296	2.748	1.255	1.408	2.270	1.385	0.133
15.254	10.492	15.251	1.120	3.825	4.559	7.665	4.507	0.804
7.735	5.096	7.199	1.289	0.956	1.265	1.925	1.236	0.115
11.062	9.776	9.388	5.048	2.352	2.598	3.900	2.577	0.353

BMJ Open: first published as 10.1136/bmjopen-2022-063051 on 8 November 2022. Downloaded from http://bmjopen.bmj.com/ on June 10, 2025 at Agence Bibliographique de l Enseignement Superieur (ABES) .
Protected by copyright, including for uses related to text and data mining, AI training, and similar technologies.

9.022	8.308	5.532	5.605	1.258	1.403	2.566	1.369	0.125
32.342	25.628	30.344	9.085	21.842	22.485	32.901	22.541	9.061
3.400	2.107	3.340	0.103	0.171	0.249	0.382	0.247	0.010
5.047	4.006	3.660	0.257	0.368	0.480	0.802	0.479	0.028
3.134	1.819	3.062	0.002	0.128	0.204	0.325	0.203	0.007
13.558	11.007	11.469	5.880	3.372	4.048	5.907	3.950	0.645
8.282	6.772	7.749	2.957	1.357	1.578	2.227	1.567	0.170
5.390	3.909	3.582	0.036	0.363	0.503	0.917	0.497	0.029
5.401	3.552	5.038	1.301	0.435	0.613	0.917	0.611	0.042
3.966	2.604	3.799	0.123	0.269	0.369	0.506	0.368	0.019
5.633	4.386	4.464	0.942	0.531	0.621	1.001	0.614	0.039
3.149	1.664	3.147	0.170	0.102	0.155	0.311	0.153	0.005
3.784	2.577	3.258	0.475	0.191	0.258	0.454	0.256	0.011
7.951	6.459	5.903	0.045	0.885	1.210	2.142	1.167	0.093
6.817	4.506	6.387	1.055	0.691	0.886	1.462	0.880	0.067
7.784	6.322	6.895	2.712	1.231	1.415	1.903	1.412	0.152
12.441	7.739	12.162	1.572	2.313	2.941	4.898	2.904	0.402
16.422	12.513	15.861	2.894	4.492	4.998	8.482	4.966	0.797
27.009	21.425	25.069	8.693	14.959	16.042	22.918	16.010	5.763
8.947	7.350	6.990	2.234	1.135	1.351	2.515	1.341	0.128
13.291	8.491	13.104	0.615	2.474	3.251	5.883	3.166	0.379
5.671	2.993	5.671	0.100	0.283	0.495	1.011	0.489	0.019
8.214	5.554	7.968	1.932	1.237	1.574	2.124	1.572	0.170
5.584	4.790	4.319	2.528	0.481	0.539	0.980	0.527	0.031
9.725	6.554	9.274	1.314	1.459	1.953	2.971	1.944	0.238
16.284	12.471	15.055	0.726	3.620	4.000	8.331	3.963	0.645
3.707	2.472	3.379	0.531	0.221	0.311	0.445	0.309	0.014
16.159	11.384	16.159	4.627	3.858	4.256	8.203	4.029	0.506
4.053	2.688	3.620	0.707	0.258	0.349	0.516	0.347	0.016
3.744	1.985	3.743	0.076	0.186	0.285	0.442	0.282	0.011
6.956	5.626	4.803	1.591	0.669	0.821	1.525	0.808	0.058
7.936	6.362	7.128	3.081	1.178	1.318	2.163	1.302	0.120
9.195	6.126	7.318	1.738	1.708	1.836	2.661	1.858	0.209
17.009	8.810	16.189	0.942	2.437	3.849	9.088	3.752	0.562
9.263	7.602	7.208	3.536	1.222	1.383	2.696	1.338	0.114
10.514	8.759	7.409	3.082	1.494	1.771	3.482	1.712	0.151
10.231	8.838	7.094	2.851	1.488	1.803	3.372	1.739	0.166
6.100	4.339	5.591	0.679	0.516	0.732	1.220	0.722	0.048
17.012	13.949	16.935	6.552	6.058	6.416	9.100	6.386	1.433
18.621	14.380	14.373	6.548	4.829	5.408	10.893	5.328	0.999
9.774	6.785	8.878	1.968	1.741	2.204	3.001	2.190	0.285
10.375	7.553	9.325	3.307	1.779	2.280	3.443	2.262	0.286
11.542	9.849	7.908	4.661	2.103	2.433	4.190	2.390	0.308
8.757	6.907	8.753	2.415	1.552	1.848	2.420	1.841	0.224
6.793	4.234	6.753	0.367	0.597	0.920	1.502	0.910	0.068
6.195	5.019	5.753	2.072	0.634	0.738	1.213	0.721	0.049
2.123	1.222	2.050	0.099	0.062	0.091	0.144	0.089	0.002
7.276	4.568	7.267	1.827	0.795	0.957	1.663	0.935	0.073
2.744	1.425	2.563	0.133	0.078	0.128	0.237	0.123	0.003
10.853	8.721	9.956	2.319	2.269	2.569	3.723	2.547	0.342

For peer review only

BMJ Open: first published as 10.1136/bmjopen-2022-063051 on 8 November 2022. Downloaded from http://bmjopen.bmj.com/ on June 10, 2025 at Agence Bibliographique de l Enseignement Superieur (ABES) . Protected by copyright, including for uses related to text and data mining, AI training, and similar technologies.

6.386	4.271	6.267	1.450	0.622	0.798	1.282	0.779	0.052
7.385	6.025	5.712	3.287	0.847	0.981	1.714	0.961	0.077
6.224	4.693	5.826	1.532	0.584	0.710	1.218	0.686	0.040
2.739	1.458	2.699	0.000	0.079	0.137	0.248	0.129	0.003
6.758	5.613	6.202	3.057	0.747	0.850	1.552	0.826	0.060
8.335	5.295	8.154	0.578	0.472	0.673	2.182	0.626	0.032
24.223	19.791	22.453	9.808	12.666	13.149	18.524	13.126	4.170
9.429	7.753	9.246	3.668	1.763	2.018	2.881	1.991	0.233
7.279	5.501	6.496	1.296	0.962	1.180	1.701	1.156	0.093
4.951	3.068	4.238	0.721	0.311	0.403	0.770	0.396	0.018
3.677	3.075	2.630	1.197	0.197	0.240	0.431	0.230	0.008
3.184	1.674	2.913	0.185	0.096	0.166	0.322	0.159	0.004
4.432	3.209	4.075	1.200	0.283	0.349	0.626	0.346	0.016
8.784	7.818	6.956	3.946	1.370	1.477	2.435	1.460	0.148
13.905	9.021	13.148	0.801	2.857	3.336	6.331	3.136	0.362
7.117	5.697	7.117	1.111	0.959	1.100	1.716	1.067	0.083
4.398	3.418	3.652	1.122	0.260	0.319	0.609	0.314	0.014
4.263	2.616	3.714	0.022	0.236	0.323	0.576	0.316	0.014
3.378	1.853	3.377	0.224	0.119	0.210	0.389	0.196	0.005
5.130	2.891	4.336	0.308	0.177	0.292	0.827	0.275	0.008
5.027	3.392	4.348	1.368	0.315	0.392	0.795	0.385	0.019
2.603	1.519	2.548	0.128	0.096	0.144	0.214	0.138	0.004
8.733	7.733	5.173	2.236	1.000	1.104	2.399	1.082	0.087
6.282	4.788	4.997	1.219	0.529	0.634	1.242	0.623	0.038
6.960	6.297	6.263	3.045	0.617	0.691	1.556	0.649	0.035
6.109	4.679	5.536	1.914	0.602	0.685	1.173	0.680	0.047
8.258	5.056	7.901	0.962	0.957	1.190	2.143	1.166	0.099
21.893	19.479	15.008	5.305	5.825	6.171	15.090	6.046	1.094
7.690	6.527	5.130	2.092	0.820	0.984	1.861	0.906	0.058
4.236	3.327	2.935	1.359	0.267	0.320	0.564	0.310	0.014
7.909	6.999	6.604	1.846	1.191	1.329	1.991	1.306	0.123
5.815	3.677	4.000	0.846	0.324	0.434	1.062	0.406	0.019
7.097	4.213	6.014	0.103	0.332	0.541	1.582	0.515	0.023
2.628	1.504	2.617	0.126	0.075	0.129	0.227	0.120	0.003
6.801	6.385	4.171	3.307	0.723	0.806	1.476	0.797	0.058
5.605	3.754	5.144	1.846	0.487	0.608	0.987	0.597	0.037
6.085	4.188	5.097	1.013	0.566	0.707	1.164	0.693	0.046
10.066	6.868	9.700	2.978	1.972	2.370	3.227	2.338	0.291
11.565	10.869	9.066	5.115	2.694	2.806	4.206	2.801	0.417
10.003	8.861	9.695	3.555	2.151	2.310	3.143	2.295	0.306
6.948	6.210	4.669	2.279	0.766	0.840	1.517	0.825	0.061
8.098	6.481	7.268	3.584	1.033	1.168	2.064	1.144	0.093
15.923	12.736	11.639	3.653	3.319	3.922	7.966	3.711	0.511
9.220	8.728	6.525	5.970	1.325	1.489	2.729	1.424	0.127
8.947	7.049	8.891	2.469	1.606	1.828	2.595	1.814	0.208
3.410	2.529	3.319	1.196	0.188	0.222	0.369	0.217	0.008
6.977	5.759	5.449	1.556	0.777	0.934	1.530	0.903	0.066
1.627	0.900	1.540	0.310	0.031	0.050	0.090	0.047	0.001
1.571	0.846	1.511	0.124	0.026	0.044	0.080	0.041	0.001
4.670	3.829	3.715	0.862	0.374	0.442	0.707	0.433	0.023

BMJ Open: first published as 10.1136/bmjopen-2022-063051 on 8 November 2022. Downloaded from http://bmjopen.bmj.com/ on June 10, 2025 at Agence Bibliographique de l Enseignement Superieur (ABES) .
Protected by copyright, including for uses related to text and data mining, AI training, and similar technologies.

2.495	1.472	2.180	0.087	0.072	0.103	0.196	0.100	0.002
2.449	1.457	2.325	0.046	0.086	0.131	0.194	0.125	0.003
9.599	6.040	9.240	1.954	1.225	1.478	2.895	1.465	0.128
7.998	6.644	5.913	3.660	1.019	1.183	2.072	1.148	0.100
7.328	5.848	5.773	2.070	0.814	0.905	1.687	0.887	0.066
6.486	5.072	6.312	0.846	0.639	0.755	1.334	0.750	0.052
7.722	6.054	7.580	2.357	1.147	1.296	1.910	1.270	0.117
4.784	3.869	4.102	1.291	0.329	0.390	0.719	0.383	0.019
15.603	11.496	14.341	7.003	4.024	4.638	7.675	4.569	0.809
5.647	3.274	5.306	0.026	0.355	0.466	1.003	0.451	0.021
4.724	3.696	4.160	1.815	0.429	0.518	0.707	0.510	0.030
6.943	5.844	5.841	1.209	0.657	0.807	1.560	0.764	0.049
11.331	8.473	9.336	2.050	1.711	1.957	4.035	1.938	0.218
3.405	1.788	3.124	0.171	0.121	0.195	0.369	0.189	0.005
3.375	1.970	3.356	0.117	0.146	0.221	0.377	0.215	0.007
2.674	2.099	2.427	0.125	0.119	0.164	0.251	0.160	0.005
6.651	5.678	4.727	3.075	0.642	0.716	1.397	0.705	0.049
4.557	3.452	4.551	1.438	0.388	0.466	0.672	0.457	0.025
6.241	5.711	6.021	2.024	0.837	0.928	1.273	0.922	0.073
4.200	3.054	3.431	0.180	0.273	0.358	0.574	0.350	0.016
4.277	3.071	4.011	1.379	0.341	0.433	0.576	0.427	0.023
7.789	6.371	6.026	2.151	0.819	0.987	1.906	0.932	0.060
2.779	2.123	2.323	0.573	0.137	0.172	0.243	0.171	0.006
3.590	2.777	3.414	1.580	0.240	0.286	0.408	0.278	0.012
6.957	6.079	6.471	2.907	0.713	0.780	1.524	0.750	0.048
5.784	5.145	4.269	1.733	0.498	0.560	1.051	0.547	0.030
5.795	4.770	4.652	1.961	0.401	0.530	1.068	0.476	0.021
5.333	3.786	4.835	0.986	0.424	0.507	0.893	0.498	0.028
7.607	6.500	4.457	3.691	0.723	0.793	1.818	0.773	0.053
4.095	3.019	3.578	1.043	0.276	0.374	0.556	0.364	0.017
5.900	5.509	4.218	3.215	0.545	0.570	1.098	0.557	0.031
5.574	3.949	5.005	1.532	0.505	0.630	0.977	0.624	0.041
5.053	3.735	4.455	1.533	0.398	0.461	0.803	0.454	0.025
9.075	6.193	9.068	2.564	1.532	1.753	2.802	1.731	0.191
7.748	7.232	7.453	3.980	1.306	1.395	1.963	1.378	0.139
7.203	5.799	5.440	1.852	0.826	0.957	1.631	0.925	0.070
15.720	12.308	14.026	4.352	4.479	5.063	7.782	5.036	0.977
5.186	4.052	3.267	1.796	0.280	0.347	0.845	0.322	0.012
5.388	2.932	4.739	0.773	0.335	0.421	0.912	0.407	0.018
6.487	5.148	5.922	1.965	0.654	0.765	1.340	0.742	0.050
5.446	3.837	5.297	1.539	0.461	0.549	0.932	0.537	0.031
4.406	3.846	4.243	1.228	0.391	0.445	0.653	0.440	0.025
5.714	4.684	5.562	1.815	0.544	0.612	1.026	0.588	0.034
5.047	4.191	3.070	1.619	0.276	0.311	0.801	0.289	0.012
7.755	6.941	4.725	4.013	0.823	0.909	1.891	0.893	0.066
2.901	1.778	2.668	0.019	0.107	0.158	0.278	0.150	0.004
6.661	5.753	4.657	1.227	0.646	0.769	1.394	0.738	0.048

For peer review only

BMJ Open: first published as 10.1136/bmjopen-2022-063051 on 8 November 2022. Downloaded from http://bmjopen.bmj.com/ on June 10, 2025 at Agence Bibliographique de l Enseignement Superieur (ABES) .
Protected by copyright, including for uses related to text and data mining, AI training, and similar technologies.

convex hull	minimal bo	minimum n	maximum r	neck perim	equivalent	neck area	elliptical ne	aspect ratic
V_CH	V_MBS	D_neck,mir	D_neck,ma	P_neck	D_neck,equ	A_neck	A_neck,elli	AR
ml	ml	mm	mm	mm	mm	cm^2	cm^2	-
0.091	0.172	2.903	3.885	13.086	3.537	0.116	0.089	1.479
0.372	0.943	2.992	5.434	17.029	3.417	0.145	0.128	1.520
0.071	0.204	3.276	4.862	14.831	3.926	0.146	0.125	1.239
0.105	0.262	2.412	3.903	13.317	3.147	0.105	0.074	1.460
0.087	0.217	2.835	4.497	15.471	3.260	0.126	0.100	1.260
0.076	0.134	4.243	5.252	19.040	4.336	0.206	0.175	0.543
4.299	7.404	7.102	11.374	37.990	7.833	0.744	0.634	1.721
0.080	0.160	2.937	5.732	18.940	3.767	0.178	0.132	0.733
0.062	0.108	3.700	5.163	19.585	4.624	0.226	0.150	0.735
0.062	0.145	3.135	3.555	11.360	3.390	0.096	0.088	1.421
0.219	0.337	4.061	6.687	22.302	4.713	0.263	0.213	1.015
0.211	0.747	2.896	4.022	12.395	3.169	0.098	0.091	1.892
0.343	0.775	4.591	6.207	19.420	4.961	0.241	0.224	1.314
0.064	0.205	3.911	6.350	21.036	4.791	0.252	0.195	0.400
0.028	0.058	3.525	4.157	13.267	3.968	0.132	0.115	0.769
0.567	1.327	4.216	6.408	19.835	4.605	0.228	0.212	1.496
0.006	0.014	1.920	2.875	8.841	2.356	0.052	0.043	0.654
0.765	1.591	5.778	6.676	22.660	5.667	0.321	0.303	1.837
0.018	0.028	2.370	2.886	9.061	2.653	0.060	0.054	0.967
0.045	0.096	2.781	3.684	11.481	3.120	0.090	0.080	1.230
0.110	0.260	3.374	4.360	13.771	3.700	0.127	0.116	1.284
0.085	0.144	4.129	4.939	15.345	4.263	0.164	0.160	1.048
0.535	1.061	5.283	6.859	21.247	5.494	0.292	0.285	1.541
0.116	0.316	4.399	6.782	20.002	4.982	0.249	0.234	0.732
0.349	0.459	5.692	6.345	21.843	5.642	0.308	0.284	1.246
0.144	0.334	5.051	7.400	24.248	5.730	0.347	0.294	0.621
0.027	0.067	3.554	4.752	15.381	4.143	0.159	0.133	0.612
1.148	1.661	6.103	13.945	53.525	9.693	1.297	0.668	0.608
0.096	0.244	3.241	5.421	18.057	4.145	0.187	0.138	0.776
0.131	0.322	4.742	5.937	19.016	4.669	0.222	0.221	0.774
0.140	0.592	3.148	5.233	16.748	4.119	0.172	0.129	1.047
0.640	2.049	6.067	6.812	24.497	5.741	0.352	0.325	1.876
0.065	0.121	3.929	4.537	15.469	3.986	0.154	0.140	0.899
0.057	0.156	2.964	5.044	16.782	3.982	0.167	0.117	0.622
0.049	0.161	2.859	4.073	13.567	3.522	0.119	0.091	1.249
0.015	0.026	2.338	3.094	9.103	3.028	0.069	0.057	0.878
0.065	0.154	3.388	4.395	14.337	3.683	0.132	0.117	1.134
0.150	0.300	4.221	5.874	20.243	4.553	0.230	0.195	0.773
1.618	2.628	7.460	14.252	45.129	8.355	0.943	0.835	0.665
0.118	0.270	3.389	5.919	16.909	4.575	0.193	0.158	1.049
0.048	0.080	4.100	4.888	16.858	4.339	0.183	0.157	0.692
0.413	1.134	4.955	5.832	21.532	4.829	0.260	0.227	2.005
5.489	8.192	4.856	13.272	38.744	6.453	0.625	0.506	1.563
0.166	0.381	4.146	5.861	19.226	4.767	0.229	0.191	0.946
0.471	1.692	4.251	6.311	19.493	5.268	0.257	0.211	1.331
0.068	0.159	3.330	4.548	14.206	3.568	0.127	0.119	0.943
1.284	2.125	5.828	7.791	26.972	5.678	0.383	0.357	1.769

For peer review only

BMJ Open: first published as 10.1136/bmjopen-2022-063051 on 8 November 2022. Downloaded from http://bmjopen.bmj.com/ on June 10, 2025 at Agence Bibliographique de l Enseignement Superieur (ABES) .
Protected by copyright, including for uses related to text and data mining, AI training, and similar technologies.

0.065	0.142	2.869	6.280	18.787	4.153	0.195	0.141	0.685
0.140	0.274	5.099	5.722	19.742	4.850	0.239	0.229	1.030
0.723	2.721	9.411	15.328	45.262	10.554	1.194	1.133	0.448
0.076	0.204	3.921	5.390	19.347	4.578	0.221	0.166	0.782
0.025	0.057	4.072	4.605	15.924	4.153	0.165	0.147	0.524
0.025	0.052	2.544	3.498	10.509	2.840	0.075	0.070	1.001
0.027	0.055	3.973	4.537	15.822	4.355	0.172	0.142	0.506
0.671	1.245	5.067	6.060	20.235	5.028	0.254	0.241	1.844
0.067	0.188	4.039	6.019	18.197	4.473	0.203	0.191	0.770
0.024	0.058	3.349	4.139	15.221	3.971	0.151	0.109	0.532
1.284	3.227	3.904	8.491	26.453	5.140	0.340	0.260	2.001
0.334	0.821	3.698	5.097	15.808	3.937	0.156	0.148	1.489
0.088	0.171	3.652	5.028	14.943	4.393	0.164	0.144	1.004
0.021	0.037	2.695	3.182	10.976	3.122	0.086	0.067	0.874
0.296	0.742	3.682	4.035	12.878	3.887	0.125	0.117	1.693
0.047	0.156	3.958	5.126	15.600	4.569	0.178	0.159	0.948
0.065	0.125	3.926	6.009	20.114	5.003	0.252	0.185	0.554
0.015	0.043	3.044	3.841	13.047	3.343	0.109	0.092	0.545
0.048	0.111	3.747	4.646	14.887	4.055	0.151	0.137	0.609
0.032	0.064	1.743	2.212	6.685	2.312	0.039	0.030	1.934
0.146	0.446	3.494	4.013	13.901	3.573	0.124	0.110	1.223
0.026	0.044	3.340	4.165	13.007	3.667	0.119	0.109	0.616
0.158	0.271	3.373	5.696	18.626	4.310	0.201	0.151	1.161
0.006	0.013	2.149	2.798	9.586	2.605	0.062	0.047	0.549
0.059	0.133	4.544	5.666	18.559	4.809	0.223	0.202	0.554
0.088	0.241	3.240	5.327	15.348	3.834	0.147	0.136	0.751
0.106	0.272	3.982	5.445	15.999	4.286	0.171	0.170	0.895
0.635	1.332	5.655	8.968	30.914	6.682	0.516	0.398	0.953
0.031	0.056	3.242	4.090	14.393	3.732	0.134	0.104	0.775
0.352	1.309	4.023	4.674	15.332	4.004	0.153	0.148	2.325
0.062	0.129	3.028	3.756	12.271	3.335	0.102	0.089	1.209
0.072	0.167	3.273	4.162	13.626	3.661	0.125	0.107	1.327
1.971	3.931	5.400	6.936	23.221	5.117	0.297	0.294	1.995
0.349	0.644	6.668	7.542	25.103	7.353	0.461	0.395	1.030
0.057	0.157	2.954	5.757	18.913	3.839	0.182	0.134	0.634
0.060	0.138	3.374	4.303	14.245	4.211	0.150	0.114	0.937
0.048	0.126	4.114	6.204	23.009	4.885	0.281	0.200	0.431
0.410	1.556	4.088	5.305	16.784	4.591	0.193	0.170	2.214
0.073	0.116	2.687	5.335	20.340	3.712	0.189	0.113	0.513
0.049	0.104	2.559	5.530	16.327	3.620	0.148	0.111	0.666
0.647	1.666	5.581	7.501	23.891	6.226	0.372	0.329	1.329
0.041	0.072	3.421	4.484	14.463	4.178	0.151	0.120	0.841
0.133	0.611	2.123	4.861	12.221	2.913	0.089	0.081	1.572
0.064	0.171	4.645	6.823	21.514	6.082	0.327	0.249	0.355
0.029	0.066	3.453	4.611	16.463	4.059	0.167	0.125	0.494
0.028	0.124	2.466	2.877	9.725	2.697	0.066	0.056	1.584
0.144	0.322	2.931	4.907	13.849	3.745	0.130	0.113	1.014
0.831	1.995	3.693	15.254	44.240	6.164	0.682	0.442	0.666
0.123	0.251	3.660	5.911	21.822	5.129	0.280	0.170	0.849
0.370	0.724	4.471	5.481	18.185	4.966	0.226	0.193	1.679

BMJ Open: first published as 10.1136/bmjopen-2022-063051 on 8 November 2022. Downloaded from http://bmjopen.bmj.com/ on June 10, 2025 at Agence Bibliographique de l Enseignement Superieur (ABES) . Protected by copyright, including for uses related to text and data mining, AI training, and similar technologies.

0.138	0.387	3.088	3.831	12.450	3.565	0.111	0.093	2.122
9.561	17.746	2.961	18.027	50.338	5.556	0.699	0.419	1.193
0.010	0.022	2.536	3.340	10.417	2.938	0.077	0.067	0.611
0.028	0.068	2.961	3.628	12.388	3.587	0.111	0.084	1.019
0.007	0.017	2.669	3.062	9.724	3.065	0.075	0.064	0.485
0.709	1.350	6.233	9.921	32.559	7.095	0.578	0.486	1.059
0.177	0.312	3.682	5.598	18.267	4.597	0.210	0.162	1.131
0.030	0.083	3.109	3.713	13.372	4.008	0.134	0.091	0.945
0.043	0.083	2.949	4.596	16.118	4.349	0.175	0.106	0.652
0.019	0.034	3.058	3.824	11.763	3.366	0.099	0.092	0.673
0.041	0.094	2.402	3.999	11.654	2.840	0.083	0.075	0.993
0.005	0.016	1.871	3.149	9.064	2.252	0.051	0.046	0.473
0.011	0.029	2.480	2.749	9.781	2.680	0.066	0.054	0.838
0.105	0.295	5.164	6.092	19.890	5.675	0.282	0.247	0.940
0.071	0.166	3.647	5.591	18.794	4.024	0.189	0.160	0.718
0.154	0.247	3.845	5.198	17.087	4.221	0.180	0.157	1.182
0.433	1.019	7.600	9.255	32.052	7.377	0.591	0.552	0.759
0.946	2.323	5.854	9.288	29.079	6.525	0.474	0.427	1.117
5.822	10.316	10.249	12.646	43.430	9.687	1.052	1.018	1.517
0.133	0.375	4.577	4.981	16.951	4.848	0.205	0.179	1.257
0.457	1.342	6.603	9.821	38.845	7.126	0.692	0.509	0.530
0.021	0.096	4.180	5.671	18.176	4.536	0.206	0.186	0.300
0.173	0.291	5.563	7.294	22.990	5.826	0.335	0.319	0.738
0.033	0.091	1.425	2.956	8.692	2.091	0.045	0.033	1.531
0.242	0.482	6.692	7.545	27.655	7.023	0.486	0.397	0.804
0.673	2.261	4.714	7.341	25.595	5.352	0.342	0.272	0.918
0.014	0.028	3.033	3.304	11.382	3.083	0.088	0.079	0.715
0.705	2.209	3.936	5.479	16.917	4.038	0.171	0.169	1.545
0.017	0.035	2.888	3.555	11.320	3.126	0.088	0.081	0.700
0.012	0.028	2.723	3.744	12.259	3.122	0.096	0.080	0.511
0.062	0.177	3.927	4.189	14.081	3.967	0.140	0.129	1.205
0.129	0.299	3.261	4.724	14.375	3.444	0.124	0.121	1.255
0.223	0.408	1.690	6.942	22.424	2.675	0.150	0.092	0.807
0.604	2.576	9.516	16.051	57.167	9.204	1.315	1.200	0.288
0.133	0.416	3.427	4.118	13.379	3.487	0.117	0.111	1.722
0.190	0.611	4.209	5.875	18.330	4.775	0.219	0.194	1.392
0.200	0.582	4.580	5.781	20.002	5.026	0.251	0.208	1.487
0.052	0.127	4.276	4.986	17.482	4.697	0.205	0.167	0.779
1.463	2.581	5.536	7.179	23.516	5.577	0.328	0.312	1.939
1.064	3.380	4.917	12.472	34.457	5.794	0.499	0.482	1.010
0.294	0.489	4.505	8.378	31.391	5.719	0.449	0.296	0.719
0.301	0.601	6.063	8.092	28.011	6.899	0.483	0.385	0.865
0.323	0.806	3.486	7.314	23.602	4.859	0.287	0.200	1.297
0.227	0.354	3.933	6.501	22.813	5.068	0.289	0.201	0.960
0.072	0.173	4.796	6.793	21.520	5.804	0.312	0.256	0.533
0.054	0.126	2.981	3.763	11.219	3.091	0.087	0.088	1.153
0.002	0.005	1.667	2.050	6.305	1.717	0.027	0.027	0.561
0.080	0.202	3.798	4.688	14.879	3.770	0.140	0.140	0.865
0.003	0.011	2.058	2.646	8.188	2.184	0.045	0.043	0.390
0.364	0.676	4.880	7.274	20.777	5.344	0.278	0.279	1.165

For peer review only

BMJ Open: first published as 10.1136/bmjopen-2022-063051 on 8 November 2022. Downloaded from http://bmjopen.bmj.com/ on June 10, 2025 at Agence Bibliographique de l Enseignement Superieur (ABES) . Protected by copyright, including for uses related to text and data mining, AI training, and similar technologies.

0.059	0.136	3.633	5.216	16.163	3.879	0.157	0.149	0.784
0.083	0.211	3.466	3.933	13.148	3.467	0.114	0.107	1.281
0.049	0.126	3.027	4.428	12.646	3.207	0.101	0.105	1.023
0.004	0.012	2.254	2.739	9.026	2.224	0.050	0.048	0.413
0.066	0.182	2.509	4.164	11.013	2.871	0.079	0.082	1.172
0.040	0.303	3.046	6.031	16.366	3.781	0.155	0.144	0.385
4.307	7.497	4.943	11.565	29.411	6.256	0.460	0.449	1.617
0.251	0.460	3.312	6.808	19.810	4.592	0.227	0.177	0.979
0.109	0.209	4.469	5.198	17.058	4.553	0.194	0.182	1.006
0.020	0.064	2.612	4.202	11.337	3.013	0.085	0.086	0.710
0.010	0.027	1.673	2.354	6.665	1.998	0.033	0.031	1.238
0.005	0.017	2.558	3.184	9.667	2.606	0.063	0.064	0.377
0.017	0.047	2.537	3.163	9.173	2.730	0.063	0.063	0.845
0.156	0.357	3.105	3.630	11.718	3.059	0.090	0.089	1.984
0.496	1.498	3.688	7.971	23.076	4.837	0.279	0.231	1.062
0.097	0.211	3.514	3.858	12.669	3.425	0.108	0.106	1.402
0.015	0.045	2.234	2.843	9.386	2.324	0.055	0.050	0.937
0.015	0.041	3.000	3.715	10.778	2.970	0.080	0.088	0.565
0.007	0.023	2.662	3.378	11.376	2.694	0.077	0.071	0.423
0.010	0.071	2.885	4.088	12.580	3.113	0.098	0.093	0.312
0.020	0.067	2.674	3.641	10.202	2.743	0.070	0.076	0.774
0.005	0.009	1.941	2.438	8.082	2.096	0.042	0.037	0.530
0.094	0.349	2.932	3.509	10.841	3.047	0.083	0.081	2.044
0.042	0.130	2.598	4.490	11.942	3.133	0.094	0.092	0.946
0.044	0.182	1.604	2.311	6.687	1.877	0.031	0.029	2.104
0.049	0.119	2.818	3.448	10.414	2.988	0.078	0.076	1.158
0.112	0.295	4.647	5.228	18.128	4.607	0.209	0.191	0.834
1.181	5.512	3.626	7.662	19.509	4.543	0.222	0.218	2.164
0.078	0.239	2.966	3.629	11.960	2.882	0.086	0.085	1.665
0.016	0.040	2.054	2.604	8.405	2.090	0.044	0.042	1.193
0.133	0.264	3.526	4.008	13.454	3.419	0.115	0.111	1.572
0.023	0.103	2.488	4.181	11.759	2.758	0.081	0.082	0.733
0.028	0.187	3.376	6.094	16.842	4.360	0.184	0.162	0.395
0.003	0.010	2.058	2.628	8.482	2.109	0.045	0.042	0.422
0.060	0.169	2.876	3.210	9.865	3.022	0.075	0.072	1.979
0.041	0.092	2.534	4.791	13.958	3.151	0.110	0.095	0.683
0.051	0.118	3.367	4.437	14.181	3.586	0.127	0.117	0.909
0.323	0.545	4.747	9.608	24.939	5.860	0.365	0.358	0.651
0.424	0.811	2.828	4.463	12.938	3.306	0.107	0.099	2.356
0.315	0.524	3.432	4.980	14.519	3.980	0.144	0.134	1.701
0.066	0.176	2.482	3.060	9.082	2.609	0.059	0.060	1.963
0.108	0.279	2.829	4.298	13.230	3.376	0.112	0.095	1.206
0.639	2.114	4.957	9.395	25.968	6.032	0.392	0.366	1.109
0.148	0.424	3.121	3.948	11.926	3.295	0.098	0.097	2.209
0.221	0.393	3.803	6.053	18.164	4.583	0.208	0.181	1.031
0.009	0.021	1.782	2.158	6.541	1.799	0.029	0.030	0.933
0.077	0.178	3.345	4.520	13.440	3.752	0.126	0.119	1.234
0.001	0.003	1.249	1.627	4.931	1.263	0.016	0.016	0.420
0.001	0.002	1.171	1.571	5.218	1.191	0.016	0.014	0.365
0.025	0.056	2.550	2.828	9.049	2.602	0.059	0.057	1.291

For peer review only

BMJ Open: first published as 10.1136/bmjopen-2022-063051 on 8 November 2022. Downloaded from http://bmjopen.bmj.com/ on June 10, 2025 at Agence Bibliographique de l Enseignement Superieur (ABES) .
Protected by copyright, including for uses related to text and data mining, AI training, and similar technologies.

0.003	0.008	1.614	2.232	6.529	1.706	0.028	0.028	0.544
0.004	0.008	2.024	2.328	7.829	1.956	0.038	0.037	0.595
0.152	0.463	3.752	6.083	20.202	4.746	0.240	0.179	0.764
0.110	0.280	3.307	5.198	14.592	3.553	0.130	0.135	1.248
0.074	0.206	2.337	3.921	10.721	2.726	0.073	0.072	1.265
0.054	0.145	3.253	4.288	12.309	3.606	0.111	0.110	0.924
0.130	0.248	3.443	4.427	13.709	3.601	0.123	0.120	1.325
0.020	0.057	2.337	2.977	8.842	2.448	0.054	0.055	1.207
0.875	1.999	5.504	11.272	31.139	6.996	0.545	0.487	0.882
0.025	0.094	2.229	5.284	13.469	2.867	0.097	0.093	0.481
0.033	0.056	2.807	3.647	10.997	2.972	0.082	0.080	0.984
0.058	0.183	3.309	4.297	13.094	3.291	0.108	0.112	1.192
0.230	0.762	4.694	6.020	17.946	5.054	0.227	0.222	1.171
0.006	0.021	2.550	3.222	9.787	2.806	0.069	0.065	0.377
0.008	0.022	2.539	3.357	10.019	2.758	0.069	0.067	0.526
0.006	0.012	1.792	2.444	7.653	2.150	0.041	0.034	0.834
0.051	0.155	2.582	3.108	9.392	2.699	0.063	0.063	1.671
0.027	0.052	2.791	3.230	9.826	2.820	0.069	0.071	1.005
0.078	0.135	3.086	3.614	10.669	3.209	0.086	0.088	1.562
0.018	0.041	2.968	3.431	10.338	2.993	0.077	0.080	0.871
0.025	0.041	2.996	3.439	10.693	3.209	0.086	0.081	0.826
0.080	0.247	3.390	4.303	13.330	3.390	0.113	0.115	1.321
0.006	0.011	1.980	2.183	6.667	2.038	0.034	0.034	0.957
0.013	0.024	1.860	2.600	7.731	1.939	0.037	0.038	0.960
0.057	0.177	1.771	2.520	7.349	2.020	0.037	0.035	1.909
0.034	0.101	2.142	2.834	8.480	2.306	0.049	0.048	1.758
0.030	0.104	2.525	3.927	10.784	2.783	0.075	0.078	0.972
0.031	0.079	2.552	3.426	10.614	2.776	0.074	0.069	0.998
0.058	0.230	2.391	2.810	8.625	2.316	0.050	0.053	1.969
0.019	0.039	3.067	3.601	11.501	3.064	0.088	0.087	0.793
0.036	0.108	0.981	1.591	4.414	1.106	0.012	0.012	2.888
0.043	0.091	3.448	4.293	13.109	3.606	0.118	0.116	0.848
0.027	0.068	2.188	3.205	9.355	2.372	0.055	0.055	1.086
0.204	0.441	4.669	5.375	16.745	4.748	0.199	0.197	1.128
0.145	0.259	2.815	3.184	10.027	2.889	0.072	0.070	2.243
0.079	0.196	3.412	3.903	11.686	3.419	0.100	0.105	1.424
1.014	2.041	6.801	10.575	28.975	7.694	0.557	0.565	1.066
0.016	0.073	1.988	2.577	7.813	2.160	0.042	0.040	1.274
0.022	0.082	2.507	3.337	10.511	2.750	0.072	0.066	0.695
0.056	0.146	3.141	3.432	11.178	3.152	0.088	0.085	1.217
0.034	0.085	2.409	3.774	10.852	2.821	0.077	0.071	0.845
0.026	0.050	2.316	2.781	8.572	2.264	0.049	0.051	1.334
0.040	0.098	2.113	2.553	7.909	2.222	0.044	0.042	1.627
0.014	0.067	1.016	1.949	4.922	1.111	0.014	0.016	1.743
0.071	0.245	2.801	3.116	10.051	2.771	0.070	0.069	2.029
0.005	0.014	1.964	2.682	8.337	2.070	0.043	0.041	0.565
0.056	0.155	3.187	3.553	11.772	3.139	0.092	0.089	1.483

For peer review only

BMJ Open: first published as 10.1136/bmjopen-2022-063051 on 8 November 2022. Downloaded from http://bmjopen.bmj.com/ on June 10, 2025 at Agence Bibliographique de l Enseignement Superieur (ABES) . Protected by copyright, including for uses related to text and data mining, AI training, and similar technologies.

aspect ratic	bottleneck	bulge locat	nonspericit	aneurysm v	aneurysm s	undulation	ellipticity ir	mean of m
eAR	BF	BL	NSI	AVSV	AASA	UI	EI	MAA
-	-	-	-	-	-	-	-	mm^-1
1.625	1.471	0.153	0.270	0.485	0.671	0.079	0.240	0.318
2.417	2.012	0.364	0.370	0.285	0.545	0.277	0.271	0.254
1.534	1.000	0.052	0.311	0.311	0.529	0.101	0.282	0.322
1.811	1.836	0.626	0.278	0.370	0.567	0.077	0.255	0.302
1.739	1.358	0.340	0.270	0.390	0.580	0.023	0.264	0.325
0.657	1.101	0.202	0.249	0.549	0.709	0.034	0.237	0.322
2.499	2.064	0.491	0.257	0.555	0.721	0.045	0.234	0.090
1.115	1.117	0.351	0.254	0.478	0.650	0.043	0.240	0.324
0.821	1.004	0.019	0.258	0.555	0.723	0.037	0.247	0.308
1.490	1.649	0.475	0.279	0.407	0.605	0.046	0.267	0.354
1.441	1.113	0.499	0.236	0.639	0.770	0.018	0.231	0.239
2.401	2.536	0.414	0.304	0.261	0.465	0.077	0.284	0.259
1.644	1.768	0.543	0.249	0.431	0.603	0.027	0.240	0.216
0.531	1.148	0.113	0.299	0.285	0.491	0.079	0.275	0.356
0.805	1.000	0.010	0.291	0.460	0.667	0.039	0.276	0.401
2.082	1.729	0.453	0.261	0.396	0.579	0.073	0.245	0.185
0.798	1.000	0.031	0.289	0.441	0.647	0.037	0.277	0.666
2.164	1.847	0.528	0.267	0.459	0.644	0.047	0.251	0.163
1.052	1.172	0.466	0.239	0.628	0.766	0.017	0.233	0.524
1.452	1.214	0.464	0.260	0.454	0.633	0.029	0.251	0.389
1.513	1.531	0.674	0.275	0.390	0.584	0.074	0.252	0.292
1.214	1.180	0.285	0.266	0.562	0.737	0.054	0.248	0.315
1.924	1.583	0.324	0.243	0.494	0.655	0.022	0.235	0.179
0.997	1.153	0.390	0.278	0.354	0.550	0.034	0.266	0.283
1.402	1.454	0.443	0.226	0.748	0.845	0.016	0.220	0.200
0.802	0.986	0.424	0.286	0.396	0.600	0.079	0.259	0.239
0.701	0.998	0.026	0.297	0.377	0.589	0.080	0.272	0.357
0.874	0.993	0.153	0.232	0.680	0.799	0.016	0.226	0.132
1.016	1.204	0.520	0.299	0.349	0.561	0.112	0.264	0.321
0.985	1.417	0.453	0.271	0.385	0.577	0.053	0.253	0.303
1.330	1.958	0.536	0.354	0.188	0.404	0.204	0.300	0.317
2.226	1.674	0.290	0.322	0.275	0.496	0.119	0.276	0.176
1.023	1.178	0.492	0.254	0.522	0.690	0.024	0.245	0.337
0.787	1.281	0.383	0.279	0.344	0.540	0.066	0.257	0.354
1.444	1.163	0.261	0.307	0.277	0.486	0.099	0.278	0.371
0.897	1.049	0.432	0.258	0.539	0.709	0.039	0.243	0.499
1.353	1.145	0.347	0.266	0.404	0.591	0.042	0.253	0.325
0.998	1.361	0.313	0.263	0.473	0.654	0.055	0.246	0.271
1.134	1.112	0.234	0.247	0.595	0.746	0.033	0.231	0.128
1.358	1.027	0.320	0.288	0.400	0.605	0.087	0.256	0.284
0.780	1.024	0.204	0.259	0.578	0.743	0.032	0.248	0.335
2.421	1.532	0.475	0.270	0.351	0.541	0.036	0.259	0.193
3.215	1.713	0.478	0.224	0.662	0.777	0.012	0.220	0.088
1.163	1.378	0.409	0.268	0.413	0.601	0.055	0.254	0.274
1.594	2.251	0.194	0.327	0.241	0.456	0.136	0.277	0.212
1.202	1.308	0.446	0.255	0.413	0.591	0.032	0.242	0.336
2.428	1.802	0.503	0.242	0.588	0.734	0.027	0.232	0.135

For peer review only

BMJ Open: first published as 10.1136/bmjopen-2022-063051 on 8 November 2022. Downloaded from http://bmjopen.bmj.com/ on June 10, 2025 at Agence Bibliographique de l Enseignement Superieur (ABES) .
Protected by copyright, including for uses related to text and data mining, AI training, and similar technologies.

1.036	0.977	0.145	0.297	0.405	0.618	0.109	0.264	0.331
1.215	1.183	0.417	0.254	0.499	0.669	0.022	0.244	0.258
0.651	1.059	0.327	0.319	0.256	0.470	0.037	0.304	0.154
0.920	1.169	0.349	0.271	0.352	0.543	0.052	0.257	0.345
0.581	1.000	0.015	0.318	0.415	0.647	0.050	0.301	0.368
1.233	1.019	0.561	0.280	0.437	0.635	0.069	0.258	0.435
0.527	1.000	0.154	0.309	0.456	0.680	0.067	0.284	0.343
2.223	1.872	0.519	0.236	0.528	0.679	0.019	0.229	0.169
1.037	1.000	0.024	0.329	0.323	0.556	0.099	0.287	0.313
0.555	1.091	0.219	0.279	0.399	0.596	0.047	0.265	0.413
3.305	1.703	0.484	0.262	0.382	0.566	0.041	0.252	0.142
1.927	2.168	0.604	0.306	0.347	0.565	0.145	0.256	0.232
1.149	1.205	0.410	0.246	0.503	0.666	0.026	0.237	0.314
0.890	1.187	0.333	0.238	0.559	0.706	0.019	0.231	0.494
1.757	2.633	0.381	0.268	0.380	0.569	0.049	0.251	0.223
1.063	1.000	0.054	0.332	0.264	0.489	0.126	0.292	0.373
0.666	0.999	0.185	0.282	0.488	0.685	0.059	0.262	0.302
0.626	1.000	0.072	0.336	0.313	0.550	0.102	0.301	0.437
0.698	1.278	0.503	0.299	0.383	0.597	0.104	0.257	0.391
1.850	1.899	0.554	0.259	0.479	0.656	0.059	0.239	0.432
1.374	2.359	0.431	0.279	0.312	0.506	0.047	0.264	0.285
0.700	1.000	0.077	0.267	0.568	0.742	0.027	0.255	0.443
1.534	1.155	0.439	0.242	0.569	0.719	0.027	0.233	0.261
0.590	0.998	0.009	0.309	0.405	0.630	0.084	0.281	0.578
0.653	1.067	0.304	0.284	0.437	0.638	0.025	0.274	0.355
1.043	1.303	0.312	0.347	0.290	0.533	0.202	0.281	0.330
1.137	1.351	0.350	0.262	0.379	0.563	0.031	0.253	0.321
1.279	1.434	0.449	0.258	0.453	0.630	0.051	0.244	0.176
0.850	0.997	0.026	0.264	0.531	0.708	0.044	0.248	0.397
2.714	1.699	0.589	0.288	0.251	0.443	0.067	0.270	0.220
1.361	1.480	0.572	0.244	0.470	0.635	0.018	0.238	0.367
1.509	1.147	0.305	0.255	0.420	0.597	0.025	0.247	0.326
2.705	2.766	0.544	0.245	0.488	0.652	0.027	0.235	0.119
1.056	1.184	0.275	0.268	0.505	0.688	0.068	0.237	0.167
0.951	0.962	0.134	0.271	0.346	0.537	0.041	0.258	0.334
0.957	1.203	0.325	0.298	0.388	0.602	0.103	0.263	0.331
0.547	0.970	0.043	0.307	0.353	0.572	0.072	0.283	0.258
2.558	2.061	0.539	0.335	0.221	0.436	0.163	0.293	0.213
0.738	0.964	0.338	0.238	0.616	0.754	0.029	0.228	0.320
1.018	0.996	0.078	0.276	0.444	0.639	0.063	0.252	0.293
1.601	1.728	0.463	0.272	0.366	0.558	0.059	0.250	0.157
0.902	0.999	0.139	0.280	0.526	0.718	0.069	0.254	0.354
2.623	1.546	0.263	0.339	0.185	0.389	0.152	0.296	0.310
0.398	0.991	0.076	0.300	0.349	0.562	0.070	0.277	0.298
0.561	1.013	0.325	0.291	0.396	0.605	0.081	0.264	0.374
1.690	1.350	0.455	0.324	0.203	0.405	0.088	0.304	0.462
1.328	1.691	0.552	0.279	0.413	0.610	0.078	0.251	0.273
1.649	1.000	0.110	0.263	0.403	0.588	0.033	0.255	0.148
0.979	1.218	0.257	0.267	0.457	0.642	0.070	0.248	0.296
1.853	1.713	0.549	0.256	0.488	0.661	0.045	0.239	0.181

For peer review only

BMJ Open: first published as 10.1136/bmjopen-2022-063051 on 8 November 2022. Downloaded from http://bmjopen.bmj.com/ on June 10, 2025 at Agence Bibliographique de l Enseignement Superieur (ABES) .
Protected by copyright, including for uses related to text and data mining, AI training, and similar technologies.

2.281	1.444	0.689	0.298	0.324	0.534	0.091	0.270	0.297
3.872	1.683	0.422	0.260	0.511	0.685	0.052	0.231	0.073
0.694	1.000	0.050	0.295	0.436	0.647	0.057	0.271	0.532
1.031	1.009	0.069	0.257	0.417	0.597	0.009	0.255	0.456
0.485	1.000	0.001	0.301	0.407	0.623	0.018	0.296	0.593
1.480	1.156	0.560	0.275	0.478	0.669	0.091	0.246	0.152
1.377	1.384	0.467	0.247	0.545	0.704	0.039	0.232	0.241
0.875	0.965	0.010	0.278	0.346	0.542	0.053	0.260	0.393
0.689	1.096	0.434	0.238	0.511	0.666	0.017	0.232	0.406
0.765	0.994	0.048	0.262	0.556	0.727	0.021	0.253	0.494
1.398	1.116	0.237	0.278	0.416	0.613	0.051	0.261	0.401
0.661	0.999	0.114	0.313	0.276	0.490	0.059	0.295	0.631
0.860	1.185	0.206	0.270	0.375	0.565	0.042	0.255	0.565
1.009	0.969	0.008	0.325	0.315	0.545	0.115	0.294	0.283
0.998	1.142	0.263	0.277	0.406	0.602	0.047	0.259	0.353
1.456	1.326	0.441	0.227	0.614	0.742	0.012	0.222	0.274
0.952	1.314	0.224	0.280	0.395	0.593	0.070	0.253	0.198
1.590	1.708	0.279	0.336	0.343	0.586	0.158	0.260	0.163
1.980	1.982	0.453	0.229	0.559	0.699	0.010	0.226	0.088
1.291	1.403	0.357	0.271	0.343	0.533	0.037	0.258	0.286
0.730	1.334	0.118	0.365	0.283	0.538	0.170	0.299	0.230
0.375	1.000	0.059	0.449	0.195	0.484	0.115	0.409	0.320
0.924	1.092	0.359	0.251	0.584	0.740	0.016	0.244	0.268
2.164	1.461	0.559	0.277	0.342	0.538	0.060	0.263	0.453
0.864	1.229	0.217	0.241	0.495	0.654	0.016	0.236	0.243
1.259	2.051	0.108	0.277	0.285	0.476	0.041	0.263	0.182
0.767	1.023	0.225	0.293	0.487	0.695	0.054	0.271	0.483
2.097	2.949	0.546	0.395	0.229	0.491	0.282	0.285	0.215
0.796	1.018	0.284	0.285	0.471	0.672	0.044	0.267	0.482
0.613	1.000	0.040	0.335	0.390	0.637	0.134	0.277	0.535
1.273	1.147	0.315	0.288	0.328	0.530	0.064	0.268	0.354
1.722	1.509	0.519	0.283	0.401	0.602	0.072	0.256	0.303
2.094	1.054	0.310	0.272	0.512	0.698	0.064	0.230	0.254
0.503	1.009	0.204	0.303	0.218	0.413	0.069	0.288	0.174
2.034	1.750	0.499	0.327	0.273	0.496	0.148	0.275	0.304
1.712	1.261	0.377	0.364	0.247	0.492	0.205	0.283	0.281
1.711	1.227	0.332	0.334	0.285	0.516	0.172	0.271	0.255
0.827	1.121	0.175	0.298	0.379	0.592	0.071	0.272	0.346
2.496	2.359	0.471	0.236	0.555	0.702	0.021	0.229	0.137
2.173	1.152	0.520	0.280	0.296	0.489	0.061	0.260	0.138
1.053	1.060	0.327	0.241	0.584	0.730	0.029	0.230	0.197
1.015	1.152	0.472	0.264	0.475	0.657	0.052	0.243	0.184
1.953	1.081	0.491	0.267	0.382	0.570	0.046	0.258	0.206
1.232	1.346	0.387	0.231	0.633	0.761	0.013	0.227	0.245
0.624	0.994	0.101	0.300	0.390	0.606	0.056	0.281	0.278
1.404	1.529	0.477	0.289	0.388	0.594	0.095	0.258	0.401
0.669	1.000	0.086	0.317	0.389	0.619	0.083	0.295	0.974
1.076	1.550	0.450	0.282	0.363	0.562	0.090	0.253	0.328
0.472	0.969	0.129	0.365	0.268	0.520	0.154	0.315	0.791
1.586	1.369	0.274	0.262	0.507	0.684	0.060	0.238	0.198

For peer review only

BMJ Open: first published as 10.1136/bmjopen-2022-063051 on 8 November 2022. Downloaded from http://bmjopen.bmj.com/ on June 10, 2025 at Agence Bibliographique de l Enseignement Superieur (ABES) .
Protected by copyright, including for uses related to text and data mining, AI training, and similar technologies.

1.054	1.201	0.355	0.310	0.384	0.608	0.117	0.267	0.349
1.453	1.452	0.652	0.279	0.363	0.561	0.078	0.254	0.339
1.412	1.316	0.338	0.345	0.316	0.563	0.180	0.278	0.418
0.509	0.985	0.000	0.415	0.237	0.520	0.241	0.341	0.717
1.700	1.489	0.626	0.290	0.329	0.532	0.091	0.265	0.359
0.615	1.352	0.249	0.387	0.104	0.287	0.215	0.329	0.418
2.990	1.941	0.524	0.242	0.556	0.709	0.032	0.227	0.092
1.452	1.358	0.550	0.269	0.507	0.691	0.070	0.243	0.237
1.149	1.250	0.248	0.317	0.447	0.680	0.142	0.259	0.296
0.990	1.009	0.242	0.339	0.281	0.514	0.113	0.296	0.459
1.459	1.117	0.411	0.319	0.310	0.533	0.146	0.276	0.646
0.461	0.915	0.154	0.420	0.217	0.495	0.213	0.349	0.588
0.979	1.289	0.449	0.293	0.344	0.552	0.055	0.274	0.566
2.355	1.916	0.548	0.264	0.415	0.599	0.051	0.247	0.269
1.750	1.650	0.095	0.378	0.242	0.495	0.270	0.279	0.226
1.580	1.845	0.205	0.313	0.394	0.622	0.141	0.263	0.347
1.146	1.285	0.421	0.284	0.318	0.516	0.080	0.254	0.594
0.706	1.000	0.010	0.303	0.334	0.548	0.075	0.282	0.538
0.530	1.000	0.157	0.402	0.233	0.503	0.195	0.355	0.507
0.410	1.061	0.241	0.443	0.113	0.333	0.239	0.370	0.537
1.027	1.194	0.485	0.299	0.280	0.485	0.078	0.273	0.501
0.617	1.045	0.099	0.340	0.394	0.647	0.200	0.262	0.841
2.354	1.474	0.312	0.305	0.248	0.451	0.079	0.280	0.315
1.355	1.113	0.287	0.305	0.291	0.501	0.098	0.269	0.398
2.590	2.710	0.626	0.371	0.190	0.417	0.218	0.305	0.462
1.336	1.605	0.479	0.265	0.392	0.579	0.050	0.246	0.397
0.946	1.511	0.221	0.295	0.336	0.544	0.118	0.249	0.289
3.649	1.959	0.320	0.326	0.199	0.401	0.074	0.305	0.151
2.097	1.414	0.346	0.366	0.243	0.487	0.261	0.285	0.355
1.486	1.127	0.438	0.271	0.360	0.551	0.091	0.247	0.546
1.842	1.648	0.293	0.274	0.465	0.656	0.076	0.247	0.279
1.112	0.957	0.276	0.323	0.186	0.382	0.159	0.290	0.471
0.552	0.987	0.043	0.396	0.123	0.326	0.180	0.344	0.392
0.526	0.996	0.113	0.357	0.279	0.527	0.180	0.317	0.764
2.102	1.299	0.521	0.280	0.343	0.540	0.042	0.268	0.364
1.039	1.074	0.564	0.284	0.403	0.605	0.100	0.246	0.419
1.125	1.149	0.251	0.288	0.390	0.595	0.102	0.251	0.378
1.068	1.010	0.476	0.279	0.533	0.725	0.101	0.237	0.207
3.180	2.032	0.487	0.236	0.514	0.666	0.017	0.229	0.207
2.128	1.947	0.420	0.240	0.584	0.730	0.029	0.230	0.211
2.303	1.525	0.379	0.275	0.350	0.544	0.072	0.252	0.354
1.536	1.691	0.692	0.313	0.333	0.554	0.138	0.256	0.331
1.728	1.239	0.351	0.339	0.242	0.466	0.201	0.274	0.189
2.647	1.653	0.685	0.319	0.299	0.522	0.142	0.279	0.284
1.362	1.469	0.396	0.257	0.529	0.699	0.059	0.233	0.244
1.119	1.538	0.595	0.288	0.384	0.589	0.086	0.261	0.685
1.487	1.206	0.279	0.306	0.371	0.590	0.138	0.259	0.331
0.542	0.946	0.453	0.346	0.283	0.523	0.186	0.289	1.245
0.481	0.962	0.216	0.379	0.260	0.520	0.222	0.310	1.290
1.403	1.314	0.236	0.291	0.404	0.612	0.096	0.258	0.498

For peer review only

BMJ Open: first published as 10.1136/bmjopen-2022-063051 on 8 November 2022. Downloaded from http://bmjopen.bmj.com/ on June 10, 2025 at Agence Bibliographique de l Enseignement Superieur (ABES) .
Protected by copyright, including for uses related to text and data mining, AI training, and similar technologies.

0.711	0.977	0.072	0.350	0.270	0.510	0.175	0.286	0.960
0.708	0.998	0.033	0.322	0.406	0.642	0.142	0.283	0.778
0.980	1.519	0.420	0.333	0.277	0.506	0.154	0.261	0.273
1.826	1.137	0.564	0.281	0.356	0.554	0.090	0.257	0.286
1.820	1.472	0.417	0.290	0.323	0.526	0.097	0.255	0.339
1.099	1.472	0.213	0.286	0.359	0.562	0.041	0.272	0.360
1.629	1.712	0.402	0.277	0.472	0.665	0.101	0.240	0.288
1.468	1.378	0.359	0.288	0.330	0.533	0.071	0.266	0.513
1.421	1.272	0.704	0.270	0.405	0.595	0.075	0.243	0.158
0.887	1.004	0.010	0.354	0.222	0.450	0.172	0.290	0.503
1.207	1.141	0.506	0.268	0.543	0.721	0.073	0.241	0.427
1.556	1.359	0.236	0.324	0.270	0.490	0.155	0.284	0.360
1.395	1.551	0.291	0.282	0.286	0.480	0.051	0.264	0.222
0.432	0.970	0.141	0.391	0.247	0.513	0.180	0.323	0.548
0.640	1.000	0.066	0.355	0.317	0.572	0.129	0.310	0.553
0.948	0.993	0.061	0.298	0.422	0.637	0.094	0.267	0.685
1.924	1.521	0.592	0.274	0.314	0.505	0.048	0.261	0.385
1.151	1.409	0.443	0.276	0.489	0.680	0.078	0.251	0.443
1.759	1.666	0.358	0.272	0.542	0.725	0.062	0.245	0.330
0.999	1.000	0.060	0.308	0.387	0.610	0.109	0.270	0.463
0.886	1.166	0.485	0.265	0.569	0.741	0.067	0.240	0.439
1.677	1.400	0.378	0.369	0.242	0.489	0.251	0.278	0.358
1.025	1.064	0.274	0.260	0.532	0.704	0.026	0.252	0.717
1.287	1.313	0.633	0.284	0.481	0.681	0.112	0.248	0.603
2.382	2.568	0.604	0.321	0.273	0.492	0.156	0.268	0.404
2.160	1.506	0.348	0.320	0.298	0.521	0.102	0.286	0.439
1.372	1.184	0.514	0.395	0.198	0.446	0.325	0.294	0.524
1.231	1.411	0.288	0.294	0.349	0.557	0.099	0.256	0.453
2.389	1.586	0.667	0.295	0.232	0.425	0.075	0.276	0.374
0.932	0.994	0.365	0.305	0.434	0.655	0.102	0.272	0.483
4.155	2.651	0.700	0.325	0.284	0.507	0.137	0.272	0.473
1.009	1.166	0.421	0.266	0.454	0.639	0.044	0.252	0.377
1.468	1.390	0.440	0.274	0.372	0.565	0.063	0.254	0.475
1.277	1.687	0.423	0.265	0.432	0.618	0.063	0.242	0.231
2.472	2.341	0.557	0.254	0.537	0.702	0.046	0.239	0.274
1.625	1.394	0.333	0.295	0.358	0.568	0.111	0.263	0.329
1.466	1.326	0.386	0.250	0.478	0.647	0.037	0.235	0.142
1.520	1.268	0.547	0.363	0.169	0.381	0.221	0.303	0.600
0.843	1.420	0.333	0.352	0.220	0.447	0.171	0.290	0.536
1.325	1.726	0.471	0.302	0.340	0.554	0.113	0.265	0.381
1.130	1.404	0.483	0.289	0.371	0.576	0.088	0.261	0.405
1.639	1.526	0.331	0.261	0.497	0.674	0.048	0.244	0.474
1.870	2.178	0.437	0.320	0.344	0.573	0.168	0.262	0.442
3.059	1.575	0.476	0.309	0.176	0.361	0.142	0.289	0.651
2.282	1.516	0.635	0.300	0.269	0.472	0.077	0.275	0.360
0.732	0.995	0.012	0.324	0.313	0.541	0.148	0.286	0.680
1.679	1.311	0.233	0.310	0.313	0.530	0.136	0.269	0.383

For peer review only

BMJ Open: first published as 10.1136/bmjopen-2022-063051 on 8 November 2022. Downloaded from http://bmjopen.bmj.com/ on June 10, 2025 at Agence Bibliographique de l Enseignement Superieur (ABES) .
Protected by copyright, including for uses related to text and data mining, AI training, and similar technologies.

mean of m	standard d	high mean c	L2-norm of	mean of Ga	mean of m	standard d	high Gaussia	L2-norm of
absMAA	MSD	HMC	MLN	GAA	absGAA	GSD	HGC	GLN
mm^-1	mm^-1	%	-	mm^-2	mm^-2	mm^-2	%	-
0.370	0.303	27.483	0.329	0.069	0.227	0.376	170.270	2.699
0.328	0.307	99.650	0.491	0.034	0.179	0.308	561.209	5.898
0.382	0.330	39.608	0.316	0.048	0.220	0.383	193.206	2.283
0.343	0.255	35.989	0.317	0.050	0.192	0.287	202.369	2.361
0.337	0.247	25.724	0.306	0.081	0.152	0.244	111.783	1.818
0.348	0.234	10.601	0.264	0.090	0.155	0.217	56.300	1.293
0.140	0.155	68.740	0.506	0.006	0.030	0.072	337.335	7.205
0.379	0.315	27.518	0.311	0.080	0.199	0.306	125.715	1.876
0.325	0.237	-4.035	0.233	0.076	0.159	0.256	38.871	1.205
0.376	0.331	22.618	0.325	0.092	0.203	0.412	115.984	2.393
0.248	0.178	7.167	0.294	0.047	0.083	0.136	54.474	1.768
0.294	0.242	65.689	0.374	0.041	0.130	0.235	310.560	3.334
0.232	0.170	32.321	0.326	0.042	0.071	0.102	131.248	1.942
0.380	0.249	39.230	0.262	0.102	0.203	0.260	172.089	1.276
0.404	0.211	-2.756	0.215	0.132	0.193	0.229	12.202	0.746
0.215	0.197	46.687	0.382	0.024	0.082	0.158	281.687	4.003
0.671	0.414	-0.486	0.222	0.361	0.563	0.758	23.583	0.845
0.199	0.192	44.389	0.398	0.020	0.063	0.127	232.352	4.009
0.543	0.286	2.134	0.252	0.241	0.363	0.400	28.454	1.043
0.399	0.190	13.360	0.256	0.120	0.191	0.207	54.113	1.056
0.307	0.212	21.546	0.290	0.053	0.152	0.204	138.982	1.721
0.340	0.239	10.459	0.284	0.081	0.165	0.226	74.818	1.560
0.203	0.158	28.289	0.329	0.028	0.056	0.096	122.201	2.377
0.315	0.227	33.131	0.287	0.073	0.131	0.186	133.613	1.570
0.216	0.119	3.469	0.271	0.036	0.056	0.064	27.970	1.247
0.271	0.231	16.426	0.271	0.038	0.130	0.217	140.469	1.842
0.382	0.264	-3.851	0.197	0.096	0.246	0.282	55.765	0.735
0.140	0.088	2.641	0.257	0.016	0.025	0.033	36.799	1.203
0.387	0.372	50.037	0.365	0.077	0.284	0.468	327.761	3.296
0.333	0.246	41.619	0.324	0.085	0.154	0.209	177.817	1.951
0.354	0.270	84.214	0.364	0.055	0.217	0.303	487.876	2.950
0.237	0.244	86.955	0.450	0.019	0.087	0.200	441.938	5.629
0.371	0.235	13.847	0.266	0.100	0.161	0.201	51.703	1.185
0.439	0.399	46.462	0.326	0.087	0.306	0.492	240.832	2.349
0.407	0.281	37.388	0.281	0.076	0.231	0.343	163.135	1.613
0.570	0.384	4.723	0.241	0.184	0.475	0.580	60.221	1.122
0.362	0.272	20.362	0.280	0.081	0.167	0.275	85.294	1.573
0.308	0.246	27.931	0.317	0.060	0.144	0.226	147.719	2.208
0.164	0.148	40.176	0.378	0.015	0.033	0.059	142.546	2.862
0.343	0.312	37.421	0.341	0.048	0.213	0.351	242.425	2.908
0.387	0.269	3.259	0.237	0.098	0.204	0.253	45.488	1.042
0.226	0.209	46.111	0.364	0.027	0.073	0.137	206.103	2.868
0.096	0.068	19.469	0.339	0.007	0.012	0.020	92.486	2.471
0.289	0.212	30.106	0.314	0.061	0.121	0.182	145.513	1.983
0.281	0.269	107.395	0.461	0.030	0.133	0.249	629.400	5.743
0.393	0.319	32.247	0.311	0.093	0.194	0.294	119.328	1.750
0.165	0.153	31.289	0.381	0.015	0.037	0.066	136.383	2.960

For peer review only

BMJ Open: first published as 10.1136/bmjopen-2022-063051 on 8 November 2022. Downloaded from http://bmjopen.bmj.com/ on June 10, 2025 at Agence Bibliographique de l Enseignement Superieur (ABES) .
Protected by copyright, including for uses related to text and data mining, AI training, and similar technologies.

0.350	0.247	13.398	0.258	0.070	0.203	0.269	112.222	1.370
0.287	0.208	15.684	0.280	0.052	0.102	0.226	66.441	2.078
0.182	0.175	57.716	0.334	0.022	0.042	0.081	218.754	2.151
0.356	0.234	30.075	0.275	0.096	0.198	0.247	164.159	1.450
0.388	0.259	-7.566	0.195	0.122	0.195	0.277	10.566	0.715
0.460	0.300	6.766	0.251	0.122	0.315	0.390	69.545	1.155
0.407	0.329	-3.969	0.208	0.118	0.246	0.302	36.806	0.780
0.203	0.182	35.467	0.372	0.023	0.063	0.105	179.517	3.037
0.419	0.407	48.732	0.337	0.078	0.257	0.381	224.679	2.102
0.473	0.333	13.718	0.224	0.139	0.309	0.393	78.607	0.935
0.161	0.146	47.887	0.385	0.015	0.043	0.081	264.046	3.689
0.278	0.232	61.744	0.390	0.035	0.115	0.193	289.460	3.489
0.343	0.232	18.223	0.283	0.082	0.158	0.233	88.126	1.628
0.516	0.267	7.079	0.243	0.221	0.329	0.340	41.759	0.958
0.275	0.261	54.542	0.398	0.039	0.108	0.207	242.212	3.573
0.402	0.312	34.161	0.275	0.096	0.248	0.417	176.386	1.726
0.327	0.269	1.580	0.244	0.071	0.179	0.283	72.216	1.339
0.523	0.441	13.316	0.229	0.147	0.443	0.626	107.707	1.104
0.491	0.422	46.646	0.329	0.120	0.372	0.524	231.396	2.211
0.484	0.309	19.917	0.289	0.080	0.373	0.597	129.208	2.242
0.318	0.236	50.879	0.336	0.061	0.135	0.240	202.896	2.567
0.463	0.263	1.081	0.234	0.180	0.269	0.319	28.479	0.951
0.298	0.229	19.650	0.310	0.057	0.120	0.208	94.046	2.157
0.601	0.450	-12.547	0.189	0.274	0.589	0.757	24.710	0.673
0.368	0.232	16.362	0.257	0.120	0.161	0.209	60.852	1.110
0.385	0.324	48.503	0.340	0.063	0.256	0.413	281.276	2.831
0.340	0.253	36.700	0.321	0.085	0.162	0.290	161.584	2.334
0.205	0.197	40.081	0.374	0.025	0.068	0.150	216.724	3.849
0.437	0.302	3.354	0.240	0.136	0.240	0.328	34.409	1.029
0.234	0.160	59.080	0.336	0.034	0.082	0.108	276.784	2.173
0.374	0.216	17.165	0.279	0.114	0.175	0.261	71.811	1.539
0.356	0.235	21.604	0.277	0.073	0.173	0.277	101.693	1.713
0.163	0.184	59.477	0.479	0.013	0.047	0.138	347.994	8.316
0.268	0.333	43.610	0.421	0.021	0.093	0.193	166.645	3.114
0.398	0.341	33.368	0.288	0.094	0.204	0.327	128.610	1.558
0.415	0.393	32.874	0.323	0.084	0.229	0.342	134.917	1.756
0.320	0.293	-0.625	0.200	0.038	0.168	0.269	62.166	0.895
0.255	0.212	83.131	0.388	0.023	0.103	0.163	433.185	3.457
0.379	0.308	14.760	0.291	0.088	0.207	0.331	89.730	1.849
0.395	0.322	15.166	0.254	0.043	0.241	0.361	105.098	1.550
0.201	0.181	48.023	0.352	0.012	0.064	0.109	248.305	2.981
0.392	0.291	1.273	0.245	0.094	0.233	0.293	55.595	1.109
0.368	0.321	93.888	0.400	0.051	0.203	0.379	462.490	3.849
0.350	0.276	20.654	0.231	0.081	0.163	0.223	93.445	0.961
0.428	0.351	7.344	0.228	0.100	0.274	0.369	72.784	0.947
0.478	0.292	47.932	0.282	0.105	0.283	0.429	171.297	1.482
0.348	0.308	47.938	0.367	0.054	0.186	0.289	236.237	2.935
0.167	0.145	30.251	0.322	0.010	0.043	0.078	162.837	2.388
0.343	0.294	34.369	0.325	0.075	0.203	0.309	211.068	2.415
0.234	0.207	30.349	0.335	0.016	0.074	0.146	129.073	2.742

BMJ Open: first published as 10.1136/bmjopen-2022-063051 on 8 November 2022. Downloaded from http://bmjopen.bmj.com/ on June 10, 2025 at Agence Bibliographique de l Enseignement Superieur (ABES) . Protected by copyright, including for uses related to text and data mining, AI training, and similar technologies.

0.310	0.203	40.308	0.321	0.062	0.127	0.156	158.831	1.680
0.134	0.159	116.852	0.652	0.004	0.032	0.070	729.119	12.129
0.582	0.368	1.515	0.213	0.245	0.414	0.448	25.923	0.694
0.456	0.212	15.229	0.243	0.171	0.207	0.272	32.309	0.940
0.596	0.330	-4.095	0.194	0.295	0.427	0.550	10.610	0.637
0.198	0.195	35.769	0.362	0.010	0.071	0.132	235.187	3.551
0.287	0.219	20.911	0.302	0.047	0.113	0.167	100.239	1.872
0.442	0.314	19.405	0.241	0.102	0.267	0.354	94.929	1.064
0.422	0.250	13.919	0.250	0.164	0.215	0.238	56.828	1.001
0.523	0.306	4.891	0.240	0.221	0.313	0.342	26.158	0.871
0.462	0.355	30.353	0.311	0.127	0.265	0.410	111.064	1.816
0.694	0.535	9.189	0.210	0.239	0.801	1.159	98.527	0.957
0.632	0.437	20.122	0.248	0.262	0.507	0.657	83.067	1.073
0.287	0.214	18.435	0.266	0.052	0.111	0.229	88.334	1.656
0.384	0.290	31.078	0.302	0.114	0.181	0.260	109.950	1.561
0.289	0.180	12.421	0.289	0.069	0.095	0.137	43.848	1.499
0.240	0.200	49.804	0.341	0.036	0.079	0.118	206.468	2.274
0.240	0.234	97.060	0.481	0.018	0.087	0.128	487.833	4.638
0.095	0.071	28.605	0.350	0.007	0.012	0.023	123.417	2.849
0.302	0.200	35.247	0.296	0.068	0.112	0.147	124.830	1.462
0.324	0.338	121.985	0.512	0.040	0.148	0.249	593.122	4.969
0.334	0.280	-5.348	0.180	0.085	0.189	0.332	52.250	0.772
0.271	0.137	11.424	0.266	0.071	0.080	0.092	34.642	1.143
0.472	0.278	31.700	0.294	0.131	0.275	0.419	114.179	1.681
0.246	0.119	19.664	0.260	0.058	0.064	0.064	51.720	1.000
0.233	0.223	89.689	0.436	0.028	0.080	0.135	433.125	3.965
0.534	0.370	0.416	0.228	0.195	0.369	0.501	30.857	0.949
0.312	0.312	151.925	0.593	0.026	0.159	0.256	935.858	7.911
0.526	0.357	6.666	0.243	0.197	0.375	0.483	54.078	1.073
0.559	0.295	4.862	0.210	0.250	0.355	0.369	25.014	0.660
0.363	0.233	26.305	0.276	0.093	0.198	0.265	140.458	1.494
0.359	0.305	48.969	0.371	0.077	0.185	0.285	219.141	2.764
0.335	0.338	54.332	0.440	0.050	0.171	0.468	262.402	6.402
0.199	0.168	69.450	0.300	0.016	0.056	0.091	303.266	1.787
0.363	0.302	68.165	0.377	0.052	0.219	0.295	369.005	2.910
0.349	0.311	83.616	0.408	0.044	0.209	0.311	478.957	3.737
0.334	0.316	73.015	0.394	0.042	0.195	0.284	424.433	3.396
0.377	0.293	17.496	0.259	0.093	0.191	0.292	85.111	1.259
0.154	0.123	31.337	0.360	0.016	0.033	0.058	137.452	2.922
0.155	0.120	44.422	0.320	0.010	0.037	0.061	224.235	2.390
0.227	0.165	11.027	0.270	0.029	0.076	0.109	80.816	1.565
0.255	0.255	33.511	0.334	0.026	0.107	0.171	194.240	2.452
0.209	0.129	20.799	0.280	0.026	0.060	0.102	100.045	1.762
0.253	0.159	10.847	0.290	0.056	0.080	0.103	53.801	1.446
0.317	0.254	9.439	0.232	0.058	0.141	0.240	68.197	1.174
0.436	0.318	35.395	0.324	0.115	0.280	0.420	170.562	2.199
0.974	0.334	4.159	0.204	0.852	0.945	0.784	8.047	0.571
0.372	0.298	35.316	0.314	0.074	0.231	0.414	206.100	2.662
0.791	0.300	8.528	0.188	0.627	0.663	0.529	24.912	0.511
0.225	0.170	22.277	0.313	0.034	0.068	0.114	101.540	2.151

BMJ Open: first published as 10.1136/bmjopen-2022-063051 on 8 November 2022. Downloaded from http://bmjopen.bmj.com/ on June 10, 2025 at Agence Bibliographique de l Enseignement Superieur (ABES) . Protected by copyright, including for uses related to text and data mining, AI training, and similar technologies.

0.395	0.337	26.292	0.304	0.106	0.215	0.343	119.503	1.779
0.345	0.208	27.427	0.291	0.095	0.150	0.229	104.142	1.671
0.481	0.370	49.783	0.340	0.141	0.339	0.471	228.326	2.284
0.717	0.172	0.717	0.165	0.476	0.494	0.292	-2.452	0.350
0.360	0.183	26.541	0.277	0.083	0.154	0.221	89.651	1.407
0.420	0.192	75.210	0.252	0.135	0.181	0.207	215.113	0.927
0.114	0.110	38.262	0.407	0.008	0.019	0.049	180.146	5.047
0.242	0.132	15.827	0.287	0.046	0.076	0.105	73.711	1.611
0.363	0.333	33.399	0.348	0.076	0.189	0.303	155.409	2.388
0.545	0.457	35.031	0.288	0.193	0.368	0.588	125.531	1.531
0.664	0.437	23.027	0.275	0.240	0.730	0.921	150.513	1.489
0.589	0.286	-5.813	0.161	0.347	0.429	0.381	9.752	0.395
0.568	0.184	26.758	0.252	0.283	0.309	0.258	53.829	0.861
0.297	0.218	30.931	0.323	0.053	0.124	0.194	140.585	2.194
0.290	0.329	105.626	0.537	0.032	0.148	0.425	646.131	9.678
0.393	0.341	45.084	0.379	0.096	0.269	0.401	266.984	3.148
0.594	0.180	30.718	0.252	0.316	0.331	0.285	60.140	0.880
0.569	0.351	21.800	0.248	0.239	0.421	1.604	92.936	3.043
0.523	0.311	-7.988	0.163	0.232	0.306	0.414	-5.200	0.449
0.543	0.371	39.201	0.218	0.241	0.362	0.570	137.911	0.872
0.546	0.364	37.232	0.277	0.195	0.408	0.621	157.810	1.634
0.873	0.447	13.886	0.235	0.691	0.832	0.948	41.574	0.896
0.341	0.238	48.851	0.314	0.055	0.157	0.237	200.304	1.940
0.440	0.311	38.254	0.292	0.125	0.259	0.359	156.080	1.601
0.524	0.447	84.399	0.402	0.138	0.440	0.790	445.200	3.938
0.431	0.279	31.785	0.299	0.136	0.222	0.294	107.420	1.554
0.362	0.304	49.502	0.326	0.067	0.191	0.295	224.935	2.304
0.165	0.136	80.958	0.391	0.015	0.035	0.074	323.417	3.489
0.391	0.288	50.280	0.329	0.069	0.237	0.307	251.364	2.052
0.551	0.257	16.638	0.248	0.216	0.402	0.423	80.139	1.007
0.322	0.285	28.080	0.346	0.058	0.168	0.298	165.452	2.882
0.482	0.297	40.044	0.252	0.141	0.354	0.464	199.146	1.251
0.407	0.307	44.513	0.228	0.099	0.252	0.444	217.488	1.200
0.767	0.275	3.142	0.177	0.594	0.632	0.378	14.077	0.420
0.364	0.139	24.614	0.263	0.095	0.133	0.144	56.210	0.992
0.425	0.219	19.227	0.263	0.137	0.223	0.314	75.266	1.328
0.403	0.274	22.733	0.279	0.113	0.232	0.333	114.462	1.583
0.264	0.252	33.935	0.365	0.031	0.116	0.252	198.855	3.979
0.223	0.159	28.928	0.341	0.039	0.065	0.143	118.067	3.175
0.256	0.244	28.024	0.377	0.031	0.105	0.236	163.323	4.077
0.381	0.243	32.272	0.299	0.085	0.197	0.259	138.150	1.661
0.385	0.313	55.871	0.369	0.082	0.234	0.360	283.973	3.034
0.241	0.245	92.100	0.448	0.020	0.098	0.167	521.985	4.429
0.308	0.213	43.675	0.325	0.043	0.134	0.208	190.504	2.243
0.276	0.227	25.543	0.336	0.051	0.108	0.209	122.525	2.754
0.703	0.413	20.526	0.276	0.370	0.689	0.789	102.406	1.304
0.387	0.315	34.960	0.321	0.076	0.237	0.340	188.784	2.155
1.246	0.507	5.409	0.190	1.456	1.771	1.521	26.783	0.528
1.290	0.436	2.759	0.174	1.617	1.792	1.226	13.602	0.418
0.520	0.377	23.268	0.304	0.197	0.380	0.577	113.641	1.815

BMJ Open: first published as 10.1136/bmjopen-2022-063051 on 8 November 2022. Downloaded from http://bmjopen.bmj.com/ on June 10, 2025 at Agence Bibliographique de l Enseignement Superieur (ABES) .
Protected by copyright, including for uses related to text and data mining, AI training, and similar technologies.

0.978	0.554	22.089	0.237	0.888	1.297	1.236	102.055	0.872
0.793	0.359	-1.413	0.201	0.561	0.741	0.666	14.568	0.599
0.371	0.370	78.107	0.406	0.058	0.229	0.371	427.990	3.659
0.320	0.265	29.756	0.313	0.050	0.157	0.273	158.021	2.246
0.414	0.326	51.809	0.338	0.073	0.248	0.370	232.553	2.444
0.395	0.282	28.826	0.291	0.104	0.216	0.310	129.108	1.660
0.349	0.308	36.082	0.359	0.061	0.192	0.311	192.483	2.890
0.566	0.434	35.500	0.307	0.218	0.438	0.681	150.907	1.871
0.201	0.237	57.108	0.454	0.011	0.091	0.499	454.480	15.975
0.572	0.377	61.654	0.298	0.184	0.483	0.553	285.505	1.644
0.450	0.243	6.697	0.256	0.150	0.274	0.309	54.358	1.170
0.423	0.363	49.203	0.329	0.083	0.279	0.447	246.705	2.375
0.270	0.257	52.916	0.353	0.041	0.090	0.158	189.102	2.229
0.677	0.576	15.981	0.220	0.295	0.543	0.734	59.595	0.760
0.615	0.430	6.457	0.213	0.291	0.469	0.609	40.678	0.786
0.717	0.438	1.433	0.223	0.383	0.619	0.769	23.782	0.812
0.394	0.224	31.241	0.284	0.101	0.197	0.275	118.561	1.495
0.501	0.363	15.854	0.284	0.148	0.372	0.510	98.952	1.638
0.416	0.481	32.256	0.425	-0.035	0.396	3.326	301.410	22.151
0.517	0.364	10.600	0.245	0.156	0.394	0.477	79.837	1.090
0.474	0.330	1.492	0.255	0.155	0.349	0.439	60.040	1.264
0.443	0.394	72.470	0.383	0.091	0.325	0.686	393.159	4.508
0.717	0.244	-0.307	0.223	0.459	0.548	0.439	5.803	0.691
0.631	0.386	13.614	0.279	0.315	0.503	0.598	63.297	1.292
0.436	0.294	51.879	0.336	0.092	0.240	0.339	190.884	1.993
0.492	0.408	42.402	0.337	0.126	0.340	0.542	184.095	2.209
0.552	0.458	60.888	0.351	0.111	0.581	0.852	393.852	2.740
0.518	0.409	38.234	0.316	0.150	0.401	0.663	185.284	2.293
0.418	0.324	58.963	0.335	0.073	0.282	0.490	307.733	2.848
0.529	0.450	11.413	0.276	0.194	0.421	0.745	86.600	1.692
0.609	0.623	80.026	0.459	0.130	0.591	1.244	415.731	5.422
0.409	0.258	14.050	0.259	0.115	0.203	0.303	57.781	1.302
0.498	0.281	25.777	0.277	0.205	0.274	0.301	75.337	1.155
0.297	0.299	40.100	0.372	0.042	0.133	0.260	195.973	3.215
0.297	0.221	17.446	0.320	0.050	0.129	0.218	100.845	2.327
0.380	0.315	37.038	0.330	0.069	0.253	0.385	228.068	2.567
0.171	0.152	34.278	0.350	0.015	0.043	0.100	163.667	3.608
0.611	0.415	58.447	0.307	0.181	0.614	0.818	313.327	1.864
0.594	0.462	60.049	0.326	0.204	0.578	0.816	319.459	2.242
0.424	0.366	38.583	0.340	0.107	0.296	0.508	215.801	2.702
0.486	0.372	32.390	0.297	0.110	0.312	0.450	131.456	1.699
0.513	0.295	16.990	0.278	0.186	0.333	0.424	73.202	1.443
0.511	0.407	46.090	0.352	0.083	0.447	0.953	264.583	4.138
0.653	0.286	64.988	0.297	0.187	0.566	0.711	260.920	1.612
0.397	0.269	54.190	0.324	0.089	0.203	0.300	205.775	2.049
0.742	0.476	10.353	0.216	0.421	0.637	0.722	40.798	0.712
0.478	0.451	59.272	0.379	0.099	0.390	0.685	332.115	3.557

For peer review only

BMJ Open: first published as 10.1136/bmjopen-2022-063051 on 8 November 2022. Downloaded from http://bmjopen.bmj.com/ on June 10, 2025 at Agence Bibliographique de l Enseignement Superieur (ABES) .
Protected by copyright, including for uses related to text and data mining, AI training, and similar technologies.

Gaussian curvature

For peer review only

BMJ Open: first published as 10.1136/bmjopen-2022-063051 on 8 November 2022. Downloaded from http://bmjopen.bmj.com/ on June 10, 2025 at Agence Bibliographique de l Enseignement Superieur (ABES) .
Protected by copyright, including for uses related to text and data mining, AI training, and similar technologies.

BMJ Open

Geometric uncertainty in intracranial aneurysm rupture status discrimination: a two-site retrospective study.

Journal:	*BMJ Open*
Manuscript ID	bmjopen-2022-063051.R1
Article Type:	Original research
Date Submitted by the Author:	07-Jul-2022
Complete List of Authors:	Hellmeier, Florian; Charité – Universitätsmedizin Berlin, Institute for Computer-Assisted Cardiovascular Medicine Brüning, Jan; Charité Universitätsmedizin Berlin, Insitute for Computer-Assisted Cardiovascular Medicine Berg, Philipp; University of Magdeburg, Fluid Dynamics and Technical Flows Saalfeld, Sylvia; University of Magdeburg 'Otto von Guericke', Department of Simulation and Graphics Spuler, Andreas; Helios Klinikum Berlin-Buch Sandalcioglu, I. Erol; Otto von Guericke Universitat Magdeburg, Department of Neurosurgery Beuing, Oliver; AMEOS Hospital Bernburg, Deparment of Radiology Larsen, Naomi; University Medical Center Schleswig-Holstein, Department of Radiology and Neuroradiology Schaller, Jens; Charité – Universitätsmedizin Berlin Goubergrits, Leonid ; Charite Universitatsmedizin Berlin, Institute for Computer-Assisted Cardiovascular Medicine
Primary Subject Heading:	Research methods
Secondary Subject Heading:	Neurology, Radiology and imaging
Keywords:	Neurology < INTERNAL MEDICINE, Neuroradiology < RADIOLOGY & IMAGING, Neurosurgery < SURGERY

SCHOLARONE™
Manuscripts

BMJ Open: first published as 10.1136/bmjopen-2022-063051 on 8 November 2022. Downloaded from http://bmjopen.bmj.com/ on June 10, 2025 at Agence Bibliographique de l Enseignement Superieur (ABES) .
Protected by copyright, including for uses related to text and data mining, AI training, and similar technologies.

I, the Submitting Author has the right to grant and does grant on behalf of all authors of the Work (as defined in the below author licence), an exclusive licence and/or a non-exclusive licence for contributions from authors who are: i) UK Crown employees; ii) where BMJ has agreed a CC-BY licence shall apply, and/or iii) in accordance with the terms applicable for US Federal Government officers or employees acting as part of their official duties; on a worldwide, perpetual, irrevocable, royalty-free basis to BMJ Publishing Group Ltd ("BMJ") its licensees and where the relevant Journal is co-owned by BMJ to the co-owners of the Journal, to publish the Work in this journal and any other BMJ products and to exploit all rights, as set out in our licence.

The Submitting Author accepts and understands that any supply made under these terms is made by BMJ to the Submitting Author unless you are acting as an employee on behalf of your employer or a postgraduate student of an affiliated institution which is paying any applicable article publishing charge ("APC") for Open Access articles. Where the Submitting Author wishes to make the Work available on an Open Access basis (and intends to pay the relevant APC), the terms of reuse of such Open Access shall be governed by a Creative Commons licence – details of these licences and which Creative Commons licence will apply to this Work are set out in our licence referred to above.

Other than as permitted in any relevant BMJ Author's Self Archiving Policies, I confirm this Work has not been accepted for publication elsewhere, is not being considered for publication elsewhere and does not duplicate material already published. I confirm all authors consent to publication of this Work and authorise the granting of this licence.

For peer review only

Enseignement Superieur (ABES) .
Protected by copyright, including for uses related to text and data mining, AI training, and similar technologies.

BMJ Open: first published as 10.1136/bmjopen-2022-063051 on 8 November 2022. Downloaded from http://bmjopen.bmj.com/ on June 10, 2025 at Agence Bibliographique de l Enseignement Superieur (ABES) . Protected by copyright, including for uses related to text and data mining, AI training, and similar technologies.

Geometric uncertainty in intracranial aneurysm rupture status discrimination: a two-site retrospective study.

Florian Hellmeier[1], Jan Brüning[1], Philipp Berg[2,3], Sylvia Saalfeld[3,4], Andreas Spuler[5], I. Erol Sandalcioglu[6], Oliver Beuing[7], Naomi Larsen[8], Jens Schaller[1], Leonid Goubergrits[1,9]

[1] Institute of Computer-assisted Cardiovascular Medicine, Charité – Universitätsmedizin Berlin, Berlin, Germany

[2] Laboratory of Fluid Dynamics and Technical Flows, University of Magdeburg, Magdeburg, Germany

[3] Research Campus *STIMULATE*, University of Magdeburg, Magdeburg, Germany

[4] Department of Simulation and Graphics, University of Magdeburg, Magdeburg, Germany

[5] Helios Klinikum Berlin-Buch, Berlin, Germany

[6] Department of Neurosurgery, University Hospital Magdeburg, Magdeburg, Germany

[7] Department of Radiology, AMEOS Hospital, Bernburg, Germany

[8] Department of Radiology and Neuroradiology, University Medical Center Schleswig-Holstein (UKSH), Kiel, Germany

[9] Einstein Center Digital Future, Berlin, Germany

Correspondence:

Jan Brüning

Email: jan.bruening@charite.de

Telephone: +49 30 450 553 879

Telefax: +49 30 450 553 838

Charité – Universitätsmedizin Berlin
Institute of Computer-assisted Cardiovascular Medicine
Augustenburger Platz 1
13353 Berlin
Germany

Keywords: intracranial aneurysms; uncertainty analysis; rupture risk assessment;

Word count: 4,003

For peer review only

For peer review only

BMJ Open: first published as 10.1136/bmjopen-2022-063051 on 8 November 2022. Downloaded from http://bmjopen.bmj.com/ on June 10, 2025 at Agence Bibliographique de l Enseignement Superieur (ABES) .
Protected by copyright, including for uses related to text and data mining, AI training, and similar technologies.

Abstract

Objectives: Assessing the risk associated with unruptured intracranial aneurysms (IA) is essential in clinical decision making. Several geometric risk parameters have been proposed for this purpose. However, performance of these parameters has been inconsistent. This study evaluates the performance and robustness of geometric risk parameters on two datasets and compare it to the uncertainty inherent in assessing these parameters and quantifies inter-parameter correlations.

Methods: Two datasets containing 244 IA geometries from 178 patients were retrospectively analyzed. IAs were stratified by anatomical region, based on the PHASES score locations. 37 geometric risk parameters representing four groups (size, neck, non-dimensional, and curvature parameters) were assessed. Analysis included standardized absolute differences (SAD) between ruptured and unruptured IAs, ratios of SAD to median relative uncertainty (MRU) associated with the parameters, and inter-parameter correlation.

Results: The ratio of SAD to MRU was lower for higher-dimensional size parameters (i.e., areas and volumes) than for one-dimensional size parameters. Non-dimensional size parameters performed comparatively well with regard to SAD and MRU. SAD was higher in the posterior anatomical region. Correlation of parameters was strongest within parameter (sub)groups and between size and curvature parameters, while anatomical region did not strongly affect correlation patterns.

Conclusion: Non-dimensional parameters and few parameters from other groups were comparatively robust, suggesting that they might generalize better to other datasets. The data on discriminative performance and inter-parameter correlations presented in this study may aid in developing and choosing robust geometric risk parameters for use in rupture risk models.

For peer review only

BMJ Open: first published as 10.1136/bmjopen-2022-063051 on 8 November 2022. Downloaded from http://bmjopen.bmj.com/ on June 10, 2025 at Agence Bibliographique de l Enseignement Superieur (ABES) .
Protected by copyright, including for uses related to text and data mining, AI training, and similar technologies.

Strengths and limitations of this study

- This study provides location-specific estimates of the discriminative ability of a large set of geometric risk parameters for IA rupture risk assessment, while also considering uncertainty.
- The analysis was performed on two independent datasets to assess robustness of the findings.
- Even though the relative uncertainty in acquisition of each geometric risk parameter was evaluated based on more than 20 individual segmentations performed during the Multiple Aneurysms Anatomy Challenge, this evaluation was only performed on five aneurysms in total.

For peer review only

BMJ Open: first published as 10.1136/bmjopen-2022-063051 on 8 November 2022. Downloaded from http://bmjopen.bmj.com/ on June 10, 2025 at Agence Bibliographique de l Enseignement Superieur (ABES) .
Protected by copyright, including for uses related to text and data mining, AI training, and similar technologies.

BMJ Open: first published as 10.1136/bmjopen-2022-063051 on 8 November 2022. Downloaded from http://bmjopen.bmj.com/ on June 10, 2025 at Agence Bibliographique de l Enseignement Superieur (ABES) . Protected by copyright, including for uses related to text and data mining, AI training, and similar technologies.

Introduction

A relevant part of the general population harbors one or more unruptured intracranial aneurysms (IAs), with the overall prevalence estimated around 3% [1]. While most IAs do not rupture [2], the question of whether and when to treat them remains relevant due to the poor prognosis of ruptured IAs [3, 4] as well as the risk of intervention [3, 5]. Current American Heart Association/American Stroke Association guidelines list several modifiable and non-modifiable risk factors for IA growth and/or rupture, including IA location, growth rate, morphology, smoking status, alcohol consumption, hypertension, age, sex, previous IA, and family history [6]. Attempts have been made to develop scoring systems to quantify rupture risk, growth risk, and/or support treatment decisions, these include the PHASES score by Greving et al. [7], the UIATS by Etminan et al. [8] and the ELAPSS score by Backes et al. [9]. All three of these scores are based on clinically available data and all include geometric rupture risk parameters: IA size in case of the PHASES score [7], surface irregularity, size ratio, as well as aspect ratio in case of the UIATS [8], and IA size as well as surface irregularity for the ELAPSS score [9]. While these metrics were designed to support clinical decision making, performance on clinical data has been mixed [10-12] and improvements, particularly for patients harboring multiple IAs, are desired by clinicians [13].

The aim of this paper is to assess the ability of a broad number of proposed geometric risk parameters to differentiate between unruptured and ruptured IAs while also comparing their discriminative ability relative to the uncertainty encountered in determining them. Any acquisition of patient-specific IA geometries and subsequent use of these geometries to derive geometric risk parameters is affected by a number of uncertainty-introducing factors. Starting with the medical imaging acquisition itself, which is followed by image data pre-processing, segmentation, geometry reconstruction including post-processing (e.g., smoothing, checking of topology), and finally calculation of the geometric risk parameters. All these processing steps are associated with some errors, resulting in uncertainty, which negatively affects the ability of parameters to discriminate IA rupture status. Discrimination of rupture status on an individual IA level is, however, necessary if these parameters are to support the clinical decision-making process, including any decisions regarding treatment modalities. Previous studies found high variability in the uncertainty of different geometric risk parameters as well as differences in their ability to differentiate between ruptured and unruptured IAs [14-16]. Furthermore, for geometric risk parameters with multiple alternative definitions, the specific implementation can affect the discriminative performance of the parameter itself and any derived parameters, as demonstrated by Lauric et al. for parameters incorporating IA and neck size [17].

The current study was performed to facilitate optimal selection of geometric rupture risk parameters by identifying geometric parameters, which are good discriminators while also exhibiting low uncertainty. The analysis is performed on two datasets processed by different research groups and is differentiated by

For peer review only

anatomical region, in order to assess how the predictive suitability of the geometric risk parameters is affected by geometry processing as well as anatomical location. Additionally, correlation of the geometric risk parameters with each other is assessed.

For peer review only

BMJ Open: first published as 10.1136/bmjopen-2022-063051 on 8 November 2022. Downloaded from http://bmjopen.bmj.com/ on June 10, 2025 at Agence Bibliographique de l Enseignement Superieur (ABES) .
Protected by copyright, including for uses related to text and data mining, AI training, and similar technologies.

BMJ Open: first published as 10.1136/bmjopen-2022-063051 on 8 November 2022. Downloaded from http://bmjopen.bmj.com/ on June 10, 2025 at Agence Bibliographique de l Enseignement Superieur (ABES) . Protected by copyright, including for uses related to text and data mining, AI training, and similar technologies.

Methods

Medical imaging data

IA geometries were retrospectively reconstructed and segmented from 3D rotational angiography data acquired for routine clinical indications. Data was collected consecutively. The inclusion criteria of the datasets were imaging modality and the corresponding acquisition resolution. Cases with considerable segmentation artifacts such as close vessels that appear to be merged or holes in the segmented lumen were rejected from the analysis. 142 IAs were acquired in the Helios Klinikum Berlin-Buch (Berlin, Germany), 38 in KRH Klinikum Nordstadt (Hanover, Germany), 23 in the University Medical Center Schleswig-Holstein (UKSH) (Kiel, Germany), and 41 in the University Hospital Magdeburg (Magdeburg, Germany). Processing of the imaging data, including segmentation, was performed at two sites: Berlin, which processed 142 IAs from Helios Klinikum Berlin-Buch (dataset 1), and Magdeburg, which processed 102 IAs from KRH Klinikum Nordstadt, UKSH, and University Hospital Magdeburg (dataset 2). Overall, 244 IAs from 178 patients were included, from which geometric risk parameters were subsequently calculated. Based on the PHASES score [7], aneurysm location was classified into four anatomical regions: internal carotid artery (ICA), middle cerebral artery (MCA), anterior region (all vessels anterior of the ICA/MCA), and posterior region (all vessels posterior of the ICA/MCA). The distribution of the individual IA locations and their assignment to the four anatomical regions are shown in Table 1.

Table 1: Frequency and rupture status of individual IA locations by dataset. ACA: anterior cerebral artery, AComA: anterior communicating artery, AChA: anterior choroidal artery, ICA: internal carotid artery, MCA: middle cerebral artery, PComA: posterior communicating artery, PCA: posterior cerebral artery, SCA: superior cerebellar artery, BA: basilar artery, PICA: posterior inferior cerebellar artery, VA: vertebral artery.

Anatomical region	Vessel	Dataset 1 unruptured	Dataset 1 ruptured	Dataset 2 unruptured	Dataset 2 ruptured
Anterior	ACA	3	1	2	2
	AComA	10	22	11	5
ICA	AChA	0	1	1	2
	ICA	29	8	19	4
MCA	MCA	28	10	31	8
Posterior	PComA	8	10	2	4
	PCA	0	1	0	0
	SCA	0	0	1	1
	BA	4	3	3	4
	PICA	0	4	1	0
	VA	0	0	0	1

Geometric risk parameters

Historically, several geometric parameters for IA rupture risk assessment have been proposed. In order to have access to information on parameter uncertainty, the parameters chosen for this study were limited to a subset of the parameters reported in Goubergrits et al. [14], a parameter uncertainty study performed on segmentation data obtained during the Multiple Aneurysms AnaTomy Challenge (MATCH) 2018 [18]. The major outcome of this study was the median relative uncertainty (MRU) of geometric parameters. Briefly, five aneurysms were segmented and reconstructed by 26 international research groups, which participated in the MATCH challenge. These segmentations were used to calculate the median and the 68.3% range between the 84.13th and the 15.87th percentile for each of the five aneurysms. The uncertainty range was selected with respect to the range of ± one standard deviation for normally distributed data reported in other studies. The uncertainty was defined as the uncertainty range divided by the median value and calculated for each geometric parameter. Finally, the average of all five aneurysms was calculated to define the MRU. For a detailed description of the parameters and the rationale for choosing the parameters, the interested reader is referred to Goubergrits et al. [14]. Briefly, most of the proposed geometric parameters describe aneurysm and/or aneurysmal neck size or shape, or irregularity. These parameters were previously proposed as predictors for rupture risk. Table 2 lists the geometric parameters, their abbreviations and MRU values.

Table 2: List of the investigated geometric parameters, their descriptions, and median relative uncertainties (MRU). Note that terminology and implementation in the references might differ subtly. Derived and modified from tables 1-5 from Goubergrits et al. [14], used under Creative Commons Attribution License (CC BY 4.0). The CC BY 4.0 license text is available at https://creativecommons.org/licenses/by/4.0/.

Parameter group	Parameter name, unit [exemplary reference]	Parameter abbreviation	Short description	MRU
Size	Height, mm [19]	H	Maximum perpendicular distance from the neck plane to the aneurysm surface	0.140
	Maximum dimension, mm [20]	L_{max}	Maximum distance between two points on the aneurysm surface	0.157
	Maximum height, mm [15]	H_{max}	Maximum distance between the centroid of the neck and the aneurysm surface	0.123
	Maximum diameter, mm [17]	D_{max}	Maximum neck plane-parallel distance between two points on the aneurysm surface	0.169
	Bulge height, mm [19]	H_b	Distance between the neck plane and the maximum diameter	0.373
	Surface area, mm^2 [15]	A	Surface area of the aneurysm	0.215

BMJ Open: first published as 10.1136/bmjopen-2022-063051 on 8 November 2022. Downloaded from http://bmjopen.bmj.com/ on June 10, 2025 at Agence Bibliographique de l Enseignement Superieur (ABES) . Protected by copyright, including for uses related to text and data mining, AI training, and similar technologies.

For peer review only

	Convex hull surface area, mm² [15]	A_{CH}	Surface area of the aneurysm's convex hull	0.277
	Minimal bounding sphere surface area, mm² [21]	A_{MBS}	Surface area of the aneurysm's minimal bounding sphere	0.305
	Closed surface area, mm²	A_{closed}	Surface area of the neck-closed aneurysm	0.283
	Volume, mm³ [15]	V	Volume of the neck-closed aneurysm	0.392
	Convex hull volume, mm³ [15]	V_{CH}	Volume of the aneurysm's convex hull	0.399
	Minimal bounding sphere volume, mm³ [21]	V_{MBS}	Volume of the aneurysm's minimal bounding sphere	0.451
Neck	Minimum neck diameter, mm [17]	$D_{neck,min}$	Minimum distance between two opposite points on the neck perimeter	0.306
	Maximum neck diameter, mm [22]	$D_{neck,max}$	Maximum distance between two points on the neck perimeter	0.348
	Neck perimeter, mm [19]	P_{neck}	Perimeter of the aneurysm neck	0.374
	Equivalent neck diameter, mm [19]	$D_{neck,equiv}$	Hydraulic diameter of the aneurysm neck	0.276
	Neck area, mm² [19]	A_{neck}	Area of the aneurysm neck	0.593
	Elliptical neck area, mm²	$A_{neck,elliptical}$	Neck area calculated as the product of the minimum and maximum neck diameter	0.650
Non-dimensional	Aspect ratio [22]	AR	Ratio of height to maximum neck diameter	0.293
	Equivalent aspect ratio [19]	eAR	Ratio of height to equivalent neck diameter	0.326
	Bottleneck factor [19]	BF	Ratio of maximum diameter to maximum neck diameter	0.201
	Bulge location [19]	BL	Ratio of bulge height to height	0.301
	Nonsphericity index [15]	NSI	Normalized ratio of volume to surface area relative to a hemisphere	0.108
	Aneurysm volume to bounding sphere volume [21]	AVSV	Ratio of volume to minimal bounding sphere volume	0.173
	Aneurysm surface area to bounding sphere area [21]	AASA	Ratio of surface area to minimal bounding sphere surface area	0.095

For peer review only

BMJ Open: first published as 10.1136/bmjopen-2022-063051 on 8 November 2022. Downloaded from http://bmjopen.bmj.com/ on June 10, 2025 at Agence Bibliographique de l Enseignement Superieur (ABES) .
Protected by copyright, including for uses related to text and data mining, AI training, and similar technologies.

	Undulation index [15]	UI	1 minus the ratio of volume to convex hull volume	0.709
	Ellipticity index [15]	EI	Normalized ratio of convex hull volume to convex hull surface area relative to a hemisphere	0.051
Curvature	Mean of mean curvature, mm^{-1} [19]	MAA	Surface average of local mean curvature	0.136
	Mean of absolute mean curvature, mm^{-1}	absMAA	Surface average of the magnitude of the local mean curvature	0.133
	Standard deviation of mean curvature, mm^{-1}	MSD	Standard deviation of the local mean curvature	1.011
	High mean curvature, % [21]	HMC	Relative increase of the mean of absolute mean curvature over the mean curvature of the minimal bounding sphere	0.396
	L2-norm of mean curvature [19]	MLN	Scale invariant measure of surface irregularity, uses mean curvature	0.150
	Mean of Gaussian curvature, mm^{-2} [19]	GAA	Surface average of local Gaussian curvature	0.344
	Mean of absolute Gaussian curvature, mm^{-2}	absGAA	Surface average of the magnitude of the local Gaussian curvature	0.485
	Standard deviation of Gaussian curvature, mm^{-2}	GSD	Standard deviation of the local Gaussian curvature	1.798
	High Gaussian curvature, % [21]	HGC	Relative increase of the mean of absolute Gaussian curvature over the Gaussian curvature of the minimal bounding sphere	0.822
	L2-norm of Gaussian curvature [19]	GLN	Scale invariant measure of surface irregularity, uses Gaussian curvature	0.545

Since the diameter of the parent vessel was not available for all IAs studied, size ratio could not be calculated and was excluded. Furthermore, UI and CR as well as NSI and NPR are directly related through $CR = 1 - UI$ and $IPR = \frac{\sqrt[3]{18\pi}}{1-NSI}$, respectively. CR and IPR were therefore not included in the analysis, in order to avoid redundancy. Geometric risk parameters were calculated from the IA geometries using MATLAB (version R2017b, MathWorks, Natick, USA), Python (version 3.7.1, Python Software Foundation, Delaware, USA), and ZIBAmira (version 2015.28, Zuse Institute Berlin, Germany). The individual parameter values, IA location, and rupture status for each IA in this study, as well as the exact

BMJ Open: first published as 10.1136/bmjopen-2022-063051 on 8 November 2022. Downloaded from http://bmjopen.bmj.com/ on June 10, 2025 at Agence Bibliographique de l Enseignement Superieur (ABES) . Protected by copyright, including for uses related to text and data mining, AI training, and similar technologies.

values of the inter-parameter correlation coefficients are provided as supplemental material 1 and 2 respectively.

Statistical analysis

Since most of the geometric risk parameters were non-normally distributed, as assessed by Q-Q plots and Shapiro-Wilk tests, the median was used to quantify central tendency and the interquartile range was used to quantify dispersion. Correlations were quantified using Pearson's r with correlations $|r| \geq 0.75$ referred to as strong, while those with $0.75 > |r| \geq 0.25$ and $|r| < 0.25$ referred to as moderate and weak, respectively. Statistical analysis was performed using SPSS (version 28.0.0.0, IBM, Armonk, USA) and MATLAB.

The discriminative ability of the individual parameters was assessed by standardizing the absolute difference between the medians of the ruptured and unruptured IAs with the weighted arithmetic mean of the IQRs of the two groups. This measure of effect size will be referred to as the standardized absolute group difference (SAD). Furthermore, the ratio of the SAD to the relative uncertainty, a measure of the uncertainty associated with parameter calculation, from Goubergrits et al. [14] was calculated for all parameters and will be referred to as the group difference-uncertainty ratio (DUR). The equations for SAD and DUR are thus $SAD = \frac{(n_r + n_u) \cdot |m_r - m_u|}{n_r IQR_r + n_u IQR_u}$ and $DUR = \frac{SAD}{MRU}$, where n_i, m_i, and IQR_i are the sample sizes, median values, and interquartile ranges of the ruptured (subscript *r*) and unruptured (subscript *u*) samples, while MRU is the median relative uncertainty from Goubergrits et al. [14], which is also listed in Table 2. SAD and DUR may take any value ≥0 with higher values indicating stronger discriminative ability and a better ratio of discriminative ability to uncertainty, respectively. SAD and DUR values of zero would indicate no discriminative ability and the worst possible ratio of discriminative ability to uncertainty, respectively. Additionally, the correlation coefficients between the parameters were calculated. Analysis of SAD and DUR as well as the correlation coefficients was performed individually for each anatomical region and each dataset.

Patient and public involvement

Due to the purely retrospective manner of this study, no involvement of patients or the general public was considered.

For peer review only

BMJ Open: first published as 10.1136/bmjopen-2022-063051 on 8 November 2022. Downloaded from http://bmjopen.bmj.com/ on June 10, 2025 at Agence Bibliographique de l Enseignement Superieur (ABES) . Protected by copyright, including for uses related to text and data mining, AI training, and similar technologies.

Results

Figure 1 shows SAD for all geometric risk parameters by anatomical region and dataset. Considering both datasets, the following parameters achieved the comparatively highest SAD for each anatomical region: curvature (HMC, MLN, HGC, GLN) and non-dimensional (AR, eAR, AVSV, AASA) parameters in the anterior region, curvature (HMC, HGC) and non-dimensional (NSI, AASA, EI) parameters in the ICA, non-dimensional (AR, eAR, BL, AVSV, AASA) parameters in the MCA, and size (H, L_{max}, A, A_{MBS}) and curvature (MSD, absGAA, GSD) parameters in the posterior region. Compared to the other anatomical regions, SAD was higher in the posterior region and more parameters exhibited relatively high SAD. Looking at all anatomical regions combined, curvature (HMC, MLN, absGAA, HGC, GLN) and non-dimensional (AR, eAR, AVSV, AASA) parameters as well as one neck ($D_{neck,min}$) and one size (H_b) parameter show comparatively high SAD in both datasets. Furthermore, the differences between the two datasets become less pronounced when combining all anatomical regions. Moreover, this combined evaluation resulted in SAD being higher for the size parameters in site 2 compared to site 1. Here, it is worthwhile to note that the SAD of this combined assessment is not the average of the SAD of all four region-specific evaluations. Thus, pooling for some parameters can result in the absolute difference between the ruptured and unruptured groups to be close to zero, which results in SAD values close to zero as observed for the one-dimensional size parameters of the site 1 dataset.

Figure 2 shows DUR for all geometric risk parameters by anatomical region and dataset. Considering both datasets, the following parameters achieved the comparatively highest DUR for each anatomical region: non-dimensional (AASA, EI) and one curvature (MLN) parameter in the anterior region, non-dimensional (EI, AASA, NSI) parameters in the ICA, non-dimensional (AASA, EI) parameters in the MCA, and size parameters (H, L_{max}, H_{max}, A), curvature (MAA, absMAA), and one non-dimensional (EI) parameter in the posterior region. Similar to SAD, DUR in the posterior region was overall higher and more parameters exhibited relatively high DUR, compared to the other anatomical regions. Looking at all anatomical regions combined, non-dimensional (NSI, AVSV, AASA, EI) and curvature (absMAA, MLN) parameters show comparatively high DUR in both datasets. As for SAD, the differences between the two datasets are less pronounced when looking at all anatomical regions combined.

Figures 3 and 4 show correlation coefficients between the geometric risk parameters by anatomical region for both datasets. The following general features are present in most data correlation plots: The size parameters (H, L_{max}, H_{max}, D_{max}, H_b, A, A_{CH}, A_{MBS}, A_{closed}, V, V_{CH}, V_{MBS}) are generally strongly correlated with each other. Similarly, the neck parameters ($D_{neck,min}$, $D_{neck,max}$, P_{neck}, $D_{neck,equiv}$, A_{neck}, $A_{neck,elliptical}$) are also generally strongly correlated with each other.

BMJ Open: first published as 10.1136/bmjopen-2022-063051 on 8 November 2022. Downloaded from http://bmjopen.bmj.com/ on June 10, 2025 at Agence Bibliographique de l Enseignement Superieur (ABES) . Protected by copyright, including for uses related to text and data mining, AI training, and similar technologies.

Within the non-dimensional parameter group, there are two distinct subgroups in most plots: one formed by AR, eAR, BF, and BL and one formed by NSI, AVSV, AASA, UI, and EI. Within the latter subgroup, several of the correlations are negative but their magnitude is overall moderate to strong. The curvature parameters also form two subgroups, one formed by dimensional curvature parameters (MAA, absMAA, MDS, GAA, absGAA, GSD) and one by non-dimensional curvature parameters (HMC, MLN, HGC, GLN). With regard to correlations between parameter groups, there is generally moderate to strong correlation between the size and neck parameters. Additionally, the size and neck parameters are generally moderately correlated with the curvature parameters, the direction of the correlation being positive for the non-dimensional curvature parameters and negative for the dimensional curvature parameters.

For peer review only

BMJ Open: first published as 10.1136/bmjopen-2022-063051 on 8 November 2022. Downloaded from http://bmjopen.bmj.com/ on June 10, 2025 at Agence Bibliographique de l Enseignement Superieur (ABES) .
Protected by copyright, including for uses related to text and data mining, AI training, and similar technologies.

Discussion

Previous research has assessed the impact of uncertainty on geometric risk parameters in a limited fashion. Ma et al. examined the influence of random noise on the calculation of 14 geometric risk parameters, finding curvature parameters more susceptible to random noise than size, neck, and non-dimensional parameters [19]. Others have examined the influence of imaging modality [23] and CT angiography reconstruction kernel [24] on geometric risk parameters. Regarding image acquisition, Ramachandran et al. have examined the influence of imaging modality [23], while O'Meara et al. [24] and Berg et al. [25] have focused on the reconstruction kernel's effect on geometric and hemodynamic risk parameters, respectively. The current study as well as the earlier uncertainty study based on the MATCH challenge were both based on 3D rotational angiography imaging, which is the routine imaging modality in both centers involved in this study. Other sensitivity and uncertainty aspects of computational fluid dynamics approaches to IAs have been explored, e.g., by Cebral et al. [26], Sarrami-Foroushani et al. [27], and Schneiders et al. [28]. To the authors' knowledge there is, however, no comprehensive publication relating discriminative performance and uncertainty of geometric risk parameters, while also providing detailed data on their correlation with each other.

Looking at the parameter groups examined in this study, the following findings can be made: the size and neck parameters measuring areas (A, A_{CH}, A_{MBS}, A_{closed}, A_{neck}, $A_{neck,elliptical}$) and volumes (V, V_{CH}, V_{MBS}) generally do not achieve high DUR, despite having SAD similar to the size and neck parameters measuring length (H, L_{max}, H_{max}, D_{max}, H_b, $D_{neck,min}$, $D_{neck,max}$, P_{neck}, $D_{neck,equiv}$). The cause is the higher uncertainty encountered in determining the higher-dimensional parameters when compared to the one-dimensional parameters [14]. This suggests that higher-dimensional size parameters tend to be less robust and thus less suitable for use in practical risk models than one-dimensional size parameters. Like Lauric et al. [17], there are instances of noticeable differences in the discriminative performance of parameters capturing the same aspect of IA geometry, e.g., for the neck size parameters. The non-dimensional parameters exhibit comparatively high SAD and DUR, except for BL and UI, which exhibit lower discriminative ability and/or higher uncertainty in their calculation. The curvature parameters show substantial variability in SAD and DUR depending on the anatomical region and the parameter, with MLN performing comparatively well overall. It is notable that the posterior region tends to exhibit higher SAD and DUR than the other regions, indicating more pronounced geometric differences between ruptured and unruptured IAs in this region. Regarding the differences in SAD and DUR between datasets 1 and 2, it is likely that differences in the patient collectives, subsample sizes, and reconstruction techniques are the main causes. The latter could in the future be tackled by machine learning-based segmentation methods, which can reduce operator-induced uncertainty. Examples of such methods have previously been presented, e.g., in the context of the CADA challenge [29].

BMJ Open: first published as 10.1136/bmjopen-2022-063051 on 8 November 2022. Downloaded from http://bmjopen.bmj.com/ on June 10, 2025 at Agence Bibliographique de l Enseignement Superieur (ABES) . Protected by copyright, including for uses related to text and data mining, AI training, and similar technologies.

BMJ Open: first published as 10.1136/bmjopen-2022-063051 on 8 November 2022. Downloaded from http://bmjopen.bmj.com/ on June 10, 2025 at Agence Bibliographique de l Enseignement Superieur (ABES) . Protected by copyright, including for uses related to text and data mining, AI training, and similar technologies.

Regarding the correlation patterns, there is substantial similarity between all analyzed anatomical regions and datasets. Parameters tend to be most strongly correlated with other parameters from the same parameter group, except for the non-dimensional and curvature parameters, which form two subgroups each. This is reasonable, given that the parameters within each parameter group capture similar aspects of IA geometry. For the size and neck parameter groups this is obvious, since they both capture aspects of IA and neck size, respectively. The two distinct correlation subgroups within the non-dimensional parameter group are likely caused by the underlying parameter subgroups capturing different aspects of aneurysm shape. While the parameters of the first subgroup (AR, eAR, BF, BL) are simply ratios of one-dimensional size parameters, the second subgroup (NSI, AVSV, AASA, UI, EI) is formed by parameters relating aneurysm area and/or volume to geometric reference objects, e.g., the minimal bounding sphere or convex hull. The negative correlation between AVSV and AASA with the other parameters from the second subgroup is due to the parameter definitions, which cause AVSV and AASA to increase with increasing sphericity, while the other parameters tend to decrease with increasing sphericity. The curvature parameters also form two subgroups, with the first subgroup consisting of the dimensional parameters quantifying the mean or dispersion of IA surface curvature (MAA, absMAA, MSD, GAA, absGAA, GSD) and the second subgroup consisting of non-dimensional, scale invariant curvature parameters (HMC, MLN, HGC, GLN). Since the former parameters intrinsically decrease with IA size, while the latter parameters increase with IA size, the negative correlation of the two subgroups with each other makes sense. It should be noted that the positive correlation of the non-dimensional curvature parameters with IA size is not an intrinsic property of the non-dimensional parameters themselves, since they are designed to be scale invariant. It rather indicates that curvature and irregularities of the IA surface increase in larger IAs.

For a geometric risk parameter to be a good candidate for rupture risk prediction, it should generally have a high SAD, in order to be able to differentiate between ruptured and unruptured IAs. Additionally, DUR should be high, indicating low sensitivity of the parameter to the imaging, segmentation, and calculation workflow, by which it is calculated. This is desirable because it allows models including such parameters to generalize well to other datasets. Finally, when choosing a set of parameters, data from the correlation analysis can be used to identify parameters that are not strongly correlated. Neyazi et al. have previously used this method to derive a two-parameter rupture status prediction model from a set of 49 geometric and hemodynamic rupture risk parameters, identifying AR and the maximal relative residence time as the most suitable model parameters [13]. Other attempts to identify suitable rupture status prediction models based on geometric risk parameters have been attempted, e.g., Dhar et al. [15] and Zhang et al. [30], but results have generally been inconsistent. Possible reasons for the discrepant findings regarding optimal parameter choice are the sample sizes used and the uncertainty inherent in the workflow by which the parameters are calculated. This may lead to the selection of less robust parameters that perform well on a given dataset but generalize less well to others. Based on the results of this study and considering SAD, DUR, as well as the correlation between geometric risk parameters, examples of more robust parameter choices could look as follows:

- H_{max}, $D_{neck,min}$, AR, AASA, and MLN for the anterior region.
- L_{max}, P_{neck}, AR, AASA, and HGC for the ICA.
- D_{max}, $D_{neck,min}$, eAR, AASA, and HMC for the MCA.
- L_{max}, $D_{neck,min}$, BL, EI, and absMAA for the posterior region.
- H_b, $D_{neck,min}$, AR, AASA, and MLN if looking at all anatomical regions combined.

Overall, while individual size, neck, and curvature parameters achieved good discriminative performance and robustness, the non-dimensional parameters tended to perform well as a group. This suggests that non-dimensional geometric risk parameters can provide comparatively good discriminative performance, while the nondimensionalization itself mitigates some of the uncertainty introduced through the workflow by which the parameters are calculated [14]. Neither did we attempt to develop a novel aneurysm rupture risk prediction model, nor did we test earlier published models [16, 31]. We decided against this analysis due to the large variety of published proposed risk models. Testing them as well as the propagation of the parameter's uncertainty towards assessment of rupture risk should be tested in a separate study. Finally, elaborated models will also require further information such as hypertension status, earlier SAH as well as hemodynamic parameters, which were unavailable within this study.

Limitations

IAs were grouped by anatomical region because IA location is an important determinant of rupture risk, as demonstrated by its weight in current risk scores [7-9]. However, by analyzing the datasets by anatomical region, some subsamples become quite small. Small sample size might affect the accuracy of the median and interquartile range estimates derived from these groups. This limitation is, however, partially mitigated by also analyzing all anatomical regions combined and using two datasets, in order to get a more comprehensive picture of the risk parameters' performance. The major focus of the study was the analysis of the performance and robustness of 37 geometric risk parameters. Thus, not all findings of this study could be assessed in depth. For example, we decided for grouping of aneurysms by anatomical regions as recommended by clinical scores, such as such as PHASES score [7]. While we observed differences in both SAD and DUR based on the aneurysms' location within the circulation, the underlying mechanisms for these differences cannot be assessed by the available data. However, Tykocki & Kostkiewicz found significant differences between some geometric parameters (parent artery size, size ratio and aspect ratio) of aneurysms for the anterior and the posterior regions [32]. They associated the difference in these parameters to different impacts on the intra-aneurysmal hemodynamics such as vortex formation and wall

For peer review only

BMJ Open: first published as 10.1136/bmjopen-2022-063051 on 8 November 2022. Downloaded from http://bmjopen.bmj.com/ on June 10, 2025 at Agence Bibliographique de l Enseignement Superieur (ABES) . Protected by copyright, including for uses related to text and data mining, AI training, and similar technologies.

BMJ Open: first published as 10.1136/bmjopen-2022-063051 on 8 November 2022. Downloaded from http://bmjopen.bmj.com/ on June 10, 2025 at Agence Bibliographique de l Enseignement Superieur (ABES) . Protected by copyright, including for uses related to text and data mining, AI training, and similar technologies.

shear stress. Why these geometric parameters might result in different hemodynamic conditions and rupture risks must be investigated in a dedicated study. This is especially important as this study's findings demonstrated differences in the SAD not only between locations and the cohorts, but also when all aneurysm locations were evaluated together.

Furthermore, the underlying motivation for the chosen geometric parameters to be used for risk prediction. All parameters were chosen as they were discussed in existing literature as potential risk parameters. The investigated parameters as well as their respective references are summarized in the table 2. Respectively, most of rupture risk models used in frames of the MATCH challenge [18] included both geometric and hemodynamic parameters.

Another potential limitation are the uncertainty values from Goubergrits et al. [14], which were used to calculate DUR. These values were calculated on a sample containing MCA and posterior region IAs [14]. While it does not seem particularly probable, it is possible that IA location and size might affect the uncertainty inherent in calculating the geometric risk parameters in a relevant manner, which in turn could influence DUR results. Respectively the generalization of MRU values from the uncertainty study [14] should be considered with caution, especially as those values were calculated only based on five aneurysms. A more fundamental limitations is the focus on geometric risk parameters. These parameters serve as proxies for the pathophysiological processes leading to IA rupture through the latter's influence on the geometry of the IA surface. Due to their nature, geometric risk parameters cannot directly capture the hemodynamic, mechanical, or biochemical aspects of IA rupture. Nevertheless, they are among the most intensely researched types of IA rupture risk parameters, due to the comparative ease with which they can be calculated from clinical data.

Note that the list of parameters investigated in this study is not exhaustive. More proposed geometric parameters can be found in recent literature [33]. The parameters investigated here are limited to a set of parameters investigated earlier in frames of the uncertainty study [14]. Second, these parameters were constrained to parameters, which can be calculated automatically. Furthermore, we excluded parameters such as Writhe-based indices or indices based on Zernike moments due to high sensitivity of these parameter to the reconstruction process (e.g., surface smoothing algorithms). However, some of the novel parameters (e.g. conicity index [33]) can be calculated based on parameters provided in this study.

Finally, the calculation of geometric parameters including the ostium plane depends on a sufficient reference plane selection. Recently, Berg et al. quantified the potential effect of neck curve variations on hemodynamic predictions [34]. These findings could be transferred to the cases included in this study in future work.

For peer review only

Conclusion

Based on datasets from two research groups, the present study provides location-specific estimates of the discriminative ability of a large set of geometric risk parameters for IA rupture risk assessment, while also considering uncertainty. Additionally, correlation patterns between the parameters are identified. The presented data is potentially useful in evaluating geometric risk parameters for use in rupture risk models or when choosing input parameters for machine learning approaches to rupture risk prediction. It may also be helpful when designing future geometric risk parameters for clinical use.

For peer review only

BMJ Open: first published as 10.1136/bmjopen-2022-063051 on 8 November 2022. Downloaded from http://bmjopen.bmj.com/ on June 10, 2025 at Agence Bibliographique de l Enseignement Superieur (ABES) .
Protected by copyright, including for uses related to text and data mining, AI training, and similar technologies.

Conflict of interest statement

The authors declare that there is no conflict of interest.

Acknowledgments

The authors kindly acknowledge PD Dr. Belal Neyazi (Department of Neurosurgery, University Hospital Magdeburg) for his assistance during data acquisition as well as Adriano Schlief (Institute of Computer-assisted Cardiovascular Medicine, Charité – Universitätsmedizin Berlin) for his help in checking the topology and scaling of the IA geometries.

Data Availability Statement

All individual parameter values as well as the correlation coefficients are made available as supplemental material.

- supplemental material 1: individual parameter values, IA location, and rupture status for each IA
- supplemental material 2: exact values of the inter-parameter correlation coefficients

Ethical approval statements

In this study, patient-specific 3D reconstructions of intracranial aneurysms based on routine information were evaluated retrospectively. Use of retrospective data was approved by the local ethics committees (Ethikkommission der Charité - Universitätsmedizin Berlin: EA2/222/19; Ethikkommission der Med. Hochschule Hannover: NOVA Nr. 68/20).

Funding

This study was partly funded by the Federal Ministry of Education and Research in Germany within the Forschungscampus *STIMULATE* (grant number 13GW0473A) and the German Research Foundation (grant number SA 3461/2-1, BE 6230/2-1).

Author contributions

All roles according to CRediT (contributor roles taxonomy). Conceptualization: LG, JS, FH, JB, and PB. Methodology: FH, JS, and LG. Resources: AS, IES, OB, NL, SS, and PB. Investigation: JB, FH, and JS. Formal Analysis: FH. Funding acquisition: LG, PB, and SS. Supervision: LG. Writing – original draft: FH, LG, and JB. Writing – review & editing: PB, SS, AS, IES, OB, NL, and JS.

For peer review only

BMJ Open: first published as 10.1136/bmjopen-2022-063051 on 8 November 2022. Downloaded from http://bmjopen.bmj.com/ on June 10, 2025 at Agence Bibliographique de l Enseignement Superieur (ABES) . Protected by copyright, including for uses related to text and data mining, AI training, and similar technologies.

References

1. Vlak, M.H., A. Algra, R. Brandenburg, and G.J. Rinkel, *Prevalence of unruptured intracranial aneurysms, with emphasis on sex, age, comorbidity, country, and time period: a systematic review and meta-analysis.* Lancet Neurol, 2011. **10**(7): p. 626-36.
2. Brown, R.D., Jr. and J.P. Broderick, *Unruptured intracranial aneurysms: epidemiology, natural history, management options, and familial screening.* Lancet Neurol, 2014. **13**(4): p. 393-404.
3. Wiebers, D.O., J.P. Whisnant, J. Huston, 3rd, I. Meissner, R.D. Brown, Jr., D.G. Piepgras, G.S. Forbes, K. Thielen, D. Nichols, W.M. O'Fallon, J. Peacock, L. Jaeger, N.F. Kassell, G.L. Kongable-Beckman, J.C. Torner, and I. International Study of Unruptured Intracranial Aneurysms, *Unruptured intracranial aneurysms: natural history, clinical outcome, and risks of surgical and endovascular treatment.* Lancet, 2003. **362**(9378): p. 103-10.
4. Rackauskaite, D., E. Svanborg, E. Andersson, K. Lowhagen, L. Csajbok, and B. Nellgard, *Prospective study: Long-term outcome at 12-15 years after aneurysmal subarachnoid hemorrhage.* Acta Neurol Scand, 2018. **138**(5): p. 400-407.
5. Pontes, F.G.B., E.M. da Silva, J.C. Baptista-Silva, and V. Vasconcelos, *Treatments for unruptured intracranial aneurysms.* Cochrane Database Syst Rev, 2021. **5**: p. CD013312.
6. Thompson, B.G., et al., *Guidelines for the Management of Patients With Unruptured Intracranial Aneurysms: A Guideline for Healthcare Professionals From the American Heart Association/American Stroke Association.* Stroke, 2015. **46**(8): p. 2368-400.
7. Greving, J.P., M.J. Wermer, R.D. Brown, Jr., A. Morita, S. Juvela, M. Yonekura, T. Ishibashi, J.C. Torner, T. Nakayama, G.J. Rinkel, and A. Algra, *Development of the PHASES score for prediction of risk of rupture of intracranial aneurysms: a pooled analysis of six prospective cohort studies.* Lancet Neurol, 2014. **13**(1): p. 59-66.
8. Etminan, N., et al., *The unruptured intracranial aneurysm treatment score: a multidisciplinary consensus.* Neurology, 2015. **85**(10): p. 881-9.
9. Backes, D., et al., *ELAPSS score for prediction of risk of growth of unruptured intracranial aneurysms.* Neurology, 2017. **88**(17): p. 1600-1606.
10. Juvela, S., *PHASES score and treatment scoring with cigarette smoking in the long-term prediction of rupturing of unruptured intracranial aneurysms.* J Neurosurg, 2022. **136**(1): p. 156-162.
11. Molenberg, R., M.W. Aalbers, A. Mazuri, G.J. Luijckx, J.D.M. Metzemaekers, R.J.M. Groen, M. Uyttenboogaart, and J.M.C. van Dijk, *The Unruptured Intracranial Aneurysm Treatment Score as a predictor of aneurysm growth or rupture.* Eur J Neurol, 2021. **28**(3): p. 837-843.
12. Hernandez-Duran, S., D. Mielke, V. Rohde, and V. Malinova, *Is the unruptured intracranial aneurysm treatment score (UIATS) sensitive enough to detect aneurysms at risk of rupture?* Neurosurg Rev, 2021. **44**(2): p. 987-993.
13. Neyazi, B., V.M. Swiatek, M. Skalej, O. Beuing, K.P. Stein, J. Hattingen, B. Preim, P. Berg, S. Saalfeld, and I.E. Sandalcioglu, *Rupture risk assessment for multiple intracranial aneurysms: why there is no need for dozens of clinical, morphological and hemodynamic parameters.* Ther Adv Neurol Disord, 2020. **13**: p. 1756286420966159.
14. Goubergrits, L., F. Hellmeier, J. Bruening, A. Spuler, H.C. Hege, S. Voss, G. Janiga, S. Saalfeld, O. Beuing, and P. Berg, *Multiple Aneurysms AnaTomy CHallenge 2018 (MATCH): uncertainty quantification of geometric rupture risk parameters.* Biomed Eng Online, 2019. **18**(1): p. 35.
15. Dhar, S., M. Tremmel, J. Mocco, M. Kim, J. Yamamoto, A.H. Siddiqui, L.N. Hopkins, and H. Meng, *Morphology parameters for intracranial aneurysm rupture risk assessment.* Neurosurgery, 2008. **63**(2): p. 185-96; discussion 196-7.
16. Detmer, F.J., B.J. Chung, F. Mut, M. Slawski, F. Hamzei-Sichani, C. Putman, C. Jimenez, and J.R. Cebral, *Development and internal validation of an aneurysm rupture probability model based on patient characteristics and aneurysm location, morphology, and hemodynamics.* Int J Comput Assist Radiol Surg, 2018. **13**(11): p. 1767-1779.

BMJ Open: first published as 10.1136/bmjopen-2022-063051 on 8 November 2022. Downloaded from http://bmjopen.bmj.com/ on June 10, 2025 at Agence Bibliographique de l Enseignement Superieur (ABES) . Protected by copyright, including for uses related to text and data mining, AI training, and similar technologies.

17. Lauric, A., M.I. Baharoglu, and A.M. Malek, *Ruptured status discrimination performance of aspect ratio, height/width, and bottleneck factor is highly dependent on aneurysm sizing methodology.* Neurosurgery, 2012. **71**(1): p. 38-45.
18. Berg, P., et al., *Multiple Aneurysms AnaTomy CHallenge 2018 (MATCH): Phase I: Segmentation.* Cardiovasc Eng Technol, 2018. **9**(4): p. 565-581.
19. Ma, B., R.E. Harbaugh, and M.L. Raghavan, *Three-dimensional geometrical characterization of cerebral aneurysms.* Ann Biomed Eng, 2004. **32**(2): p. 264-73.
20. Lauric, A., E.L. Miller, M.I. Baharoglu, and A.M. Malek, *3D shape analysis of intracranial aneurysms using the writhe number as a discriminant for rupture.* Ann Biomed Eng, 2011. **39**(5): p. 1457-69.
21. Chien, A., J. Sayre, and F. Vinuela, *Comparative morphological analysis of the geometry of ruptured and unruptured aneurysms.* Neurosurgery, 2011. **69**(2): p. 349-56.
22. Ujiie, H., Y. Tamano, K. Sasaki, and T. Hori, *Is the aspect ratio a reliable index for predicting the rupture of a saccular aneurysm?* Neurosurgery, 2001. **48**(3): p. 495-502; discussion 502-3.
23. Ramachandran, M., R. Retarekar, R.E. Harbaugh, D. Hasan, B. Policeni, R. Rosenwasser, C. Ogilvy, and M.L. Raghavan, *Sensitivity of Quantified Intracranial Aneurysm Geometry to Imaging Modality.* Cardiovasc Eng Technol, 2013. **4**(1): p. 75-86.
24. O'Meara, B., J.P. Rahal, A. Lauric, and A.M. Malek, *Benefit of a sharp computed tomography angiography reconstruction kernel for improved characterization of intracranial aneurysms.* Neurosurgery, 2014. **10 Suppl 1**: p. 97-105; discussion 105.
25. Berg, P., S. Saalfeld, S. Voss, T. Redel, B. Preim, G. Janiga, and O. Beuing, *Does the DSA reconstruction kernel affect hemodynamic predictions in intracranial aneurysms? An analysis of geometry and blood flow variations.* J Neurointerv Surg, 2018. **10**(3): p. 290-296.
26. Cebral, J.R., M.A. Castro, S. Appanaboyina, C.M. Putman, D. Millan, and A.F. Frangi, *Efficient pipeline for image-based patient-specific analysis of cerebral aneurysm hemodynamics: technique and sensitivity.* IEEE Trans Med Imaging, 2005. **24**(4): p. 457-67.
27. Sarrami-Foroushani, A., T. Lassila, and A.F. Frangi, *Virtual endovascular treatment of intracranial aneurysms: models and uncertainty.* Wiley Interdiscip Rev Syst Biol Med, 2017. **9**(4).
28. Schneiders, J.J., H.A. Marquering, L. Antiga, R. van den Berg, E. VanBavel, and C.B. Majoie, *Intracranial aneurysm neck size overestimation with 3D rotational angiography: the impact on intra-aneurysmal hemodynamics simulated with computational fluid dynamics.* AJNR Am J Neuroradiol, 2013. **34**(1): p. 121-8.
29. Ivantsits, M., et al., *Detection and analysis of cerebral aneurysms based on X-ray rotational angiography - the CADA 2020 challenge.* Med Image Anal, 2021. **77**: p. 102333.
30. Zheng, Y., F. Xu, J. Ren, Q. Xu, Y. Liu, Y. Tian, and B. Leng, *Assessment of intracranial aneurysm rupture based on morphology parameters and anatomical locations.* J Neurointerv Surg, 2016. **8**(12): p. 1240-1246.
31. Lall, R.R., C.S. Eddleman, B.R. Bendok, and H.H. Batjer, *Unruptured intracranial aneurysms and the assessment of rupture risk based on anatomical and morphological factors: sifting through the sands of data.* Neurosurg Focus, 2009. **26**(5): p. E2.
32. Tykocki, T. and B. Kostkiewicz, *Aneurysms of the anterior and posterior cerebral circulation: comparison of the morphometric features.* Acta Neurochir (Wien), 2014. **156**(9): p. 1647-54.
33. Juchler, N., S. Schilling, P. Bijlenga, V. Kurtcuoglu, and S. Hirsch, *Shape Trumps Size: Image-Based Morphological Analysis Reveals That the 3D Shape Discriminates Intracranial Aneurysm Disease Status Better Than Aneurysm Size.* Front Neurol, 2022. **13**: p. 809391.
34. Berg, P., B. Behrendt, S. Voss, O. Beuing, B. Neyazi, I.E. Sandalcioglu, B. Preim, and S. Saalfeld, *VICTORIA: VIrtual neck Curve and True Ostium Reconstruction of Intracranial Aneurysms.* Cardiovasc Eng Technol, 2021. **12**(4): p. 454-465.

For peer review only

BMJ Open: first published as 10.1136/bmjopen-2022-063051 on 8 November 2022. Downloaded from http://bmjopen.bmj.com/ on June 10, 2025 at Agence Bibliographique de l Enseignement Superieur (ABES) . Protected by copyright, including for uses related to text and data mining, AI training, and similar technologies.

Figures

Figure 1: Standardized absolute group difference (SAD) for each anatomical region and dataset.

Figure 2: Group difference-uncertainty ratio (DUR) for each anatomical region and dataset.

Figure 3: Pearson's r for correlation between geometric risk parameters by anatomical region for dataset 1.

Figure 4: Pearson's r for correlation between geometric risk parameters by anatomical region for dataset 2.

For peer review only

BMJ Open: first published as 10.1136/bmjopen-2022-063051 on 8 November 2022. Downloaded from http://bmjopen.bmj.com/ on June 10, 2025 at Agence Bibliographique de l Enseignement Superieur (ABES) . Protected by copyright, including for uses related to text and data mining, AI training, and similar technologies.

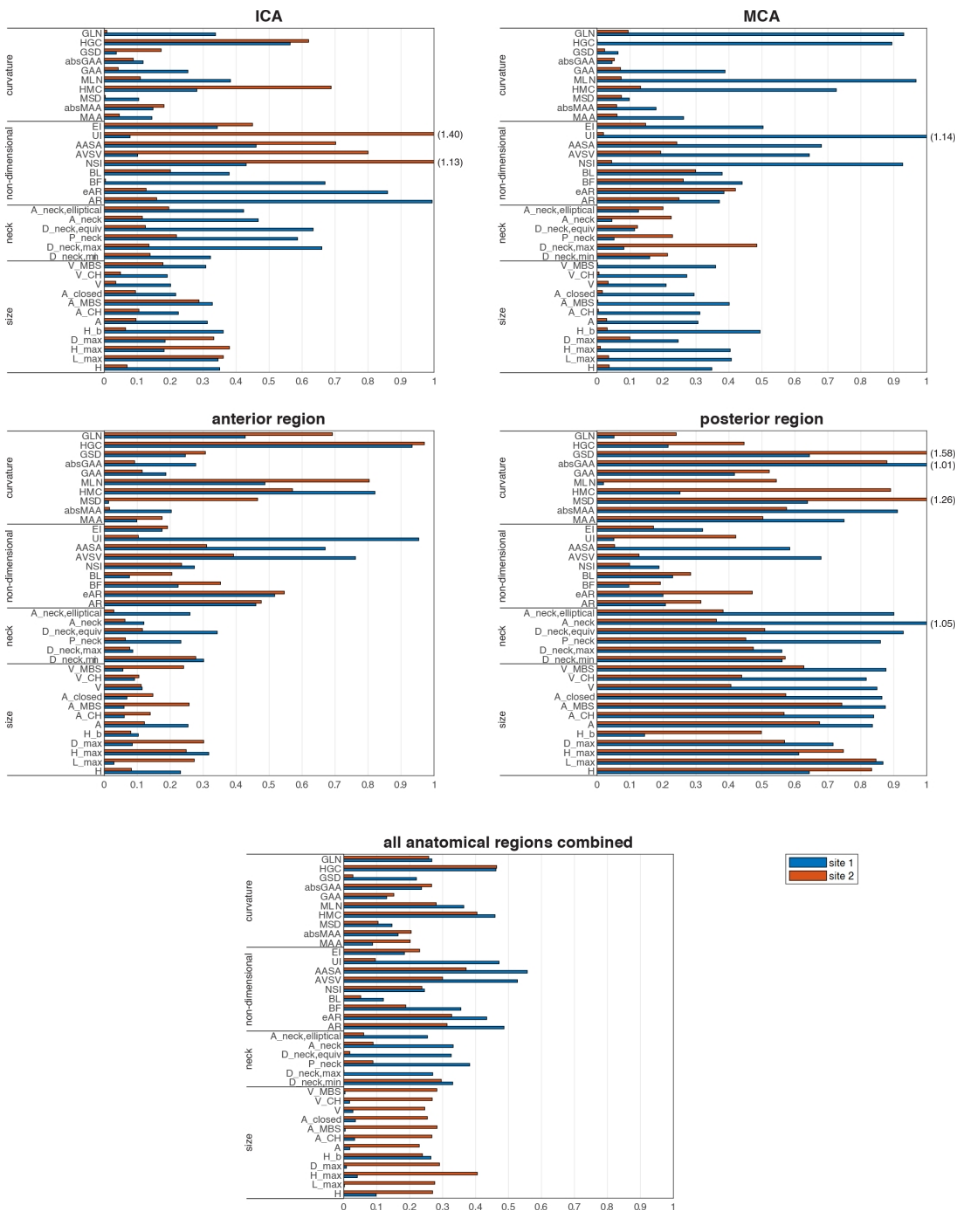

196x248mm (300 x 300 DPI)

BMJ Open: first published as 10.1136/bmjopen-2022-063051 on 8 November 2022. Downloaded from http://bmjopen.bmj.com/ on June 10, 2025 at Agence Bibliographique de l Enseignement Superieur (ABES) .
Protected by copyright, including for uses related to text and data mining, AI training, and similar technologies.

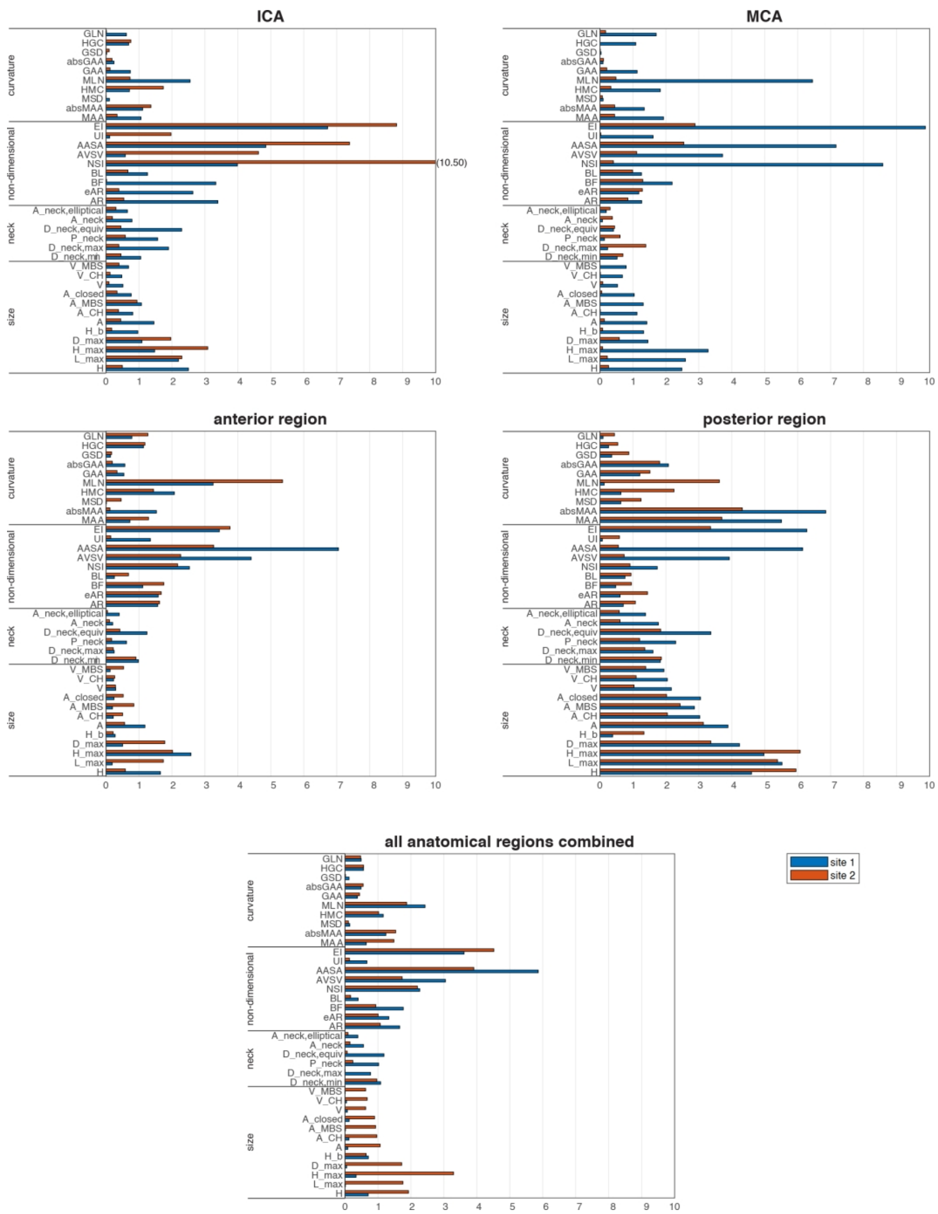

192x248mm (300 x 300 DPI)

BMJ Open: first published as 10.1136/bmjopen-2022-063051 on 8 November 2022. Downloaded from http://bmjopen.bmj.com/ on June 10, 2025 at Agence Bibliographique de l Enseignement Superieur (ABES) . Protected by copyright, including for uses related to text and data mining, AI training, and similar technologies.

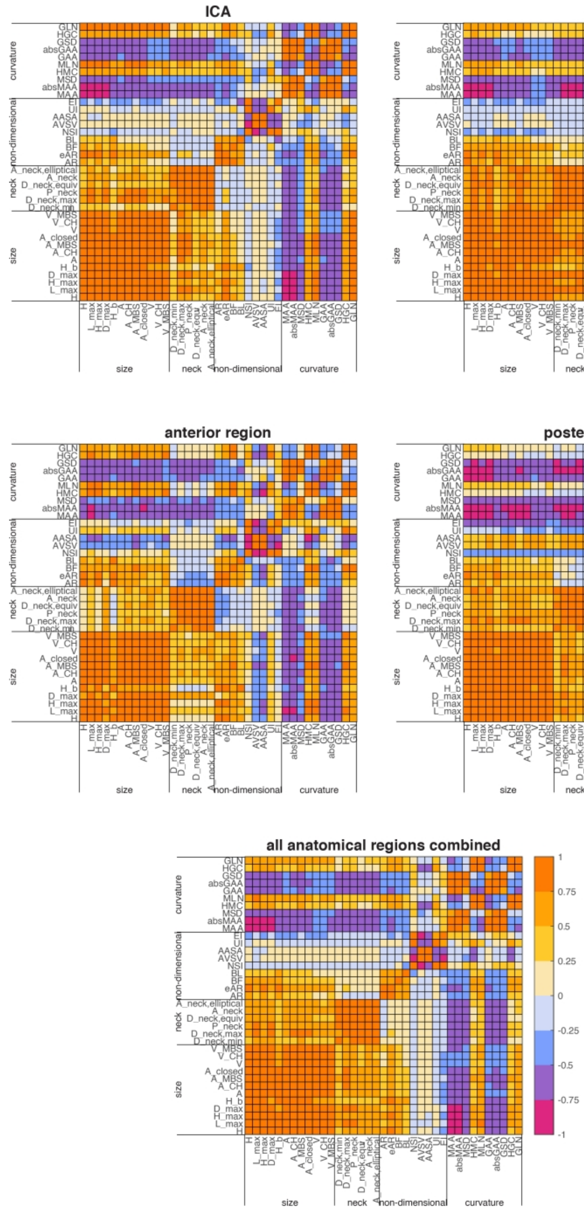

198x325mm (300 x 300 DPI)

BMJ Open: first published as 10.1136/bmjopen-2022-063051 on 8 November 2022. Downloaded from http://bmjopen.bmj.com/ on June 10, 2025 at Agence Bibliographique de l Enseignement Superieur (ABES) .
Protected by copyright, including for uses related to text and data mining, AI training, and similar technologies.

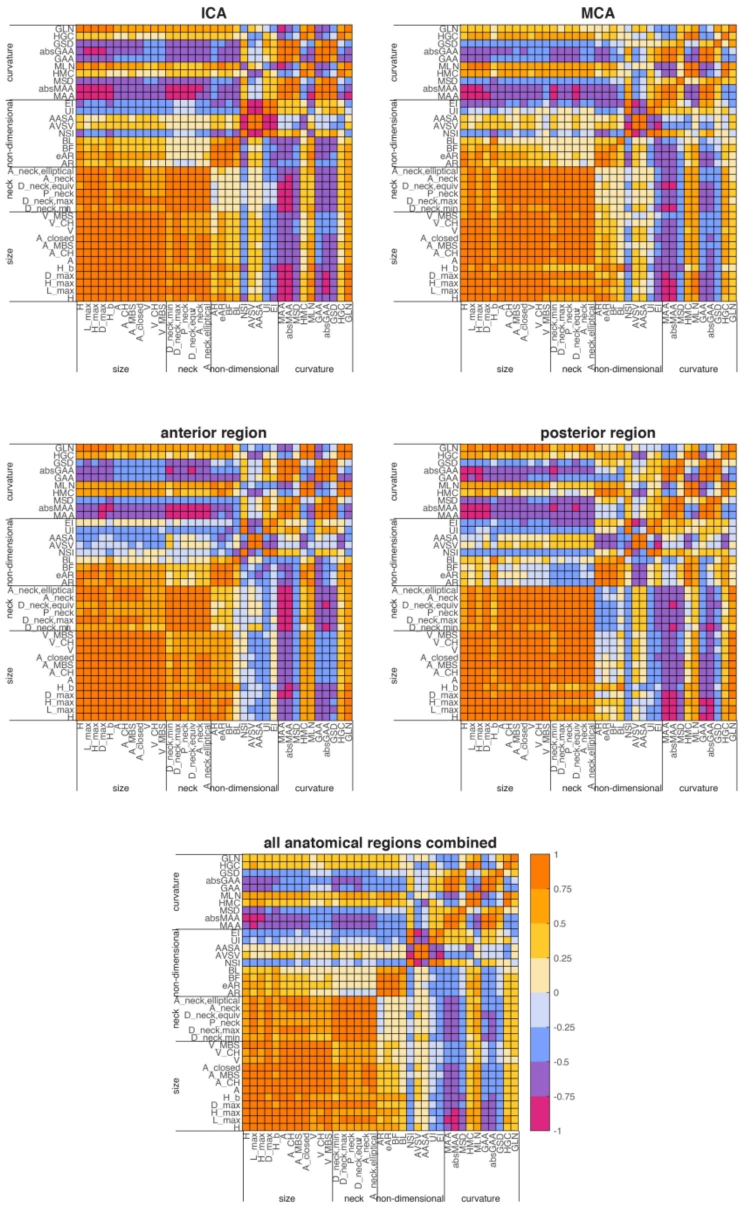

BMJ Open: first published as 10.1136/bmjopen-2022-063051 on 8 November 2022. Downloaded from http://bmjopen.bmj.com/ on June 10, 2025 at Agence Bibliographique de l Enseignement Superieur (ABES) .
Protected by copyright, including for uses related to text and data mining, AI training, and similar technologies.

Pearson's r	H	L_max	H_max	D_max	H_b	A	A_CH
H	1.000	0.872	0.968	0.610	0.836	0.867	0.830
L_max	0.872	1.000	0.950	0.884	0.648	0.962	0.960
H_max	0.968	0.950	1.000	0.728	0.783	0.922	0.894
D_max	0.610	0.884	0.728	1.000	0.349	0.873	0.900
H_b	0.836	0.648	0.783	0.349	1.000	0.653	0.605
A	0.867	0.962	0.922	0.873	0.653	1.000	0.993
A_CH	0.830	0.960	0.894	0.900	0.605	0.993	1.000
A_MBS	0.835	0.973	0.919	0.863	0.596	0.967	0.957
A_closed	0.827	0.957	0.890	0.899	0.606	0.992	1.000
V	0.779	0.917	0.842	0.869	0.565	0.980	0.988
V_CH	0.778	0.924	0.846	0.880	0.548	0.982	0.988
V_MBS	0.769	0.918	0.857	0.822	0.522	0.934	0.919
D_neck,mi	0.220	0.402	0.246	0.535	0.125	0.415	0.484
D_neck,ma	0.153	0.466	0.248	0.642	-0.049	0.426	0.520
P_neck	0.059	0.376	0.158	0.554	-0.075	0.353	0.454
D_neck,eq	0.159	0.428	0.224	0.609	-0.014	0.417	0.508
A_neck	0.089	0.392	0.170	0.583	-0.064	0.390	0.491
A_neck,elli	0.179	0.448	0.240	0.630	0.028	0.450	0.541
AR	0.867	0.582	0.784	0.236	0.849	0.579	0.503
eAR	0.879	0.639	0.819	0.304	0.801	0.608	0.536
BF	0.701	0.727	0.749	0.684	0.595	0.735	0.682
BL	0.627	0.461	0.580	0.273	0.884	0.464	0.423
NSI	0.173	0.275	0.235	0.216	-0.021	0.142	0.129
AVSV	-0.393	-0.491	-0.481	-0.331	-0.275	-0.315	-0.287
AASA	-0.455	-0.558	-0.551	-0.378	-0.337	-0.380	-0.350
UI	0.405	0.494	0.463	0.437	0.137	0.365	0.356
EI	0.012	0.091	0.067	0.013	-0.075	-0.034	-0.050
MAA	-0.661	-0.763	-0.698	-0.727	-0.481	-0.702	-0.740
absMAA	-0.692	-0.755	-0.711	-0.701	-0.547	-0.710	-0.747
MSD	-0.504	-0.453	-0.465	-0.370	-0.517	-0.489	-0.513
HMC	0.672	0.801	0.776	0.698	0.434	0.706	0.672
MLN	0.727	0.775	0.790	0.706	0.500	0.745	0.704
GAA	-0.627	-0.693	-0.655	-0.632	-0.443	-0.590	-0.621
absGAA	-0.647	-0.688	-0.659	-0.626	-0.534	-0.639	-0.672
GSD	-0.547	-0.567	-0.541	-0.507	-0.511	-0.550	-0.584
HGC	0.618	0.783	0.727	0.735	0.322	0.710	0.685
GLN	0.614	0.729	0.698	0.731	0.300	0.711	0.681

BMJ Open: first published as 10.1136/bmjopen-2022-063051 on 8 November 2022. Downloaded from http://bmjopen.bmj.com/ on June 10, 2025 at Agence Bibliographique de l Enseignement Superieur (ABES) . Protected by copyright, including for uses related to text and data mining, AI training, and similar technologies.

A_MBS	A_closed	V	V_CH	V_MBS	D_neck,min	D_neck,max	P_neck
0.835	0.827	0.779	0.778	0.769	0.220	0.153	0.059
0.973	0.957	0.917	0.924	0.918	0.402	0.466	0.376
0.919	0.890	0.842	0.846	0.857	0.246	0.248	0.158
0.863	0.899	0.869	0.880	0.822	0.535	0.642	0.554
0.596	0.606	0.565	0.548	0.522	0.125	-0.049	-0.075
0.967	0.992	0.980	0.982	0.934	0.415	0.426	0.353
0.957	1.000	0.988	0.988	0.919	0.484	0.520	0.454
1.000	0.952	0.939	0.953	0.984	0.346	0.375	0.290
0.952	1.000	0.989	0.988	0.913	0.494	0.526	0.462
0.939	0.989	1.000	0.998	0.920	0.486	0.503	0.457
0.953	0.988	0.998	1.000	0.940	0.460	0.485	0.430
0.984	0.913	0.920	0.940	1.000	0.298	0.302	0.223
0.346	0.494	0.486	0.460	0.298	1.000	0.685	0.681
0.375	0.526	0.503	0.485	0.302	0.685	1.000	0.952
0.290	0.462	0.457	0.430	0.223	0.681	0.952	1.000
0.361	0.516	0.504	0.485	0.310	0.907	0.870	0.857
0.321	0.500	0.503	0.477	0.263	0.780	0.944	0.974
0.377	0.550	0.543	0.517	0.316	0.909	0.909	0.886
0.568	0.498	0.454	0.459	0.527	-0.127	-0.328	-0.375
0.610	0.529	0.473	0.480	0.553	-0.208	-0.214	-0.304
0.753	0.675	0.643	0.668	0.743	0.043	-0.096	-0.153
0.362	0.427	0.370	0.348	0.268	0.087	-0.061	-0.064
0.334	0.113	0.080	0.131	0.361	-0.197	-0.061	-0.176
-0.501	-0.273	-0.225	-0.261	-0.486	0.179	0.068	0.160
-0.558	-0.337	-0.288	-0.320	-0.535	0.160	0.041	0.130
0.494	0.340	0.273	0.321	0.477	-0.152	0.134	-0.008
0.166	-0.065	-0.072	-0.032	0.209	-0.227	-0.193	-0.269
-0.636	-0.743	-0.667	-0.654	-0.529	-0.582	-0.679	-0.648
-0.627	-0.752	-0.683	-0.661	-0.516	-0.646	-0.664	-0.637
-0.379	-0.521	-0.510	-0.474	-0.310	-0.620	-0.396	-0.402
0.801	0.661	0.604	0.639	0.770	-0.028	0.133	-0.011
0.753	0.697	0.631	0.658	0.708	-0.009	0.127	-0.014
-0.547	-0.622	-0.527	-0.520	-0.433	-0.446	-0.584	-0.543
-0.551	-0.678	-0.607	-0.582	-0.440	-0.652	-0.603	-0.580
-0.453	-0.592	-0.545	-0.515	-0.360	-0.695	-0.549	-0.547
0.811	0.672	0.627	0.670	0.805	-0.029	0.180	0.038
0.748	0.672	0.626	0.664	0.737	-0.038	0.158	0.024

For peer review only

BMJ Open: first published as 10.1136/bmjopen-2022-063051 on 8 November 2022. Downloaded from http://bmjopen.bmj.com/ on June 10, 2025 at Agence Bibliographique de l Enseignement Superieur (ABES) . Protected by copyright, including for uses related to text and data mining, AI training, and similar technologies.

D_neck,equi	A_neck	A_neck,ellipt	AR	eAR	BF	BL	NSI
0.159	0.089	0.179	0.867	0.879	0.701	0.627	0.173
0.428	0.392	0.448	0.582	0.639	0.727	0.461	0.275
0.224	0.170	0.240	0.784	0.819	0.749	0.580	0.235
0.609	0.583	0.630	0.236	0.304	0.684	0.273	0.216
-0.014	-0.064	0.028	0.849	0.801	0.595	0.884	-0.021
0.417	0.390	0.450	0.579	0.608	0.735	0.464	0.142
0.508	0.491	0.541	0.503	0.536	0.682	0.423	0.129
0.361	0.321	0.377	0.568	0.610	0.753	0.362	0.334
0.516	0.500	0.550	0.498	0.529	0.675	0.427	0.113
0.504	0.503	0.543	0.454	0.473	0.643	0.370	0.080
0.485	0.477	0.517	0.459	0.480	0.668	0.348	0.131
0.310	0.263	0.316	0.527	0.553	0.743	0.268	0.361
0.907	0.780	0.909	-0.127	-0.208	0.043	0.087	-0.197
0.870	0.944	0.909	-0.328	-0.214	-0.096	-0.061	-0.061
0.857	0.974	0.886	-0.375	-0.304	-0.153	-0.064	-0.176
1.000	0.927	0.953	-0.267	-0.298	-0.034	-0.040	-0.113
0.927	1.000	0.949	-0.353	-0.317	-0.119	-0.074	-0.157
0.953	0.949	1.000	-0.266	-0.247	-0.036	0.004	-0.155
-0.267	-0.353	-0.266	1.000	0.946	0.687	0.672	0.175
-0.298	-0.317	-0.247	0.946	1.000	0.669	0.627	0.253
-0.034	-0.119	-0.036	0.687	0.669	1.000	0.525	0.300
-0.040	-0.074	0.004	0.672	0.627	0.525	1.000	-0.267
-0.113	-0.157	-0.155	0.175	0.253	0.300	-0.267	1.000
0.141	0.175	0.161	-0.403	-0.468	-0.491	-0.075	-0.823
0.129	0.153	0.138	-0.450	-0.524	-0.532	-0.148	-0.751
0.019	-0.021	-0.047	0.320	0.427	0.442	-0.027	0.824
-0.219	-0.243	-0.226	0.085	0.141	0.157	-0.325	0.922
-0.656	-0.622	-0.632	-0.337	-0.379	-0.384	-0.446	0.044
-0.678	-0.632	-0.667	-0.377	-0.393	-0.371	-0.492	0.103
-0.516	-0.461	-0.553	-0.319	-0.252	-0.158	-0.456	0.370
0.017	-0.024	0.030	0.536	0.649	0.764	0.318	0.542
0.022	-0.028	0.035	0.591	0.685	0.804	0.463	0.314
-0.543	-0.499	-0.495	-0.365	-0.417	-0.365	-0.436	-0.045
-0.634	-0.575	-0.635	-0.368	-0.375	-0.327	-0.513	0.183
-0.631	-0.563	-0.640	-0.296	-0.265	-0.203	-0.488	0.303
0.077	0.033	0.055	0.449	0.560	0.753	0.186	0.602
0.064	0.022	0.042	0.453	0.551	0.779	0.234	0.427

For peer review only

BMJ Open: first published as 10.1136/bmjopen-2022-063051 on 8 November 2022. Downloaded from http://bmjopen.bmj.com/ on June 10, 2025 at Agence Bibliographique de l Enseignement Superieur (ABES) . Protected by copyright, including for uses related to text and data mining, AI training, and similar technologies.

AVSV	AASA	UI	EI	MAA	absMAA	MSD	HMC
-0.393	-0.455	0.405	0.012	-0.661	-0.692	-0.504	0.672
-0.491	-0.558	0.494	0.091	-0.763	-0.755	-0.453	0.801
-0.481	-0.551	0.463	0.067	-0.698	-0.711	-0.465	0.776
-0.331	-0.378	0.437	0.013	-0.727	-0.701	-0.370	0.698
-0.275	-0.337	0.137	-0.075	-0.481	-0.547	-0.517	0.434
-0.315	-0.380	0.365	-0.034	-0.702	-0.710	-0.489	0.706
-0.287	-0.350	0.356	-0.050	-0.740	-0.747	-0.513	0.672
-0.501	-0.558	0.494	0.166	-0.636	-0.627	-0.379	0.801
-0.273	-0.337	0.340	-0.065	-0.743	-0.752	-0.521	0.661
-0.225	-0.288	0.273	-0.072	-0.667	-0.683	-0.510	0.604
-0.261	-0.320	0.321	-0.032	-0.654	-0.661	-0.474	0.639
-0.486	-0.535	0.477	0.209	-0.529	-0.516	-0.310	0.770
0.179	0.160	-0.152	-0.227	-0.582	-0.646	-0.620	-0.028
0.068	0.041	0.134	-0.193	-0.679	-0.664	-0.396	0.133
0.160	0.130	-0.008	-0.269	-0.648	-0.637	-0.402	-0.011
0.141	0.129	0.019	-0.219	-0.656	-0.678	-0.516	0.017
0.175	0.153	-0.021	-0.243	-0.622	-0.632	-0.461	-0.024
0.161	0.138	-0.047	-0.226	-0.632	-0.667	-0.553	0.030
-0.403	-0.450	0.320	0.085	-0.337	-0.377	-0.319	0.536
-0.468	-0.524	0.427	0.141	-0.379	-0.393	-0.252	0.649
-0.491	-0.532	0.442	0.157	-0.384	-0.371	-0.158	0.764
-0.075	-0.148	-0.027	-0.325	-0.446	-0.492	-0.456	0.318
-0.823	-0.751	0.824	0.922	0.044	0.103	0.370	0.542
1.000	0.988	-0.699	-0.776	0.120	0.070	-0.205	-0.736
0.988	1.000	-0.667	-0.702	0.177	0.129	-0.138	-0.785
-0.699	-0.667	1.000	0.556	-0.297	-0.203	0.211	0.706
-0.776	-0.702	0.556	1.000	0.257	0.273	0.377	0.341
0.120	0.177	-0.297	0.257	1.000	0.974	0.558	-0.424
0.070	0.129	-0.203	0.273	0.974	1.000	0.709	-0.339
-0.205	-0.138	0.211	0.377	0.558	0.709	1.000	0.032
-0.736	-0.785	0.706	0.341	-0.424	-0.339	0.032	1.000
-0.488	-0.536	0.586	0.075	-0.511	-0.427	0.009	0.912
0.207	0.254	-0.399	0.184	0.968	0.923	0.460	-0.446
0.021	0.088	-0.094	0.314	0.933	0.973	0.764	-0.290
-0.118	-0.050	0.060	0.393	0.798	0.880	0.904	-0.119
-0.689	-0.718	0.778	0.366	-0.422	-0.320	0.097	0.961
-0.487	-0.516	0.661	0.173	-0.452	-0.345	0.122	0.881

For peer review only

BMJ Open: first published as 10.1136/bmjopen-2022-063051 on 8 November 2022. Downloaded from http://bmjopen.bmj.com/ on June 10, 2025 at Agence Bibliographique de l Enseignement Superieur (ABES) . Protected by copyright, including for uses related to text and data mining, AI training, and similar technologies.

MLN	GAA	absGAA	GSD	HGC	GLN
0.727	-0.627	-0.647	-0.547	0.618	0.614
0.775	-0.693	-0.688	-0.567	0.783	0.729
0.790	-0.655	-0.659	-0.541	0.727	0.698
0.706	-0.632	-0.626	-0.507	0.735	0.731
0.500	-0.443	-0.534	-0.511	0.322	0.300
0.745	-0.590	-0.639	-0.550	0.710	0.711
0.704	-0.621	-0.672	-0.584	0.685	0.681
0.753	-0.547	-0.551	-0.453	0.811	0.748
0.697	-0.622	-0.678	-0.592	0.672	0.672
0.631	-0.527	-0.607	-0.545	0.627	0.626
0.658	-0.520	-0.582	-0.515	0.670	0.664
0.708	-0.433	-0.440	-0.360	0.805	0.737
-0.009	-0.446	-0.652	-0.695	-0.029	-0.038
0.127	-0.584	-0.603	-0.549	0.180	0.158
-0.014	-0.543	-0.580	-0.547	0.038	0.024
0.022	-0.543	-0.634	-0.631	0.077	0.064
-0.028	-0.499	-0.575	-0.563	0.033	0.022
0.035	-0.495	-0.635	-0.640	0.055	0.042
0.591	-0.365	-0.368	-0.296	0.449	0.453
0.685	-0.417	-0.375	-0.265	0.560	0.551
0.804	-0.365	-0.327	-0.203	0.753	0.779
0.463	-0.436	-0.513	-0.488	0.186	0.234
0.314	-0.045	0.183	0.303	0.602	0.427
-0.488	0.207	0.021	-0.118	-0.689	-0.487
-0.536	0.254	0.088	-0.050	-0.718	-0.516
0.586	-0.399	-0.094	0.060	0.778	0.661
0.075	0.184	0.314	0.393	0.366	0.173
-0.511	0.968	0.933	0.798	-0.422	-0.452
-0.427	0.923	0.973	0.880	-0.320	-0.345
0.009	0.460	0.764	0.904	0.097	0.122
0.912	-0.446	-0.290	-0.119	0.961	0.881
1.000	-0.519	-0.372	-0.166	0.886	0.941
-0.519	1.000	0.888	0.724	-0.438	-0.459
-0.372	0.888	1.000	0.937	-0.231	-0.256
-0.166	0.724	0.937	1.000	-0.051	-0.034
0.886	-0.438	-0.231	-0.051	1.000	0.939
0.941	-0.459	-0.256	-0.034	0.939	1.000

For peer review only

BMJ Open: first published as 10.1136/bmjopen-2022-063051 on 8 November 2022. Downloaded from http://bmjopen.bmj.com/ on June 10, 2025 at Agence Bibliographique de l Enseignement Superieur (ABES) .
Protected by copyright, including for uses related to text and data mining, AI training, and similar technologies.

parameter name	patient and ane	site supplyin	site processir	IA location	IA anatomi	rupture sta	height
abbreviation	-	-	-	-	-	-	H
unit	-	-	-	-	-	1=ruptured	mm
	1	Berlin	Berlin	AComA	anterior	1	5.748
	2	Berlin	Berlin	PComA	posterior	0	8.261
	3	Berlin	Berlin	PICA	posterior	1	6.023
	4	Berlin	Berlin	AComA	anterior	1	5.698
	5	Berlin	Berlin	ACA	anterior	0	5.667
	6	Berlin	Berlin	MCA	MCA	0	2.849
	7	Berlin	Berlin	ICA	ICA	0	19.575
	8	Berlin	Berlin	MCA	MCA	0	4.199
	9	Berlin	Berlin	MCA	MCA	0	3.795
	10	Berlin	Berlin	AComA	anterior	1	5.051
	11	Berlin	Berlin	MCA	MCA	0	6.789
	12	Berlin	Berlin	ICA	ICA	1	7.610
	13	Berlin	Berlin	MCA	MCA	0	8.157
	14	Berlin	Berlin	AComA	anterior	1	2.542
	15	Berlin	Berlin	PComA	posterior	1	3.196
	16A	Berlin	Berlin	ICA	ICA	1	9.587
	16B	Berlin	Berlin	ACA	anterior	0	1.879
	17A	Berlin	Berlin	ICA	ICA	0	12.261
	17B	Berlin	Berlin	ICA	ICA	0	2.791
	17C	Berlin	Berlin	AComA	anterior	0	4.530
	18	Berlin	Berlin	MCA	MCA	1	5.597
	19	Berlin	Berlin	AComA	anterior	1	5.177
	20	Berlin	Berlin	PComA	posterior	1	10.569
	21	Berlin	Berlin	ICA	ICA	0	4.966
	22	Berlin	Berlin	ICA	ICA	0	7.908
	23	Berlin	Berlin	MCA	MCA	1	4.598
	24	Berlin	Berlin	ICA	ICA	0	2.906
	25	Berlin	Berlin	BA	posterior	0	8.473
	26	Berlin	Berlin	MCA	MCA	1	4.210
	27	Berlin	Berlin	AComA	anterior	1	4.597
	28	Berlin	Berlin	MCA	MCA	1	5.480
	29	Berlin	Berlin	ICA	ICA	0	12.780
	30A	Berlin	Berlin	ICA	ICA	0	4.078
	30B	Berlin	Berlin	AComA	anterior	0	3.135
	30C	Berlin	Berlin	AComA	anterior	1	5.085
	30D	Berlin	Berlin	MCA	MCA	0	2.715
	30E	Berlin	Berlin	PICA	posterior	1	4.983
	31	Berlin	Berlin	MCA	MCA	0	4.542
	32	Berlin	Berlin	ICA	ICA	0	9.475
	33	Berlin	Berlin	AComA	anterior	1	6.212
	34	Berlin	Berlin	AComA	anterior	0	3.383
	35	Berlin	Berlin	ICA	ICA	1	11.690
	36	Berlin	Berlin	BA	posterior	0	20.748
	37	Berlin	Berlin	AComA	anterior	1	5.543
	38	Berlin	Berlin	AComA	anterior	0	8.400
	39	Berlin	Berlin	ICA	ICA	1	4.290
	40	Berlin	Berlin	PComA	posterior	1	13.786

For peer review only

BMJ Open: first published as 10.1136/bmjopen-2022-063051 on 8 November 2022. Downloaded from http://bmjopen.bmj.com/ on June 10, 2025 at Agence Bibliographique de l Enseignement Superieur (ABES) .
Protected by copyright, including for uses related to text and data mining, AI training, and similar technologies.

41	Berlin	Berlin	AComA	anterior	1	4.301
42	Berlin	Berlin	PComA	posterior	0	5.891
43	Berlin	Berlin	ICA	ICA	0	6.872
44	Berlin	Berlin	PICA	posterior	1	4.213
45A	Berlin	Berlin	ICA	ICA	0	2.414
45B	Berlin	Berlin	ICA	ICA	1	3.501
45C	Berlin	Berlin	ICA	ICA	0	2.297
46	Berlin	Berlin	BA	posterior	0	11.175
47	Berlin	Berlin	ICA	ICA	0	4.636
48	Berlin	Berlin	MCA	MCA	0	2.204
49	Berlin	Berlin	MCA	MCA	1	16.986
50	Berlin	Berlin	PComA	posterior	1	7.588
51	Berlin	Berlin	AComA	anterior	0	5.047
52	Berlin	Berlin	ACA	anterior	1	2.779
53	Berlin	Berlin	AChA	ICA	1	6.830
54	Berlin	Berlin	PComA	posterior	1	4.857
55	Berlin	Berlin	AComA	anterior	0	3.330
56	Berlin	Berlin	MCA	MCA	1	2.092
57A	Berlin	Berlin	ICA	ICA	0	2.831
57B	Berlin	Berlin	ICA	ICA	0	4.277
57C	Berlin	Berlin	ICA	ICA	0	4.910
57D	Berlin	Berlin	AComA	anterior	1	2.565
57E	Berlin	Berlin	MCA	MCA	0	6.612
57F	Berlin	Berlin	MCA	MCA	0	1.536
57G	Berlin	Berlin	MCA	MCA	0	3.139
58	Berlin	Berlin	PComA	posterior	1	3.998
59	Berlin	Berlin	ICA	ICA	0	4.875
60A	Berlin	Berlin	MCA	MCA	0	8.547
60B	Berlin	Berlin	MCA	MCA	0	3.172
61	Berlin	Berlin	AComA	anterior	1	10.866
62	Berlin	Berlin	ICA	ICA	1	4.541
63	Berlin	Berlin	AComA	anterior	1	5.524
64	Berlin	Berlin	ICA	ICA	1	13.839
65	Berlin	Berlin	ICA	ICA	0	7.768
66	Berlin	Berlin	AComA	anterior	1	3.652
67	Berlin	Berlin	MCA	MCA	1	4.031
68	Berlin	Berlin	AComA	anterior	1	2.672
69	Berlin	Berlin	ICA	ICA	0	11.746
70	Berlin	Berlin	AComA	anterior	1	2.739
71	Berlin	Berlin	PComA	posterior	0	3.684
72A	Berlin	Berlin	PComA	posterior	0	9.969
72B	Berlin	Berlin	AComA	anterior	0	3.769
73	Berlin	Berlin	AComA	anterior	1	7.640
74	Berlin	Berlin	ICA	ICA	0	2.422
75A	Berlin	Berlin	PComA	posterior	0	2.277
75B	Berlin	Berlin	BA	posterior	1	4.556
76	Berlin	Berlin	PComA	posterior	1	4.974
77	Berlin	Berlin	MCA	MCA	0	10.165
78	Berlin	Berlin	MCA	MCA	0	5.020
79	Berlin	Berlin	ICA	ICA	0	9.202

BMJ Open: first published as 10.1136/bmjopen-2022-063051 on 8 November 2022. Downloaded from http://bmjopen.bmj.com/ on June 10, 2025 at Agence Bibliographique de l Enseignement Superieur (ABES) .
Protected by copyright, including for uses related to text and data mining, AI training, and similar technologies.
For peer review only

80	Berlin	Berlin	AComA	anterior	1	8.132
81	Berlin	Berlin	ICA	ICA	0	21.514
82A	Berlin	Berlin	ICA	ICA	0	2.039
82B	Berlin	Berlin	MCA	MCA	0	3.698
82C	Berlin	Berlin	ACA	anterior	0	1.486
83	Berlin	Berlin	PComA	posterior	0	10.503
84A	Berlin	Berlin	ICA	ICA	0	6.331
84B	Berlin	Berlin	MCA	MCA	0	3.509
85	Berlin	Berlin	MCA	MCA	0	2.996
86	Berlin	Berlin	MCA	MCA	0	2.575
87	Berlin	Berlin	AComA	anterior	1	3.971
88A	Berlin	Berlin	MCA	MCA	0	1.489
88B	Berlin	Berlin	MCA	MCA	0	2.304
89	Berlin	Berlin	ICA	ICA	0	5.728
90	Berlin	Berlin	MCA	MCA	0	4.016
91	Berlin	Berlin	AComA	anterior	0	6.147
92	Berlin	Berlin	PComA	posterior	0	7.023
93	Berlin	Berlin	PComA	posterior	1	10.373
94	Berlin	Berlin	MCA	MCA	0	19.183
95	Berlin	Berlin	AComA	anterior	1	6.261
96	Berlin	Berlin	ICA	ICA	0	5.202
97A	Berlin	Berlin	ICA	ICA	0	1.702
97B	Berlin	Berlin	AComA	anterior	0	5.381
98	Berlin	Berlin	PICA	posterior	1	4.524
99	Berlin	Berlin	PComA	posterior	0	6.067
100A	Berlin	Berlin	MCA	MCA	1	6.738
100B	Berlin	Berlin	ICA	ICA	0	2.364
100C	Berlin	Berlin	ICA	ICA	0	8.467
100D	Berlin	Berlin	MCA	MCA	0	2.488
100E	Berlin	Berlin	MCA	MCA	0	1.914
101	Berlin	Berlin	PComA	posterior	1	5.048
102	Berlin	Berlin	AComA	anterior	1	5.931
103	Berlin	Berlin	PCA	posterior	1	5.602
104	Berlin	Berlin	MCA	MCA	0	4.629
105	Berlin	Berlin	ICA	ICA	1	7.092
106	Berlin	Berlin	MCA	MCA	1	8.177
107	Berlin	Berlin	PComA	posterior	1	8.598
108	Berlin	Berlin	AComA	anterior	1	3.886
109	Berlin	Berlin	BA	posterior	1	13.918
110	Berlin	Berlin	BA	posterior	0	12.591
111	Berlin	Berlin	AComA	anterior	0	6.025
112	Berlin	Berlin	BA	posterior	1	7.000
113A	Berlin	Berlin	MCA	MCA	0	9.488
113B	Berlin	Berlin	MCA	MCA	0	6.242
114	Berlin	Berlin	MCA	MCA	1	3.622
115A	Hanover	Magdeburg	MCA	MCA	1	4.340
115B	Hanover	Magdeburg	MCA	MCA	0	1.149
116A	Hanover	Magdeburg	AComA	anterior	1	4.055
116B	Hanover	Magdeburg	AComA	anterior	0	1.031
117A	Hanover	Magdeburg	BA	posterior	1	8.476

BMJ Open: first published as 10.1136/bmjopen-2022-063051 on 8 November 2022. Downloaded from http://bmjopen.bmj.com/ on June 10, 2025 at Agence Bibliographique de l Enseignement Superieur (ABES) .
Protected by copyright, including for uses related to text and data mining, AI training, and similar technologies.

117B	Hanover	Magdeburg	AComA	anterior	0	4.088
118A	Hanover	Magdeburg	AComA	anterior	0	5.039
118B	Hanover	Magdeburg	PComA	posterior	1	4.528
119	Hanover	Magdeburg	MCA	MCA	1	1.132
120A	Hanover	Magdeburg	MCA	MCA	1	4.881
120B	Hanover	Magdeburg	ICA	ICA	1	2.325
121	Hanover	Magdeburg	ICA	ICA	1	18.704
122	Hanover	Magdeburg	ICA	ICA	0	6.667
123A	Hanover	Magdeburg	PComA	posterior	1	5.230
123B	Hanover	Magdeburg	MCA	MCA	0	2.984
124A	Hanover	Magdeburg	ACA	anterior	1	2.914
124B	Hanover	Magdeburg	AComA	anterior	0	1.201
124C	Hanover	Magdeburg	AComA	anterior	0	2.671
125	Hanover	Magdeburg	ICA	ICA	0	7.204
126A	Hanover	Magdeburg	MCA	MCA	1	8.466
126B	Hanover	Magdeburg	MCA	MCA	0	5.410
127A	Hanover	Magdeburg	AComA	anterior	1	2.663
127B	Hanover	Magdeburg	MCA	MCA	0	2.098
128A	Hanover	Magdeburg	ICA	ICA	1	1.429
128B	Hanover	Magdeburg	ICA	ICA	0	1.275
129A	Hanover	Magdeburg	BA	posterior	1	2.818
129B	Hanover	Magdeburg	SCA	posterior	0	1.293
130A	Hanover	Magdeburg	MCA	MCA	1	7.171
130B	Hanover	Magdeburg	AComA	anterior	0	4.247
131A	Hanover	Magdeburg	BA	posterior	0	4.863
131B	Hanover	Magdeburg	BA	posterior	1	3.992
132A	Hanover	Magdeburg	PComA	posterior	0	4.359
132B	Hanover	Magdeburg	AComA	anterior	1	16.578
133A	Hanover	Magdeburg	BA	posterior	1	6.042
133B	Hanover	Magdeburg	AComA	anterior	0	3.105
134A	Hanover	Magdeburg	MCA	MCA	1	6.298
134B	Hanover	Magdeburg	MCA	MCA	0	3.067
135	Hanover	Magdeburg	ICA	ICA	0	2.406
136A	Kiel	Magdeburg	MCA	MCA	0	1.108
136B	Kiel	Magdeburg	MCA	MCA	0	6.352
137	Kiel	Magdeburg	MCA	MCA	0	3.274
138	Kiel	Magdeburg	MCA	MCA	0	4.033
139	Kiel	Magdeburg	MCA	MCA	0	6.259
140	Kiel	Magdeburg	MCA	MCA	0	10.513
141	Kiel	Magdeburg	MCA	MCA	0	8.471
142	Kiel	Magdeburg	MCA	MCA	0	6.008
143	Kiel	Magdeburg	MCA	MCA	0	5.184
144	Kiel	Magdeburg	MCA	MCA	0	10.421
145	Kiel	Magdeburg	MCA	MCA	0	8.720
146A	Kiel	Magdeburg	MCA	MCA	0	6.242
146B	Kiel	Magdeburg	ACA	anterior	0	2.012
147A	Kiel	Magdeburg	MCA	MCA	0	5.580
147B	Kiel	Magdeburg	MCA	MCA	0	0.684
147C	Kiel	Magdeburg	MCA	MCA	0	0.573
147D	Kiel	Magdeburg	ACA	anterior	0	3.651

For peer review only

BMJ Open: first published as 10.1136/bmjopen-2022-063051 on 8 November 2022. Downloaded from http://bmjopen.bmj.com/ on June 10, 2025 at Agence Bibliographique de l Enseignement Superieur (ABES) .
Protected by copyright, including for uses related to text and data mining, AI training, and similar technologies.

147E	Kiel	Magdeburg	AComA	anterior	0	1.213
147F	Kiel	Magdeburg	AComA	anterior	0	1.384
148	Kiel	Magdeburg	MCA	MCA	0	4.650
149	Kiel	Magdeburg	MCA	MCA	0	6.489
150	Kiel	Magdeburg	MCA	MCA	0	4.962
151	Kiel	Magdeburg	MCA	MCA	0	3.962
152	Magdeburg	Magdeburg	MCA	MCA	0	5.866
153	Magdeburg	Magdeburg	ACA	anterior	1	3.594
154	Magdeburg	Magdeburg	PComA	posterior	1	9.941
155A	Magdeburg	Magdeburg	AComA	anterior	1	2.543
155B	Magdeburg	Magdeburg	AComA	anterior	0	3.589
155C	Magdeburg	Magdeburg	MCA	MCA	0	5.120
156A	Magdeburg	Magdeburg	ICA	ICA	0	7.048
156B	Magdeburg	Magdeburg	ICA	ICA	0	1.214
156C	Magdeburg	Magdeburg	ICA	ICA	0	1.765
156D	Magdeburg	Magdeburg	ICA	ICA	0	2.037
157	Magdeburg	Magdeburg	VA	posterior	1	5.194
158	Magdeburg	Magdeburg	AChA	ICA	0	3.248
159	Magdeburg	Magdeburg	MCA	MCA	0	5.645
160A	Magdeburg	Magdeburg	AChA	ICA	1	2.988
160B	Magdeburg	Magdeburg	ICA	ICA	0	2.842
161A	Magdeburg	Magdeburg	ICA	ICA	1	5.684
161B	Magdeburg	Magdeburg	ICA	ICA	0	2.089
161C	Magdeburg	Magdeburg	PICA	posterior	0	2.497
162	Magdeburg	Magdeburg	AChA	ICA	1	4.811
163	Magdeburg	Magdeburg	ICA	ICA	0	4.981
164	Magdeburg	Magdeburg	MCA	MCA	0	3.817
165A	Magdeburg	Magdeburg	MCA	MCA	0	3.419
165B	Magdeburg	Magdeburg	PComA	posterior	0	5.533
165C	Magdeburg	Magdeburg	BA	posterior	0	2.856
165D	Magdeburg	Magdeburg	SCA	posterior	1	4.595
166	Magdeburg	Magdeburg	ICA	ICA	0	3.638
167	Magdeburg	Magdeburg	ICA	ICA	0	3.481
168	Magdeburg	Magdeburg	ICA	ICA	0	6.061
169	Magdeburg	Magdeburg	ICA	ICA	0	7.142
170	Magdeburg	Magdeburg	ICA	ICA	0	5.557
171	Magdeburg	Magdeburg	ICA	ICA	0	11.276
172A	Magdeburg	Magdeburg	AComA	anterior	1	3.283
172B	Magdeburg	Magdeburg	MCA	MCA	0	2.319
173A	Magdeburg	Magdeburg	MCA	MCA	1	4.176
173B	Magdeburg	Magdeburg	ICA	ICA	0	3.188
174	Magdeburg	Magdeburg	ICA	ICA	0	3.711
175	Magdeburg	Magdeburg	MCA	MCA	0	4.156
176	Magdeburg	Magdeburg	AComA	anterior	0	3.397
177A	Magdeburg	Magdeburg	PComA	posterior	1	6.322
177B	Magdeburg	Magdeburg	BA	posterior	0	1.516
178	Magdeburg	Magdeburg	MCA	MCA	1	5.269

For peer review only

BMJ Open: first published as 10.1136/bmjopen-2022-063051 on 8 November 2022. Downloaded from http://bmjopen.bmj.com/ on June 10, 2025 at Agence Bibliographique de l Enseignement Superieur (ABES) . Protected by copyright, including for uses related to text and data mining, AI training, and similar technologies.

maximum c	maximum h	maximum c	bulge heigh	surface are	convex hull	minimal bo	closed aneu	volume
L_max	H_max	D_max	H_b	A	A_CH	A_MBS	A_closed	V
mm	mm	mm	mm	cm^2	cm^2	cm^2	cm^2	ml
6.629	5.790	5.713	0.877	0.887	1.018	1.495	1.003	0.083
11.888	8.544	10.931	3.003	2.391	2.722	4.652	2.537	0.269
7.306	6.133	4.862	0.313	0.742	0.914	1.677	0.888	0.064
7.867	6.544	7.165	3.567	1.018	1.146	1.979	1.122	0.097
7.336	6.315	6.104	1.929	0.888	1.022	1.749	1.014	0.085
6.275	4.482	5.783	0.575	0.693	0.906	1.269	0.900	0.074
23.888	20.508	23.475	9.621	12.495	13.243	18.371	13.239	4.106
6.597	4.534	6.403	1.473	0.746	0.934	1.422	0.924	0.076
5.837	3.939	5.183	0.070	0.568	0.802	1.099	0.795	0.060
6.518	5.449	5.861	2.398	0.713	0.822	1.338	0.809	0.059
8.495	6.902	7.441	3.391	1.540	1.813	2.341	1.803	0.215
11.246	9.797	10.200	3.153	1.755	1.899	3.981	1.853	0.195
11.394	8.611	10.972	4.429	2.218	2.475	4.079	2.459	0.334
7.308	4.479	7.292	0.287	0.574	0.844	1.684	0.826	0.059
4.672	3.411	4.157	0.033	0.354	0.489	0.729	0.486	0.027
13.627	11.834	11.081	4.341	3.153	3.480	5.839	3.381	0.526
2.875	1.899	2.875	0.057	0.126	0.180	0.276	0.178	0.006
14.303	12.591	12.333	6.473	3.921	4.285	6.591	4.242	0.730
3.763	2.874	3.382	1.302	0.281	0.342	0.445	0.341	0.018
5.669	4.725	4.473	2.104	0.553	0.648	1.015	0.643	0.044
7.910	6.289	6.673	3.770	1.024	1.175	1.970	1.151	0.101
6.439	5.233	5.830	1.474	0.815	0.991	1.327	0.978	0.081
12.632	11.229	10.859	3.425	3.001	3.307	5.029	3.293	0.523
8.453	6.020	7.820	1.936	0.987	1.244	2.245	1.236	0.112
9.521	8.035	9.229	3.504	2.125	2.439	2.878	2.433	0.344
8.530	5.733	7.294	1.949	1.050	1.420	2.328	1.397	0.132
4.793	3.005	4.741	0.075	0.310	0.479	0.797	0.470	0.025
14.667	10.280	13.848	1.293	4.122	5.440	6.782	5.419	1.129
7.677	4.990	6.526	2.190	0.873	1.094	1.890	1.060	0.085
8.500	5.691	8.412	2.083	1.088	1.325	2.270	1.310	0.124
10.420	6.548	10.246	2.938	1.204	1.480	3.411	1.377	0.112
15.754	13.711	11.401	3.704	3.516	3.937	7.802	3.868	0.564
6.137	4.508	5.343	2.007	0.663	0.820	1.184	0.817	0.063
6.677	3.854	6.460	1.201	0.590	0.769	1.402	0.757	0.054
6.751	5.481	4.736	1.330	0.577	0.716	1.432	0.696	0.045
3.661	2.760	3.246	1.172	0.232	0.303	0.424	0.301	0.014
6.655	5.163	5.034	1.727	0.691	0.832	1.391	0.823	0.062
8.135	5.839	7.993	1.423	1.186	1.438	2.167	1.417	0.142
16.986	10.740	15.845	2.213	5.926	6.882	9.209	6.869	1.564
7.950	6.713	6.080	1.989	1.030	1.244	2.022	1.224	0.108
5.212	3.563	5.005	0.689	0.483	0.669	0.895	0.665	0.046
12.891	11.777	8.932	5.558	2.584	2.875	5.260	2.844	0.398
24.926	21.090	22.734	9.915	14.654	15.321	19.652	15.279	5.424
8.946	6.977	8.075	2.268	1.298	1.555	2.541	1.527	0.157
14.786	10.742	14.206	1.633	2.875	3.216	6.868	3.132	0.407
6.715	5.085	5.948	1.913	0.712	0.843	1.420	0.839	0.066
15.827	13.957	14.042	6.937	5.487	5.906	7.992	5.870	1.249

For peer review only

BMJ Open: first published as 10.1136/bmjopen-2022-063051 on 8 November 2022. Downloaded from http://bmjopen.bmj.com/ on June 10, 2025 at Agence Bibliographique de l Enseignement Superieur (ABES) .
Protected by copyright, including for uses related to text and data mining, AI training, and similar technologies.

6.419	4.551	6.134	0.624	0.618	0.839	1.316	0.813	0.058
8.062	6.217	6.768	2.455	1.126	1.368	2.042	1.365	0.137
17.188	10.658	16.238	2.250	3.236	4.445	9.425	4.430	0.696
7.303	4.996	6.301	1.470	0.688	0.925	1.676	0.910	0.072
4.605	2.692	4.603	0.037	0.296	0.466	0.713	0.462	0.023
4.605	3.619	3.564	1.963	0.355	0.438	0.677	0.430	0.023
4.653	2.599	4.537	0.354	0.303	0.480	0.698	0.475	0.025
13.326	11.629	11.342	5.799	3.546	3.816	5.596	3.800	0.658
7.105	4.947	6.019	0.113	0.678	0.891	1.586	0.882	0.061
4.777	2.888	4.516	0.482	0.282	0.439	0.727	0.433	0.023
18.334	17.219	14.463	8.226	5.638	6.064	10.560	5.978	1.232
11.513	9.974	11.050	4.580	2.241	2.481	4.240	2.396	0.285
6.880	5.489	6.061	2.068	0.829	0.999	1.492	0.993	0.086
4.149	2.840	3.778	0.926	0.297	0.384	0.541	0.382	0.021
11.234	7.779	10.623	2.600	2.129	2.279	3.965	2.254	0.282
6.535	5.085	5.126	0.262	0.507	0.706	1.400	0.685	0.041
6.195	3.881	6.006	0.616	0.577	0.840	1.210	0.829	0.061
4.282	2.759	3.841	0.151	0.216	0.331	0.590	0.325	0.013
5.968	3.703	5.938	1.423	0.517	0.678	1.119	0.668	0.043
4.773	4.310	4.200	2.368	0.467	0.513	0.771	0.506	0.031
9.479	6.686	9.469	2.116	1.305	1.446	2.823	1.429	0.139
4.362	2.739	4.165	0.197	0.326	0.447	0.600	0.445	0.025
7.928	6.831	6.578	2.903	1.256	1.465	2.026	1.456	0.154
2.798	1.593	2.792	0.014	0.105	0.170	0.266	0.167	0.005
6.330	3.703	6.047	0.954	0.580	0.806	1.259	0.803	0.058
7.668	6.509	6.943	1.249	0.852	1.054	1.873	0.999	0.070
8.038	5.767	7.357	1.708	0.972	1.152	2.030	1.143	0.103
13.384	9.880	12.864	3.835	3.174	3.751	5.854	3.690	0.603
4.583	3.361	4.077	0.084	0.364	0.502	0.704	0.498	0.030
13.573	12.129	7.940	6.398	2.411	2.619	5.788	2.564	0.328
6.253	4.782	5.560	2.596	0.679	0.785	1.232	0.782	0.060
6.774	5.738	4.776	1.687	0.752	0.882	1.467	0.876	0.070
19.580	14.862	19.183	7.524	7.554	7.889	12.044	7.851	1.917
10.702	7.977	8.927	2.139	2.019	2.495	3.606	2.481	0.325
6.698	4.629	5.540	0.489	0.576	0.764	1.410	0.757	0.055
6.354	4.692	5.177	1.312	0.626	0.795	1.289	0.776	0.053
6.204	3.207	6.016	0.114	0.413	0.706	1.215	0.694	0.044
14.376	13.009	10.934	6.325	2.638	2.994	6.492	2.830	0.343
6.016	4.460	5.142	0.926	0.678	0.873	1.149	0.866	0.071
5.832	3.890	5.511	0.286	0.536	0.691	1.071	0.684	0.046
14.708	12.119	12.964	4.615	3.419	3.829	6.796	3.791	0.609
5.100	3.825	4.479	0.525	0.452	0.611	0.840	0.603	0.038
10.529	8.923	7.517	2.011	1.266	1.421	3.483	1.355	0.113
6.886	3.607	6.764	0.185	0.510	0.851	1.490	0.837	0.060
4.974	3.155	4.670	0.739	0.312	0.487	0.792	0.479	0.026
6.182	5.235	3.884	2.072	0.422	0.503	1.203	0.487	0.025
8.405	5.927	8.296	2.748	1.255	1.408	2.270	1.385	0.133
15.254	10.492	15.251	1.120	3.825	4.559	7.665	4.507	0.804
7.735	5.096	7.199	1.289	0.956	1.265	1.925	1.236	0.115
11.062	9.776	9.388	5.048	2.352	2.598	3.900	2.577	0.353

For peer review only

BMJ Open: first published as 10.1136/bmjopen-2022-063051 on 8 November 2022. Downloaded from http://bmjopen.bmj.com/ on June 10, 2025 at Agence Bibliographique de l Enseignement Superieur (ABES) .
Protected by copyright, including for uses related to text and data mining, AI training, and similar technologies.

9.022	8.308	5.532	5.605	1.258	1.403	2.566	1.369	0.125
32.342	25.628	30.344	9.085	21.842	22.485	32.901	22.541	9.061
3.400	2.107	3.340	0.103	0.171	0.249	0.382	0.247	0.010
5.047	4.006	3.660	0.257	0.368	0.480	0.802	0.479	0.028
3.134	1.819	3.062	0.002	0.128	0.204	0.325	0.203	0.007
13.558	11.007	11.469	5.880	3.372	4.048	5.907	3.950	0.645
8.282	6.772	7.749	2.957	1.357	1.578	2.227	1.567	0.170
5.390	3.909	3.582	0.036	0.363	0.503	0.917	0.497	0.029
5.401	3.552	5.038	1.301	0.435	0.613	0.917	0.611	0.042
3.966	2.604	3.799	0.123	0.269	0.369	0.506	0.368	0.019
5.633	4.386	4.464	0.942	0.531	0.621	1.001	0.614	0.039
3.149	1.664	3.147	0.170	0.102	0.155	0.311	0.153	0.005
3.784	2.577	3.258	0.475	0.191	0.258	0.454	0.256	0.011
7.951	6.459	5.903	0.045	0.885	1.210	2.142	1.167	0.093
6.817	4.506	6.387	1.055	0.691	0.886	1.462	0.880	0.067
7.784	6.322	6.895	2.712	1.231	1.415	1.903	1.412	0.152
12.441	7.739	12.162	1.572	2.313	2.941	4.898	2.904	0.402
16.422	12.513	15.861	2.894	4.492	4.998	8.482	4.966	0.797
27.009	21.425	25.069	8.693	14.959	16.042	22.918	16.010	5.763
8.947	7.350	6.990	2.234	1.135	1.351	2.515	1.341	0.128
13.291	8.491	13.104	0.615	2.474	3.251	5.883	3.166	0.379
5.671	2.993	5.671	0.100	0.283	0.495	1.011	0.489	0.019
8.214	5.554	7.968	1.932	1.237	1.574	2.124	1.572	0.170
5.584	4.790	4.319	2.528	0.481	0.539	0.980	0.527	0.031
9.725	6.554	9.274	1.314	1.459	1.953	2.971	1.944	0.238
16.284	12.471	15.055	0.726	3.620	4.000	8.331	3.963	0.645
3.707	2.472	3.379	0.531	0.221	0.311	0.445	0.309	0.014
16.159	11.384	16.159	4.627	3.858	4.256	8.203	4.029	0.506
4.053	2.688	3.620	0.707	0.258	0.349	0.516	0.347	0.016
3.744	1.985	3.743	0.076	0.186	0.285	0.442	0.282	0.011
6.956	5.626	4.803	1.591	0.669	0.821	1.525	0.808	0.058
7.936	6.362	7.128	3.081	1.178	1.318	2.163	1.302	0.120
9.195	6.126	7.318	1.738	1.708	1.836	2.661	1.858	0.209
17.009	8.810	16.189	0.942	2.437	3.849	9.088	3.752	0.562
9.263	7.602	7.208	3.536	1.222	1.383	2.696	1.338	0.114
10.514	8.759	7.409	3.082	1.494	1.771	3.482	1.712	0.151
10.231	8.838	7.094	2.851	1.488	1.803	3.372	1.739	0.166
6.100	4.339	5.591	0.679	0.516	0.732	1.220	0.722	0.048
17.012	13.949	16.935	6.552	6.058	6.416	9.100	6.386	1.433
18.621	14.380	14.373	6.548	4.829	5.408	10.893	5.328	0.999
9.774	6.785	8.878	1.968	1.741	2.204	3.001	2.190	0.285
10.375	7.553	9.325	3.307	1.779	2.280	3.443	2.262	0.286
11.542	9.849	7.908	4.661	2.103	2.433	4.190	2.390	0.308
8.757	6.907	8.753	2.415	1.552	1.848	2.420	1.841	0.224
6.793	4.234	6.753	0.367	0.597	0.920	1.502	0.910	0.068
6.195	5.019	5.753	2.072	0.634	0.738	1.213	0.721	0.049
2.123	1.222	2.050	0.099	0.062	0.091	0.144	0.089	0.002
7.276	4.568	7.267	1.827	0.795	0.957	1.663	0.935	0.073
2.744	1.425	2.563	0.133	0.078	0.128	0.237	0.123	0.003
10.853	8.721	9.956	2.319	2.269	2.569	3.723	2.547	0.342

For peer review only

BMJ Open: first published as 10.1136/bmjopen-2022-063051 on 8 November 2022. Downloaded from http://bmjopen.bmj.com/ on June 10, 2025 at Agence Bibliographique de l Enseignement Superieur (ABES) . Protected by copyright, including for uses related to text and data mining, AI training, and similar technologies.

6.386	4.271	6.267	1.450	0.622	0.798	1.282	0.779	0.052
7.385	6.025	5.712	3.287	0.847	0.981	1.714	0.961	0.077
6.224	4.693	5.826	1.532	0.584	0.710	1.218	0.686	0.040
2.739	1.458	2.699	0.000	0.079	0.137	0.248	0.129	0.003
6.758	5.613	6.202	3.057	0.747	0.850	1.552	0.826	0.060
8.335	5.295	8.154	0.578	0.472	0.673	2.182	0.626	0.032
24.223	19.791	22.453	9.808	12.666	13.149	18.524	13.126	4.170
9.429	7.753	9.246	3.668	1.763	2.018	2.881	1.991	0.233
7.279	5.501	6.496	1.296	0.962	1.180	1.701	1.156	0.093
4.951	3.068	4.238	0.721	0.311	0.403	0.770	0.396	0.018
3.677	3.075	2.630	1.197	0.197	0.240	0.431	0.230	0.008
3.184	1.674	2.913	0.185	0.096	0.166	0.322	0.159	0.004
4.432	3.209	4.075	1.200	0.283	0.349	0.626	0.346	0.016
8.784	7.818	6.956	3.946	1.370	1.477	2.435	1.460	0.148
13.905	9.021	13.148	0.801	2.857	3.336	6.331	3.136	0.362
7.117	5.697	7.117	1.111	0.959	1.100	1.716	1.067	0.083
4.398	3.418	3.652	1.122	0.260	0.319	0.609	0.314	0.014
4.263	2.616	3.714	0.022	0.236	0.323	0.576	0.316	0.014
3.378	1.853	3.377	0.224	0.119	0.210	0.389	0.196	0.005
5.130	2.891	4.336	0.308	0.177	0.292	0.827	0.275	0.008
5.027	3.392	4.348	1.368	0.315	0.392	0.795	0.385	0.019
2.603	1.519	2.548	0.128	0.096	0.144	0.214	0.138	0.004
8.733	7.733	5.173	2.236	1.000	1.104	2.399	1.082	0.087
6.282	4.788	4.997	1.219	0.529	0.634	1.242	0.623	0.038
6.960	6.297	6.263	3.045	0.617	0.691	1.556	0.649	0.035
6.109	4.679	5.536	1.914	0.602	0.685	1.173	0.680	0.047
8.258	5.056	7.901	0.962	0.957	1.190	2.143	1.166	0.099
21.893	19.479	15.008	5.305	5.825	6.171	15.090	6.046	1.094
7.690	6.527	5.130	2.092	0.820	0.984	1.861	0.906	0.058
4.236	3.327	2.935	1.359	0.267	0.320	0.564	0.310	0.014
7.909	6.999	6.604	1.846	1.191	1.329	1.991	1.306	0.123
5.815	3.677	4.000	0.846	0.324	0.434	1.062	0.406	0.019
7.097	4.213	6.014	0.103	0.332	0.541	1.582	0.515	0.023
2.628	1.504	2.617	0.126	0.075	0.129	0.227	0.120	0.003
6.801	6.385	4.171	3.307	0.723	0.806	1.476	0.797	0.058
5.605	3.754	5.144	1.846	0.487	0.608	0.987	0.597	0.037
6.085	4.188	5.097	1.013	0.566	0.707	1.164	0.693	0.046
10.066	6.868	9.700	2.978	1.972	2.370	3.227	2.338	0.291
11.565	10.869	9.066	5.115	2.694	2.806	4.206	2.801	0.417
10.003	8.861	9.695	3.555	2.151	2.310	3.143	2.295	0.306
6.948	6.210	4.669	2.279	0.766	0.840	1.517	0.825	0.061
8.098	6.481	7.268	3.584	1.033	1.168	2.064	1.144	0.093
15.923	12.736	11.639	3.653	3.319	3.922	7.966	3.711	0.511
9.220	8.728	6.525	5.970	1.325	1.489	2.729	1.424	0.127
8.947	7.049	8.891	2.469	1.606	1.828	2.595	1.814	0.208
3.410	2.529	3.319	1.196	0.188	0.222	0.369	0.217	0.008
6.977	5.759	5.449	1.556	0.777	0.934	1.530	0.903	0.066
1.627	0.900	1.540	0.310	0.031	0.050	0.090	0.047	0.001
1.571	0.846	1.511	0.124	0.026	0.044	0.080	0.041	0.001
4.670	3.829	3.715	0.862	0.374	0.442	0.707	0.433	0.023

BMJ Open: first published as 10.1136/bmjopen-2022-063051 on 8 November 2022. Downloaded from http://bmjopen.bmj.com/ on June 10, 2025 at Agence Bibliographique de l Enseignement Superieur (ABES) .
Protected by copyright, including for uses related to text and data mining, AI training, and similar technologies.

2.495	1.472	2.180	0.087	0.072	0.103	0.196	0.100	0.002
2.449	1.457	2.325	0.046	0.086	0.131	0.194	0.125	0.003
9.599	6.040	9.240	1.954	1.225	1.478	2.895	1.465	0.128
7.998	6.644	5.913	3.660	1.019	1.183	2.072	1.148	0.100
7.328	5.848	5.773	2.070	0.814	0.905	1.687	0.887	0.066
6.486	5.072	6.312	0.846	0.639	0.755	1.334	0.750	0.052
7.722	6.054	7.580	2.357	1.147	1.296	1.910	1.270	0.117
4.784	3.869	4.102	1.291	0.329	0.390	0.719	0.383	0.019
15.603	11.496	14.341	7.003	4.024	4.638	7.675	4.569	0.809
5.647	3.274	5.306	0.026	0.355	0.466	1.003	0.451	0.021
4.724	3.696	4.160	1.815	0.429	0.518	0.707	0.510	0.030
6.943	5.844	5.841	1.209	0.657	0.807	1.560	0.764	0.049
11.331	8.473	9.336	2.050	1.711	1.957	4.035	1.938	0.218
3.405	1.788	3.124	0.171	0.121	0.195	0.369	0.189	0.005
3.375	1.970	3.356	0.117	0.146	0.221	0.377	0.215	0.007
2.674	2.099	2.427	0.125	0.119	0.164	0.251	0.160	0.005
6.651	5.678	4.727	3.075	0.642	0.716	1.397	0.705	0.049
4.557	3.452	4.551	1.438	0.388	0.466	0.672	0.457	0.025
6.241	5.711	6.021	2.024	0.837	0.928	1.273	0.922	0.073
4.200	3.054	3.431	0.180	0.273	0.358	0.574	0.350	0.016
4.277	3.071	4.011	1.379	0.341	0.433	0.576	0.427	0.023
7.789	6.371	6.026	2.151	0.819	0.987	1.906	0.932	0.060
2.779	2.123	2.323	0.573	0.137	0.172	0.243	0.171	0.006
3.590	2.777	3.414	1.580	0.240	0.286	0.408	0.278	0.012
6.957	6.079	6.471	2.907	0.713	0.780	1.524	0.750	0.048
5.784	5.145	4.269	1.733	0.498	0.560	1.051	0.547	0.030
5.795	4.770	4.652	1.961	0.401	0.530	1.068	0.476	0.021
5.333	3.786	4.835	0.986	0.424	0.507	0.893	0.498	0.028
7.607	6.500	4.457	3.691	0.723	0.793	1.818	0.773	0.053
4.095	3.019	3.578	1.043	0.276	0.374	0.556	0.364	0.017
5.900	5.509	4.218	3.215	0.545	0.570	1.098	0.557	0.031
5.574	3.949	5.005	1.532	0.505	0.630	0.977	0.624	0.041
5.053	3.735	4.455	1.533	0.398	0.461	0.803	0.454	0.025
9.075	6.193	9.068	2.564	1.532	1.753	2.802	1.731	0.191
7.748	7.232	7.453	3.980	1.306	1.395	1.963	1.378	0.139
7.203	5.799	5.440	1.852	0.826	0.957	1.631	0.925	0.070
15.720	12.308	14.026	4.352	4.479	5.063	7.782	5.036	0.977
5.186	4.052	3.267	1.796	0.280	0.347	0.845	0.322	0.012
5.388	2.932	4.739	0.773	0.335	0.421	0.912	0.407	0.018
6.487	5.148	5.922	1.965	0.654	0.765	1.340	0.742	0.050
5.446	3.837	5.297	1.539	0.461	0.549	0.932	0.537	0.031
4.406	3.846	4.243	1.228	0.391	0.445	0.653	0.440	0.025
5.714	4.684	5.562	1.815	0.544	0.612	1.026	0.588	0.034
5.047	4.191	3.070	1.619	0.276	0.311	0.801	0.289	0.012
7.755	6.941	4.725	4.013	0.823	0.909	1.891	0.893	0.066
2.901	1.778	2.668	0.019	0.107	0.158	0.278	0.150	0.004
6.661	5.753	4.657	1.227	0.646	0.769	1.394	0.738	0.048

For peer review only

BMJ Open: first published as 10.1136/bmjopen-2022-063051 on 8 November 2022. Downloaded from http://bmjopen.bmj.com/ on June 10, 2025 at Agence Bibliographique de l Enseignement Superieur (ABES) .
Protected by copyright, including for uses related to text and data mining, AI training, and similar technologies.

convex hull	minimal bo	minimum n	maximum r	neck perim	equivalent	neck area	elliptical ne	aspect ratic
V_CH	V_MBS	D_neck,mir	D_neck,ma:	P_neck	D_neck,equ	A_neck	A_neck,elli	AR
ml	ml	mm	mm	mm	mm	cm^2	cm^2	-
0.091	0.172	2.903	3.885	13.086	3.537	0.116	0.089	1.479
0.372	0.943	2.992	5.434	17.029	3.417	0.145	0.128	1.520
0.071	0.204	3.276	4.862	14.831	3.926	0.146	0.125	1.239
0.105	0.262	2.412	3.903	13.317	3.147	0.105	0.074	1.460
0.087	0.217	2.835	4.497	15.471	3.260	0.126	0.100	1.260
0.076	0.134	4.243	5.252	19.040	4.336	0.206	0.175	0.543
4.299	7.404	7.102	11.374	37.990	7.833	0.744	0.634	1.721
0.080	0.160	2.937	5.732	18.940	3.767	0.178	0.132	0.733
0.062	0.108	3.700	5.163	19.585	4.624	0.226	0.150	0.735
0.062	0.145	3.135	3.555	11.360	3.390	0.096	0.088	1.421
0.219	0.337	4.061	6.687	22.302	4.713	0.263	0.213	1.015
0.211	0.747	2.896	4.022	12.395	3.169	0.098	0.091	1.892
0.343	0.775	4.591	6.207	19.420	4.961	0.241	0.224	1.314
0.064	0.205	3.911	6.350	21.036	4.791	0.252	0.195	0.400
0.028	0.058	3.525	4.157	13.267	3.968	0.132	0.115	0.769
0.567	1.327	4.216	6.408	19.835	4.605	0.228	0.212	1.496
0.006	0.014	1.920	2.875	8.841	2.356	0.052	0.043	0.654
0.765	1.591	5.778	6.676	22.660	5.667	0.321	0.303	1.837
0.018	0.028	2.370	2.886	9.061	2.653	0.060	0.054	0.967
0.045	0.096	2.781	3.684	11.481	3.120	0.090	0.080	1.230
0.110	0.260	3.374	4.360	13.771	3.700	0.127	0.116	1.284
0.085	0.144	4.129	4.939	15.345	4.263	0.164	0.160	1.048
0.535	1.061	5.283	6.859	21.247	5.494	0.292	0.285	1.541
0.116	0.316	4.399	6.782	20.002	4.982	0.249	0.234	0.732
0.349	0.459	5.692	6.345	21.843	5.642	0.308	0.284	1.246
0.144	0.334	5.051	7.400	24.248	5.730	0.347	0.294	0.621
0.027	0.067	3.554	4.752	15.381	4.143	0.159	0.133	0.612
1.148	1.661	6.103	13.945	53.525	9.693	1.297	0.668	0.608
0.096	0.244	3.241	5.421	18.057	4.145	0.187	0.138	0.776
0.131	0.322	4.742	5.937	19.016	4.669	0.222	0.221	0.774
0.140	0.592	3.148	5.233	16.748	4.119	0.172	0.129	1.047
0.640	2.049	6.067	6.812	24.497	5.741	0.352	0.325	1.876
0.065	0.121	3.929	4.537	15.469	3.986	0.154	0.140	0.899
0.057	0.156	2.964	5.044	16.782	3.982	0.167	0.117	0.622
0.049	0.161	2.859	4.073	13.567	3.522	0.119	0.091	1.249
0.015	0.026	2.338	3.094	9.103	3.028	0.069	0.057	0.878
0.065	0.154	3.388	4.395	14.337	3.683	0.132	0.117	1.134
0.150	0.300	4.221	5.874	20.243	4.553	0.230	0.195	0.773
1.618	2.628	7.460	14.252	45.129	8.355	0.943	0.835	0.665
0.118	0.270	3.389	5.919	16.909	4.575	0.193	0.158	1.049
0.048	0.080	4.100	4.888	16.858	4.339	0.183	0.157	0.692
0.413	1.134	4.955	5.832	21.532	4.829	0.260	0.227	2.005
5.489	8.192	4.856	13.272	38.744	6.453	0.625	0.506	1.563
0.166	0.381	4.146	5.861	19.226	4.767	0.229	0.191	0.946
0.471	1.692	4.251	6.311	19.493	5.268	0.257	0.211	1.331
0.068	0.159	3.330	4.548	14.206	3.568	0.127	0.119	0.943
1.284	2.125	5.828	7.791	26.972	5.678	0.383	0.357	1.769

BMJ Open: first published as 10.1136/bmjopen-2022-063051 on 8 November 2022. Downloaded from http://bmjopen.bmj.com/ on June 10, 2025 at Agence Bibliographique de l Enseignement Superieur (ABES) . Protected by copyright, including for uses related to text and data mining, AI training, and similar technologies.

0.065	0.142	2.869	6.280	18.787	4.153	0.195	0.141	0.685
0.140	0.274	5.099	5.722	19.742	4.850	0.239	0.229	1.030
0.723	2.721	9.411	15.328	45.262	10.554	1.194	1.133	0.448
0.076	0.204	3.921	5.390	19.347	4.578	0.221	0.166	0.782
0.025	0.057	4.072	4.605	15.924	4.153	0.165	0.147	0.524
0.025	0.052	2.544	3.498	10.509	2.840	0.075	0.070	1.001
0.027	0.055	3.973	4.537	15.822	4.355	0.172	0.142	0.506
0.671	1.245	5.067	6.060	20.235	5.028	0.254	0.241	1.844
0.067	0.188	4.039	6.019	18.197	4.473	0.203	0.191	0.770
0.024	0.058	3.349	4.139	15.221	3.971	0.151	0.109	0.532
1.284	3.227	3.904	8.491	26.453	5.140	0.340	0.260	2.001
0.334	0.821	3.698	5.097	15.808	3.937	0.156	0.148	1.489
0.088	0.171	3.652	5.028	14.943	4.393	0.164	0.144	1.004
0.021	0.037	2.695	3.182	10.976	3.122	0.086	0.067	0.874
0.296	0.742	3.682	4.035	12.878	3.887	0.125	0.117	1.693
0.047	0.156	3.958	5.126	15.600	4.569	0.178	0.159	0.948
0.065	0.125	3.926	6.009	20.114	5.003	0.252	0.185	0.554
0.015	0.043	3.044	3.841	13.047	3.343	0.109	0.092	0.545
0.048	0.111	3.747	4.646	14.887	4.055	0.151	0.137	0.609
0.032	0.064	1.743	2.212	6.685	2.312	0.039	0.030	1.934
0.146	0.446	3.494	4.013	13.901	3.573	0.124	0.110	1.223
0.026	0.044	3.340	4.165	13.007	3.667	0.119	0.109	0.616
0.158	0.271	3.373	5.696	18.626	4.310	0.201	0.151	1.161
0.006	0.013	2.149	2.798	9.586	2.605	0.062	0.047	0.549
0.059	0.133	4.544	5.666	18.559	4.809	0.223	0.202	0.554
0.088	0.241	3.240	5.327	15.348	3.834	0.147	0.136	0.751
0.106	0.272	3.982	5.445	15.999	4.286	0.171	0.170	0.895
0.635	1.332	5.655	8.968	30.914	6.682	0.516	0.398	0.953
0.031	0.056	3.242	4.090	14.393	3.732	0.134	0.104	0.775
0.352	1.309	4.023	4.674	15.332	4.004	0.153	0.148	2.325
0.062	0.129	3.028	3.756	12.271	3.335	0.102	0.089	1.209
0.072	0.167	3.273	4.162	13.626	3.661	0.125	0.107	1.327
1.971	3.931	5.400	6.936	23.221	5.117	0.297	0.294	1.995
0.349	0.644	6.668	7.542	25.103	7.353	0.461	0.395	1.030
0.057	0.157	2.954	5.757	18.913	3.839	0.182	0.134	0.634
0.060	0.138	3.374	4.303	14.245	4.211	0.150	0.114	0.937
0.048	0.126	4.114	6.204	23.009	4.885	0.281	0.200	0.431
0.410	1.556	4.088	5.305	16.784	4.591	0.193	0.170	2.214
0.073	0.116	2.687	5.335	20.340	3.712	0.189	0.113	0.513
0.049	0.104	2.559	5.530	16.327	3.620	0.148	0.111	0.666
0.647	1.666	5.581	7.501	23.891	6.226	0.372	0.329	1.329
0.041	0.072	3.421	4.484	14.463	4.178	0.151	0.120	0.841
0.133	0.611	2.123	4.861	12.221	2.913	0.089	0.081	1.572
0.064	0.171	4.645	6.823	21.514	6.082	0.327	0.249	0.355
0.029	0.066	3.453	4.611	16.463	4.059	0.167	0.125	0.494
0.028	0.124	2.466	2.877	9.725	2.697	0.066	0.056	1.584
0.144	0.322	2.931	4.907	13.849	3.745	0.130	0.113	1.014
0.831	1.995	3.693	15.254	44.240	6.164	0.682	0.442	0.666
0.123	0.251	3.660	5.911	21.822	5.129	0.280	0.170	0.849
0.370	0.724	4.471	5.481	18.185	4.966	0.226	0.193	1.679

For peer review only

BMJ Open: first published as 10.1136/bmjopen-2022-063051 on 8 November 2022. Downloaded from http://bmjopen.bmj.com/ on June 10, 2025 at Agence Bibliographique de l Enseignement Superieur (ABES) . Protected by copyright, including for uses related to text and data mining, AI training, and similar technologies.

0.138	0.387	3.088	3.831	12.450	3.565	0.111	0.093	2.122
9.561	17.746	2.961	18.027	50.338	5.556	0.699	0.419	1.193
0.010	0.022	2.536	3.340	10.417	2.938	0.077	0.067	0.611
0.028	0.068	2.961	3.628	12.388	3.587	0.111	0.084	1.019
0.007	0.017	2.669	3.062	9.724	3.065	0.075	0.064	0.485
0.709	1.350	6.233	9.921	32.559	7.095	0.578	0.486	1.059
0.177	0.312	3.682	5.598	18.267	4.597	0.210	0.162	1.131
0.030	0.083	3.109	3.713	13.372	4.008	0.134	0.091	0.945
0.043	0.083	2.949	4.596	16.118	4.349	0.175	0.106	0.652
0.019	0.034	3.058	3.824	11.763	3.366	0.099	0.092	0.673
0.041	0.094	2.402	3.999	11.654	2.840	0.083	0.075	0.993
0.005	0.016	1.871	3.149	9.064	2.252	0.051	0.046	0.473
0.011	0.029	2.480	2.749	9.781	2.680	0.066	0.054	0.838
0.105	0.295	5.164	6.092	19.890	5.675	0.282	0.247	0.940
0.071	0.166	3.647	5.591	18.794	4.024	0.189	0.160	0.718
0.154	0.247	3.845	5.198	17.087	4.221	0.180	0.157	1.182
0.433	1.019	7.600	9.255	32.052	7.377	0.591	0.552	0.759
0.946	2.323	5.854	9.288	29.079	6.525	0.474	0.427	1.117
5.822	10.316	10.249	12.646	43.430	9.687	1.052	1.018	1.517
0.133	0.375	4.577	4.981	16.951	4.848	0.205	0.179	1.257
0.457	1.342	6.603	9.821	38.845	7.126	0.692	0.509	0.530
0.021	0.096	4.180	5.671	18.176	4.536	0.206	0.186	0.300
0.173	0.291	5.563	7.294	22.990	5.826	0.335	0.319	0.738
0.033	0.091	1.425	2.956	8.692	2.091	0.045	0.033	1.531
0.242	0.482	6.692	7.545	27.655	7.023	0.486	0.397	0.804
0.673	2.261	4.714	7.341	25.595	5.352	0.342	0.272	0.918
0.014	0.028	3.033	3.304	11.382	3.083	0.088	0.079	0.715
0.705	2.209	3.936	5.479	16.917	4.038	0.171	0.169	1.545
0.017	0.035	2.888	3.555	11.320	3.126	0.088	0.081	0.700
0.012	0.028	2.723	3.744	12.259	3.122	0.096	0.080	0.511
0.062	0.177	3.927	4.189	14.081	3.967	0.140	0.129	1.205
0.129	0.299	3.261	4.724	14.375	3.444	0.124	0.121	1.255
0.223	0.408	1.690	6.942	22.424	2.675	0.150	0.092	0.807
0.604	2.576	9.516	16.051	57.167	9.204	1.315	1.200	0.288
0.133	0.416	3.427	4.118	13.379	3.487	0.117	0.111	1.722
0.190	0.611	4.209	5.875	18.330	4.775	0.219	0.194	1.392
0.200	0.582	4.580	5.781	20.002	5.026	0.251	0.208	1.487
0.052	0.127	4.276	4.986	17.482	4.697	0.205	0.167	0.779
1.463	2.581	5.536	7.179	23.516	5.577	0.328	0.312	1.939
1.064	3.380	4.917	12.472	34.457	5.794	0.499	0.482	1.010
0.294	0.489	4.505	8.378	31.391	5.719	0.449	0.296	0.719
0.301	0.601	6.063	8.092	28.011	6.899	0.483	0.385	0.865
0.323	0.806	3.486	7.314	23.602	4.859	0.287	0.200	1.297
0.227	0.354	3.933	6.501	22.813	5.068	0.289	0.201	0.960
0.072	0.173	4.796	6.793	21.520	5.804	0.312	0.256	0.533
0.054	0.126	2.981	3.763	11.219	3.091	0.087	0.088	1.153
0.002	0.005	1.667	2.050	6.305	1.717	0.027	0.027	0.561
0.080	0.202	3.798	4.688	14.879	3.770	0.140	0.140	0.865
0.003	0.011	2.058	2.646	8.188	2.184	0.045	0.043	0.390
0.364	0.676	4.880	7.274	20.777	5.344	0.278	0.279	1.165

BMJ Open: first published as 10.1136/bmjopen-2022-063051 on 8 November 2022. Downloaded from http://bmjopen.bmj.com/ on June 10, 2025 at Agence Bibliographique de l Enseignement Superieur (ABES) .
Protected by copyright, including for uses related to text and data mining, AI training, and similar technologies.

For peer review only

0.059	0.136	3.633	5.216	16.163	3.879	0.157	0.149	0.784
0.083	0.211	3.466	3.933	13.148	3.467	0.114	0.107	1.281
0.049	0.126	3.027	4.428	12.646	3.207	0.101	0.105	1.023
0.004	0.012	2.254	2.739	9.026	2.224	0.050	0.048	0.413
0.066	0.182	2.509	4.164	11.013	2.871	0.079	0.082	1.172
0.040	0.303	3.046	6.031	16.366	3.781	0.155	0.144	0.385
4.307	7.497	4.943	11.565	29.411	6.256	0.460	0.449	1.617
0.251	0.460	3.312	6.808	19.810	4.592	0.227	0.177	0.979
0.109	0.209	4.469	5.198	17.058	4.553	0.194	0.182	1.006
0.020	0.064	2.612	4.202	11.337	3.013	0.085	0.086	0.710
0.010	0.027	1.673	2.354	6.665	1.998	0.033	0.031	1.238
0.005	0.017	2.558	3.184	9.667	2.606	0.063	0.064	0.377
0.017	0.047	2.537	3.163	9.173	2.730	0.063	0.063	0.845
0.156	0.357	3.105	3.630	11.718	3.059	0.090	0.089	1.984
0.496	1.498	3.688	7.971	23.076	4.837	0.279	0.231	1.062
0.097	0.211	3.514	3.858	12.669	3.425	0.108	0.106	1.402
0.015	0.045	2.234	2.843	9.386	2.324	0.055	0.050	0.937
0.015	0.041	3.000	3.715	10.778	2.970	0.080	0.088	0.565
0.007	0.023	2.662	3.378	11.376	2.694	0.077	0.071	0.423
0.010	0.071	2.885	4.088	12.580	3.113	0.098	0.093	0.312
0.020	0.067	2.674	3.641	10.202	2.743	0.070	0.076	0.774
0.005	0.009	1.941	2.438	8.082	2.096	0.042	0.037	0.530
0.094	0.349	2.932	3.509	10.841	3.047	0.083	0.081	2.044
0.042	0.130	2.598	4.490	11.942	3.133	0.094	0.092	0.946
0.044	0.182	1.604	2.311	6.687	1.877	0.031	0.029	2.104
0.049	0.119	2.818	3.448	10.414	2.988	0.078	0.076	1.158
0.112	0.295	4.647	5.228	18.128	4.607	0.209	0.191	0.834
1.181	5.512	3.626	7.662	19.509	4.543	0.222	0.218	2.164
0.078	0.239	2.966	3.629	11.960	2.882	0.086	0.085	1.665
0.016	0.040	2.054	2.604	8.405	2.090	0.044	0.042	1.193
0.133	0.264	3.526	4.008	13.454	3.419	0.115	0.111	1.572
0.023	0.103	2.488	4.181	11.759	2.758	0.081	0.082	0.733
0.028	0.187	3.376	6.094	16.842	4.360	0.184	0.162	0.395
0.003	0.010	2.058	2.628	8.482	2.109	0.045	0.042	0.422
0.060	0.169	2.876	3.210	9.865	3.022	0.075	0.072	1.979
0.041	0.092	2.534	4.791	13.958	3.151	0.110	0.095	0.683
0.051	0.118	3.367	4.437	14.181	3.586	0.127	0.117	0.909
0.323	0.545	4.747	9.608	24.939	5.860	0.365	0.358	0.651
0.424	0.811	2.828	4.463	12.938	3.306	0.107	0.099	2.356
0.315	0.524	3.432	4.980	14.519	3.980	0.144	0.134	1.701
0.066	0.176	2.482	3.060	9.082	2.609	0.059	0.060	1.963
0.108	0.279	2.829	4.298	13.230	3.376	0.112	0.095	1.206
0.639	2.114	4.957	9.395	25.968	6.032	0.392	0.366	1.109
0.148	0.424	3.121	3.948	11.926	3.295	0.098	0.097	2.209
0.221	0.393	3.803	6.053	18.164	4.583	0.208	0.181	1.031
0.009	0.021	1.782	2.158	6.541	1.799	0.029	0.030	0.933
0.077	0.178	3.345	4.520	13.440	3.752	0.126	0.119	1.234
0.001	0.003	1.249	1.627	4.931	1.263	0.016	0.016	0.420
0.001	0.002	1.171	1.571	5.218	1.191	0.016	0.014	0.365
0.025	0.056	2.550	2.828	9.049	2.602	0.059	0.057	1.291

BMJ Open: first published as 10.1136/bmjopen-2022-063051 on 8 November 2022. Downloaded from http://bmjopen.bmj.com/ on June 10, 2025 at Agence Bibliographique de l Enseignement Superieur (ABES) .
Protected by copyright, including for uses related to text and data mining, AI training, and similar technologies.

0.003	0.008	1.614	2.232	6.529	1.706	0.028	0.028	0.544
0.004	0.008	2.024	2.328	7.829	1.956	0.038	0.037	0.595
0.152	0.463	3.752	6.083	20.202	4.746	0.240	0.179	0.764
0.110	0.280	3.307	5.198	14.592	3.553	0.130	0.135	1.248
0.074	0.206	2.337	3.921	10.721	2.726	0.073	0.072	1.265
0.054	0.145	3.253	4.288	12.309	3.606	0.111	0.110	0.924
0.130	0.248	3.443	4.427	13.709	3.601	0.123	0.120	1.325
0.020	0.057	2.337	2.977	8.842	2.448	0.054	0.055	1.207
0.875	1.999	5.504	11.272	31.139	6.996	0.545	0.487	0.882
0.025	0.094	2.229	5.284	13.469	2.867	0.097	0.093	0.481
0.033	0.056	2.807	3.647	10.997	2.972	0.082	0.080	0.984
0.058	0.183	3.309	4.297	13.094	3.291	0.108	0.112	1.192
0.230	0.762	4.694	6.020	17.946	5.054	0.227	0.222	1.171
0.006	0.021	2.550	3.222	9.787	2.806	0.069	0.065	0.377
0.008	0.022	2.539	3.357	10.019	2.758	0.069	0.067	0.526
0.006	0.012	1.792	2.444	7.653	2.150	0.041	0.034	0.834
0.051	0.155	2.582	3.108	9.392	2.699	0.063	0.063	1.671
0.027	0.052	2.791	3.230	9.826	2.820	0.069	0.071	1.005
0.078	0.135	3.086	3.614	10.669	3.209	0.086	0.088	1.562
0.018	0.041	2.968	3.431	10.338	2.993	0.077	0.080	0.871
0.025	0.041	2.996	3.439	10.693	3.209	0.086	0.081	0.826
0.080	0.247	3.390	4.303	13.330	3.390	0.113	0.115	1.321
0.006	0.011	1.980	2.183	6.667	2.038	0.034	0.034	0.957
0.013	0.024	1.860	2.600	7.731	1.939	0.037	0.038	0.960
0.057	0.177	1.771	2.520	7.349	2.020	0.037	0.035	1.909
0.034	0.101	2.142	2.834	8.480	2.306	0.049	0.048	1.758
0.030	0.104	2.525	3.927	10.784	2.783	0.075	0.078	0.972
0.031	0.079	2.552	3.426	10.614	2.776	0.074	0.069	0.998
0.058	0.230	2.391	2.810	8.625	2.316	0.050	0.053	1.969
0.019	0.039	3.067	3.601	11.501	3.064	0.088	0.087	0.793
0.036	0.108	0.981	1.591	4.414	1.106	0.012	0.012	2.888
0.043	0.091	3.448	4.293	13.109	3.606	0.118	0.116	0.848
0.027	0.068	2.188	3.205	9.355	2.372	0.055	0.055	1.086
0.204	0.441	4.669	5.375	16.745	4.748	0.199	0.197	1.128
0.145	0.259	2.815	3.184	10.027	2.889	0.072	0.070	2.243
0.079	0.196	3.412	3.903	11.686	3.419	0.100	0.105	1.424
1.014	2.041	6.801	10.575	28.975	7.694	0.557	0.565	1.066
0.016	0.073	1.988	2.577	7.813	2.160	0.042	0.040	1.274
0.022	0.082	2.507	3.337	10.511	2.750	0.072	0.066	0.695
0.056	0.146	3.141	3.432	11.178	3.152	0.088	0.085	1.217
0.034	0.085	2.409	3.774	10.852	2.821	0.077	0.071	0.845
0.026	0.050	2.316	2.781	8.572	2.264	0.049	0.051	1.334
0.040	0.098	2.113	2.553	7.909	2.222	0.044	0.042	1.627
0.014	0.067	1.016	1.949	4.922	1.111	0.014	0.016	1.743
0.071	0.245	2.801	3.116	10.051	2.771	0.070	0.069	2.029
0.005	0.014	1.964	2.682	8.337	2.070	0.043	0.041	0.565
0.056	0.155	3.187	3.553	11.772	3.139	0.092	0.089	1.483

For peer review only

BMJ Open: first published as 10.1136/bmjopen-2022-063051 on 8 November 2022. Downloaded from http://bmjopen.bmj.com/ on June 10, 2025 at Agence Bibliographique de l Enseignement Superieur (ABES) .
Protected by copyright, including for uses related to text and data mining, AI training, and similar technologies.

aspect ratic	bottleneck	bulge locat	nonspericit	aneurysm v	aneurysm s	undulation	ellipticity ir	mean of m
eAR	BF	BL	NSI	AVSV	AASA	UI	EI	MAA
-	-	-	-	-	-	-	-	mm^-1
1.625	1.471	0.153	0.270	0.485	0.671	0.079	0.240	0.318
2.417	2.012	0.364	0.370	0.285	0.545	0.277	0.271	0.254
1.534	1.000	0.052	0.311	0.311	0.529	0.101	0.282	0.322
1.811	1.836	0.626	0.278	0.370	0.567	0.077	0.255	0.302
1.739	1.358	0.340	0.270	0.390	0.580	0.023	0.264	0.325
0.657	1.101	0.202	0.249	0.549	0.709	0.034	0.237	0.322
2.499	2.064	0.491	0.257	0.555	0.721	0.045	0.234	0.090
1.115	1.117	0.351	0.254	0.478	0.650	0.043	0.240	0.324
0.821	1.004	0.019	0.258	0.555	0.723	0.037	0.247	0.308
1.490	1.649	0.475	0.279	0.407	0.605	0.046	0.267	0.354
1.441	1.113	0.499	0.236	0.639	0.770	0.018	0.231	0.239
2.401	2.536	0.414	0.304	0.261	0.465	0.077	0.284	0.259
1.644	1.768	0.543	0.249	0.431	0.603	0.027	0.240	0.216
0.531	1.148	0.113	0.299	0.285	0.491	0.079	0.275	0.356
0.805	1.000	0.010	0.291	0.460	0.667	0.039	0.276	0.401
2.082	1.729	0.453	0.261	0.396	0.579	0.073	0.245	0.185
0.798	1.000	0.031	0.289	0.441	0.647	0.037	0.277	0.666
2.164	1.847	0.528	0.267	0.459	0.644	0.047	0.251	0.163
1.052	1.172	0.466	0.239	0.628	0.766	0.017	0.233	0.524
1.452	1.214	0.464	0.260	0.454	0.633	0.029	0.251	0.389
1.513	1.531	0.674	0.275	0.390	0.584	0.074	0.252	0.292
1.214	1.180	0.285	0.266	0.562	0.737	0.054	0.248	0.315
1.924	1.583	0.324	0.243	0.494	0.655	0.022	0.235	0.179
0.997	1.153	0.390	0.278	0.354	0.550	0.034	0.266	0.283
1.402	1.454	0.443	0.226	0.748	0.845	0.016	0.220	0.200
0.802	0.986	0.424	0.286	0.396	0.600	0.079	0.259	0.239
0.701	0.998	0.026	0.297	0.377	0.589	0.080	0.272	0.357
0.874	0.993	0.153	0.232	0.680	0.799	0.016	0.226	0.132
1.016	1.204	0.520	0.299	0.349	0.561	0.112	0.264	0.321
0.985	1.417	0.453	0.271	0.385	0.577	0.053	0.253	0.303
1.330	1.958	0.536	0.354	0.188	0.404	0.204	0.300	0.317
2.226	1.674	0.290	0.322	0.275	0.496	0.119	0.276	0.176
1.023	1.178	0.492	0.254	0.522	0.690	0.024	0.245	0.337
0.787	1.281	0.383	0.279	0.344	0.540	0.066	0.257	0.354
1.444	1.163	0.261	0.307	0.277	0.486	0.099	0.278	0.371
0.897	1.049	0.432	0.258	0.539	0.709	0.039	0.243	0.499
1.353	1.145	0.347	0.266	0.404	0.591	0.042	0.253	0.325
0.998	1.361	0.313	0.263	0.473	0.654	0.055	0.246	0.271
1.134	1.112	0.234	0.247	0.595	0.746	0.033	0.231	0.128
1.358	1.027	0.320	0.288	0.400	0.605	0.087	0.256	0.284
0.780	1.024	0.204	0.259	0.578	0.743	0.032	0.248	0.335
2.421	1.532	0.475	0.270	0.351	0.541	0.036	0.259	0.193
3.215	1.713	0.478	0.224	0.662	0.777	0.012	0.220	0.088
1.163	1.378	0.409	0.268	0.413	0.601	0.055	0.254	0.274
1.594	2.251	0.194	0.327	0.241	0.456	0.136	0.277	0.212
1.202	1.308	0.446	0.255	0.413	0.591	0.032	0.242	0.336
2.428	1.802	0.503	0.242	0.588	0.734	0.027	0.232	0.135

For peer review only

BMJ Open: first published as 10.1136/bmjopen-2022-063051 on 8 November 2022. Downloaded from http://bmjopen.bmj.com/ on June 10, 2025 at Agence Bibliographique de l Enseignement Superieur (ABES) . Protected by copyright, including for uses related to text and data mining, AI training, and similar technologies.

1.036	0.977	0.145	0.297	0.405	0.618	0.109	0.264	0.331
1.215	1.183	0.417	0.254	0.499	0.669	0.022	0.244	0.258
0.651	1.059	0.327	0.319	0.256	0.470	0.037	0.304	0.154
0.920	1.169	0.349	0.271	0.352	0.543	0.052	0.257	0.345
0.581	1.000	0.015	0.318	0.415	0.647	0.050	0.301	0.368
1.233	1.019	0.561	0.280	0.437	0.635	0.069	0.258	0.435
0.527	1.000	0.154	0.309	0.456	0.680	0.067	0.284	0.343
2.223	1.872	0.519	0.236	0.528	0.679	0.019	0.229	0.169
1.037	1.000	0.024	0.329	0.323	0.556	0.099	0.287	0.313
0.555	1.091	0.219	0.279	0.399	0.596	0.047	0.265	0.413
3.305	1.703	0.484	0.262	0.382	0.566	0.041	0.252	0.142
1.927	2.168	0.604	0.306	0.347	0.565	0.145	0.256	0.232
1.149	1.205	0.410	0.246	0.503	0.666	0.026	0.237	0.314
0.890	1.187	0.333	0.238	0.559	0.706	0.019	0.231	0.494
1.757	2.633	0.381	0.268	0.380	0.569	0.049	0.251	0.223
1.063	1.000	0.054	0.332	0.264	0.489	0.126	0.292	0.373
0.666	0.999	0.185	0.282	0.488	0.685	0.059	0.262	0.302
0.626	1.000	0.072	0.336	0.313	0.550	0.102	0.301	0.437
0.698	1.278	0.503	0.299	0.383	0.597	0.104	0.257	0.391
1.850	1.899	0.554	0.259	0.479	0.656	0.059	0.239	0.432
1.374	2.359	0.431	0.279	0.312	0.506	0.047	0.264	0.285
0.700	1.000	0.077	0.267	0.568	0.742	0.027	0.255	0.443
1.534	1.155	0.439	0.242	0.569	0.719	0.027	0.233	0.261
0.590	0.998	0.009	0.309	0.405	0.630	0.084	0.281	0.578
0.653	1.067	0.304	0.284	0.437	0.638	0.025	0.274	0.355
1.043	1.303	0.312	0.347	0.290	0.533	0.202	0.281	0.330
1.137	1.351	0.350	0.262	0.379	0.563	0.031	0.253	0.321
1.279	1.434	0.449	0.258	0.453	0.630	0.051	0.244	0.176
0.850	0.997	0.026	0.264	0.531	0.708	0.044	0.248	0.397
2.714	1.699	0.589	0.288	0.251	0.443	0.067	0.270	0.220
1.361	1.480	0.572	0.244	0.470	0.635	0.018	0.238	0.367
1.509	1.147	0.305	0.255	0.420	0.597	0.025	0.247	0.326
2.705	2.766	0.544	0.245	0.488	0.652	0.027	0.235	0.119
1.056	1.184	0.275	0.268	0.505	0.688	0.068	0.237	0.167
0.951	0.962	0.134	0.271	0.346	0.537	0.041	0.258	0.334
0.957	1.203	0.325	0.298	0.388	0.602	0.103	0.263	0.331
0.547	0.970	0.043	0.307	0.353	0.572	0.072	0.283	0.258
2.558	2.061	0.539	0.335	0.221	0.436	0.163	0.293	0.213
0.738	0.964	0.338	0.238	0.616	0.754	0.029	0.228	0.320
1.018	0.996	0.078	0.276	0.444	0.639	0.063	0.252	0.293
1.601	1.728	0.463	0.272	0.366	0.558	0.059	0.250	0.157
0.902	0.999	0.139	0.280	0.526	0.718	0.069	0.254	0.354
2.623	1.546	0.263	0.339	0.185	0.389	0.152	0.296	0.310
0.398	0.991	0.076	0.300	0.349	0.562	0.070	0.277	0.298
0.561	1.013	0.325	0.291	0.396	0.605	0.081	0.264	0.374
1.690	1.350	0.455	0.324	0.203	0.405	0.088	0.304	0.462
1.328	1.691	0.552	0.279	0.413	0.610	0.078	0.251	0.273
1.649	1.000	0.110	0.263	0.403	0.588	0.033	0.255	0.148
0.979	1.218	0.257	0.267	0.457	0.642	0.070	0.248	0.296
1.853	1.713	0.549	0.256	0.488	0.661	0.045	0.239	0.181

BMJ Open: first published as 10.1136/bmjopen-2022-063051 on 8 November 2022. Downloaded from http://bmjopen.bmj.com/ on June 10, 2025 at Agence Bibliographique de l Enseignement Superieur (ABES) . Protected by copyright, including for uses related to text and data mining, AI training, and similar technologies.

For peer review only

2.281	1.444	0.689	0.298	0.324	0.534	0.091	0.270	0.297
3.872	1.683	0.422	0.260	0.511	0.685	0.052	0.231	0.073
0.694	1.000	0.050	0.295	0.436	0.647	0.057	0.271	0.532
1.031	1.009	0.069	0.257	0.417	0.597	0.009	0.255	0.456
0.485	1.000	0.001	0.301	0.407	0.623	0.018	0.296	0.593
1.480	1.156	0.560	0.275	0.478	0.669	0.091	0.246	0.152
1.377	1.384	0.467	0.247	0.545	0.704	0.039	0.232	0.241
0.875	0.965	0.010	0.278	0.346	0.542	0.053	0.260	0.393
0.689	1.096	0.434	0.238	0.511	0.666	0.017	0.232	0.406
0.765	0.994	0.048	0.262	0.556	0.727	0.021	0.253	0.494
1.398	1.116	0.237	0.278	0.416	0.613	0.051	0.261	0.401
0.661	0.999	0.114	0.313	0.276	0.490	0.059	0.295	0.631
0.860	1.185	0.206	0.270	0.375	0.565	0.042	0.255	0.565
1.009	0.969	0.008	0.325	0.315	0.545	0.115	0.294	0.283
0.998	1.142	0.263	0.277	0.406	0.602	0.047	0.259	0.353
1.456	1.326	0.441	0.227	0.614	0.742	0.012	0.222	0.274
0.952	1.314	0.224	0.280	0.395	0.593	0.070	0.253	0.198
1.590	1.708	0.279	0.336	0.343	0.586	0.158	0.260	0.163
1.980	1.982	0.453	0.229	0.559	0.699	0.010	0.226	0.088
1.291	1.403	0.357	0.271	0.343	0.533	0.037	0.258	0.286
0.730	1.334	0.118	0.365	0.283	0.538	0.170	0.299	0.230
0.375	1.000	0.059	0.449	0.195	0.484	0.115	0.409	0.320
0.924	1.092	0.359	0.251	0.584	0.740	0.016	0.244	0.268
2.164	1.461	0.559	0.277	0.342	0.538	0.060	0.263	0.453
0.864	1.229	0.217	0.241	0.495	0.654	0.016	0.236	0.243
1.259	2.051	0.108	0.277	0.285	0.476	0.041	0.263	0.182
0.767	1.023	0.225	0.293	0.487	0.695	0.054	0.271	0.483
2.097	2.949	0.546	0.395	0.229	0.491	0.282	0.285	0.215
0.796	1.018	0.284	0.285	0.471	0.672	0.044	0.267	0.482
0.613	1.000	0.040	0.335	0.390	0.637	0.134	0.277	0.535
1.273	1.147	0.315	0.288	0.328	0.530	0.064	0.268	0.354
1.722	1.509	0.519	0.283	0.401	0.602	0.072	0.256	0.303
2.094	1.054	0.310	0.272	0.512	0.698	0.064	0.230	0.254
0.503	1.009	0.204	0.303	0.218	0.413	0.069	0.288	0.174
2.034	1.750	0.499	0.327	0.273	0.496	0.148	0.275	0.304
1.712	1.261	0.377	0.364	0.247	0.492	0.205	0.283	0.281
1.711	1.227	0.332	0.334	0.285	0.516	0.172	0.271	0.255
0.827	1.121	0.175	0.298	0.379	0.592	0.071	0.272	0.346
2.496	2.359	0.471	0.236	0.555	0.702	0.021	0.229	0.137
2.173	1.152	0.520	0.280	0.296	0.489	0.061	0.260	0.138
1.053	1.060	0.327	0.241	0.584	0.730	0.029	0.230	0.197
1.015	1.152	0.472	0.264	0.475	0.657	0.052	0.243	0.184
1.953	1.081	0.491	0.267	0.382	0.570	0.046	0.258	0.206
1.232	1.346	0.387	0.231	0.633	0.761	0.013	0.227	0.245
0.624	0.994	0.101	0.300	0.390	0.606	0.056	0.281	0.278
1.404	1.529	0.477	0.289	0.388	0.594	0.095	0.258	0.401
0.669	1.000	0.086	0.317	0.389	0.619	0.083	0.295	0.974
1.076	1.550	0.450	0.282	0.363	0.562	0.090	0.253	0.328
0.472	0.969	0.129	0.365	0.268	0.520	0.154	0.315	0.791
1.586	1.369	0.274	0.262	0.507	0.684	0.060	0.238	0.198

For peer review only

BMJ Open: first published as 10.1136/bmjopen-2022-063051 on 8 November 2022. Downloaded from http://bmjopen.bmj.com/ on June 10, 2025 at Agence Bibliographique de l Enseignement Superieur (ABES) .
Protected by copyright, including for uses related to text and data mining, AI training, and similar technologies.

1.054	1.201	0.355	0.310	0.384	0.608	0.117	0.267	0.349
1.453	1.452	0.652	0.279	0.363	0.561	0.078	0.254	0.339
1.412	1.316	0.338	0.345	0.316	0.563	0.180	0.278	0.418
0.509	0.985	0.000	0.415	0.237	0.520	0.241	0.341	0.717
1.700	1.489	0.626	0.290	0.329	0.532	0.091	0.265	0.359
0.615	1.352	0.249	0.387	0.104	0.287	0.215	0.329	0.418
2.990	1.941	0.524	0.242	0.556	0.709	0.032	0.227	0.092
1.452	1.358	0.550	0.269	0.507	0.691	0.070	0.243	0.237
1.149	1.250	0.248	0.317	0.447	0.680	0.142	0.259	0.296
0.990	1.009	0.242	0.339	0.281	0.514	0.113	0.296	0.459
1.459	1.117	0.411	0.319	0.310	0.533	0.146	0.276	0.646
0.461	0.915	0.154	0.420	0.217	0.495	0.213	0.349	0.588
0.979	1.289	0.449	0.293	0.344	0.552	0.055	0.274	0.566
2.355	1.916	0.548	0.264	0.415	0.599	0.051	0.247	0.269
1.750	1.650	0.095	0.378	0.242	0.495	0.270	0.279	0.226
1.580	1.845	0.205	0.313	0.394	0.622	0.141	0.263	0.347
1.146	1.285	0.421	0.284	0.318	0.516	0.080	0.254	0.594
0.706	1.000	0.010	0.303	0.334	0.548	0.075	0.282	0.538
0.530	1.000	0.157	0.402	0.233	0.503	0.195	0.355	0.507
0.410	1.061	0.241	0.443	0.113	0.333	0.239	0.370	0.537
1.027	1.194	0.485	0.299	0.280	0.485	0.078	0.273	0.501
0.617	1.045	0.099	0.340	0.394	0.647	0.200	0.262	0.841
2.354	1.474	0.312	0.305	0.248	0.451	0.079	0.280	0.315
1.355	1.113	0.287	0.305	0.291	0.501	0.098	0.269	0.398
2.590	2.710	0.626	0.371	0.190	0.417	0.218	0.305	0.462
1.336	1.605	0.479	0.265	0.392	0.579	0.050	0.246	0.397
0.946	1.511	0.221	0.295	0.336	0.544	0.118	0.249	0.289
3.649	1.959	0.320	0.326	0.199	0.401	0.074	0.305	0.151
2.097	1.414	0.346	0.366	0.243	0.487	0.261	0.285	0.355
1.486	1.127	0.438	0.271	0.360	0.551	0.091	0.247	0.546
1.842	1.648	0.293	0.274	0.465	0.656	0.076	0.247	0.279
1.112	0.957	0.276	0.323	0.186	0.382	0.159	0.290	0.471
0.552	0.987	0.043	0.396	0.123	0.326	0.180	0.344	0.392
0.526	0.996	0.113	0.357	0.279	0.527	0.180	0.317	0.764
2.102	1.299	0.521	0.280	0.343	0.540	0.042	0.268	0.364
1.039	1.074	0.564	0.284	0.403	0.605	0.100	0.246	0.419
1.125	1.149	0.251	0.288	0.390	0.595	0.102	0.251	0.378
1.068	1.010	0.476	0.279	0.533	0.725	0.101	0.237	0.207
3.180	2.032	0.487	0.236	0.514	0.666	0.017	0.229	0.207
2.128	1.947	0.420	0.240	0.584	0.730	0.029	0.230	0.211
2.303	1.525	0.379	0.275	0.350	0.544	0.072	0.252	0.354
1.536	1.691	0.692	0.313	0.333	0.554	0.138	0.256	0.331
1.728	1.239	0.351	0.339	0.242	0.466	0.201	0.274	0.189
2.647	1.653	0.685	0.319	0.299	0.522	0.142	0.279	0.284
1.362	1.469	0.396	0.257	0.529	0.699	0.059	0.233	0.244
1.119	1.538	0.595	0.288	0.384	0.589	0.086	0.261	0.685
1.487	1.206	0.279	0.306	0.371	0.590	0.138	0.259	0.331
0.542	0.946	0.453	0.346	0.283	0.523	0.186	0.289	1.245
0.481	0.962	0.216	0.379	0.260	0.520	0.222	0.310	1.290
1.403	1.314	0.236	0.291	0.404	0.612	0.096	0.258	0.498

For peer review only

BMJ Open: first published as 10.1136/bmjopen-2022-063051 on 8 November 2022. Downloaded from http://bmjopen.bmj.com/ on June 10, 2025 at Agence Bibliographique de l Enseignement Superieur (ABES) .
Protected by copyright, including for uses related to text and data mining, AI training, and similar technologies.

0.711	0.977	0.072	0.350	0.270	0.510	0.175	0.286	0.960
0.708	0.998	0.033	0.322	0.406	0.642	0.142	0.283	0.778
0.980	1.519	0.420	0.333	0.277	0.506	0.154	0.261	0.273
1.826	1.137	0.564	0.281	0.356	0.554	0.090	0.257	0.286
1.820	1.472	0.417	0.290	0.323	0.526	0.097	0.255	0.339
1.099	1.472	0.213	0.286	0.359	0.562	0.041	0.272	0.360
1.629	1.712	0.402	0.277	0.472	0.665	0.101	0.240	0.288
1.468	1.378	0.359	0.288	0.330	0.533	0.071	0.266	0.513
1.421	1.272	0.704	0.270	0.405	0.595	0.075	0.243	0.158
0.887	1.004	0.010	0.354	0.222	0.450	0.172	0.290	0.503
1.207	1.141	0.506	0.268	0.543	0.721	0.073	0.241	0.427
1.556	1.359	0.236	0.324	0.270	0.490	0.155	0.284	0.360
1.395	1.551	0.291	0.282	0.286	0.480	0.051	0.264	0.222
0.432	0.970	0.141	0.391	0.247	0.513	0.180	0.323	0.548
0.640	1.000	0.066	0.355	0.317	0.572	0.129	0.310	0.553
0.948	0.993	0.061	0.298	0.422	0.637	0.094	0.267	0.685
1.924	1.521	0.592	0.274	0.314	0.505	0.048	0.261	0.385
1.151	1.409	0.443	0.276	0.489	0.680	0.078	0.251	0.443
1.759	1.666	0.358	0.272	0.542	0.725	0.062	0.245	0.330
0.999	1.000	0.060	0.308	0.387	0.610	0.109	0.270	0.463
0.886	1.166	0.485	0.265	0.569	0.741	0.067	0.240	0.439
1.677	1.400	0.378	0.369	0.242	0.489	0.251	0.278	0.358
1.025	1.064	0.274	0.260	0.532	0.704	0.026	0.252	0.717
1.287	1.313	0.633	0.284	0.481	0.681	0.112	0.248	0.603
2.382	2.568	0.604	0.321	0.273	0.492	0.156	0.268	0.404
2.160	1.506	0.348	0.320	0.298	0.521	0.102	0.286	0.439
1.372	1.184	0.514	0.395	0.198	0.446	0.325	0.294	0.524
1.231	1.411	0.288	0.294	0.349	0.557	0.099	0.256	0.453
2.389	1.586	0.667	0.295	0.232	0.425	0.075	0.276	0.374
0.932	0.994	0.365	0.305	0.434	0.655	0.102	0.272	0.483
4.155	2.651	0.700	0.325	0.284	0.507	0.137	0.272	0.473
1.009	1.166	0.421	0.266	0.454	0.639	0.044	0.252	0.377
1.468	1.390	0.440	0.274	0.372	0.565	0.063	0.254	0.475
1.277	1.687	0.423	0.265	0.432	0.618	0.063	0.242	0.231
2.472	2.341	0.557	0.254	0.537	0.702	0.046	0.239	0.274
1.625	1.394	0.333	0.295	0.358	0.568	0.111	0.263	0.329
1.466	1.326	0.386	0.250	0.478	0.647	0.037	0.235	0.142
1.520	1.268	0.547	0.363	0.169	0.381	0.221	0.303	0.600
0.843	1.420	0.333	0.352	0.220	0.447	0.171	0.290	0.536
1.325	1.726	0.471	0.302	0.340	0.554	0.113	0.265	0.381
1.130	1.404	0.483	0.289	0.371	0.576	0.088	0.261	0.405
1.639	1.526	0.331	0.261	0.497	0.674	0.048	0.244	0.474
1.870	2.178	0.437	0.320	0.344	0.573	0.168	0.262	0.442
3.059	1.575	0.476	0.309	0.176	0.361	0.142	0.289	0.651
2.282	1.516	0.635	0.300	0.269	0.472	0.077	0.275	0.360
0.732	0.995	0.012	0.324	0.313	0.541	0.148	0.286	0.680
1.679	1.311	0.233	0.310	0.313	0.530	0.136	0.269	0.383

BMJ Open: first published as 10.1136/bmjopen-2022-063051 on 8 November 2022. Downloaded from http://bmjopen.bmj.com/ on June 10, 2025 at Agence Bibliographique de l Enseignement Superieur (ABES) .
Protected by copyright, including for uses related to text and data mining, AI training, and similar technologies.

mean of m	standard d	high mean c	L2-norm of	mean of G	mean of m	standard d	high Gaussia	L2-norm of
absMAA	MSD	HMC	MLN	GAA	absGAA	GSD	HGC	GLN
mm^-1	mm^-1	%	-	mm^-2	mm^-2	mm^-2	%	-
0.370	0.303	27.483	0.329	0.069	0.227	0.376	170.270	2.699
0.328	0.307	99.650	0.491	0.034	0.179	0.308	561.209	5.898
0.382	0.330	39.608	0.316	0.048	0.220	0.383	193.206	2.283
0.343	0.255	35.989	0.317	0.050	0.192	0.287	202.369	2.361
0.337	0.247	25.724	0.306	0.081	0.152	0.244	111.783	1.818
0.348	0.234	10.601	0.264	0.090	0.155	0.217	56.300	1.293
0.140	0.155	68.740	0.506	0.006	0.030	0.072	337.335	7.205
0.379	0.315	27.518	0.311	0.080	0.199	0.306	125.715	1.876
0.325	0.237	-4.035	0.233	0.076	0.159	0.256	38.871	1.205
0.376	0.331	22.618	0.325	0.092	0.203	0.412	115.984	2.393
0.248	0.178	7.167	0.294	0.047	0.083	0.136	54.474	1.768
0.294	0.242	65.689	0.374	0.041	0.130	0.235	310.560	3.334
0.232	0.170	32.321	0.326	0.042	0.071	0.102	131.248	1.942
0.380	0.249	39.230	0.262	0.102	0.203	0.260	172.089	1.276
0.404	0.211	-2.756	0.215	0.132	0.193	0.229	12.202	0.746
0.215	0.197	46.687	0.382	0.024	0.082	0.158	281.687	4.003
0.671	0.414	-0.486	0.222	0.361	0.563	0.758	23.583	0.845
0.199	0.192	44.389	0.398	0.020	0.063	0.127	232.352	4.009
0.543	0.286	2.134	0.252	0.241	0.363	0.400	28.454	1.043
0.399	0.190	13.360	0.256	0.120	0.191	0.207	54.113	1.056
0.307	0.212	21.546	0.290	0.053	0.152	0.204	138.982	1.721
0.340	0.239	10.459	0.284	0.081	0.165	0.226	74.818	1.560
0.203	0.158	28.289	0.329	0.028	0.056	0.096	122.201	2.377
0.315	0.227	33.131	0.287	0.073	0.131	0.186	133.613	1.570
0.216	0.119	3.469	0.271	0.036	0.056	0.064	27.970	1.247
0.271	0.231	16.426	0.271	0.038	0.130	0.217	140.469	1.842
0.382	0.264	-3.851	0.197	0.096	0.246	0.282	55.765	0.735
0.140	0.088	2.641	0.257	0.016	0.025	0.033	36.799	1.203
0.387	0.372	50.037	0.365	0.077	0.284	0.468	327.761	3.296
0.333	0.246	41.619	0.324	0.085	0.154	0.209	177.817	1.951
0.354	0.270	84.214	0.364	0.055	0.217	0.303	487.876	2.950
0.237	0.244	86.955	0.450	0.019	0.087	0.200	441.938	5.629
0.371	0.235	13.847	0.266	0.100	0.161	0.201	51.703	1.185
0.439	0.399	46.462	0.326	0.087	0.306	0.492	240.832	2.349
0.407	0.281	37.388	0.281	0.076	0.231	0.343	163.135	1.613
0.570	0.384	4.723	0.241	0.184	0.475	0.580	60.221	1.122
0.362	0.272	20.362	0.280	0.081	0.167	0.275	85.294	1.573
0.308	0.246	27.931	0.317	0.060	0.144	0.226	147.719	2.208
0.164	0.148	40.176	0.378	0.015	0.033	0.059	142.546	2.862
0.343	0.312	37.421	0.341	0.048	0.213	0.351	242.425	2.908
0.387	0.269	3.259	0.237	0.098	0.204	0.253	45.488	1.042
0.226	0.209	46.111	0.364	0.027	0.073	0.137	206.103	2.868
0.096	0.068	19.469	0.339	0.007	0.012	0.020	92.486	2.471
0.289	0.212	30.106	0.314	0.061	0.121	0.182	145.513	1.983
0.281	0.269	107.395	0.461	0.030	0.133	0.249	629.400	5.743
0.393	0.319	32.247	0.311	0.093	0.194	0.294	119.328	1.750
0.165	0.153	31.289	0.381	0.015	0.037	0.066	136.383	2.960

For peer review only

BMJ Open: first published as 10.1136/bmjopen-2022-063051 on 8 November 2022. Downloaded from http://bmjopen.bmj.com/ on June 10, 2025 at Agence Bibliographique de l Enseignement Superieur (ABES) .
Protected by copyright, including for uses related to text and data mining, AI training, and similar technologies.

0.350	0.247	13.398	0.258	0.070	0.203	0.269	112.222	1.370
0.287	0.208	15.684	0.280	0.052	0.102	0.226	66.441	2.078
0.182	0.175	57.716	0.334	0.022	0.042	0.081	218.754	2.151
0.356	0.234	30.075	0.275	0.096	0.198	0.247	164.159	1.450
0.388	0.259	-7.566	0.195	0.122	0.195	0.277	10.566	0.715
0.460	0.300	6.766	0.251	0.122	0.315	0.390	69.545	1.155
0.407	0.329	-3.969	0.208	0.118	0.246	0.302	36.806	0.780
0.203	0.182	35.467	0.372	0.023	0.063	0.105	179.517	3.037
0.419	0.407	48.732	0.337	0.078	0.257	0.381	224.679	2.102
0.473	0.333	13.718	0.224	0.139	0.309	0.393	78.607	0.935
0.161	0.146	47.887	0.385	0.015	0.043	0.081	264.046	3.689
0.278	0.232	61.744	0.390	0.035	0.115	0.193	289.460	3.489
0.343	0.232	18.223	0.283	0.082	0.158	0.233	88.126	1.628
0.516	0.267	7.079	0.243	0.221	0.329	0.340	41.759	0.958
0.275	0.261	54.542	0.398	0.039	0.108	0.207	242.212	3.573
0.402	0.312	34.161	0.275	0.096	0.248	0.417	176.386	1.726
0.327	0.269	1.580	0.244	0.071	0.179	0.283	72.216	1.339
0.523	0.441	13.316	0.229	0.147	0.443	0.626	107.707	1.104
0.491	0.422	46.646	0.329	0.120	0.372	0.524	231.396	2.211
0.484	0.309	19.917	0.289	0.080	0.373	0.597	129.208	2.242
0.318	0.236	50.879	0.336	0.061	0.135	0.240	202.896	2.567
0.463	0.263	1.081	0.234	0.180	0.269	0.319	28.479	0.951
0.298	0.229	19.650	0.310	0.057	0.120	0.208	94.046	2.157
0.601	0.450	-12.547	0.189	0.274	0.589	0.757	24.710	0.673
0.368	0.232	16.362	0.257	0.120	0.161	0.209	60.852	1.110
0.385	0.324	48.503	0.340	0.063	0.256	0.413	281.276	2.831
0.340	0.253	36.700	0.321	0.085	0.162	0.290	161.584	2.334
0.205	0.197	40.081	0.374	0.025	0.068	0.150	216.724	3.849
0.437	0.302	3.354	0.240	0.136	0.240	0.328	34.409	1.029
0.234	0.160	59.080	0.336	0.034	0.082	0.108	276.784	2.173
0.374	0.216	17.165	0.279	0.114	0.175	0.261	71.811	1.539
0.356	0.235	21.604	0.277	0.073	0.173	0.277	101.693	1.713
0.163	0.184	59.477	0.479	0.013	0.047	0.138	347.994	8.316
0.268	0.333	43.610	0.421	0.021	0.093	0.193	166.645	3.114
0.398	0.341	33.368	0.288	0.094	0.204	0.327	128.610	1.558
0.415	0.393	32.874	0.323	0.084	0.229	0.342	134.917	1.756
0.320	0.293	-0.625	0.200	0.038	0.168	0.269	62.166	0.895
0.255	0.212	83.131	0.388	0.023	0.103	0.163	433.185	3.457
0.379	0.308	14.760	0.291	0.088	0.207	0.331	89.730	1.849
0.395	0.322	15.166	0.254	0.043	0.241	0.361	105.098	1.550
0.201	0.181	48.023	0.352	0.012	0.064	0.109	248.305	2.981
0.392	0.291	1.273	0.245	0.094	0.233	0.293	55.595	1.109
0.368	0.321	93.888	0.400	0.051	0.203	0.379	462.490	3.849
0.350	0.276	20.654	0.231	0.081	0.163	0.223	93.445	0.961
0.428	0.351	7.344	0.228	0.100	0.274	0.369	72.784	0.947
0.478	0.292	47.932	0.282	0.105	0.283	0.429	171.297	1.482
0.348	0.308	47.938	0.367	0.054	0.186	0.289	236.237	2.935
0.167	0.145	30.251	0.322	0.010	0.043	0.078	162.837	2.388
0.343	0.294	34.369	0.325	0.075	0.203	0.309	211.068	2.415
0.234	0.207	30.349	0.335	0.016	0.074	0.146	129.073	2.742

BMJ Open: first published as 10.1136/bmjopen-2022-063051 on 8 November 2022. Downloaded from http://bmjopen.bmj.com/ on June 10, 2025 at Agence Bibliographique de l Enseignement Superieur (ABES) . Protected by copyright, including for uses related to text and data mining, AI training, and similar technologies.

0.310	0.203	40.308	0.321	0.062	0.127	0.156	158.831	1.680
0.134	0.159	116.852	0.652	0.004	0.032	0.070	729.119	12.129
0.582	0.368	1.515	0.213	0.245	0.414	0.448	25.923	0.694
0.456	0.212	15.229	0.243	0.171	0.207	0.272	32.309	0.940
0.596	0.330	-4.095	0.194	0.295	0.427	0.550	10.610	0.637
0.198	0.195	35.769	0.362	0.010	0.071	0.132	235.187	3.551
0.287	0.219	20.911	0.302	0.047	0.113	0.167	100.239	1.872
0.442	0.314	19.405	0.241	0.102	0.267	0.354	94.929	1.064
0.422	0.250	13.919	0.250	0.164	0.215	0.238	56.828	1.001
0.523	0.306	4.891	0.240	0.221	0.313	0.342	26.158	0.871
0.462	0.355	30.353	0.311	0.127	0.265	0.410	111.064	1.816
0.694	0.535	9.189	0.210	0.239	0.801	1.159	98.527	0.957
0.632	0.437	20.122	0.248	0.262	0.507	0.657	83.067	1.073
0.287	0.214	18.435	0.266	0.052	0.111	0.229	88.334	1.656
0.384	0.290	31.078	0.302	0.114	0.181	0.260	109.950	1.561
0.289	0.180	12.421	0.289	0.069	0.095	0.137	43.848	1.499
0.240	0.200	49.804	0.341	0.036	0.079	0.118	206.468	2.274
0.240	0.234	97.060	0.481	0.018	0.087	0.128	487.833	4.638
0.095	0.071	28.605	0.350	0.007	0.012	0.023	123.417	2.849
0.302	0.200	35.247	0.296	0.068	0.112	0.147	124.830	1.462
0.324	0.338	121.985	0.512	0.040	0.148	0.249	593.122	4.969
0.334	0.280	-5.348	0.180	0.085	0.189	0.332	52.250	0.772
0.271	0.137	11.424	0.266	0.071	0.080	0.092	34.642	1.143
0.472	0.278	31.700	0.294	0.131	0.275	0.419	114.179	1.681
0.246	0.119	19.664	0.260	0.058	0.064	0.064	51.720	1.000
0.233	0.223	89.689	0.436	0.028	0.080	0.135	433.125	3.965
0.534	0.370	0.416	0.228	0.195	0.369	0.501	30.857	0.949
0.312	0.312	151.925	0.593	0.026	0.159	0.256	935.858	7.911
0.526	0.357	6.666	0.243	0.197	0.375	0.483	54.078	1.073
0.559	0.295	4.862	0.210	0.250	0.355	0.369	25.014	0.660
0.363	0.233	26.305	0.276	0.093	0.198	0.265	140.458	1.494
0.359	0.305	48.969	0.371	0.077	0.185	0.285	219.141	2.764
0.335	0.338	54.332	0.440	0.050	0.171	0.468	262.402	6.402
0.199	0.168	69.450	0.300	0.016	0.056	0.091	303.266	1.787
0.363	0.302	68.165	0.377	0.052	0.219	0.295	369.005	2.910
0.349	0.311	83.616	0.408	0.044	0.209	0.311	478.957	3.737
0.334	0.316	73.015	0.394	0.042	0.195	0.284	424.433	3.396
0.377	0.293	17.496	0.259	0.093	0.191	0.292	85.111	1.259
0.154	0.123	31.337	0.360	0.016	0.033	0.058	137.452	2.922
0.155	0.120	44.422	0.320	0.010	0.037	0.061	224.235	2.390
0.227	0.165	11.027	0.270	0.029	0.076	0.109	80.816	1.565
0.255	0.255	33.511	0.334	0.026	0.107	0.171	194.240	2.452
0.209	0.129	20.799	0.280	0.026	0.060	0.102	100.045	1.762
0.253	0.159	10.847	0.290	0.056	0.080	0.103	53.801	1.446
0.317	0.254	9.439	0.232	0.058	0.141	0.240	68.197	1.174
0.436	0.318	35.395	0.324	0.115	0.280	0.420	170.562	2.199
0.974	0.334	4.159	0.204	0.852	0.945	0.784	8.047	0.571
0.372	0.298	35.316	0.314	0.074	0.231	0.414	206.100	2.662
0.791	0.300	8.528	0.188	0.627	0.663	0.529	24.912	0.511
0.225	0.170	22.277	0.313	0.034	0.068	0.114	101.540	2.151

For peer review only

BMJ Open: first published as 10.1136/bmjopen-2022-063051 on 8 November 2022. Downloaded from http://bmjopen.bmj.com/ on June 10, 2025 at Agence Bibliographique de l Enseignement Superieur (ABES) . Protected by copyright, including for uses related to text and data mining, AI training, and similar technologies.

0.395	0.337	26.292	0.304	0.106	0.215	0.343	119.503	1.779
0.345	0.208	27.427	0.291	0.095	0.150	0.229	104.142	1.671
0.481	0.370	49.783	0.340	0.141	0.339	0.471	228.326	2.284
0.717	0.172	0.717	0.165	0.476	0.494	0.292	-2.452	0.350
0.360	0.183	26.541	0.277	0.083	0.154	0.221	89.651	1.407
0.420	0.192	75.210	0.252	0.135	0.181	0.207	215.113	0.927
0.114	0.110	38.262	0.407	0.008	0.019	0.049	180.146	5.047
0.242	0.132	15.827	0.287	0.046	0.076	0.105	73.711	1.611
0.363	0.333	33.399	0.348	0.076	0.189	0.303	155.409	2.388
0.545	0.457	35.031	0.288	0.193	0.368	0.588	125.531	1.531
0.664	0.437	23.027	0.275	0.240	0.730	0.921	150.513	1.489
0.589	0.286	-5.813	0.161	0.347	0.429	0.381	9.752	0.395
0.568	0.184	26.758	0.252	0.283	0.309	0.258	53.829	0.861
0.297	0.218	30.931	0.323	0.053	0.124	0.194	140.585	2.194
0.290	0.329	105.626	0.537	0.032	0.148	0.425	646.131	9.678
0.393	0.341	45.084	0.379	0.096	0.269	0.401	266.984	3.148
0.594	0.180	30.718	0.252	0.316	0.331	0.285	60.140	0.880
0.569	0.351	21.800	0.248	0.239	0.421	1.604	92.936	3.043
0.523	0.311	-7.988	0.163	0.232	0.306	0.414	-5.200	0.449
0.543	0.371	39.201	0.218	0.241	0.362	0.570	137.911	0.872
0.546	0.364	37.232	0.277	0.195	0.408	0.621	157.810	1.634
0.873	0.447	13.886	0.235	0.691	0.832	0.948	41.574	0.896
0.341	0.238	48.851	0.314	0.055	0.157	0.237	200.304	1.940
0.440	0.311	38.254	0.292	0.125	0.259	0.359	156.080	1.601
0.524	0.447	84.399	0.402	0.138	0.440	0.790	445.200	3.938
0.431	0.279	31.785	0.299	0.136	0.222	0.294	107.420	1.554
0.362	0.304	49.502	0.326	0.067	0.191	0.295	224.935	2.304
0.165	0.136	80.958	0.391	0.015	0.035	0.074	323.417	3.489
0.391	0.288	50.280	0.329	0.069	0.237	0.307	251.364	2.052
0.551	0.257	16.638	0.248	0.216	0.402	0.423	80.139	1.007
0.322	0.285	28.080	0.346	0.058	0.168	0.298	165.452	2.882
0.482	0.297	40.044	0.252	0.141	0.354	0.464	199.146	1.251
0.407	0.307	44.513	0.228	0.099	0.252	0.444	217.488	1.200
0.767	0.275	3.142	0.177	0.594	0.632	0.378	14.077	0.420
0.364	0.139	24.614	0.263	0.095	0.133	0.144	56.210	0.992
0.425	0.219	19.227	0.263	0.137	0.223	0.314	75.266	1.328
0.403	0.274	22.733	0.279	0.113	0.232	0.333	114.462	1.583
0.264	0.252	33.935	0.365	0.031	0.116	0.252	198.855	3.979
0.223	0.159	28.928	0.341	0.039	0.065	0.143	118.067	3.175
0.256	0.244	28.024	0.377	0.031	0.105	0.236	163.323	4.077
0.381	0.243	32.272	0.299	0.085	0.197	0.259	138.150	1.661
0.385	0.313	55.871	0.369	0.082	0.234	0.360	283.973	3.034
0.241	0.245	92.100	0.448	0.020	0.098	0.167	521.985	4.429
0.308	0.213	43.675	0.325	0.043	0.134	0.208	190.504	2.243
0.276	0.227	25.543	0.336	0.051	0.108	0.209	122.525	2.754
0.703	0.413	20.526	0.276	0.370	0.689	0.789	102.406	1.304
0.387	0.315	34.960	0.321	0.076	0.237	0.340	188.784	2.155
1.246	0.507	5.409	0.190	1.456	1.771	1.521	26.783	0.528
1.290	0.436	2.759	0.174	1.617	1.792	1.226	13.602	0.418
0.520	0.377	23.268	0.304	0.197	0.380	0.577	113.641	1.815

For peer review only

BMJ Open: first published as 10.1136/bmjopen-2022-063051 on 8 November 2022. Downloaded from http://bmjopen.bmj.com/ on June 10, 2025 at Agence Bibliographique de l Enseignement Superieur (ABES) .
Protected by copyright, including for uses related to text and data mining, AI training, and similar technologies.

0.978	0.554	22.089	0.237	0.888	1.297	1.236	102.055	0.872
0.793	0.359	-1.413	0.201	0.561	0.741	0.666	14.568	0.599
0.371	0.370	78.107	0.406	0.058	0.229	0.371	427.990	3.659
0.320	0.265	29.756	0.313	0.050	0.157	0.273	158.021	2.246
0.414	0.326	51.809	0.338	0.073	0.248	0.370	232.553	2.444
0.395	0.282	28.826	0.291	0.104	0.216	0.310	129.108	1.660
0.349	0.308	36.082	0.359	0.061	0.192	0.311	192.483	2.890
0.566	0.434	35.500	0.307	0.218	0.438	0.681	150.907	1.871
0.201	0.237	57.108	0.454	0.011	0.091	0.499	454.480	15.975
0.572	0.377	61.654	0.298	0.184	0.483	0.553	285.505	1.644
0.450	0.243	6.697	0.256	0.150	0.274	0.309	54.358	1.170
0.423	0.363	49.203	0.329	0.083	0.279	0.447	246.705	2.375
0.270	0.257	52.916	0.353	0.041	0.090	0.158	189.102	2.229
0.677	0.576	15.981	0.220	0.295	0.543	0.734	59.595	0.760
0.615	0.430	6.457	0.213	0.291	0.469	0.609	40.678	0.786
0.717	0.438	1.433	0.223	0.383	0.619	0.769	23.782	0.812
0.394	0.224	31.241	0.284	0.101	0.197	0.275	118.561	1.495
0.501	0.363	15.854	0.284	0.148	0.372	0.510	98.952	1.638
0.416	0.481	32.256	0.425	-0.035	0.396	3.326	301.410	22.151
0.517	0.364	10.600	0.245	0.156	0.394	0.477	79.837	1.090
0.474	0.330	1.492	0.255	0.155	0.349	0.439	60.040	1.264
0.443	0.394	72.470	0.383	0.091	0.325	0.686	393.159	4.508
0.717	0.244	-0.307	0.223	0.459	0.548	0.439	5.803	0.691
0.631	0.386	13.614	0.279	0.315	0.503	0.598	63.297	1.292
0.436	0.294	51.879	0.336	0.092	0.240	0.339	190.884	1.993
0.492	0.408	42.402	0.337	0.126	0.340	0.542	184.095	2.209
0.552	0.458	60.888	0.351	0.111	0.581	0.852	393.852	2.740
0.518	0.409	38.234	0.316	0.150	0.401	0.663	185.284	2.293
0.418	0.324	58.963	0.335	0.073	0.282	0.490	307.733	2.848
0.529	0.450	11.413	0.276	0.194	0.421	0.745	86.600	1.692
0.609	0.623	80.026	0.459	0.130	0.591	1.244	415.731	5.422
0.409	0.258	14.050	0.259	0.115	0.203	0.303	57.781	1.302
0.498	0.281	25.777	0.277	0.205	0.274	0.301	75.337	1.155
0.297	0.299	40.100	0.372	0.042	0.133	0.260	195.973	3.215
0.297	0.221	17.446	0.320	0.050	0.129	0.218	100.845	2.327
0.380	0.315	37.038	0.330	0.069	0.253	0.385	228.068	2.567
0.171	0.152	34.278	0.350	0.015	0.043	0.100	163.667	3.608
0.611	0.415	58.447	0.307	0.181	0.614	0.818	313.327	1.864
0.594	0.462	60.049	0.326	0.204	0.578	0.816	319.459	2.242
0.424	0.366	38.583	0.340	0.107	0.296	0.508	215.801	2.702
0.486	0.372	32.390	0.297	0.110	0.312	0.450	131.456	1.699
0.513	0.295	16.990	0.278	0.186	0.333	0.424	73.202	1.443
0.511	0.407	46.090	0.352	0.083	0.447	0.953	264.583	4.138
0.653	0.286	64.988	0.297	0.187	0.566	0.711	260.920	1.612
0.397	0.269	54.190	0.324	0.089	0.203	0.300	205.775	2.049
0.742	0.476	10.353	0.216	0.421	0.637	0.722	40.798	0.712
0.478	0.451	59.272	0.379	0.099	0.390	0.685	332.115	3.557

BMJ Open: first published as 10.1136/bmjopen-2022-063051 on 8 November 2022. Downloaded from http://bmjopen.bmj.com/ on June 10, 2025 at Agence Bibliographique de l Enseignement Superieur (ABES) . Protected by copyright, including for uses related to text and data mining, AI training, and similar technologies.

Gaussian curvature

For peer review only

BMJ Open: first published as 10.1136/bmjopen-2022-063051 on 8 November 2022. Downloaded from http://bmjopen.bmj.com/ on June 10, 2025 at Agence Bibliographique de l Enseignement Superieur (ABES) .
Protected by copyright, including for uses related to text and data mining, AI training, and similar technologies.

STROBE Statement—Checklist of items that should be included in reports of ***cohort studies***

	Item No	Recommendation	Page No
Title and abstract	1	(*a*) Indicate the study's design with a commonly used term in the title or the abstract	1
		(*b*) Provide in the abstract an informative and balanced summary of what was done and what was found	2
Introduction			
Background/rationale	2	Explain the scientific background and rationale for the investigation being reported	3
Objectives	3	State specific objectives, including any prespecified hypotheses	3-4
Methods			
Study design	4	Present key elements of study design early in the paper	5-8
Setting	5	Describe the setting, locations, and relevant dates, including periods of recruitment, exposure, follow-up, and data collection	n.a.
Participants	6	(*a*) Give the eligibility criteria, and the sources and methods of selection of participants. Describe methods of follow-up (*b*) For matched studies, give matching criteria and number of exposed and unexposed	n.a.
Variables	7	Clearly define all outcomes, exposures, predictors, potential confounders, and effect modifiers. Give diagnostic criteria, if applicable	6-8
Data sources/ measurement	8*	For each variable of interest, give sources of data and details of methods of assessment (measurement). Describe comparability of assessment methods if there is more than one group	5
Bias	9	Describe any efforts to address potential sources of bias	13
Study size	10	Explain how the study size was arrived at	5
Quantitative variables	11	Explain how quantitative variables were handled in the analyses. If applicable, describe which groupings were chosen and why	6-7
Statistical methods	12	(*a*) Describe all statistical methods, including those used to control for confounding	8
		(*b*) Describe any methods used to examine subgroups and interactions	8
		(*c*) Explain how missing data were addressed	n.a.
		(*d*) If applicable, explain how loss to follow-up was addressed	n.a.
		(*e*) Describe any sensitivity analyses	5-8
Results			
Participants	13*	(a) Report numbers of individuals at each stage of study—eg numbers potentially eligible, examined for eligibility, confirmed eligible, included in the study, completing follow-up, and analysed	5
		(b) Give reasons for non-participation at each stage	n.a.
		(c) Consider use of a flow diagram	n.a.
Descriptive data	14*	(a) Give characteristics of study participants (eg demographic, clinical, social) and information on exposures and potential confounders	n.a.
		(b) Indicate number of participants with missing data for each variable of interest	n.a.
		(c) Summarise follow-up time (eg, average and total amount)	n.a.
Outcome data	15*	Report numbers of outcome events or summary measures over time	n.a.

For peer review only - http://bmjopen.bmj.com/site/about/guidelines.xhtml

Protected by copyright, including for uses related to text and data mining, AI training, and similar technologies. Enseignement Superieur (ABES) .

Main results	16	(*a*) Give unadjusted estimates and, if applicable, confounder-adjusted estimates and their precision (eg, 95% confidence interval). Make clear which confounders were adjusted for and why they were included	9-10
		(*b*) Report category boundaries when continuous variables were categorized	n.a.
		(*c*) If relevant, consider translating estimates of relative risk into absolute risk for a meaningful time period	n.a.
Other analyses	17	Report other analyses done—eg analyses of subgroups and interactions, and sensitivity analyses	9-10
Discussion			
Key results	18	Summarise key results with reference to study objectives	11
Limitations	19	Discuss limitations of the study, taking into account sources of potential bias or imprecision. Discuss both direction and magnitude of any potential bias	13
Interpretation	20	Give a cautious overall interpretation of results considering objectives, limitations, multiplicity of analyses, results from similar studies, and other relevant evidence	13
Generalisability	21	Discuss the generalisability (external validity) of the study results	11-12
Other information			
Funding	22	Give the source of funding and the role of the funders for the present study and, if applicable, for the original study on which the present article is based	14

*Give information separately for exposed and unexposed groups.

Note: An Explanation and Elaboration article discusses each checklist item and gives methodological background and published examples of transparent reporting. The STROBE checklist is best used in conjunction with this article (freely available on the Web sites of PLoS Medicine at http://www.plosmedicine.org/, Annals of Internal Medicine at http://www.annals.org/, and Epidemiology at http://www.epidem.com/). Information on the STROBE Initiative is available at http://www.strobe-statement.org.

For peer review only - http://bmjopen.bmj.com/site/about/guidelines.xhtml

For peer review only

Enseignement Superieur (ABES) .
Protected by copyright, including for uses related to text and data mining, AI training, and similar technologies.

BMJ Open

Geometric uncertainty in intracranial aneurysm rupture status discrimination: a two-site retrospective study.

Journal:	*BMJ Open*
Manuscript ID	bmjopen-2022-063051.R2
Article Type:	Original research
Date Submitted by the Author:	01-Aug-2022

Complete List of Authors:	Hellmeier, Florian; Charité – Universitätsmedizin Berlin, Institute for Computer-Assisted Cardiovascular Medicine Brüning, Jan; Charité Universitätsmedizin Berlin, Insitute for Computer-Assisted Cardiovascular Medicine Berg, Philipp; University of Magdeburg, Fluid Dynamics and Technical Flows Saalfeld, Sylvia; University of Magdeburg 'Otto von Guericke', Department of Simulation and Graphics Spuler, Andreas; Helios Klinikum Berlin-Buch Sandalcioglu, I. Erol; Otto von Guericke Universitat Magdeburg, Department of Neurosurgery Beuing, Oliver; AMEOS Hospital Bernburg, Deparment of Radiology Larsen, Naomi; University Medical Center Schleswig-Holstein, Department of Radiology and Neuroradiology Schaller, Jens; Charité – Universitätsmedizin Berlin Goubergrits, Leonid ; Charite Universitatsmedizin Berlin, Institute for Computer-Assisted Cardiovascular Medicine

Primary Subject Heading:	Research methods
Secondary Subject Heading:	Neurology, Radiology and imaging
Keywords:	Neurology < INTERNAL MEDICINE, Neuroradiology < RADIOLOGY & IMAGING, Neurosurgery < SURGERY

SCHOLARONE™ Manuscripts

BMJ Open: first published as 10.1136/bmjopen-2022-063051 on 8 November 2022. Downloaded from http://bmjopen.bmj.com/ on June 10, 2025 at Agence Bibliographique de l Enseignement Superieur (ABES) .
Protected by copyright, including for uses related to text and data mining, AI training, and similar technologies.

I, the Submitting Author has the right to grant and does grant on behalf of all authors of the Work (as defined in the below author licence), an exclusive licence and/or a non-exclusive licence for contributions from authors who are: i) UK Crown employees; ii) where BMJ has agreed a CC-BY licence shall apply, and/or iii) in accordance with the terms applicable for US Federal Government officers or employees acting as part of their official duties; on a worldwide, perpetual, irrevocable, royalty-free basis to BMJ Publishing Group Ltd ("BMJ") its licensees and where the relevant Journal is co-owned by BMJ to the co-owners of the Journal, to publish the Work in this journal and any other BMJ products and to exploit all rights, as set out in our licence.

The Submitting Author accepts and understands that any supply made under these terms is made by BMJ to the Submitting Author unless you are acting as an employee on behalf of your employer or a postgraduate student of an affiliated institution which is paying any applicable article publishing charge ("APC") for Open Access articles. Where the Submitting Author wishes to make the Work available on an Open Access basis (and intends to pay the relevant APC), the terms of reuse of such Open Access shall be governed by a Creative Commons licence – details of these licences and which Creative Commons licence will apply to this Work are set out in our licence referred to above.

Other than as permitted in any relevant BMJ Author's Self Archiving Policies, I confirm this Work has not been accepted for publication elsewhere, is not being considered for publication elsewhere and does not duplicate material already published. I confirm all authors consent to publication of this Work and authorise the granting of this licence.

For peer review only

Enseignement Superieur (ABES) .
Protected by copyright, including for uses related to text and data mining, AI training, and similar technologies.

BMJ Open: first published as 10.1136/bmjopen-2022-063051 on 8 November 2022. Downloaded from http://bmjopen.bmj.com/ on June 10, 2025 at Agence Bibliographique de l Enseignement Superieur (ABES) . Protected by copyright, including for uses related to text and data mining, AI training, and similar technologies.

Geometric uncertainty in intracranial aneurysm rupture status discrimination: a two-site retrospective study.

Florian Hellmeier[1], Jan Brüning[1], Philipp Berg[2,3], Sylvia Saalfeld[3,4], Andreas Spuler[5], I. Erol Sandalcioglu[6], Oliver Beuing[7], Naomi Larsen[8], Jens Schaller[1], Leonid Goubergrits[1,9]

[1] Institute of Computer-assisted Cardiovascular Medicine, Charité – Universitätsmedizin Berlin, Berlin, Germany

[2] Laboratory of Fluid Dynamics and Technical Flows, University of Magdeburg, Magdeburg, Germany

[3] Research Campus *STIMULATE*, University of Magdeburg, Magdeburg, Germany

[4] Department of Simulation and Graphics, University of Magdeburg, Magdeburg, Germany

[5] Helios Klinikum Berlin-Buch, Berlin, Germany

[6] Department of Neurosurgery, University Hospital Magdeburg, Magdeburg, Germany

[7] Department of Radiology, AMEOS Hospital, Bernburg, Germany

[8] Department of Radiology and Neuroradiology, University Medical Center Schleswig-Holstein (UKSH), Kiel, Germany

[9] Einstein Center Digital Future, Berlin, Germany

Correspondence:

Jan Brüning

Email: jan.bruening@charite.de

Telephone: +49 30 450 553 879

Telefax: +49 30 450 553 838

Charité – Universitätsmedizin Berlin
Institute of Computer-assisted Cardiovascular Medicine
Augustenburger Platz 1
13353 Berlin
Germany

Keywords: intracranial aneurysms; uncertainty analysis; rupture risk assessment;

Word count: 4,003

For peer review only

For peer review only

BMJ Open: first published as 10.1136/bmjopen-2022-063051 on 8 November 2022. Downloaded from http://bmjopen.bmj.com/ on June 10, 2025 at Agence Bibliographique de l Enseignement Superieur (ABES) .
Protected by copyright, including for uses related to text and data mining, AI training, and similar technologies.

BMJ Open: first published as 10.1136/bmjopen-2022-063051 on 8 November 2022. Downloaded from http://bmjopen.bmj.com/ on June 10, 2025 at Agence Bibliographique de l Enseignement Superieur (ABES) . Protected by copyright, including for uses related to text and data mining, AI training, and similar technologies.

Abstract

Objectives: Assessing the risk associated with unruptured intracranial aneurysms (IA) is essential in clinical decision making. Several geometric risk parameters have been proposed for this purpose. However, performance of these parameters has been inconsistent. This study evaluates the performance and robustness of geometric risk parameters on two datasets and compare it to the uncertainty inherent in assessing these parameters and quantifies inter-parameter correlations.

Methods: Two datasets containing 244 ruptured and unruptured IA geometries from 178 patients were retrospectively analyzed. IAs were stratified by anatomical region, based on the PHASES score locations. 37 geometric risk parameters representing four groups (size, neck, non-dimensional, and curvature parameters) were assessed. Analysis included standardized absolute differences (SAD) between ruptured and unruptured IAs, ratios of SAD to median relative uncertainty (MRU) associated with the parameters, and inter-parameter correlation.

Results: The ratio of SAD to MRU was lower for higher-dimensional size parameters (i.e., areas and volumes) than for one-dimensional size parameters. Non-dimensional size parameters performed comparatively well with regard to SAD and MRU. SAD was higher in the posterior anatomical region. Correlation of parameters was strongest within parameter (sub)groups and between size and curvature parameters, while anatomical region did not strongly affect correlation patterns.

Conclusion: Non-dimensional parameters and few parameters from other groups were comparatively robust, suggesting that they might generalize better to other datasets. The data on discriminative performance and inter-parameter correlations presented in this study may aid in developing and choosing robust geometric parameters for use in rupture risk models.

For peer review only

Strengths and limitations of this study

- This study provides location-specific estimates of the discriminative ability of a large set of geometric parameters for IA rupture status assessment, while also considering uncertainty.
- The analysis was performed on two independent datasets to assess robustness of the findings.
- Even though the relative uncertainty in acquisition of each geometric risk parameter was evaluated based on more than 20 individual segmentations performed during the Multiple Aneurysms Anatomy Challenge, this evaluation was only performed on five aneurysms in total.

For peer review only

BMJ Open: first published as 10.1136/bmjopen-2022-063051 on 8 November 2022. Downloaded from http://bmjopen.bmj.com/ on June 10, 2025 at Agence Bibliographique de l Enseignement Superieur (ABES) .
Protected by copyright, including for uses related to text and data mining, AI training, and similar technologies.

BMJ Open: first published as 10.1136/bmjopen-2022-063051 on 8 November 2022. Downloaded from http://bmjopen.bmj.com/ on June 10, 2025 at Agence Bibliographique de l Enseignement Superieur (ABES) . Protected by copyright, including for uses related to text and data mining, AI training, and similar technologies.

Introduction

A relevant part of the general population harbors one or more unruptured intracranial aneurysms (IAs), with the overall prevalence estimated around 3% [1]. While most IAs do not rupture [2], the question of whether and when to treat them remains relevant due to the poor prognosis of ruptured IAs [3, 4] as well as the risk of intervention [3, 5]. Current American Heart Association/American Stroke Association guidelines list several modifiable and non-modifiable risk factors for IA growth and/or rupture, including IA location, growth rate, morphology, smoking status, alcohol consumption, hypertension, age, sex, previous IA, and family history [6]. Attempts have been made to develop scoring systems to quantify rupture risk, growth risk, and/or support treatment decisions, these include the PHASES score by Greving et al. [7], the UIATS by Etminan et al. [8] and the ELAPSS score by Backes et al. [9]. All three of these scores are based on clinically available data and all include geometric rupture risk parameters: IA size in case of the PHASES score [7], surface irregularity, size ratio, as well as aspect ratio in case of the UIATS [8], and IA size as well as surface irregularity for the ELAPSS score [9]. While these metrics were designed to support clinical decision making, performance on clinical data has been mixed [10-12] and improvements, particularly for patients harboring multiple IAs, are desired by clinicians [13].

The aim of this paper is to assess the ability of a broad number of proposed geometric risk parameters to differentiate between unruptured and ruptured IAs while also comparing their discriminative ability relative to the uncertainty encountered in determining them. Any acquisition of patient-specific IA geometries and subsequent use of these geometries to derive geometric risk parameters is affected by a number of uncertainty-introducing factors. Starting with the medical imaging acquisition itself, which is followed by image data pre-processing, segmentation, geometry reconstruction including post-processing (e.g., smoothing, checking of topology), and finally calculation of the geometric risk parameters. All these processing steps are associated with some errors, resulting in uncertainty, which negatively affects the ability of parameters to discriminate IA rupture status. Discrimination of rupture status on an individual IA level is, however, necessary if these parameters are to support the clinical decision-making process, including any decisions regarding treatment modalities. Previous studies found high variability in the uncertainty of different geometric risk parameters as well as differences in their ability to differentiate between ruptured and unruptured IAs [14-16]. Furthermore, for geometric risk parameters with multiple alternative definitions, the specific implementation can affect the discriminative performance of the parameter itself and any derived parameters, as demonstrated by Lauric et al. for parameters incorporating IA and neck size [17].

The current study was performed to facilitate optimal selection of geometric rupture risk parameters by identifying geometric parameters, which are good discriminators while also exhibiting low uncertainty. The analysis is performed on two datasets processed by different research groups and is differentiated by anatomical region, in order to assess how the rupture status discrimination of the geometric parameters is affected by geometry processing as well as anatomical location. Additionally, correlation of the geometric risk parameters with each other is assessed.

For peer review only

BMJ Open: first published as 10.1136/bmjopen-2022-063051 on 8 November 2022. Downloaded from http://bmjopen.bmj.com/ on June 10, 2025 at Agence Bibliographique de l Enseignement Superieur (ABES) .
Protected by copyright, including for uses related to text and data mining, AI training, and similar technologies.

BMJ Open: first published as 10.1136/bmjopen-2022-063051 on 8 November 2022. Downloaded from http://bmjopen.bmj.com/ on June 10, 2025 at Agence Bibliographique de l Enseignement Superieur (ABES) . Protected by copyright, including for uses related to text and data mining, AI training, and similar technologies.

Methods

Medical imaging data

IA geometries were retrospectively reconstructed and segmented from 3D rotational angiography data acquired for routine clinical indications. Data was collected consecutively. The inclusion criteria of the datasets were imaging modality and the corresponding acquisition resolution. Cases with considerable segmentation artifacts such as close vessels that appear to be merged or holes in the segmented lumen were rejected from the analysis. 142 IAs were acquired in the Helios Klinikum Berlin-Buch (Berlin, Germany), 38 in KRH Klinikum Nordstadt (Hanover, Germany), 23 in the University Medical Center Schleswig-Holstein (UKSH) (Kiel, Germany), and 41 in the University Hospital Magdeburg (Magdeburg, Germany). Processing of the imaging data, including segmentation, was performed at two sites: Berlin, which processed 142 IAs from Helios Klinikum Berlin-Buch (dataset 1), and Magdeburg, which processed 102 IAs from KRH Klinikum Nordstadt, UKSH, and University Hospital Magdeburg (dataset 2). Overall, 244 IAs from 178 patients were included, from which geometric risk parameters were subsequently calculated. Based on the PHASES score [7], aneurysm location was classified into four anatomical regions: internal carotid artery (ICA), middle cerebral artery (MCA), anterior region (all vessels anterior of the ICA/MCA), and posterior region (all vessels posterior of the ICA/MCA). The distribution of the individual IA locations and their assignment to the four anatomical regions are shown in Table 1.

Table 1: Frequency and rupture status of individual IA locations by dataset. ACA: anterior cerebral artery, AComA: anterior communicating artery, AChA: anterior choroidal artery, ICA: internal carotid artery, MCA: middle cerebral artery, PComA: posterior communicating artery, PCA: posterior cerebral artery, SCA: superior cerebellar artery, BA: basilar artery, PICA: posterior inferior cerebellar artery, VA: vertebral artery.

Anatomical region	Vessel	Dataset 1 unruptured	Dataset 1 ruptured	Dataset 2 unruptured	Dataset 2 ruptured
Anterior	ACA	3	1	2	2
	AComA	10	22	11	5
ICA	AChA	0	1	1	2
	ICA	29	8	19	4
MCA	MCA	28	10	31	8
Posterior	PComA	8	10	2	4
	PCA	0	1	0	0
	SCA	0	0	1	1
	BA	4	3	3	4
	PICA	0	4	1	0
	VA	0	0	0	1

BMJ Open: first published as 10.1136/bmjopen-2022-063051 on 8 November 2022. Downloaded from http://bmjopen.bmj.com/ on June 10, 2025 at Agence Bibliographique de l Enseignement Superieur (ABES) . Protected by copyright, including for uses related to text and data mining, AI training, and similar technologies.

Geometric risk parameters

Historically, several geometric parameters for IA rupture risk assessment have been proposed. In order to have access to information on parameter uncertainty, the parameters chosen for this study were limited to a subset of the parameters reported in Goubergrits et al. [14], a parameter uncertainty study performed on segmentation data obtained during the Multiple Aneurysms AnaTomy Challenge (MATCH) 2018 [18]. The major outcome of this study was the median relative uncertainty (MRU) of geometric parameters. Briefly, five aneurysms were segmented and reconstructed by 26 international research groups, which participated in the MATCH challenge. These segmentations were used to calculate the median and the 68.3% range between the 84.13th and the 15.87th percentile of all selected geometric parameters for each of the five aneurysms. The uncertainty range was selected with respect to the range of ± one standard deviation for normally distributed data reported in other studies. The uncertainty was defined as the uncertainty range divided by the median value and calculated for each geometric parameter. Finally, the average of all five aneurysms was calculated to define the MRU. For a detailed description of the parameters and the rationale for choosing the parameters, the interested reader is referred to Goubergrits et al. [14]. Briefly, most of the proposed geometric parameters describe aneurysm and/or aneurysmal neck size or shape, or irregularity. These parameters were previously proposed as predictors for rupture risk. Table 2 lists the geometric parameters, their abbreviations and MRU values, as well as their respective references.

Table 2: List of the investigated geometric parameters, their descriptions, and median relative uncertainties (MRU). Note that terminology and implementation in the references might differ subtly. Derived and modified from tables 1-5 from Goubergrits et al. [14], used under Creative Commons Attribution License (CC BY 4.0). The CC BY 4.0 license text is available at https://creativecommons.org/licenses/by/4.0/.

Parameter group	Parameter name, unit [exemplary reference]	Parameter abbreviation	Short description	MRU
Size	Height, mm [19]	H	Maximum perpendicular distance from the neck plane to the aneurysm surface	0.140
	Maximum dimension, mm [20]	L_{max}	Maximum distance between two points on the aneurysm surface	0.157
	Maximum height, mm [15]	H_{max}	Maximum distance between the centroid of the neck and the aneurysm surface	0.123
	Maximum diameter, mm [17]	D_{max}	Maximum neck plane-parallel distance between two points on the aneurysm surface	0.169
	Bulge height, mm [19]	H_b	Distance between the neck plane and the maximum diameter	0.373
	Surface area, mm^2 [15]	A	Surface area of the aneurysm	0.215

	Convex hull surface area, mm^2 [15]	A_{CH}	Surface area of the aneurysm's convex hull	0.277
	Minimal bounding sphere surface area, mm^2 [21]	A_{MBS}	Surface area of the aneurysm's minimal bounding sphere	0.305
	Closed surface area, mm^2	A_{closed}	Surface area of the neck-closed aneurysm	0.283
	Volume, mm^3 [15]	V	Volume of the neck-closed aneurysm	0.392
	Convex hull volume, mm^3 [15]	V_{CH}	Volume of the aneurysm's convex hull	0.399
	Minimal bounding sphere volume, mm^3 [21]	V_{MBS}	Volume of the aneurysm's minimal bounding sphere	0.451
Neck	Minimum neck diameter, mm [17]	$D_{neck,min}$	Minimum distance between two opposite points on the neck perimeter	0.306
	Maximum neck diameter, mm [22]	$D_{neck,max}$	Maximum distance between two points on the neck perimeter	0.348
	Neck perimeter, mm [19]	P_{neck}	Perimeter of the aneurysm neck	0.374
	Equivalent neck diameter, mm [19]	$D_{neck,equiv}$	Hydraulic diameter of the aneurysm neck	0.276
	Neck area, mm^2 [19]	A_{neck}	Area of the aneurysm neck	0.593
	Elliptical neck area, mm^2	$A_{neck,elliptical}$	Neck area calculated as the product of the minimum and maximum neck diameter	0.650
Non-dimensional	Aspect ratio [22]	AR	Ratio of height to maximum neck diameter	0.293
	Equivalent aspect ratio [19]	eAR	Ratio of height to equivalent neck diameter	0.326
	Bottleneck factor [19]	BF	Ratio of maximum diameter to maximum neck diameter	0.201
	Bulge location [19]	BL	Ratio of bulge height to height	0.301
	Nonsphericity index [15]	NSI	Normalized ratio of volume to surface area relative to a hemisphere	0.108
	Aneurysm volume to bounding sphere volume [21]	AVSV	Ratio of volume to minimal bounding sphere volume	0.173
	Aneurysm surface area to bounding sphere area [21]	AASA	Ratio of surface area to minimal bounding sphere surface area	0.095

For peer review only

BMJ Open: first published as 10.1136/bmjopen-2022-063051 on 8 November 2022. Downloaded from http://bmjopen.bmj.com/ on June 10, 2025 at Agence Bibliographique de l Enseignement Superieur (ABES) . Protected by copyright, including for uses related to text and data mining, AI training, and similar technologies.

	Undulation index [15]	UI	1 minus the ratio of volume to convex hull volume	0.709
	Ellipticity index [15]	EI	Normalized ratio of convex hull volume to convex hull surface area relative to a hemisphere	0.051
Curvature	Mean of mean curvature, mm^{-1} [19]	MAA	Surface average of local mean curvature	0.136
	Mean of absolute mean curvature, mm^{-1}	absMAA	Surface average of the magnitude of the local mean curvature	0.133
	Standard deviation of mean curvature, mm^{-1}	MSD	Standard deviation of the local mean curvature	1.011
	High mean curvature, % [21]	HMC	Relative increase of the mean of absolute mean curvature over the mean curvature of the minimal bounding sphere	0.396
	L2-norm of mean curvature [19]	MLN	Scale invariant measure of surface irregularity, uses mean curvature	0.150
	Mean of Gaussian curvature, mm^{-2} [19]	GAA	Surface average of local Gaussian curvature	0.344
	Mean of absolute Gaussian curvature, mm^{-2}	absGAA	Surface average of the magnitude of the local Gaussian curvature	0.485
	Standard deviation of Gaussian curvature, mm^{-2}	GSD	Standard deviation of the local Gaussian curvature	1.798
	High Gaussian curvature, % [21]	HGC	Relative increase of the mean of absolute Gaussian curvature over the Gaussian curvature of the minimal bounding sphere	0.822
	L2-norm of Gaussian curvature [19]	GLN	Scale invariant measure of surface irregularity, uses Gaussian curvature	0.545

Since the diameter of the parent vessel was not available for all IAs studied, size ratio could not be calculated and was excluded. Furthermore, UI and CR as well as NSI and NPR are directly related through $CR = 1 - UI$ and $IPR = \frac{\sqrt[3]{18\pi}}{1 - NSI}$, respectively. CR and IPR were therefore not included in the analysis, in order to avoid redundancy. Geometric risk parameters were calculated from the IA geometries using MATLAB (version R2017b, MathWorks, Natick, USA), Python (version 3.7.1, Python Software Foundation, Delaware, USA), and ZIBAmira (version 2015.28, Zuse Institute Berlin, Germany). The individual parameter values, IA location, and rupture status for each IA in this study, as well as the exact

BMJ Open: first published as 10.1136/bmjopen-2022-063051 on 8 November 2022. Downloaded from http://bmjopen.bmj.com/ on June 10, 2025 at Agence Bibliographique de l Enseignement Superieur (ABES) . Protected by copyright, including for uses related to text and data mining, AI training, and similar technologies.

BMJ Open: first published as 10.1136/bmjopen-2022-063051 on 8 November 2022. Downloaded from http://bmjopen.bmj.com/ on June 10, 2025 at Agence Bibliographique de l Enseignement Superieur (ABES) . Protected by copyright, including for uses related to text and data mining, AI training, and similar technologies.

values of the inter-parameter correlation coefficients are provided as supplemental material 1 and 2 respectively.

Statistical analysis

Since most of the geometric risk parameters were non-normally distributed, as assessed by Q-Q plots and Shapiro-Wilk tests, the median was used to quantify central tendency and the interquartile range was used to quantify dispersion. Correlations were quantified using Pearson's r with correlations $|r| \geq 0.75$ referred to as strong, while those with $0.75 > |r| \geq 0.25$ and $|r| < 0.25$ referred to as moderate and weak, respectively. Statistical analysis was performed using SPSS (version 28.0.0.0, IBM, Armonk, USA) and MATLAB.

The discriminative ability of the individual parameters was assessed by standardizing the absolute difference between the medians of the ruptured and unruptured IAs with the weighted arithmetic mean of the IQRs of the two groups. This measure of effect size will be referred to as the standardized absolute group difference (SAD). Furthermore, the ratio of the SAD to the relative uncertainty, a measure of the uncertainty associated with parameter calculation, from Goubergrits et al. [14] was calculated for all parameters and will be referred to as the group difference-uncertainty ratio (DUR). The equations for SAD and DUR are thus $SAD = \frac{(n_r + n_u) \cdot |m_r - m_u|}{n_r IQR_r + n_u IQR_u}$ and $DUR = \frac{SAD}{MRU}$, where n_i, m_i, and IQR_i are the sample sizes, median values, and interquartile ranges of the geometric parameters evaluated for ruptured (subscript *r*) and unruptured (subscript *u*) samples, while MRU is the median relative uncertainty from Goubergrits et al. [14], which is also listed in Table 2. SAD and DUR may take any value ≥0 with higher values indicating stronger discriminative ability and a better ratio of discriminative ability to uncertainty, respectively. SAD and DUR values of zero would indicate no discriminative ability and the worst possible ratio of discriminative ability to uncertainty, respectively. Additionally, the correlation coefficients between the parameters were calculated. Analysis of SAD and DUR as well as the correlation coefficients was performed individually for each anatomical region and each dataset.

Patient and public involvement

Due to the purely retrospective manner of this study, no involvement of patients or the general public was considered.

Results

Figure 1 shows SAD for all geometric risk parameters by anatomical region and dataset. Considering both datasets, the following parameters achieved the comparatively highest SAD for each anatomical region: curvature (HMC, MLN, HGC, GLN) and non-dimensional (AR, eAR, AVSV, AASA) parameters in the anterior region, curvature (HMC, HGC) and non-dimensional (NSI, AASA, EI) parameters in the ICA, non-dimensional (AR, eAR, BL, AVSV, AASA) parameters in the MCA, and size (H, L_{max}, A, A_{MBS}) and curvature (MSD, absGAA, GSD) parameters in the posterior region. Compared to the other anatomical regions, SAD was higher in the posterior region and more parameters exhibited relatively high SAD. Looking at all anatomical regions combined, curvature (HMC, MLN, absGAA, HGC, GLN) and non-dimensional (AR, eAR, AVSV, AASA) parameters as well as one neck ($D_{neck,min}$) and one size (H_b) parameter show comparatively high SAD in both datasets. Furthermore, the differences between the two datasets become less pronounced when combining all anatomical regions. Moreover, this combined evaluation resulted in SAD being higher for the size parameters in site 2 compared to site 1. Here, it is worthwhile to note that the SAD of this combined assessment is not the average of the SAD of all four region-specific evaluations. Thus, pooling for some parameters can result in the absolute difference between the ruptured and unruptured groups to be close to zero, which results in SAD values close to zero as observed for the one-dimensional size parameters of the site 1 dataset.

Figure 2 shows DUR for all geometric risk parameters by anatomical region and dataset. Considering both datasets, the following parameters achieved the comparatively highest DUR for each anatomical region: non-dimensional (AASA, EI) and one curvature (MLN) parameter in the anterior region, non-dimensional (EI, AASA, NSI) parameters in the ICA, non-dimensional (AASA, EI) parameters in the MCA, and size parameters (H, L_{max}, H_{max}, A), curvature (MAA, absMAA), and one non-dimensional (EI) parameter in the posterior region. Similar to SAD, DUR in the posterior region was overall higher and more parameters exhibited relatively high DUR, compared to the other anatomical regions. Looking at all anatomical regions combined, non-dimensional (NSI, AVSV, AASA, EI) and curvature (absMAA, MLN) parameters show comparatively high DUR in both datasets. As for SAD, the differences between the two datasets are less pronounced when looking at all anatomical regions combined.

Figures 3 and 4 show correlation coefficients between the geometric risk parameters by anatomical region for both datasets. The following general features are present in most data correlation plots: The size parameters (H, L_{max}, H_{max}, D_{max}, H_b, A, A_{CH}, A_{MBS}, A_{closed}, V, V_{CH}, V_{MBS}) are generally strongly correlated with each other. Similarly, the neck parameters ($D_{neck,min}$, $D_{neck,max}$, P_{neck}, $D_{neck,equiv}$, A_{neck}, $A_{neck,elliptical}$) are also generally strongly correlated with each other.

BMJ Open: first published as 10.1136/bmjopen-2022-063051 on 8 November 2022. Downloaded from http://bmjopen.bmj.com/ on June 10, 2025 at Agence Bibliographique de l Enseignement Superieur (ABES) . Protected by copyright, including for uses related to text and data mining, AI training, and similar technologies.

BMJ Open: first published as 10.1136/bmjopen-2022-063051 on 8 November 2022. Downloaded from http://bmjopen.bmj.com/ on June 10, 2025 at Agence Bibliographique de l Enseignement Superieur (ABES) . Protected by copyright, including for uses related to text and data mining, AI training, and similar technologies.

Within the non-dimensional parameter group, there are two distinct subgroups in most plots: one formed by AR, eAR, BF, and BL and one formed by NSI, AVSV, AASA, UI, and EI. Within the latter subgroup, several of the correlations are negative but their magnitude is overall moderate to strong. The curvature parameters also form two subgroups, one formed by dimensional curvature parameters (MAA, absMAA, MDS, GAA, absGAA, GSD) and one by non-dimensional curvature parameters (HMC, MLN, HGC, GLN). With regard to correlations between parameter groups, there is generally moderate to strong correlation between the size and neck parameters. Additionally, the size and neck parameters are generally moderately correlated with the curvature parameters, the direction of the correlation being positive for the non-dimensional curvature parameters and negative for the dimensional curvature parameters.

For peer review only

Discussion

Previous research has assessed the impact of uncertainty on geometric risk parameters in a limited fashion. Ma et al. examined the influence of random noise on the calculation of 14 geometric risk parameters, finding curvature parameters more susceptible to random noise than size, neck, and non-dimensional parameters [19]. Others have examined the influence of imaging modality [23] and CT angiography reconstruction kernel [24] on geometric risk parameters. Regarding image acquisition, Ramachandran et al. have examined the influence of imaging modality [23], while O'Meara et al. [24] and Berg et al. [25] have focused on the reconstruction kernel's effect on geometric and hemodynamic risk parameters, respectively. The current study as well as the earlier uncertainty study based on the MATCH challenge were both based on 3D rotational angiography imaging, which is the routine imaging modality in both centers involved in this study. Other sensitivity and uncertainty aspects of computational fluid dynamics approaches to IAs have been explored, e.g., by Cebral et al. [26], Sarrami-Foroushani et al. [27], and Schneiders et al. [28]. To the authors' knowledge there is, however, no comprehensive publication relating discriminative performance and uncertainty of geometric risk parameters, while also providing detailed data on their correlation with each other.

Looking at the parameter groups examined in this study, the following findings can be made: the size and neck parameters measuring areas (A, A_{CH}, A_{MBS}, A_{closed}, A_{neck}, $A_{neck,elliptical}$) and volumes (V, V_{CH}, V_{MBS}) generally do not achieve high DUR, despite having SAD similar to the size and neck parameters measuring length (H, L_{max}, H_{max}, D_{max}, H_b, $D_{neck,min}$, $D_{neck,max}$, P_{neck}, $D_{neck,equiv}$). The cause is the higher uncertainty encountered in determining the higher-dimensional parameters when compared to the one-dimensional parameters [14]. This suggests that higher-dimensional size parameters tend to be less robust and thus less suitable for use in practical risk models than one-dimensional size parameters. Like Lauric et al. [17], there are instances of noticeable differences in the discriminative performance of parameters capturing the same aspect of IA geometry, e.g., for the neck size parameters. The non-dimensional parameters exhibit comparatively high SAD and DUR, except for BL and UI, which exhibit lower discriminative ability and/or higher uncertainty in their calculation. The curvature parameters show substantial variability in SAD and DUR depending on the anatomical region and the parameter, with MLN performing comparatively well overall. It is notable that the posterior region tends to exhibit higher SAD and DUR than the other regions, indicating more pronounced geometric differences between ruptured and unruptured IAs in this region. Regarding the differences in SAD and DUR between datasets 1 and 2, it is likely that differences in the patient collectives, subsample sizes, and reconstruction techniques are the main causes. The latter could in the future be tackled by machine learning-based segmentation methods, which can reduce operator-induced uncertainty. Examples of such methods have previously been presented, e.g., in the context of the CADA challenge [29].

BMJ Open: first published as 10.1136/bmjopen-2022-063051 on 8 November 2022. Downloaded from http://bmjopen.bmj.com/ on June 10, 2025 at Agence Bibliographique de l Enseignement Superieur (ABES) . Protected by copyright, including for uses related to text and data mining, AI training, and similar technologies.

Regarding the correlation patterns, there is substantial similarity between all analyzed anatomical regions and datasets. Parameters tend to be most strongly correlated with other parameters from the same parameter group, except for the non-dimensional and curvature parameters, which form two subgroups each. This is reasonable, given that the parameters within each parameter group capture similar aspects of IA geometry. For the size and neck parameter groups this is obvious, since they both capture aspects of IA and neck size, respectively. The two distinct correlation subgroups within the non-dimensional parameter group are likely caused by the underlying parameter subgroups capturing different aspects of aneurysm shape. While the parameters of the first subgroup (AR, eAR, BF, BL) are simply ratios of one-dimensional size parameters, the second subgroup (NSI, AVSV, AASA, UI, EI) is formed by parameters relating aneurysm area and/or volume to geometric reference objects, e.g., the minimal bounding sphere or convex hull. The negative correlation between AVSV and AASA with the other parameters from the second subgroup is due to the parameter definitions, which cause AVSV and AASA to increase with increasing sphericity, while the other parameters tend to decrease with increasing sphericity. The curvature parameters also form two subgroups, with the first subgroup consisting of the dimensional parameters quantifying the mean or dispersion of IA surface curvature (MAA, absMAA, MSD, GAA, absGAA, GSD) and the second subgroup consisting of non-dimensional, scale invariant curvature parameters (HMC, MLN, HGC, GLN). Since the former parameters intrinsically decrease with IA size, while the latter parameters increase with IA size, the negative correlation of the two subgroups with each other makes sense. It should be noted that the positive correlation of the non-dimensional curvature parameters with IA size is not an intrinsic property of the non-dimensional parameters themselves, since they are designed to be scale invariant. It rather indicates that curvature and irregularities of the IA surface increase in larger IAs.

For a geometric risk parameter to be a good candidate for rupture risk prediction, it should generally have a high SAD, in order to be able to differentiate between ruptured and unruptured IAs. Additionally, DUR should be high, indicating low sensitivity of the parameter to the imaging, segmentation, and calculation workflow, by which it is calculated. This is desirable because it allows models including such parameters to generalize well to other datasets. Finally, when choosing a set of parameters, data from the correlation analysis can be used to identify parameters that are not strongly correlated. Neyazi et al. have previously used this method to derive a two-parameter rupture status prediction model from a set of 49 geometric and hemodynamic rupture risk parameters, identifying AR and the maximal relative residence time as the most suitable model parameters [13]. Other attempts to identify suitable rupture status prediction models based on geometric risk parameters have been attempted, e.g., Dhar et al. [15] and Zhang et al. [30], but results have generally been inconsistent. Possible reasons for the discrepant findings regarding optimal parameter choice are the sample sizes used and the uncertainty inherent in the workflow by which the parameters are calculated. This may lead to the selection of less robust parameters that perform well on a given dataset but

For peer review only

BMJ Open: first published as 10.1136/bmjopen-2022-063051 on 8 November 2022. Downloaded from http://bmjopen.bmj.com/ on June 10, 2025 at Agence Bibliographique de l Enseignement Superieur (ABES) .
Protected by copyright, including for uses related to text and data mining, AI training, and similar technologies.

generalize less well to others. Based on the results of this study and considering SAD, DUR, as well as the correlation between geometric risk parameters, examples of more robust parameter choices could look as follows:

- H_{max}, $D_{neck,min}$, AR, AASA, and MLN for the anterior region.
- L_{max}, P_{neck}, AR, AASA, and HGC for the ICA.
- D_{max}, $D_{neck,min}$, eAR, AASA, and HMC for the MCA.
- L_{max}, $D_{neck,min}$, BL, EI, and absMAA for the posterior region.
- H_b, $D_{neck,min}$, AR, AASA, and MLN if looking at all anatomical regions combined.

Overall, while individual size, neck, and curvature parameters achieved good discriminative performance and robustness, the non-dimensional parameters tended to perform well as a group. This suggests that non-dimensional geometric risk parameters can provide comparatively good discriminative performance, while the nondimensionalization itself mitigates some of the uncertainty introduced through the workflow by which the parameters are calculated [14]. Neither did we attempt to develop a novel aneurysm rupture risk prediction model, nor did we test earlier published models [16, 31]. We decided against this analysis due to the large variety of published proposed risk models. Testing them as well as the propagation of the parameter's uncertainty towards assessment of rupture risk should be tested in a separate study. Finally, elaborated models will also require further information such as hypertension status, earlier SAH as well as hemodynamic parameters, which were unavailable within this study.

Limitations

IAs were grouped by anatomical region because IA location is an important determinant of rupture risk, as demonstrated by its weight in current risk scores [7-9]. However, by analyzing the datasets by anatomical region, some subsamples become quite small. Small sample size might affect the accuracy of the median and interquartile range estimates derived from these groups. This limitation is, however, partially mitigated by also analyzing all anatomical regions combined and using two datasets, in order to get a more comprehensive picture of the risk parameters' performance. The major focus of the study was the analysis of the performance and robustness of 37 geometric risk parameters. Thus, not all findings of this study could be assessed in depth. For example, we decided for grouping of aneurysms by anatomical regions as recommended by clinical scores, such as such as PHASES score [7]. While we observed differences in both SAD and DUR based on the aneurysms' location within the circulation, the underlying mechanisms for these differences cannot be assessed by the available data. However, Tykocki & Kostkiewicz found significant differences between some geometric parameters (parent artery size, size ratio and aspect ratio) of aneurysms for the anterior and the posterior regions [32]. They associated the difference in these parameters to different impacts on the intra-aneurysmal hemodynamics such as vortex formation and wall

For peer review only

BMJ Open: first published as 10.1136/bmjopen-2022-063051 on 8 November 2022. Downloaded from http://bmjopen.bmj.com/ on June 10, 2025 at Agence Bibliographique de l Enseignement Superieur (ABES) . Protected by copyright, including for uses related to text and data mining, AI training, and similar technologies.

shear stress. Why these geometric parameters might result in different hemodynamic conditions and rupture risks must be investigated in a dedicated study. This is especially important as this study's findings demonstrated differences in the SAD not only between locations and the cohorts, but also when all aneurysm locations were evaluated together.

Another potential limitation is the uncertainty values from Goubergrits et al. [14], which were used to calculate DUR. These values were calculated on a sample containing MCA and posterior region IAs [14]. While it does not seem particularly probable, it is possible that IA location and size might affect the uncertainty inherent in calculating the geometric risk parameters in a relevant manner, which in turn could influence DUR results. Respectively the generalization of MRU values from the uncertainty study [14] should be considered with caution, especially as those values were calculated only based on five aneurysms. A more fundamental limitations is the focus on geometric risk parameters. These parameters serve as proxies for the pathophysiological processes leading to IA rupture through the latter's influence on the geometry of the IA surface. Due to their nature, geometric risk parameters cannot directly capture the hemodynamic, mechanical, or biochemical aspects of IA rupture. Nevertheless, they are among the most intensely researched types of IA rupture risk parameters, due to the comparative ease with which they can be calculated from clinical data.

All parameters included within this study have been discussed in previous literature as potential risk parameters. Note, however, that the list of parameters investigated in this study is not exhaustive. More proposed geometric parameters can be found in recent literature [33]. The parameters investigated here are limited to a set of parameters investigated earlier in frames of the uncertainty study [14]. Second, these parameters were constrained to parameters, that can be calculated automatically.

Finally, the calculation of geometric parameters including the ostium plane depends on a sufficient reference plane selection. Recently, Berg et al. quantified the potential effect of neck curve variations on hemodynamic predictions [34]. These findings could be transferred to the cases included in this study in future work.

Due to the retrospective nature of this work, only the parameters' capabilities to discriminate the rupture status could be assessed by comparing their respective values observed in ruptured or unruptured IA. To adequately assess the capabilities of any model using these parameters for rupture risk assessment, it has to be evaluated on a longitudinal cohort containing only UIA.

Conclusion

Based on datasets from two research groups, the present study provides location-specific estimates of the discriminative ability of a large set of geometric risk parameters for IA rupture status assessment, while also considering uncertainty. Additionally, correlation patterns between the parameters are identified. The

For peer review only

BMJ Open: first published as 10.1136/bmjopen-2022-063051 on 8 November 2022. Downloaded from http://bmjopen.bmj.com/ on June 10, 2025 at Agence Bibliographique de l Enseignement Superieur (ABES) . Protected by copyright, including for uses related to text and data mining, AI training, and similar technologies.

presented data is potentially useful in evaluating geometric risk parameters for use in rupture risk models or when choosing input parameters for machine learning approaches to rupture risk prediction. It may also be helpful when designing future geometric risk parameters for clinical use.

For peer review only

BMJ Open: first published as 10.1136/bmjopen-2022-063051 on 8 November 2022. Downloaded from http://bmjopen.bmj.com/ on June 10, 2025 at Agence Bibliographique de l Enseignement Superieur (ABES) . Protected by copyright, including for uses related to text and data mining, AI training, and similar technologies.

BMJ Open: first published as 10.1136/bmjopen-2022-063051 on 8 November 2022. Downloaded from http://bmjopen.bmj.com/ on June 10, 2025 at Agence Bibliographique de l Enseignement Superieur (ABES) . Protected by copyright, including for uses related to text and data mining, AI training, and similar technologies.

Conflict of interest statement

The authors declare that there is no conflict of interest.

Acknowledgments

The authors kindly acknowledge PD Dr. Belal Neyazi (Department of Neurosurgery, University Hospital Magdeburg) for his assistance during data acquisition as well as Adriano Schlief (Institute of Computer-assisted Cardiovascular Medicine, Charité – Universitätsmedizin Berlin) for his help in checking the topology and scaling of the IA geometries.

Data Availability Statement

All individual parameter values as well as the correlation coefficients are made available as supplemental material.

Ethical approval statements

In this study, patient-specific 3D reconstructions of intracranial aneurysms based on routine information were evaluated retrospectively. Use of retrospective data was approved by the local ethics committees (Ethikkommission der Charité - Universitätsmedizin Berlin: EA2/222/19; Ethikkommission der Med. Hochschule Hannover: NOVA Nr. 68/20).

Funding

This study was partly funded by the Federal Ministry of Education and Research in Germany within the Forschungscampus *STIMULATE* (grant number 13GW0473A) and the German Research Foundation (grant number SA 3461/2-1, BE 6230/2-1).

Author contributions

All roles according to CRediT (contributor roles taxonomy). Conceptualization: LG, JS, FH, JB, and PB. Methodology: FH, JS, and LG. Resources: AS, IES, OB, NL, SS, and PB. Investigation: JB, FH, and JS. Formal Analysis: FH. Funding acquisition: LG, PB, and SS. Supervision: LG. Writing – original draft: FH, LG, and JB. Writing – review & editing: PB, SS, AS, IES, OB, NL, and JS.

For peer review only

References

1. Vlak, M.H., A. Algra, R. Brandenburg, and G.J. Rinkel, *Prevalence of unruptured intracranial aneurysms, with emphasis on sex, age, comorbidity, country, and time period: a systematic review and meta-analysis.* Lancet Neurol, 2011. **10**(7): p. 626-36.
2. Brown, R.D., Jr. and J.P. Broderick, *Unruptured intracranial aneurysms: epidemiology, natural history, management options, and familial screening.* Lancet Neurol, 2014. **13**(4): p. 393-404.
3. Wiebers, D.O., J.P. Whisnant, J. Huston, 3rd, I. Meissner, R.D. Brown, Jr., D.G. Piepgras, G.S. Forbes, K. Thielen, D. Nichols, W.M. O'Fallon, J. Peacock, L. Jaeger, N.F. Kassell, G.L. Kongable-Beckman, J.C. Torner, and I. International Study of Unruptured Intracranial Aneurysms, *Unruptured intracranial aneurysms: natural history, clinical outcome, and risks of surgical and endovascular treatment.* Lancet, 2003. **362**(9378): p. 103-10.
4. Rackauskaite, D., E. Svanborg, E. Andersson, K. Lowhagen, L. Csajbok, and B. Nellgard, *Prospective study: Long-term outcome at 12-15 years after aneurysmal subarachnoid hemorrhage.* Acta Neurol Scand, 2018. **138**(5): p. 400-407.
5. Pontes, F.G.B., E.M. da Silva, J.C. Baptista-Silva, and V. Vasconcelos, *Treatments for unruptured intracranial aneurysms.* Cochrane Database Syst Rev, 2021. **5**: p. CD013312.
6. Thompson, B.G., et al., *Guidelines for the Management of Patients With Unruptured Intracranial Aneurysms: A Guideline for Healthcare Professionals From the American Heart Association/American Stroke Association.* Stroke, 2015. **46**(8): p. 2368-400.
7. Greving, J.P., M.J. Wermer, R.D. Brown, Jr., A. Morita, S. Juvela, M. Yonekura, T. Ishibashi, J.C. Torner, T. Nakayama, G.J. Rinkel, and A. Algra, *Development of the PHASES score for prediction of risk of rupture of intracranial aneurysms: a pooled analysis of six prospective cohort studies.* Lancet Neurol, 2014. **13**(1): p. 59-66.
8. Etminan, N., et al., *The unruptured intracranial aneurysm treatment score: a multidisciplinary consensus.* Neurology, 2015. **85**(10): p. 881-9.
9. Backes, D., et al., *ELAPSS score for prediction of risk of growth of unruptured intracranial aneurysms.* Neurology, 2017. **88**(17): p. 1600-1606.
10. Juvela, S., *PHASES score and treatment scoring with cigarette smoking in the long-term prediction of rupturing of unruptured intracranial aneurysms.* J Neurosurg, 2022. **136**(1): p. 156-162.
11. Molenberg, R., M.W. Aalbers, A. Mazuri, G.J. Luijckx, J.D.M. Metzemaekers, R.J.M. Groen, M. Uyttenboogaart, and J.M.C. van Dijk, *The Unruptured Intracranial Aneurysm Treatment Score as a predictor of aneurysm growth or rupture.* Eur J Neurol, 2021. **28**(3): p. 837-843.
12. Hernandez-Duran, S., D. Mielke, V. Rohde, and V. Malinova, *Is the unruptured intracranial aneurysm treatment score (UIATS) sensitive enough to detect aneurysms at risk of rupture?* Neurosurg Rev, 2021. **44**(2): p. 987-993.
13. Neyazi, B., V.M. Swiatek, M. Skalej, O. Beuing, K.P. Stein, J. Hattingen, B. Preim, P. Berg, S. Saalfeld, and I.E. Sandalcioglu, *Rupture risk assessment for multiple intracranial aneurysms: why there is no need for dozens of clinical, morphological and hemodynamic parameters.* Ther Adv Neurol Disord, 2020. **13**: p. 1756286420966159.
14. Goubergrits, L., F. Hellmeier, J. Bruening, A. Spuler, H.C. Hege, S. Voss, G. Janiga, S. Saalfeld, O. Beuing, and P. Berg, *Multiple Aneurysms AnaTomy CHallenge 2018 (MATCH): uncertainty quantification of geometric rupture risk parameters.* Biomed Eng Online, 2019. **18**(1): p. 35.
15. Dhar, S., M. Tremmel, J. Mocco, M. Kim, J. Yamamoto, A.H. Siddiqui, L.N. Hopkins, and H. Meng, *Morphology parameters for intracranial aneurysm rupture risk assessment.* Neurosurgery, 2008. **63**(2): p. 185-96; discussion 196-7.
16. Detmer, F.J., B.J. Chung, F. Mut, M. Slawski, F. Hamzei-Sichani, C. Putman, C. Jimenez, and J.R. Cebral, *Development and internal validation of an aneurysm rupture probability model based on patient characteristics and aneurysm location, morphology, and hemodynamics.* Int J Comput Assist Radiol Surg, 2018. **13**(11): p. 1767-1779.

BMJ Open: first published as 10.1136/bmjopen-2022-063051 on 8 November 2022. Downloaded from http://bmjopen.bmj.com/ on June 10, 2025 at Agence Bibliographique de l Enseignement Superieur (ABES) . Protected by copyright, including for uses related to text and data mining, AI training, and similar technologies.

17. Lauric, A., M.I. Baharoglu, and A.M. Malek, *Ruptured status discrimination performance of aspect ratio, height/width, and bottleneck factor is highly dependent on aneurysm sizing methodology.* Neurosurgery, 2012. **71**(1): p. 38-45.
18. Berg, P., et al., *Multiple Aneurysms AnaTomy CHallenge 2018 (MATCH): Phase I: Segmentation.* Cardiovasc Eng Technol, 2018. **9**(4): p. 565-581.
19. Ma, B., R.E. Harbaugh, and M.L. Raghavan, *Three-dimensional geometrical characterization of cerebral aneurysms.* Ann Biomed Eng, 2004. **32**(2): p. 264-73.
20. Lauric, A., E.L. Miller, M.I. Baharoglu, and A.M. Malek, *3D shape analysis of intracranial aneurysms using the writhe number as a discriminant for rupture.* Ann Biomed Eng, 2011. **39**(5): p. 1457-69.
21. Chien, A., J. Sayre, and F. Vinuela, *Comparative morphological analysis of the geometry of ruptured and unruptured aneurysms.* Neurosurgery, 2011. **69**(2): p. 349-56.
22. Ujiie, H., Y. Tamano, K. Sasaki, and T. Hori, *Is the aspect ratio a reliable index for predicting the rupture of a saccular aneurysm?* Neurosurgery, 2001. **48**(3): p. 495-502; discussion 502-3.
23. Ramachandran, M., R. Retarekar, R.E. Harbaugh, D. Hasan, B. Policeni, R. Rosenwasser, C. Ogilvy, and M.L. Raghavan, *Sensitivity of Quantified Intracranial Aneurysm Geometry to Imaging Modality.* Cardiovasc Eng Technol, 2013. **4**(1): p. 75-86.
24. O'Meara, B., J.P. Rahal, A. Lauric, and A.M. Malek, *Benefit of a sharp computed tomography angiography reconstruction kernel for improved characterization of intracranial aneurysms.* Neurosurgery, 2014. **10 Suppl 1**: p. 97-105; discussion 105.
25. Berg, P., S. Saalfeld, S. Voss, T. Redel, B. Preim, G. Janiga, and O. Beuing, *Does the DSA reconstruction kernel affect hemodynamic predictions in intracranial aneurysms? An analysis of geometry and blood flow variations.* J Neurointerv Surg, 2018. **10**(3): p. 290-296.
26. Cebral, J.R., M.A. Castro, S. Appanaboyina, C.M. Putman, D. Millan, and A.F. Frangi, *Efficient pipeline for image-based patient-specific analysis of cerebral aneurysm hemodynamics: technique and sensitivity.* IEEE Trans Med Imaging, 2005. **24**(4): p. 457-67.
27. Sarrami-Foroushani, A., T. Lassila, and A.F. Frangi, *Virtual endovascular treatment of intracranial aneurysms: models and uncertainty.* Wiley Interdiscip Rev Syst Biol Med, 2017. **9**(4).
28. Schneiders, J.J., H.A. Marquering, L. Antiga, R. van den Berg, E. VanBavel, and C.B. Majoie, *Intracranial aneurysm neck size overestimation with 3D rotational angiography: the impact on intra-aneurysmal hemodynamics simulated with computational fluid dynamics.* AJNR Am J Neuroradiol, 2013. **34**(1): p. 121-8.
29. Ivantsits, M., et al., *Detection and analysis of cerebral aneurysms based on X-ray rotational angiography - the CADA 2020 challenge.* Med Image Anal, 2021. **77**: p. 102333.
30. Zheng, Y., F. Xu, J. Ren, Q. Xu, Y. Liu, Y. Tian, and B. Leng, *Assessment of intracranial aneurysm rupture based on morphology parameters and anatomical locations.* J Neurointerv Surg, 2016. **8**(12): p. 1240-1246.
31. Lall, R.R., C.S. Eddleman, B.R. Bendok, and H.H. Batjer, *Unruptured intracranial aneurysms and the assessment of rupture risk based on anatomical and morphological factors: sifting through the sands of data.* Neurosurg Focus, 2009. **26**(5): p. E2.
32. Tykocki, T. and B. Kostkiewicz, *Aneurysms of the anterior and posterior cerebral circulation: comparison of the morphometric features.* Acta Neurochir (Wien), 2014. **156**(9): p. 1647-54.
33. Juchler, N., S. Schilling, P. Bijlenga, V. Kurtcuoglu, and S. Hirsch, *Shape Trumps Size: Image-Based Morphological Analysis Reveals That the 3D Shape Discriminates Intracranial Aneurysm Disease Status Better Than Aneurysm Size.* Front Neurol, 2022. **13**: p. 809391.
34. Berg, P., B. Behrendt, S. Voss, O. Beuing, B. Neyazi, I.E. Sandalcioglu, B. Preim, and S. Saalfeld, *VICTORIA: VIrtual neck Curve and True Ostium Reconstruction of Intracranial Aneurysms.* Cardiovasc Eng Technol, 2021. **12**(4): p. 454-465.

For peer review only

BMJ Open: first published as 10.1136/bmjopen-2022-063051 on 8 November 2022. Downloaded from http://bmjopen.bmj.com/ on June 10, 2025 at Agence Bibliographique de l Enseignement Superieur (ABES) . Protected by copyright, including for uses related to text and data mining, AI training, and similar technologies.

Figures

Figure 1: Standardized absolute group difference (SAD) for each anatomical region and dataset.

Figure 2: Group difference-uncertainty ratio (DUR) for each anatomical region and dataset.

Figure 3: Pearson's r for correlation between geometric risk parameters by anatomical region for dataset 1.

Figure 4: Pearson's r for correlation between geometric risk parameters by anatomical region for dataset 2.

For peer review only

BMJ Open: first published as 10.1136/bmjopen-2022-063051 on 8 November 2022. Downloaded from http://bmjopen.bmj.com/ on June 10, 2025 at Agence Bibliographique de l Enseignement Superieur (ABES) .
Protected by copyright, including for uses related to text and data mining, AI training, and similar technologies.

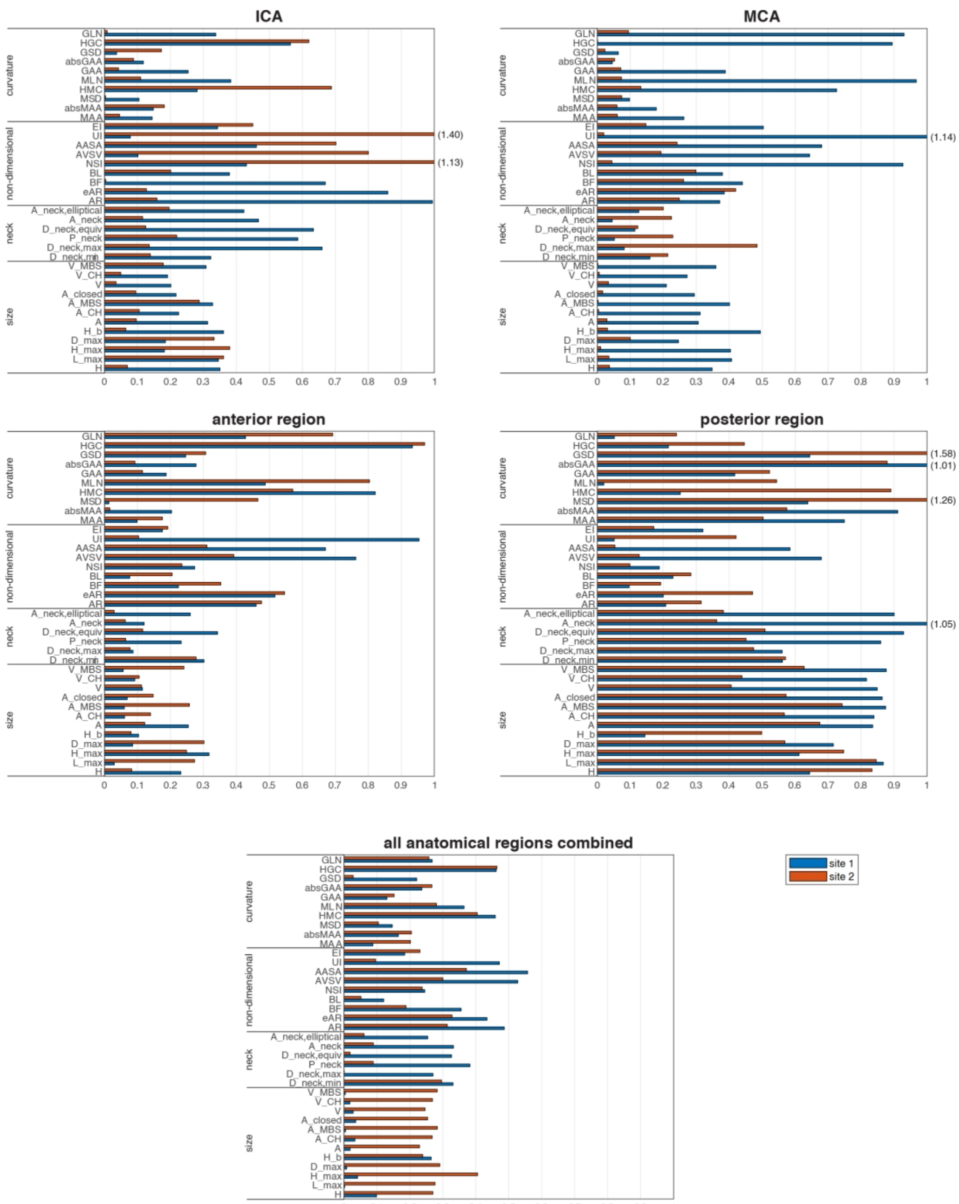

196x248mm (300 x 300 DPI)

BMJ Open: first published as 10.1136/bmjopen-2022-063051 on 8 November 2022. Downloaded from http://bmjopen.bmj.com/ on June 10, 2025 at Agence Bibliographique de l Enseignement Superieur (ABES) . Protected by copyright, including for uses related to text and data mining, AI training, and similar technologies.

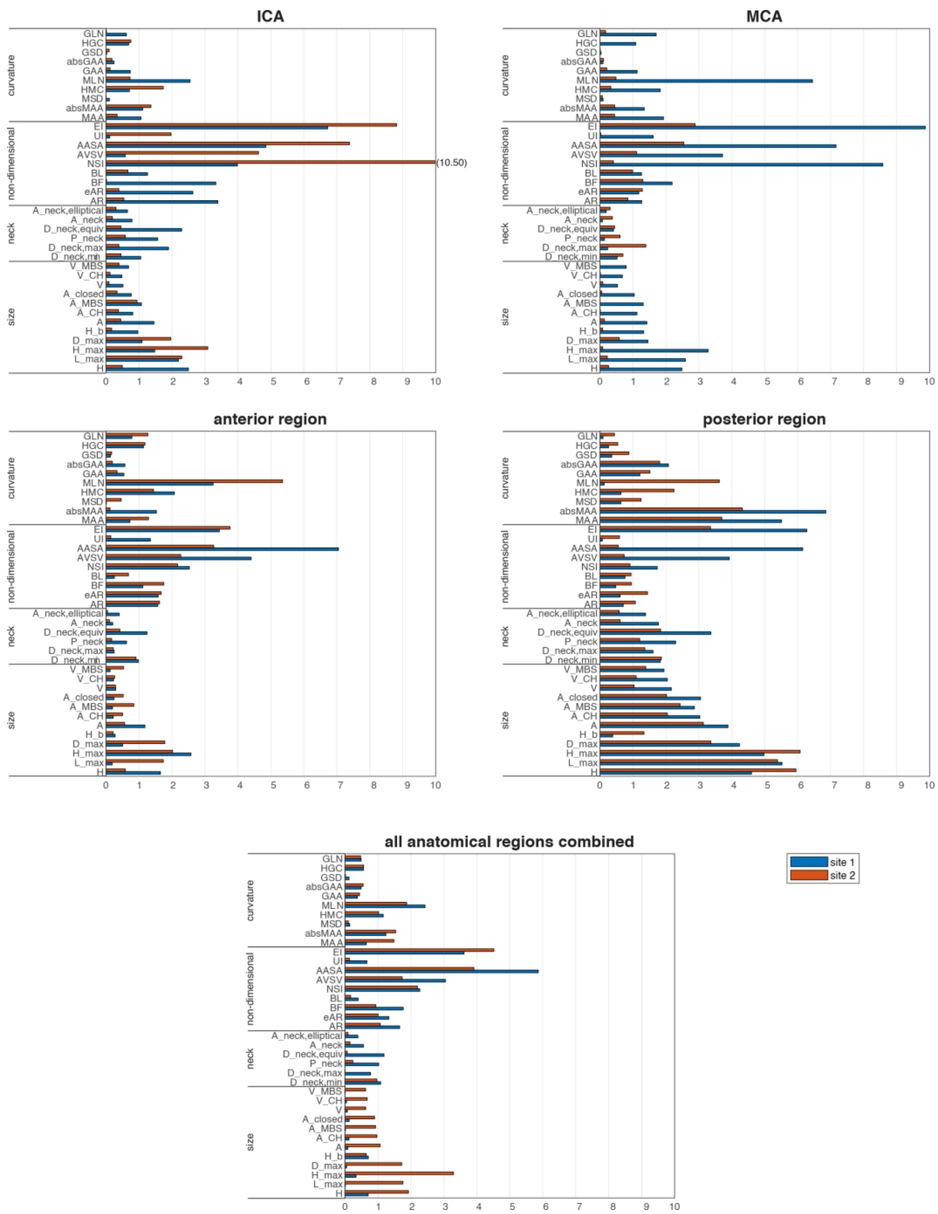

192x248mm (300 x 300 DPI)

BMJ Open: first published as 10.1136/bmjopen-2022-063051 on 8 November 2022. Downloaded from http://bmjopen.bmj.com/ on June 10, 2025 at Agence Bibliographique de l Enseignement Superieur (ABES) . Protected by copyright, including for uses related to text and data mining, AI training, and similar technologies.

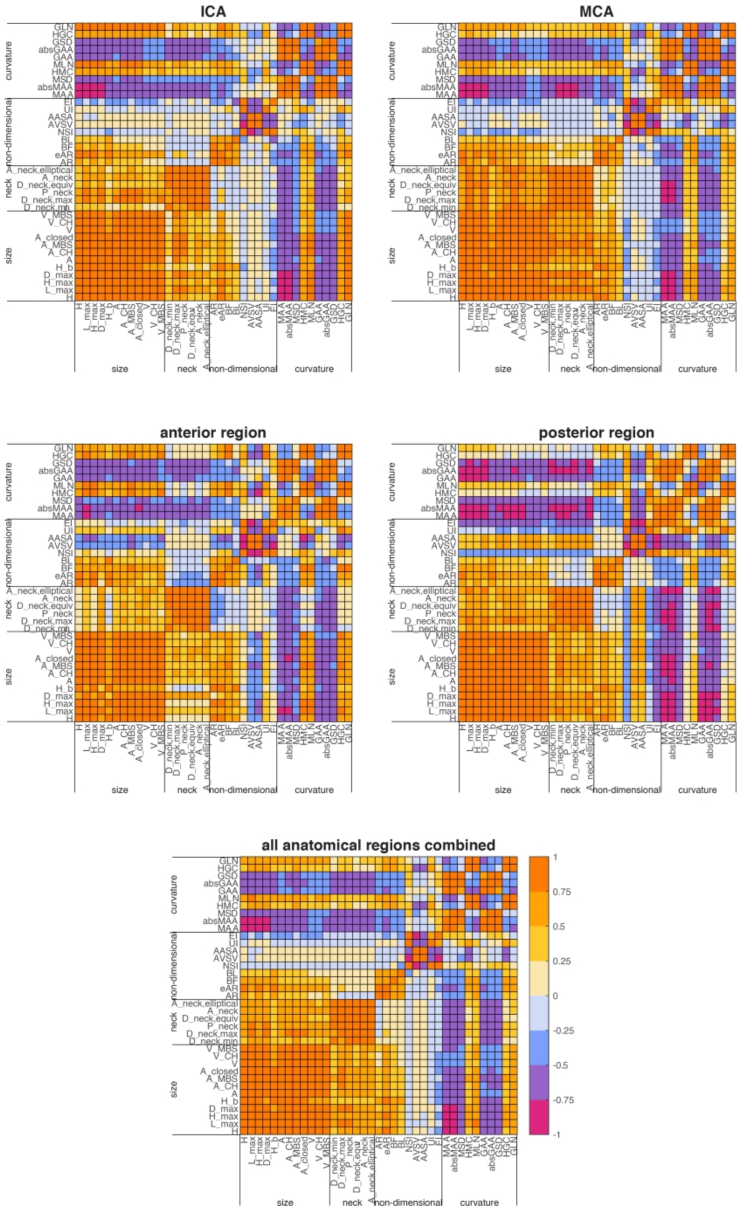

198x325mm (300 x 300 DPI)

BMJ Open: first published as 10.1136/bmjopen-2022-063051 on 8 November 2022. Downloaded from http://bmjopen.bmj.com/ on June 10, 2025 at Agence Bibliographique de l Enseignement Superieur (ABES) . Protected by copyright, including for uses related to text and data mining, AI training, and similar technologies.

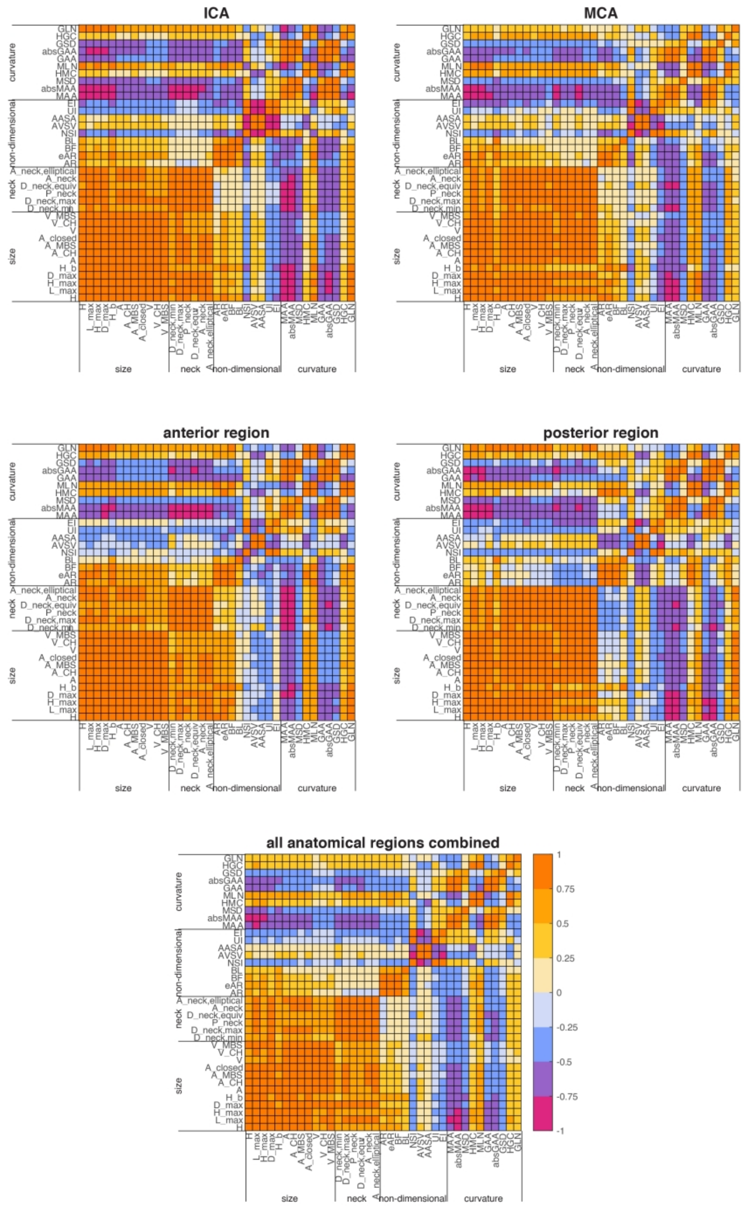

BMJ Open: first published as 10.1136/bmjopen-2022-063051 on 8 November 2022. Downloaded from http://bmjopen.bmj.com/ on June 10, 2025 at Agence Bibliographique de l Enseignement Superieur (ABES) .
Protected by copyright, including for uses related to text and data mining, AI training, and similar technologies.

Pearson's r	H	L_max	H_max	D_max	H_b	A	A_CH
H	1.000	0.872	0.968	0.610	0.836	0.867	0.830
L_max	0.872	1.000	0.950	0.884	0.648	0.962	0.960
H_max	0.968	0.950	1.000	0.728	0.783	0.922	0.894
D_max	0.610	0.884	0.728	1.000	0.349	0.873	0.900
H_b	0.836	0.648	0.783	0.349	1.000	0.653	0.605
A	0.867	0.962	0.922	0.873	0.653	1.000	0.993
A_CH	0.830	0.960	0.894	0.900	0.605	0.993	1.000
A_MBS	0.835	0.973	0.919	0.863	0.596	0.967	0.957
A_closed	0.827	0.957	0.890	0.899	0.606	0.992	1.000
V	0.779	0.917	0.842	0.869	0.565	0.980	0.988
V_CH	0.778	0.924	0.846	0.880	0.548	0.982	0.988
V_MBS	0.769	0.918	0.857	0.822	0.522	0.934	0.919
D_neck,mi	0.220	0.402	0.246	0.535	0.125	0.415	0.484
D_neck,ma	0.153	0.466	0.248	0.642	-0.049	0.426	0.520
P_neck	0.059	0.376	0.158	0.554	-0.075	0.353	0.454
D_neck,eq	0.159	0.428	0.224	0.609	-0.014	0.417	0.508
A_neck	0.089	0.392	0.170	0.583	-0.064	0.390	0.491
A_neck,elli	0.179	0.448	0.240	0.630	0.028	0.450	0.541
AR	0.867	0.582	0.784	0.236	0.849	0.579	0.503
eAR	0.879	0.639	0.819	0.304	0.801	0.608	0.536
BF	0.701	0.727	0.749	0.684	0.595	0.735	0.682
BL	0.627	0.461	0.580	0.273	0.884	0.464	0.423
NSI	0.173	0.275	0.235	0.216	-0.021	0.142	0.129
AVSV	-0.393	-0.491	-0.481	-0.331	-0.275	-0.315	-0.287
AASA	-0.455	-0.558	-0.551	-0.378	-0.337	-0.380	-0.350
UI	0.405	0.494	0.463	0.437	0.137	0.365	0.356
EI	0.012	0.091	0.067	0.013	-0.075	-0.034	-0.050
MAA	-0.661	-0.763	-0.698	-0.727	-0.481	-0.702	-0.740
absMAA	-0.692	-0.755	-0.711	-0.701	-0.547	-0.710	-0.747
MSD	-0.504	-0.453	-0.465	-0.370	-0.517	-0.489	-0.513
HMC	0.672	0.801	0.776	0.698	0.434	0.706	0.672
MLN	0.727	0.775	0.790	0.706	0.500	0.745	0.704
GAA	-0.627	-0.693	-0.655	-0.632	-0.443	-0.590	-0.621
absGAA	-0.647	-0.688	-0.659	-0.626	-0.534	-0.639	-0.672
GSD	-0.547	-0.567	-0.541	-0.507	-0.511	-0.550	-0.584
HGC	0.618	0.783	0.727	0.735	0.322	0.710	0.685
GLN	0.614	0.729	0.698	0.731	0.300	0.711	0.681

For peer review only

BMJ Open: first published as 10.1136/bmjopen-2022-063051 on 8 November 2022. Downloaded from http://bmjopen.bmj.com/ on June 10, 2025 at Agence Bibliographique de l Enseignement Superieur (ABES) .
Protected by copyright, including for uses related to text and data mining, AI training, and similar technologies.

A_MBS	A_closed	V	V_CH	V_MBS	D_neck,min	D_neck,max	P_neck
0.835	0.827	0.779	0.778	0.769	0.220	0.153	0.059
0.973	0.957	0.917	0.924	0.918	0.402	0.466	0.376
0.919	0.890	0.842	0.846	0.857	0.246	0.248	0.158
0.863	0.899	0.869	0.880	0.822	0.535	0.642	0.554
0.596	0.606	0.565	0.548	0.522	0.125	-0.049	-0.075
0.967	0.992	0.980	0.982	0.934	0.415	0.426	0.353
0.957	1.000	0.988	0.988	0.919	0.484	0.520	0.454
1.000	0.952	0.939	0.953	0.984	0.346	0.375	0.290
0.952	1.000	0.989	0.988	0.913	0.494	0.526	0.462
0.939	0.989	1.000	0.998	0.920	0.486	0.503	0.457
0.953	0.988	0.998	1.000	0.940	0.460	0.485	0.430
0.984	0.913	0.920	0.940	1.000	0.298	0.302	0.223
0.346	0.494	0.486	0.460	0.298	1.000	0.685	0.681
0.375	0.526	0.503	0.485	0.302	0.685	1.000	0.952
0.290	0.462	0.457	0.430	0.223	0.681	0.952	1.000
0.361	0.516	0.504	0.485	0.310	0.907	0.870	0.857
0.321	0.500	0.503	0.477	0.263	0.780	0.944	0.974
0.377	0.550	0.543	0.517	0.316	0.909	0.909	0.886
0.568	0.498	0.454	0.459	0.527	-0.127	-0.328	-0.375
0.610	0.529	0.473	0.480	0.553	-0.208	-0.214	-0.304
0.753	0.675	0.643	0.668	0.743	0.043	-0.096	-0.153
0.362	0.427	0.370	0.348	0.268	0.087	-0.061	-0.064
0.334	0.113	0.080	0.131	0.361	-0.197	-0.061	-0.176
-0.501	-0.273	-0.225	-0.261	-0.486	0.179	0.068	0.160
-0.558	-0.337	-0.288	-0.320	-0.535	0.160	0.041	0.130
0.494	0.340	0.273	0.321	0.477	-0.152	0.134	-0.008
0.166	-0.065	-0.072	-0.032	0.209	-0.227	-0.193	-0.269
-0.636	-0.743	-0.667	-0.654	-0.529	-0.582	-0.679	-0.648
-0.627	-0.752	-0.683	-0.661	-0.516	-0.646	-0.664	-0.637
-0.379	-0.521	-0.510	-0.474	-0.310	-0.620	-0.396	-0.402
0.801	0.661	0.604	0.639	0.770	-0.028	0.133	-0.011
0.753	0.697	0.631	0.658	0.708	-0.009	0.127	-0.014
-0.547	-0.622	-0.527	-0.520	-0.433	-0.446	-0.584	-0.543
-0.551	-0.678	-0.607	-0.582	-0.440	-0.652	-0.603	-0.580
-0.453	-0.592	-0.545	-0.515	-0.360	-0.695	-0.549	-0.547
0.811	0.672	0.627	0.670	0.805	-0.029	0.180	0.038
0.748	0.672	0.626	0.664	0.737	-0.038	0.158	0.024

For peer review only

BMJ Open: first published as 10.1136/bmjopen-2022-063051 on 8 November 2022. Downloaded from http://bmjopen.bmj.com/ on June 10, 2025 at Agence Bibliographique de l Enseignement Superieur (ABES) .
Protected by copyright, including for uses related to text and data mining, AI training, and similar technologies.

D_neck,equi	A_neck	A_neck,ellipt	AR	eAR	BF	BL	NSI
0.159	0.089	0.179	0.867	0.879	0.701	0.627	0.173
0.428	0.392	0.448	0.582	0.639	0.727	0.461	0.275
0.224	0.170	0.240	0.784	0.819	0.749	0.580	0.235
0.609	0.583	0.630	0.236	0.304	0.684	0.273	0.216
-0.014	-0.064	0.028	0.849	0.801	0.595	0.884	-0.021
0.417	0.390	0.450	0.579	0.608	0.735	0.464	0.142
0.508	0.491	0.541	0.503	0.536	0.682	0.423	0.129
0.361	0.321	0.377	0.568	0.610	0.753	0.362	0.334
0.516	0.500	0.550	0.498	0.529	0.675	0.427	0.113
0.504	0.503	0.543	0.454	0.473	0.643	0.370	0.080
0.485	0.477	0.517	0.459	0.480	0.668	0.348	0.131
0.310	0.263	0.316	0.527	0.553	0.743	0.268	0.361
0.907	0.780	0.909	-0.127	-0.208	0.043	0.087	-0.197
0.870	0.944	0.909	-0.328	-0.214	-0.096	-0.061	-0.061
0.857	0.974	0.886	-0.375	-0.304	-0.153	-0.064	-0.176
1.000	0.927	0.953	-0.267	-0.298	-0.034	-0.040	-0.113
0.927	1.000	0.949	-0.353	-0.317	-0.119	-0.074	-0.157
0.953	0.949	1.000	-0.266	-0.247	-0.036	0.004	-0.155
-0.267	-0.353	-0.266	1.000	0.946	0.687	0.672	0.175
-0.298	-0.317	-0.247	0.946	1.000	0.669	0.627	0.253
-0.034	-0.119	-0.036	0.687	0.669	1.000	0.525	0.300
-0.040	-0.074	0.004	0.672	0.627	0.525	1.000	-0.267
-0.113	-0.157	-0.155	0.175	0.253	0.300	-0.267	1.000
0.141	0.175	0.161	-0.403	-0.468	-0.491	-0.075	-0.823
0.129	0.153	0.138	-0.450	-0.524	-0.532	-0.148	-0.751
0.019	-0.021	-0.047	0.320	0.427	0.442	-0.027	0.824
-0.219	-0.243	-0.226	0.085	0.141	0.157	-0.325	0.922
-0.656	-0.622	-0.632	-0.337	-0.379	-0.384	-0.446	0.044
-0.678	-0.632	-0.667	-0.377	-0.393	-0.371	-0.492	0.103
-0.516	-0.461	-0.553	-0.319	-0.252	-0.158	-0.456	0.370
0.017	-0.024	0.030	0.536	0.649	0.764	0.318	0.542
0.022	-0.028	0.035	0.591	0.685	0.804	0.463	0.314
-0.543	-0.499	-0.495	-0.365	-0.417	-0.365	-0.436	-0.045
-0.634	-0.575	-0.635	-0.368	-0.375	-0.327	-0.513	0.183
-0.631	-0.563	-0.640	-0.296	-0.265	-0.203	-0.488	0.303
0.077	0.033	0.055	0.449	0.560	0.753	0.186	0.602
0.064	0.022	0.042	0.453	0.551	0.779	0.234	0.427

For peer review only

BMJ Open: first published as 10.1136/bmjopen-2022-063051 on 8 November 2022. Downloaded from http://bmjopen.bmj.com/ on June 10, 2025 at Agence Bibliographique de l Enseignement Superieur (ABES) .
Protected by copyright, including for uses related to text and data mining, AI training, and similar technologies.

AVSV	AASA	UI	EI	MAA	absMAA	MSD	HMC
-0.393	-0.455	0.405	0.012	-0.661	-0.692	-0.504	0.672
-0.491	-0.558	0.494	0.091	-0.763	-0.755	-0.453	0.801
-0.481	-0.551	0.463	0.067	-0.698	-0.711	-0.465	0.776
-0.331	-0.378	0.437	0.013	-0.727	-0.701	-0.370	0.698
-0.275	-0.337	0.137	-0.075	-0.481	-0.547	-0.517	0.434
-0.315	-0.380	0.365	-0.034	-0.702	-0.710	-0.489	0.706
-0.287	-0.350	0.356	-0.050	-0.740	-0.747	-0.513	0.672
-0.501	-0.558	0.494	0.166	-0.636	-0.627	-0.379	0.801
-0.273	-0.337	0.340	-0.065	-0.743	-0.752	-0.521	0.661
-0.225	-0.288	0.273	-0.072	-0.667	-0.683	-0.510	0.604
-0.261	-0.320	0.321	-0.032	-0.654	-0.661	-0.474	0.639
-0.486	-0.535	0.477	0.209	-0.529	-0.516	-0.310	0.770
0.179	0.160	-0.152	-0.227	-0.582	-0.646	-0.620	-0.028
0.068	0.041	0.134	-0.193	-0.679	-0.664	-0.396	0.133
0.160	0.130	-0.008	-0.269	-0.648	-0.637	-0.402	-0.011
0.141	0.129	0.019	-0.219	-0.656	-0.678	-0.516	0.017
0.175	0.153	-0.021	-0.243	-0.622	-0.632	-0.461	-0.024
0.161	0.138	-0.047	-0.226	-0.632	-0.667	-0.553	0.030
-0.403	-0.450	0.320	0.085	-0.337	-0.377	-0.319	0.536
-0.468	-0.524	0.427	0.141	-0.379	-0.393	-0.252	0.649
-0.491	-0.532	0.442	0.157	-0.384	-0.371	-0.158	0.764
-0.075	-0.148	-0.027	-0.325	-0.446	-0.492	-0.456	0.318
-0.823	-0.751	0.824	0.922	0.044	0.103	0.370	0.542
1.000	0.988	-0.699	-0.776	0.120	0.070	-0.205	-0.736
0.988	1.000	-0.667	-0.702	0.177	0.129	-0.138	-0.785
-0.699	-0.667	1.000	0.556	-0.297	-0.203	0.211	0.706
-0.776	-0.702	0.556	1.000	0.257	0.273	0.377	0.341
0.120	0.177	-0.297	0.257	1.000	0.974	0.558	-0.424
0.070	0.129	-0.203	0.273	0.974	1.000	0.709	-0.339
-0.205	-0.138	0.211	0.377	0.558	0.709	1.000	0.032
-0.736	-0.785	0.706	0.341	-0.424	-0.339	0.032	1.000
-0.488	-0.536	0.586	0.075	-0.511	-0.427	0.009	0.912
0.207	0.254	-0.399	0.184	0.968	0.923	0.460	-0.446
0.021	0.088	-0.094	0.314	0.933	0.973	0.764	-0.290
-0.118	-0.050	0.060	0.393	0.798	0.880	0.904	-0.119
-0.689	-0.718	0.778	0.366	-0.422	-0.320	0.097	0.961
-0.487	-0.516	0.661	0.173	-0.452	-0.345	0.122	0.881

For peer review only

BMJ Open: first published as 10.1136/bmjopen-2022-063051 on 8 November 2022. Downloaded from http://bmjopen.bmj.com/ on June 10, 2025 at Agence Bibliographique de l Enseignement Superieur (ABES) . Protected by copyright, including for uses related to text and data mining, AI training, and similar technologies.

MLN	GAA	absGAA	GSD	HGC	GLN
0.727	-0.627	-0.647	-0.547	0.618	0.614
0.775	-0.693	-0.688	-0.567	0.783	0.729
0.790	-0.655	-0.659	-0.541	0.727	0.698
0.706	-0.632	-0.626	-0.507	0.735	0.731
0.500	-0.443	-0.534	-0.511	0.322	0.300
0.745	-0.590	-0.639	-0.550	0.710	0.711
0.704	-0.621	-0.672	-0.584	0.685	0.681
0.753	-0.547	-0.551	-0.453	0.811	0.748
0.697	-0.622	-0.678	-0.592	0.672	0.672
0.631	-0.527	-0.607	-0.545	0.627	0.626
0.658	-0.520	-0.582	-0.515	0.670	0.664
0.708	-0.433	-0.440	-0.360	0.805	0.737
-0.009	-0.446	-0.652	-0.695	-0.029	-0.038
0.127	-0.584	-0.603	-0.549	0.180	0.158
-0.014	-0.543	-0.580	-0.547	0.038	0.024
0.022	-0.543	-0.634	-0.631	0.077	0.064
-0.028	-0.499	-0.575	-0.563	0.033	0.022
0.035	-0.495	-0.635	-0.640	0.055	0.042
0.591	-0.365	-0.368	-0.296	0.449	0.453
0.685	-0.417	-0.375	-0.265	0.560	0.551
0.804	-0.365	-0.327	-0.203	0.753	0.779
0.463	-0.436	-0.513	-0.488	0.186	0.234
0.314	-0.045	0.183	0.303	0.602	0.427
-0.488	0.207	0.021	-0.118	-0.689	-0.487
-0.536	0.254	0.088	-0.050	-0.718	-0.516
0.586	-0.399	-0.094	0.060	0.778	0.661
0.075	0.184	0.314	0.393	0.366	0.173
-0.511	0.968	0.933	0.798	-0.422	-0.452
-0.427	0.923	0.973	0.880	-0.320	-0.345
0.009	0.460	0.764	0.904	0.097	0.122
0.912	-0.446	-0.290	-0.119	0.961	0.881
1.000	-0.519	-0.372	-0.166	0.886	0.941
-0.519	1.000	0.888	0.724	-0.438	-0.459
-0.372	0.888	1.000	0.937	-0.231	-0.256
-0.166	0.724	0.937	1.000	-0.051	-0.034
0.886	-0.438	-0.231	-0.051	1.000	0.939
0.941	-0.459	-0.256	-0.034	0.939	1.000

For peer review only

BMJ Open: first published as 10.1136/bmjopen-2022-063051 on 8 November 2022. Downloaded from http://bmjopen.bmj.com/ on June 10, 2025 at Agence Bibliographique de l Enseignement Superieur (ABES) . Protected by copyright, including for uses related to text and data mining, AI training, and similar technologies.

parameter name	patient and ane	site supplyin	site processir	IA location	IA anatomi	rupture sta	height
abbreviation	-	-	-	-	-	-	H
unit	-	-	-	-	-	1=ruptured	mm
	1	Berlin	Berlin	AComA	anterior	1	5.748
	2	Berlin	Berlin	PComA	posterior	0	8.261
	3	Berlin	Berlin	PICA	posterior	1	6.023
	4	Berlin	Berlin	AComA	anterior	1	5.698
	5	Berlin	Berlin	ACA	anterior	0	5.667
	6	Berlin	Berlin	MCA	MCA	0	2.849
	7	Berlin	Berlin	ICA	ICA	0	19.575
	8	Berlin	Berlin	MCA	MCA	0	4.199
	9	Berlin	Berlin	MCA	MCA	0	3.795
	10	Berlin	Berlin	AComA	anterior	1	5.051
	11	Berlin	Berlin	MCA	MCA	0	6.789
	12	Berlin	Berlin	ICA	ICA	1	7.610
	13	Berlin	Berlin	MCA	MCA	0	8.157
	14	Berlin	Berlin	AComA	anterior	1	2.542
	15	Berlin	Berlin	PComA	posterior	1	3.196
	16A	Berlin	Berlin	ICA	ICA	1	9.587
	16B	Berlin	Berlin	ACA	anterior	0	1.879
	17A	Berlin	Berlin	ICA	ICA	0	12.261
	17B	Berlin	Berlin	ICA	ICA	0	2.791
	17C	Berlin	Berlin	AComA	anterior	0	4.530
	18	Berlin	Berlin	MCA	MCA	1	5.597
	19	Berlin	Berlin	AComA	anterior	1	5.177
	20	Berlin	Berlin	PComA	posterior	1	10.569
	21	Berlin	Berlin	ICA	ICA	0	4.966
	22	Berlin	Berlin	ICA	ICA	0	7.908
	23	Berlin	Berlin	MCA	MCA	1	4.598
	24	Berlin	Berlin	ICA	ICA	0	2.906
	25	Berlin	Berlin	BA	posterior	0	8.473
	26	Berlin	Berlin	MCA	MCA	1	4.210
	27	Berlin	Berlin	AComA	anterior	1	4.597
	28	Berlin	Berlin	MCA	MCA	1	5.480
	29	Berlin	Berlin	ICA	ICA	0	12.780
	30A	Berlin	Berlin	ICA	ICA	0	4.078
	30B	Berlin	Berlin	AComA	anterior	0	3.135
	30C	Berlin	Berlin	AComA	anterior	1	5.085
	30D	Berlin	Berlin	MCA	MCA	0	2.715
	30E	Berlin	Berlin	PICA	posterior	1	4.983
	31	Berlin	Berlin	MCA	MCA	0	4.542
	32	Berlin	Berlin	ICA	ICA	0	9.475
	33	Berlin	Berlin	AComA	anterior	1	6.212
	34	Berlin	Berlin	AComA	anterior	0	3.383
	35	Berlin	Berlin	ICA	ICA	1	11.690
	36	Berlin	Berlin	BA	posterior	0	20.748
	37	Berlin	Berlin	AComA	anterior	1	5.543
	38	Berlin	Berlin	AComA	anterior	0	8.400
	39	Berlin	Berlin	ICA	ICA	1	4.290
	40	Berlin	Berlin	PComA	posterior	1	13.786

For peer review only

BMJ Open: first published as 10.1136/bmjopen-2022-063051 on 8 November 2022. Downloaded from http://bmjopen.bmj.com/ on June 10, 2025 at Agence Bibliographique de l Enseignement Superieur (ABES) .
Protected by copyright, including for uses related to text and data mining, AI training, and similar technologies.

41	Berlin	Berlin	AComA	anterior	1	4.301
42	Berlin	Berlin	PComA	posterior	0	5.891
43	Berlin	Berlin	ICA	ICA	0	6.872
44	Berlin	Berlin	PICA	posterior	1	4.213
45A	Berlin	Berlin	ICA	ICA	0	2.414
45B	Berlin	Berlin	ICA	ICA	1	3.501
45C	Berlin	Berlin	ICA	ICA	0	2.297
46	Berlin	Berlin	BA	posterior	0	11.175
47	Berlin	Berlin	ICA	ICA	0	4.636
48	Berlin	Berlin	MCA	MCA	0	2.204
49	Berlin	Berlin	MCA	MCA	1	16.986
50	Berlin	Berlin	PComA	posterior	1	7.588
51	Berlin	Berlin	AComA	anterior	0	5.047
52	Berlin	Berlin	ACA	anterior	1	2.779
53	Berlin	Berlin	AChA	ICA	1	6.830
54	Berlin	Berlin	PComA	posterior	1	4.857
55	Berlin	Berlin	AComA	anterior	0	3.330
56	Berlin	Berlin	MCA	MCA	1	2.092
57A	Berlin	Berlin	ICA	ICA	0	2.831
57B	Berlin	Berlin	ICA	ICA	0	4.277
57C	Berlin	Berlin	ICA	ICA	0	4.910
57D	Berlin	Berlin	AComA	anterior	1	2.565
57E	Berlin	Berlin	MCA	MCA	0	6.612
57F	Berlin	Berlin	MCA	MCA	0	1.536
57G	Berlin	Berlin	MCA	MCA	0	3.139
58	Berlin	Berlin	PComA	posterior	1	3.998
59	Berlin	Berlin	ICA	ICA	0	4.875
60A	Berlin	Berlin	MCA	MCA	0	8.547
60B	Berlin	Berlin	MCA	MCA	0	3.172
61	Berlin	Berlin	AComA	anterior	1	10.866
62	Berlin	Berlin	ICA	ICA	1	4.541
63	Berlin	Berlin	AComA	anterior	1	5.524
64	Berlin	Berlin	ICA	ICA	1	13.839
65	Berlin	Berlin	ICA	ICA	0	7.768
66	Berlin	Berlin	AComA	anterior	1	3.652
67	Berlin	Berlin	MCA	MCA	1	4.031
68	Berlin	Berlin	AComA	anterior	1	2.672
69	Berlin	Berlin	ICA	ICA	0	11.746
70	Berlin	Berlin	AComA	anterior	1	2.739
71	Berlin	Berlin	PComA	posterior	0	3.684
72A	Berlin	Berlin	PComA	posterior	0	9.969
72B	Berlin	Berlin	AComA	anterior	0	3.769
73	Berlin	Berlin	AComA	anterior	1	7.640
74	Berlin	Berlin	ICA	ICA	0	2.422
75A	Berlin	Berlin	PComA	posterior	0	2.277
75B	Berlin	Berlin	BA	posterior	1	4.556
76	Berlin	Berlin	PComA	posterior	1	4.974
77	Berlin	Berlin	MCA	MCA	0	10.165
78	Berlin	Berlin	MCA	MCA	0	5.020
79	Berlin	Berlin	ICA	ICA	0	9.202

For peer review only

BMJ Open: first published as 10.1136/bmjopen-2022-063051 on 8 November 2022. Downloaded from http://bmjopen.bmj.com/ on June 10, 2025 at Agence Bibliographique de l Enseignement Superieur (ABES) .
Protected by copyright, including for uses related to text and data mining, AI training, and similar technologies.

80	Berlin	Berlin	AComA	anterior	1	8.132
81	Berlin	Berlin	ICA	ICA	0	21.514
82A	Berlin	Berlin	ICA	ICA	0	2.039
82B	Berlin	Berlin	MCA	MCA	0	3.698
82C	Berlin	Berlin	ACA	anterior	0	1.486
83	Berlin	Berlin	PComA	posterior	0	10.503
84A	Berlin	Berlin	ICA	ICA	0	6.331
84B	Berlin	Berlin	MCA	MCA	0	3.509
85	Berlin	Berlin	MCA	MCA	0	2.996
86	Berlin	Berlin	MCA	MCA	0	2.575
87	Berlin	Berlin	AComA	anterior	1	3.971
88A	Berlin	Berlin	MCA	MCA	0	1.489
88B	Berlin	Berlin	MCA	MCA	0	2.304
89	Berlin	Berlin	ICA	ICA	0	5.728
90	Berlin	Berlin	MCA	MCA	0	4.016
91	Berlin	Berlin	AComA	anterior	0	6.147
92	Berlin	Berlin	PComA	posterior	0	7.023
93	Berlin	Berlin	PComA	posterior	1	10.373
94	Berlin	Berlin	MCA	MCA	0	19.183
95	Berlin	Berlin	AComA	anterior	1	6.261
96	Berlin	Berlin	ICA	ICA	0	5.202
97A	Berlin	Berlin	ICA	ICA	0	1.702
97B	Berlin	Berlin	AComA	anterior	0	5.381
98	Berlin	Berlin	PICA	posterior	1	4.524
99	Berlin	Berlin	PComA	posterior	0	6.067
100A	Berlin	Berlin	MCA	MCA	1	6.738
100B	Berlin	Berlin	ICA	ICA	0	2.364
100C	Berlin	Berlin	ICA	ICA	0	8.467
100D	Berlin	Berlin	MCA	MCA	0	2.488
100E	Berlin	Berlin	MCA	MCA	0	1.914
101	Berlin	Berlin	PComA	posterior	1	5.048
102	Berlin	Berlin	AComA	anterior	1	5.931
103	Berlin	Berlin	PCA	posterior	1	5.602
104	Berlin	Berlin	MCA	MCA	0	4.629
105	Berlin	Berlin	ICA	ICA	1	7.092
106	Berlin	Berlin	MCA	MCA	1	8.177
107	Berlin	Berlin	PComA	posterior	1	8.598
108	Berlin	Berlin	AComA	anterior	1	3.886
109	Berlin	Berlin	BA	posterior	1	13.918
110	Berlin	Berlin	BA	posterior	0	12.591
111	Berlin	Berlin	AComA	anterior	0	6.025
112	Berlin	Berlin	BA	posterior	1	7.000
113A	Berlin	Berlin	MCA	MCA	0	9.488
113B	Berlin	Berlin	MCA	MCA	0	6.242
114	Berlin	Berlin	MCA	MCA	1	3.622
115A	Hanover	Magdeburg	MCA	MCA	1	4.340
115B	Hanover	Magdeburg	MCA	MCA	0	1.149
116A	Hanover	Magdeburg	AComA	anterior	1	4.055
116B	Hanover	Magdeburg	AComA	anterior	0	1.031
117A	Hanover	Magdeburg	BA	posterior	1	8.476

BMJ Open: first published as 10.1136/bmjopen-2022-063051 on 8 November 2022. Downloaded from http://bmjopen.bmj.com/ on June 10, 2025 at Agence Bibliographique de l Enseignement Superieur (ABES) .
Protected by copyright, including for uses related to text and data mining, AI training, and similar technologies.

117B	Hanover	Magdeburg	AComA	anterior	0	4.088
118A	Hanover	Magdeburg	AComA	anterior	0	5.039
118B	Hanover	Magdeburg	PComA	posterior	1	4.528
119	Hanover	Magdeburg	MCA	MCA	1	1.132
120A	Hanover	Magdeburg	MCA	MCA	1	4.881
120B	Hanover	Magdeburg	ICA	ICA	1	2.325
121	Hanover	Magdeburg	ICA	ICA	1	18.704
122	Hanover	Magdeburg	ICA	ICA	0	6.667
123A	Hanover	Magdeburg	PComA	posterior	1	5.230
123B	Hanover	Magdeburg	MCA	MCA	0	2.984
124A	Hanover	Magdeburg	ACA	anterior	1	2.914
124B	Hanover	Magdeburg	AComA	anterior	0	1.201
124C	Hanover	Magdeburg	AComA	anterior	0	2.671
125	Hanover	Magdeburg	ICA	ICA	0	7.204
126A	Hanover	Magdeburg	MCA	MCA	1	8.466
126B	Hanover	Magdeburg	MCA	MCA	0	5.410
127A	Hanover	Magdeburg	AComA	anterior	1	2.663
127B	Hanover	Magdeburg	MCA	MCA	0	2.098
128A	Hanover	Magdeburg	ICA	ICA	1	1.429
128B	Hanover	Magdeburg	ICA	ICA	0	1.275
129A	Hanover	Magdeburg	BA	posterior	1	2.818
129B	Hanover	Magdeburg	SCA	posterior	0	1.293
130A	Hanover	Magdeburg	MCA	MCA	1	7.171
130B	Hanover	Magdeburg	AComA	anterior	0	4.247
131A	Hanover	Magdeburg	BA	posterior	0	4.863
131B	Hanover	Magdeburg	BA	posterior	1	3.992
132A	Hanover	Magdeburg	PComA	posterior	0	4.359
132B	Hanover	Magdeburg	AComA	anterior	1	16.578
133A	Hanover	Magdeburg	BA	posterior	1	6.042
133B	Hanover	Magdeburg	AComA	anterior	0	3.105
134A	Hanover	Magdeburg	MCA	MCA	1	6.298
134B	Hanover	Magdeburg	MCA	MCA	0	3.067
135	Hanover	Magdeburg	ICA	ICA	0	2.406
136A	Kiel	Magdeburg	MCA	MCA	0	1.108
136B	Kiel	Magdeburg	MCA	MCA	0	6.352
137	Kiel	Magdeburg	MCA	MCA	0	3.274
138	Kiel	Magdeburg	MCA	MCA	0	4.033
139	Kiel	Magdeburg	MCA	MCA	0	6.259
140	Kiel	Magdeburg	MCA	MCA	0	10.513
141	Kiel	Magdeburg	MCA	MCA	0	8.471
142	Kiel	Magdeburg	MCA	MCA	0	6.008
143	Kiel	Magdeburg	MCA	MCA	0	5.184
144	Kiel	Magdeburg	MCA	MCA	0	10.421
145	Kiel	Magdeburg	MCA	MCA	0	8.720
146A	Kiel	Magdeburg	MCA	MCA	0	6.242
146B	Kiel	Magdeburg	ACA	anterior	0	2.012
147A	Kiel	Magdeburg	MCA	MCA	0	5.580
147B	Kiel	Magdeburg	MCA	MCA	0	0.684
147C	Kiel	Magdeburg	MCA	MCA	0	0.573
147D	Kiel	Magdeburg	ACA	anterior	0	3.651

For peer review only

BMJ Open: first published as 10.1136/bmjopen-2022-063051 on 8 November 2022. Downloaded from http://bmjopen.bmj.com/ on June 10, 2025 at Agence Bibliographique de l Enseignement Superieur (ABES) . Protected by copyright, including for uses related to text and data mining, AI training, and similar technologies.

147E	Kiel	Magdeburg	AComA	anterior	0	1.213
147F	Kiel	Magdeburg	AComA	anterior	0	1.384
148	Kiel	Magdeburg	MCA	MCA	0	4.650
149	Kiel	Magdeburg	MCA	MCA	0	6.489
150	Kiel	Magdeburg	MCA	MCA	0	4.962
151	Kiel	Magdeburg	MCA	MCA	0	3.962
152	Magdeburg	Magdeburg	MCA	MCA	0	5.866
153	Magdeburg	Magdeburg	ACA	anterior	1	3.594
154	Magdeburg	Magdeburg	PComA	posterior	1	9.941
155A	Magdeburg	Magdeburg	AComA	anterior	1	2.543
155B	Magdeburg	Magdeburg	AComA	anterior	0	3.589
155C	Magdeburg	Magdeburg	MCA	MCA	0	5.120
156A	Magdeburg	Magdeburg	ICA	ICA	0	7.048
156B	Magdeburg	Magdeburg	ICA	ICA	0	1.214
156C	Magdeburg	Magdeburg	ICA	ICA	0	1.765
156D	Magdeburg	Magdeburg	ICA	ICA	0	2.037
157	Magdeburg	Magdeburg	VA	posterior	1	5.194
158	Magdeburg	Magdeburg	AChA	ICA	0	3.248
159	Magdeburg	Magdeburg	MCA	MCA	0	5.645
160A	Magdeburg	Magdeburg	AChA	ICA	1	2.988
160B	Magdeburg	Magdeburg	ICA	ICA	0	2.842
161A	Magdeburg	Magdeburg	ICA	ICA	1	5.684
161B	Magdeburg	Magdeburg	ICA	ICA	0	2.089
161C	Magdeburg	Magdeburg	PICA	posterior	0	2.497
162	Magdeburg	Magdeburg	AChA	ICA	1	4.811
163	Magdeburg	Magdeburg	ICA	ICA	0	4.981
164	Magdeburg	Magdeburg	MCA	MCA	0	3.817
165A	Magdeburg	Magdeburg	MCA	MCA	0	3.419
165B	Magdeburg	Magdeburg	PComA	posterior	0	5.533
165C	Magdeburg	Magdeburg	BA	posterior	0	2.856
165D	Magdeburg	Magdeburg	SCA	posterior	1	4.595
166	Magdeburg	Magdeburg	ICA	ICA	0	3.638
167	Magdeburg	Magdeburg	ICA	ICA	0	3.481
168	Magdeburg	Magdeburg	ICA	ICA	0	6.061
169	Magdeburg	Magdeburg	ICA	ICA	0	7.142
170	Magdeburg	Magdeburg	ICA	ICA	0	5.557
171	Magdeburg	Magdeburg	ICA	ICA	0	11.276
172A	Magdeburg	Magdeburg	AComA	anterior	1	3.283
172B	Magdeburg	Magdeburg	MCA	MCA	0	2.319
173A	Magdeburg	Magdeburg	MCA	MCA	1	4.176
173B	Magdeburg	Magdeburg	ICA	ICA	0	3.188
174	Magdeburg	Magdeburg	ICA	ICA	0	3.711
175	Magdeburg	Magdeburg	MCA	MCA	0	4.156
176	Magdeburg	Magdeburg	AComA	anterior	0	3.397
177A	Magdeburg	Magdeburg	PComA	posterior	1	6.322
177B	Magdeburg	Magdeburg	BA	posterior	0	1.516
178	Magdeburg	Magdeburg	MCA	MCA	1	5.269

For peer review only

BMJ Open: first published as 10.1136/bmjopen-2022-063051 on 8 November 2022. Downloaded from http://bmjopen.bmj.com/ on June 10, 2025 at Agence Bibliographique de l Enseignement Superieur (ABES) . Protected by copyright, including for uses related to text and data mining, AI training, and similar technologies.

maximum c	maximum h	maximum c	bulge heigh	surface area	convex hull	minimal bo	closed aneu	volume
L_max	H_max	D_max	H_b	A	A_CH	A_MBS	A_closed	V
mm	mm	mm	mm	cm^2	cm^2	cm^2	cm^2	ml
6.629	5.790	5.713	0.877	0.887	1.018	1.495	1.003	0.083
11.888	8.544	10.931	3.003	2.391	2.722	4.652	2.537	0.269
7.306	6.133	4.862	0.313	0.742	0.914	1.677	0.888	0.064
7.867	6.544	7.165	3.567	1.018	1.146	1.979	1.122	0.097
7.336	6.315	6.104	1.929	0.888	1.022	1.749	1.014	0.085
6.275	4.482	5.783	0.575	0.693	0.906	1.269	0.900	0.074
23.888	20.508	23.475	9.621	12.495	13.243	18.371	13.239	4.106
6.597	4.534	6.403	1.473	0.746	0.934	1.422	0.924	0.076
5.837	3.939	5.183	0.070	0.568	0.802	1.099	0.795	0.060
6.518	5.449	5.861	2.398	0.713	0.822	1.338	0.809	0.059
8.495	6.902	7.441	3.391	1.540	1.813	2.341	1.803	0.215
11.246	9.797	10.200	3.153	1.755	1.899	3.981	1.853	0.195
11.394	8.611	10.972	4.429	2.218	2.475	4.079	2.459	0.334
7.308	4.479	7.292	0.287	0.574	0.844	1.684	0.826	0.059
4.672	3.411	4.157	0.033	0.354	0.489	0.729	0.486	0.027
13.627	11.834	11.081	4.341	3.153	3.480	5.839	3.381	0.526
2.875	1.899	2.875	0.057	0.126	0.180	0.276	0.178	0.006
14.303	12.591	12.333	6.473	3.921	4.285	6.591	4.242	0.730
3.763	2.874	3.382	1.302	0.281	0.342	0.445	0.341	0.018
5.669	4.725	4.473	2.104	0.553	0.648	1.015	0.643	0.044
7.910	6.289	6.673	3.770	1.024	1.175	1.970	1.151	0.101
6.439	5.233	5.830	1.474	0.815	0.991	1.327	0.978	0.081
12.632	11.229	10.859	3.425	3.001	3.307	5.029	3.293	0.523
8.453	6.020	7.820	1.936	0.987	1.244	2.245	1.236	0.112
9.521	8.035	9.229	3.504	2.125	2.439	2.878	2.433	0.344
8.530	5.733	7.294	1.949	1.050	1.420	2.328	1.397	0.132
4.793	3.005	4.741	0.075	0.310	0.479	0.797	0.470	0.025
14.667	10.280	13.848	1.293	4.122	5.440	6.782	5.419	1.129
7.677	4.990	6.526	2.190	0.873	1.094	1.890	1.060	0.085
8.500	5.691	8.412	2.083	1.088	1.325	2.270	1.310	0.124
10.420	6.548	10.246	2.938	1.204	1.480	3.411	1.377	0.112
15.754	13.711	11.401	3.704	3.516	3.937	7.802	3.868	0.564
6.137	4.508	5.343	2.007	0.663	0.820	1.184	0.817	0.063
6.677	3.854	6.460	1.201	0.590	0.769	1.402	0.757	0.054
6.751	5.481	4.736	1.330	0.577	0.716	1.432	0.696	0.045
3.661	2.760	3.246	1.172	0.232	0.303	0.424	0.301	0.014
6.655	5.163	5.034	1.727	0.691	0.832	1.391	0.823	0.062
8.135	5.839	7.993	1.423	1.186	1.438	2.167	1.417	0.142
16.986	10.740	15.845	2.213	5.926	6.882	9.209	6.869	1.564
7.950	6.713	6.080	1.989	1.030	1.244	2.022	1.224	0.108
5.212	3.563	5.005	0.689	0.483	0.669	0.895	0.665	0.046
12.891	11.777	8.932	5.558	2.584	2.875	5.260	2.844	0.398
24.926	21.090	22.734	9.915	14.654	15.321	19.652	15.279	5.424
8.946	6.977	8.075	2.268	1.298	1.555	2.541	1.527	0.157
14.786	10.742	14.206	1.633	2.875	3.216	6.868	3.132	0.407
6.715	5.085	5.948	1.913	0.712	0.843	1.420	0.839	0.066
15.827	13.957	14.042	6.937	5.487	5.906	7.992	5.870	1.249

BMJ Open: first published as 10.1136/bmjopen-2022-063051 on 8 November 2022. Downloaded from http://bmjopen.bmj.com/ on June 10, 2025 at Agence Bibliographique de l Enseignement Superieur (ABES) .
Protected by copyright, including for uses related to text and data mining, AI training, and similar technologies.

6.419	4.551	6.134	0.624	0.618	0.839	1.316	0.813	0.058
8.062	6.217	6.768	2.455	1.126	1.368	2.042	1.365	0.137
17.188	10.658	16.238	2.250	3.236	4.445	9.425	4.430	0.696
7.303	4.996	6.301	1.470	0.688	0.925	1.676	0.910	0.072
4.605	2.692	4.603	0.037	0.296	0.466	0.713	0.462	0.023
4.605	3.619	3.564	1.963	0.355	0.438	0.677	0.430	0.023
4.653	2.599	4.537	0.354	0.303	0.480	0.698	0.475	0.025
13.326	11.629	11.342	5.799	3.546	3.816	5.596	3.800	0.658
7.105	4.947	6.019	0.113	0.678	0.891	1.586	0.882	0.061
4.777	2.888	4.516	0.482	0.282	0.439	0.727	0.433	0.023
18.334	17.219	14.463	8.226	5.638	6.064	10.560	5.978	1.232
11.513	9.974	11.050	4.580	2.241	2.481	4.240	2.396	0.285
6.880	5.489	6.061	2.068	0.829	0.999	1.492	0.993	0.086
4.149	2.840	3.778	0.926	0.297	0.384	0.541	0.382	0.021
11.234	7.779	10.623	2.600	2.129	2.279	3.965	2.254	0.282
6.535	5.085	5.126	0.262	0.507	0.706	1.400	0.685	0.041
6.195	3.881	6.006	0.616	0.577	0.840	1.210	0.829	0.061
4.282	2.759	3.841	0.151	0.216	0.331	0.590	0.325	0.013
5.968	3.703	5.938	1.423	0.517	0.678	1.119	0.668	0.043
4.773	4.310	4.200	2.368	0.467	0.513	0.771	0.506	0.031
9.479	6.686	9.469	2.116	1.305	1.446	2.823	1.429	0.139
4.362	2.739	4.165	0.197	0.326	0.447	0.600	0.445	0.025
7.928	6.831	6.578	2.903	1.256	1.465	2.026	1.456	0.154
2.798	1.593	2.792	0.014	0.105	0.170	0.266	0.167	0.005
6.330	3.703	6.047	0.954	0.580	0.806	1.259	0.803	0.058
7.668	6.509	6.943	1.249	0.852	1.054	1.873	0.999	0.070
8.038	5.767	7.357	1.708	0.972	1.152	2.030	1.143	0.103
13.384	9.880	12.864	3.835	3.174	3.751	5.854	3.690	0.603
4.583	3.361	4.077	0.084	0.364	0.502	0.704	0.498	0.030
13.573	12.129	7.940	6.398	2.411	2.619	5.788	2.564	0.328
6.253	4.782	5.560	2.596	0.679	0.785	1.232	0.782	0.060
6.774	5.738	4.776	1.687	0.752	0.882	1.467	0.876	0.070
19.580	14.862	19.183	7.524	7.554	7.889	12.044	7.851	1.917
10.702	7.977	8.927	2.139	2.019	2.495	3.606	2.481	0.325
6.698	4.629	5.540	0.489	0.576	0.764	1.410	0.757	0.055
6.354	4.692	5.177	1.312	0.626	0.795	1.289	0.776	0.053
6.204	3.207	6.016	0.114	0.413	0.706	1.215	0.694	0.044
14.376	13.009	10.934	6.325	2.638	2.994	6.492	2.830	0.343
6.016	4.460	5.142	0.926	0.678	0.873	1.149	0.866	0.071
5.832	3.890	5.511	0.286	0.536	0.691	1.071	0.684	0.046
14.708	12.119	12.964	4.615	3.419	3.829	6.796	3.791	0.609
5.100	3.825	4.479	0.525	0.452	0.611	0.840	0.603	0.038
10.529	8.923	7.517	2.011	1.266	1.421	3.483	1.355	0.113
6.886	3.607	6.764	0.185	0.510	0.851	1.490	0.837	0.060
4.974	3.155	4.670	0.739	0.312	0.487	0.792	0.479	0.026
6.182	5.235	3.884	2.072	0.422	0.503	1.203	0.487	0.025
8.405	5.927	8.296	2.748	1.255	1.408	2.270	1.385	0.133
15.254	10.492	15.251	1.120	3.825	4.559	7.665	4.507	0.804
7.735	5.096	7.199	1.289	0.956	1.265	1.925	1.236	0.115
11.062	9.776	9.388	5.048	2.352	2.598	3.900	2.577	0.353

For peer review only

BMJ Open: first published as 10.1136/bmjopen-2022-063051 on 8 November 2022. Downloaded from http://bmjopen.bmj.com/ on June 10, 2025 at Agence Bibliographique de l Enseignement Superieur (ABES) .
Protected by copyright, including for uses related to text and data mining, AI training, and similar technologies.

9.022	8.308	5.532	5.605	1.258	1.403	2.566	1.369	0.125
32.342	25.628	30.344	9.085	21.842	22.485	32.901	22.541	9.061
3.400	2.107	3.340	0.103	0.171	0.249	0.382	0.247	0.010
5.047	4.006	3.660	0.257	0.368	0.480	0.802	0.479	0.028
3.134	1.819	3.062	0.002	0.128	0.204	0.325	0.203	0.007
13.558	11.007	11.469	5.880	3.372	4.048	5.907	3.950	0.645
8.282	6.772	7.749	2.957	1.357	1.578	2.227	1.567	0.170
5.390	3.909	3.582	0.036	0.363	0.503	0.917	0.497	0.029
5.401	3.552	5.038	1.301	0.435	0.613	0.917	0.611	0.042
3.966	2.604	3.799	0.123	0.269	0.369	0.506	0.368	0.019
5.633	4.386	4.464	0.942	0.531	0.621	1.001	0.614	0.039
3.149	1.664	3.147	0.170	0.102	0.155	0.311	0.153	0.005
3.784	2.577	3.258	0.475	0.191	0.258	0.454	0.256	0.011
7.951	6.459	5.903	0.045	0.885	1.210	2.142	1.167	0.093
6.817	4.506	6.387	1.055	0.691	0.886	1.462	0.880	0.067
7.784	6.322	6.895	2.712	1.231	1.415	1.903	1.412	0.152
12.441	7.739	12.162	1.572	2.313	2.941	4.898	2.904	0.402
16.422	12.513	15.861	2.894	4.492	4.998	8.482	4.966	0.797
27.009	21.425	25.069	8.693	14.959	16.042	22.918	16.010	5.763
8.947	7.350	6.990	2.234	1.135	1.351	2.515	1.341	0.128
13.291	8.491	13.104	0.615	2.474	3.251	5.883	3.166	0.379
5.671	2.993	5.671	0.100	0.283	0.495	1.011	0.489	0.019
8.214	5.554	7.968	1.932	1.237	1.574	2.124	1.572	0.170
5.584	4.790	4.319	2.528	0.481	0.539	0.980	0.527	0.031
9.725	6.554	9.274	1.314	1.459	1.953	2.971	1.944	0.238
16.284	12.471	15.055	0.726	3.620	4.000	8.331	3.963	0.645
3.707	2.472	3.379	0.531	0.221	0.311	0.445	0.309	0.014
16.159	11.384	16.159	4.627	3.858	4.256	8.203	4.029	0.506
4.053	2.688	3.620	0.707	0.258	0.349	0.516	0.347	0.016
3.744	1.985	3.743	0.076	0.186	0.285	0.442	0.282	0.011
6.956	5.626	4.803	1.591	0.669	0.821	1.525	0.808	0.058
7.936	6.362	7.128	3.081	1.178	1.318	2.163	1.302	0.120
9.195	6.126	7.318	1.738	1.708	1.836	2.661	1.858	0.209
17.009	8.810	16.189	0.942	2.437	3.849	9.088	3.752	0.562
9.263	7.602	7.208	3.536	1.222	1.383	2.696	1.338	0.114
10.514	8.759	7.409	3.082	1.494	1.771	3.482	1.712	0.151
10.231	8.838	7.094	2.851	1.488	1.803	3.372	1.739	0.166
6.100	4.339	5.591	0.679	0.516	0.732	1.220	0.722	0.048
17.012	13.949	16.935	6.552	6.058	6.416	9.100	6.386	1.433
18.621	14.380	14.373	6.548	4.829	5.408	10.893	5.328	0.999
9.774	6.785	8.878	1.968	1.741	2.204	3.001	2.190	0.285
10.375	7.553	9.325	3.307	1.779	2.280	3.443	2.262	0.286
11.542	9.849	7.908	4.661	2.103	2.433	4.190	2.390	0.308
8.757	6.907	8.753	2.415	1.552	1.848	2.420	1.841	0.224
6.793	4.234	6.753	0.367	0.597	0.920	1.502	0.910	0.068
6.195	5.019	5.753	2.072	0.634	0.738	1.213	0.721	0.049
2.123	1.222	2.050	0.099	0.062	0.091	0.144	0.089	0.002
7.276	4.568	7.267	1.827	0.795	0.957	1.663	0.935	0.073
2.744	1.425	2.563	0.133	0.078	0.128	0.237	0.123	0.003
10.853	8.721	9.956	2.319	2.269	2.569	3.723	2.547	0.342

For peer review only

BMJ Open: first published as 10.1136/bmjopen-2022-063051 on 8 November 2022. Downloaded from http://bmjopen.bmj.com/ on June 10, 2025 at Agence Bibliographique de l Enseignement Superieur (ABES) .
Protected by copyright, including for uses related to text and data mining, AI training, and similar technologies.

6.386	4.271	6.267	1.450	0.622	0.798	1.282	0.779	0.052
7.385	6.025	5.712	3.287	0.847	0.981	1.714	0.961	0.077
6.224	4.693	5.826	1.532	0.584	0.710	1.218	0.686	0.040
2.739	1.458	2.699	0.000	0.079	0.137	0.248	0.129	0.003
6.758	5.613	6.202	3.057	0.747	0.850	1.552	0.826	0.060
8.335	5.295	8.154	0.578	0.472	0.673	2.182	0.626	0.032
24.223	19.791	22.453	9.808	12.666	13.149	18.524	13.126	4.170
9.429	7.753	9.246	3.668	1.763	2.018	2.881	1.991	0.233
7.279	5.501	6.496	1.296	0.962	1.180	1.701	1.156	0.093
4.951	3.068	4.238	0.721	0.311	0.403	0.770	0.396	0.018
3.677	3.075	2.630	1.197	0.197	0.240	0.431	0.230	0.008
3.184	1.674	2.913	0.185	0.096	0.166	0.322	0.159	0.004
4.432	3.209	4.075	1.200	0.283	0.349	0.626	0.346	0.016
8.784	7.818	6.956	3.946	1.370	1.477	2.435	1.460	0.148
13.905	9.021	13.148	0.801	2.857	3.336	6.331	3.136	0.362
7.117	5.697	7.117	1.111	0.959	1.100	1.716	1.067	0.083
4.398	3.418	3.652	1.122	0.260	0.319	0.609	0.314	0.014
4.263	2.616	3.714	0.022	0.236	0.323	0.576	0.316	0.014
3.378	1.853	3.377	0.224	0.119	0.210	0.389	0.196	0.005
5.130	2.891	4.336	0.308	0.177	0.292	0.827	0.275	0.008
5.027	3.392	4.348	1.368	0.315	0.392	0.795	0.385	0.019
2.603	1.519	2.548	0.128	0.096	0.144	0.214	0.138	0.004
8.733	7.733	5.173	2.236	1.000	1.104	2.399	1.082	0.087
6.282	4.788	4.997	1.219	0.529	0.634	1.242	0.623	0.038
6.960	6.297	6.263	3.045	0.617	0.691	1.556	0.649	0.035
6.109	4.679	5.536	1.914	0.602	0.685	1.173	0.680	0.047
8.258	5.056	7.901	0.962	0.957	1.190	2.143	1.166	0.099
21.893	19.479	15.008	5.305	5.825	6.171	15.090	6.046	1.094
7.690	6.527	5.130	2.092	0.820	0.984	1.861	0.906	0.058
4.236	3.327	2.935	1.359	0.267	0.320	0.564	0.310	0.014
7.909	6.999	6.604	1.846	1.191	1.329	1.991	1.306	0.123
5.815	3.677	4.000	0.846	0.324	0.434	1.062	0.406	0.019
7.097	4.213	6.014	0.103	0.332	0.541	1.582	0.515	0.023
2.628	1.504	2.617	0.126	0.075	0.129	0.227	0.120	0.003
6.801	6.385	4.171	3.307	0.723	0.806	1.476	0.797	0.058
5.605	3.754	5.144	1.846	0.487	0.608	0.987	0.597	0.037
6.085	4.188	5.097	1.013	0.566	0.707	1.164	0.693	0.046
10.066	6.868	9.700	2.978	1.972	2.370	3.227	2.338	0.291
11.565	10.869	9.066	5.115	2.694	2.806	4.206	2.801	0.417
10.003	8.861	9.695	3.555	2.151	2.310	3.143	2.295	0.306
6.948	6.210	4.669	2.279	0.766	0.840	1.517	0.825	0.061
8.098	6.481	7.268	3.584	1.033	1.168	2.064	1.144	0.093
15.923	12.736	11.639	3.653	3.319	3.922	7.966	3.711	0.511
9.220	8.728	6.525	5.970	1.325	1.489	2.729	1.424	0.127
8.947	7.049	8.891	2.469	1.606	1.828	2.595	1.814	0.208
3.410	2.529	3.319	1.196	0.188	0.222	0.369	0.217	0.008
6.977	5.759	5.449	1.556	0.777	0.934	1.530	0.903	0.066
1.627	0.900	1.540	0.310	0.031	0.050	0.090	0.047	0.001
1.571	0.846	1.511	0.124	0.026	0.044	0.080	0.041	0.001
4.670	3.829	3.715	0.862	0.374	0.442	0.707	0.433	0.023

For peer review only

BMJ Open: first published as 10.1136/bmjopen-2022-063051 on 8 November 2022. Downloaded from http://bmjopen.bmj.com/ on June 10, 2025 at Agence Bibliographique de l Enseignement Superieur (ABES) .
Protected by copyright, including for uses related to text and data mining, AI training, and similar technologies.

2.495	1.472	2.180	0.087	0.072	0.103	0.196	0.100	0.002
2.449	1.457	2.325	0.046	0.086	0.131	0.194	0.125	0.003
9.599	6.040	9.240	1.954	1.225	1.478	2.895	1.465	0.128
7.998	6.644	5.913	3.660	1.019	1.183	2.072	1.148	0.100
7.328	5.848	5.773	2.070	0.814	0.905	1.687	0.887	0.066
6.486	5.072	6.312	0.846	0.639	0.755	1.334	0.750	0.052
7.722	6.054	7.580	2.357	1.147	1.296	1.910	1.270	0.117
4.784	3.869	4.102	1.291	0.329	0.390	0.719	0.383	0.019
15.603	11.496	14.341	7.003	4.024	4.638	7.675	4.569	0.809
5.647	3.274	5.306	0.026	0.355	0.466	1.003	0.451	0.021
4.724	3.696	4.160	1.815	0.429	0.518	0.707	0.510	0.030
6.943	5.844	5.841	1.209	0.657	0.807	1.560	0.764	0.049
11.331	8.473	9.336	2.050	1.711	1.957	4.035	1.938	0.218
3.405	1.788	3.124	0.171	0.121	0.195	0.369	0.189	0.005
3.375	1.970	3.356	0.117	0.146	0.221	0.377	0.215	0.007
2.674	2.099	2.427	0.125	0.119	0.164	0.251	0.160	0.005
6.651	5.678	4.727	3.075	0.642	0.716	1.397	0.705	0.049
4.557	3.452	4.551	1.438	0.388	0.466	0.672	0.457	0.025
6.241	5.711	6.021	2.024	0.837	0.928	1.273	0.922	0.073
4.200	3.054	3.431	0.180	0.273	0.358	0.574	0.350	0.016
4.277	3.071	4.011	1.379	0.341	0.433	0.576	0.427	0.023
7.789	6.371	6.026	2.151	0.819	0.987	1.906	0.932	0.060
2.779	2.123	2.323	0.573	0.137	0.172	0.243	0.171	0.006
3.590	2.777	3.414	1.580	0.240	0.286	0.408	0.278	0.012
6.957	6.079	6.471	2.907	0.713	0.780	1.524	0.750	0.048
5.784	5.145	4.269	1.733	0.498	0.560	1.051	0.547	0.030
5.795	4.770	4.652	1.961	0.401	0.530	1.068	0.476	0.021
5.333	3.786	4.835	0.986	0.424	0.507	0.893	0.498	0.028
7.607	6.500	4.457	3.691	0.723	0.793	1.818	0.773	0.053
4.095	3.019	3.578	1.043	0.276	0.374	0.556	0.364	0.017
5.900	5.509	4.218	3.215	0.545	0.570	1.098	0.557	0.031
5.574	3.949	5.005	1.532	0.505	0.630	0.977	0.624	0.041
5.053	3.735	4.455	1.533	0.398	0.461	0.803	0.454	0.025
9.075	6.193	9.068	2.564	1.532	1.753	2.802	1.731	0.191
7.748	7.232	7.453	3.980	1.306	1.395	1.963	1.378	0.139
7.203	5.799	5.440	1.852	0.826	0.957	1.631	0.925	0.070
15.720	12.308	14.026	4.352	4.479	5.063	7.782	5.036	0.977
5.186	4.052	3.267	1.796	0.280	0.347	0.845	0.322	0.012
5.388	2.932	4.739	0.773	0.335	0.421	0.912	0.407	0.018
6.487	5.148	5.922	1.965	0.654	0.765	1.340	0.742	0.050
5.446	3.837	5.297	1.539	0.461	0.549	0.932	0.537	0.031
4.406	3.846	4.243	1.228	0.391	0.445	0.653	0.440	0.025
5.714	4.684	5.562	1.815	0.544	0.612	1.026	0.588	0.034
5.047	4.191	3.070	1.619	0.276	0.311	0.801	0.289	0.012
7.755	6.941	4.725	4.013	0.823	0.909	1.891	0.893	0.066
2.901	1.778	2.668	0.019	0.107	0.158	0.278	0.150	0.004
6.661	5.753	4.657	1.227	0.646	0.769	1.394	0.738	0.048

For peer review only

BMJ Open: first published as 10.1136/bmjopen-2022-063051 on 8 November 2022. Downloaded from http://bmjopen.bmj.com/ on June 10, 2025 at Agence Bibliographique de l Enseignement Superieur (ABES) .
Protected by copyright, including for uses related to text and data mining, AI training, and similar technologies.

convex hull	minimal bo	minimum n	maximum r	neck perim	equivalent	neck area	elliptical ne	aspect ratio
V_CH	V_MBS	D_neck,mir	D_neck,ma	P_neck	D_neck,equ	A_neck	A_neck,elli	AR
ml	ml	mm	mm	mm	mm	cm^2	cm^2	-
0.091	0.172	2.903	3.885	13.086	3.537	0.116	0.089	1.479
0.372	0.943	2.992	5.434	17.029	3.417	0.145	0.128	1.520
0.071	0.204	3.276	4.862	14.831	3.926	0.146	0.125	1.239
0.105	0.262	2.412	3.903	13.317	3.147	0.105	0.074	1.460
0.087	0.217	2.835	4.497	15.471	3.260	0.126	0.100	1.260
0.076	0.134	4.243	5.252	19.040	4.336	0.206	0.175	0.543
4.299	7.404	7.102	11.374	37.990	7.833	0.744	0.634	1.721
0.080	0.160	2.937	5.732	18.940	3.767	0.178	0.132	0.733
0.062	0.108	3.700	5.163	19.585	4.624	0.226	0.150	0.735
0.062	0.145	3.135	3.555	11.360	3.390	0.096	0.088	1.421
0.219	0.337	4.061	6.687	22.302	4.713	0.263	0.213	1.015
0.211	0.747	2.896	4.022	12.395	3.169	0.098	0.091	1.892
0.343	0.775	4.591	6.207	19.420	4.961	0.241	0.224	1.314
0.064	0.205	3.911	6.350	21.036	4.791	0.252	0.195	0.400
0.028	0.058	3.525	4.157	13.267	3.968	0.132	0.115	0.769
0.567	1.327	4.216	6.408	19.835	4.605	0.228	0.212	1.496
0.006	0.014	1.920	2.875	8.841	2.356	0.052	0.043	0.654
0.765	1.591	5.778	6.676	22.660	5.667	0.321	0.303	1.837
0.018	0.028	2.370	2.886	9.061	2.653	0.060	0.054	0.967
0.045	0.096	2.781	3.684	11.481	3.120	0.090	0.080	1.230
0.110	0.260	3.374	4.360	13.771	3.700	0.127	0.116	1.284
0.085	0.144	4.129	4.939	15.345	4.263	0.164	0.160	1.048
0.535	1.061	5.283	6.859	21.247	5.494	0.292	0.285	1.541
0.116	0.316	4.399	6.782	20.002	4.982	0.249	0.234	0.732
0.349	0.459	5.692	6.345	21.843	5.642	0.308	0.284	1.246
0.144	0.334	5.051	7.400	24.248	5.730	0.347	0.294	0.621
0.027	0.067	3.554	4.752	15.381	4.143	0.159	0.133	0.612
1.148	1.661	6.103	13.945	53.525	9.693	1.297	0.668	0.608
0.096	0.244	3.241	5.421	18.057	4.145	0.187	0.138	0.776
0.131	0.322	4.742	5.937	19.016	4.669	0.222	0.221	0.774
0.140	0.592	3.148	5.233	16.748	4.119	0.172	0.129	1.047
0.640	2.049	6.067	6.812	24.497	5.741	0.352	0.325	1.876
0.065	0.121	3.929	4.537	15.469	3.986	0.154	0.140	0.899
0.057	0.156	2.964	5.044	16.782	3.982	0.167	0.117	0.622
0.049	0.161	2.859	4.073	13.567	3.522	0.119	0.091	1.249
0.015	0.026	2.338	3.094	9.103	3.028	0.069	0.057	0.878
0.065	0.154	3.388	4.395	14.337	3.683	0.132	0.117	1.134
0.150	0.300	4.221	5.874	20.243	4.553	0.230	0.195	0.773
1.618	2.628	7.460	14.252	45.129	8.355	0.943	0.835	0.665
0.118	0.270	3.389	5.919	16.909	4.575	0.193	0.158	1.049
0.048	0.080	4.100	4.888	16.858	4.339	0.183	0.157	0.692
0.413	1.134	4.955	5.832	21.532	4.829	0.260	0.227	2.005
5.489	8.192	4.856	13.272	38.744	6.453	0.625	0.506	1.563
0.166	0.381	4.146	5.861	19.226	4.767	0.229	0.191	0.946
0.471	1.692	4.251	6.311	19.493	5.268	0.257	0.211	1.331
0.068	0.159	3.330	4.548	14.206	3.568	0.127	0.119	0.943
1.284	2.125	5.828	7.791	26.972	5.678	0.383	0.357	1.769

For peer review only

BMJ Open: first published as 10.1136/bmjopen-2022-063051 on 8 November 2022. Downloaded from http://bmjopen.bmj.com/ on June 10, 2025 at Agence Bibliographique de l Enseignement Superieur (ABES) .
Protected by copyright, including for uses related to text and data mining, AI training, and similar technologies.

0.065	0.142	2.869	6.280	18.787	4.153	0.195	0.141	0.685
0.140	0.274	5.099	5.722	19.742	4.850	0.239	0.229	1.030
0.723	2.721	9.411	15.328	45.262	10.554	1.194	1.133	0.448
0.076	0.204	3.921	5.390	19.347	4.578	0.221	0.166	0.782
0.025	0.057	4.072	4.605	15.924	4.153	0.165	0.147	0.524
0.025	0.052	2.544	3.498	10.509	2.840	0.075	0.070	1.001
0.027	0.055	3.973	4.537	15.822	4.355	0.172	0.142	0.506
0.671	1.245	5.067	6.060	20.235	5.028	0.254	0.241	1.844
0.067	0.188	4.039	6.019	18.197	4.473	0.203	0.191	0.770
0.024	0.058	3.349	4.139	15.221	3.971	0.151	0.109	0.532
1.284	3.227	3.904	8.491	26.453	5.140	0.340	0.260	2.001
0.334	0.821	3.698	5.097	15.808	3.937	0.156	0.148	1.489
0.088	0.171	3.652	5.028	14.943	4.393	0.164	0.144	1.004
0.021	0.037	2.695	3.182	10.976	3.122	0.086	0.067	0.874
0.296	0.742	3.682	4.035	12.878	3.887	0.125	0.117	1.693
0.047	0.156	3.958	5.126	15.600	4.569	0.178	0.159	0.948
0.065	0.125	3.926	6.009	20.114	5.003	0.252	0.185	0.554
0.015	0.043	3.044	3.841	13.047	3.343	0.109	0.092	0.545
0.048	0.111	3.747	4.646	14.887	4.055	0.151	0.137	0.609
0.032	0.064	1.743	2.212	6.685	2.312	0.039	0.030	1.934
0.146	0.446	3.494	4.013	13.901	3.573	0.124	0.110	1.223
0.026	0.044	3.340	4.165	13.007	3.667	0.119	0.109	0.616
0.158	0.271	3.373	5.696	18.626	4.310	0.201	0.151	1.161
0.006	0.013	2.149	2.798	9.586	2.605	0.062	0.047	0.549
0.059	0.133	4.544	5.666	18.559	4.809	0.223	0.202	0.554
0.088	0.241	3.240	5.327	15.348	3.834	0.147	0.136	0.751
0.106	0.272	3.982	5.445	15.999	4.286	0.171	0.170	0.895
0.635	1.332	5.655	8.968	30.914	6.682	0.516	0.398	0.953
0.031	0.056	3.242	4.090	14.393	3.732	0.134	0.104	0.775
0.352	1.309	4.023	4.674	15.332	4.004	0.153	0.148	2.325
0.062	0.129	3.028	3.756	12.271	3.335	0.102	0.089	1.209
0.072	0.167	3.273	4.162	13.626	3.661	0.125	0.107	1.327
1.971	3.931	5.400	6.936	23.221	5.117	0.297	0.294	1.995
0.349	0.644	6.668	7.542	25.103	7.353	0.461	0.395	1.030
0.057	0.157	2.954	5.757	18.913	3.839	0.182	0.134	0.634
0.060	0.138	3.374	4.303	14.245	4.211	0.150	0.114	0.937
0.048	0.126	4.114	6.204	23.009	4.885	0.281	0.200	0.431
0.410	1.556	4.088	5.305	16.784	4.591	0.193	0.170	2.214
0.073	0.116	2.687	5.335	20.340	3.712	0.189	0.113	0.513
0.049	0.104	2.559	5.530	16.327	3.620	0.148	0.111	0.666
0.647	1.666	5.581	7.501	23.891	6.226	0.372	0.329	1.329
0.041	0.072	3.421	4.484	14.463	4.178	0.151	0.120	0.841
0.133	0.611	2.123	4.861	12.221	2.913	0.089	0.081	1.572
0.064	0.171	4.645	6.823	21.514	6.082	0.327	0.249	0.355
0.029	0.066	3.453	4.611	16.463	4.059	0.167	0.125	0.494
0.028	0.124	2.466	2.877	9.725	2.697	0.066	0.056	1.584
0.144	0.322	2.931	4.907	13.849	3.745	0.130	0.113	1.014
0.831	1.995	3.693	15.254	44.240	6.164	0.682	0.442	0.666
0.123	0.251	3.660	5.911	21.822	5.129	0.280	0.170	0.849
0.370	0.724	4.471	5.481	18.185	4.966	0.226	0.193	1.679

For peer review only

BMJ Open: first published as 10.1136/bmjopen-2022-063051 on 8 November 2022. Downloaded from http://bmjopen.bmj.com/ on June 10, 2025 at Agence Bibliographique de l Enseignement Superieur (ABES) . Protected by copyright, including for uses related to text and data mining, AI training, and similar technologies.

0.138	0.387	3.088	3.831	12.450	3.565	0.111	0.093	2.122
9.561	17.746	2.961	18.027	50.338	5.556	0.699	0.419	1.193
0.010	0.022	2.536	3.340	10.417	2.938	0.077	0.067	0.611
0.028	0.068	2.961	3.628	12.388	3.587	0.111	0.084	1.019
0.007	0.017	2.669	3.062	9.724	3.065	0.075	0.064	0.485
0.709	1.350	6.233	9.921	32.559	7.095	0.578	0.486	1.059
0.177	0.312	3.682	5.598	18.267	4.597	0.210	0.162	1.131
0.030	0.083	3.109	3.713	13.372	4.008	0.134	0.091	0.945
0.043	0.083	2.949	4.596	16.118	4.349	0.175	0.106	0.652
0.019	0.034	3.058	3.824	11.763	3.366	0.099	0.092	0.673
0.041	0.094	2.402	3.999	11.654	2.840	0.083	0.075	0.993
0.005	0.016	1.871	3.149	9.064	2.252	0.051	0.046	0.473
0.011	0.029	2.480	2.749	9.781	2.680	0.066	0.054	0.838
0.105	0.295	5.164	6.092	19.890	5.675	0.282	0.247	0.940
0.071	0.166	3.647	5.591	18.794	4.024	0.189	0.160	0.718
0.154	0.247	3.845	5.198	17.087	4.221	0.180	0.157	1.182
0.433	1.019	7.600	9.255	32.052	7.377	0.591	0.552	0.759
0.946	2.323	5.854	9.288	29.079	6.525	0.474	0.427	1.117
5.822	10.316	10.249	12.646	43.430	9.687	1.052	1.018	1.517
0.133	0.375	4.577	4.981	16.951	4.848	0.205	0.179	1.257
0.457	1.342	6.603	9.821	38.845	7.126	0.692	0.509	0.530
0.021	0.096	4.180	5.671	18.176	4.536	0.206	0.186	0.300
0.173	0.291	5.563	7.294	22.990	5.826	0.335	0.319	0.738
0.033	0.091	1.425	2.956	8.692	2.091	0.045	0.033	1.531
0.242	0.482	6.692	7.545	27.655	7.023	0.486	0.397	0.804
0.673	2.261	4.714	7.341	25.595	5.352	0.342	0.272	0.918
0.014	0.028	3.033	3.304	11.382	3.083	0.088	0.079	0.715
0.705	2.209	3.936	5.479	16.917	4.038	0.171	0.169	1.545
0.017	0.035	2.888	3.555	11.320	3.126	0.088	0.081	0.700
0.012	0.028	2.723	3.744	12.259	3.122	0.096	0.080	0.511
0.062	0.177	3.927	4.189	14.081	3.967	0.140	0.129	1.205
0.129	0.299	3.261	4.724	14.375	3.444	0.124	0.121	1.255
0.223	0.408	1.690	6.942	22.424	2.675	0.150	0.092	0.807
0.604	2.576	9.516	16.051	57.167	9.204	1.315	1.200	0.288
0.133	0.416	3.427	4.118	13.379	3.487	0.117	0.111	1.722
0.190	0.611	4.209	5.875	18.330	4.775	0.219	0.194	1.392
0.200	0.582	4.580	5.781	20.002	5.026	0.251	0.208	1.487
0.052	0.127	4.276	4.986	17.482	4.697	0.205	0.167	0.779
1.463	2.581	5.536	7.179	23.516	5.577	0.328	0.312	1.939
1.064	3.380	4.917	12.472	34.457	5.794	0.499	0.482	1.010
0.294	0.489	4.505	8.378	31.391	5.719	0.449	0.296	0.719
0.301	0.601	6.063	8.092	28.011	6.899	0.483	0.385	0.865
0.323	0.806	3.486	7.314	23.602	4.859	0.287	0.200	1.297
0.227	0.354	3.933	6.501	22.813	5.068	0.289	0.201	0.960
0.072	0.173	4.796	6.793	21.520	5.804	0.312	0.256	0.533
0.054	0.126	2.981	3.763	11.219	3.091	0.087	0.088	1.153
0.002	0.005	1.667	2.050	6.305	1.717	0.027	0.027	0.561
0.080	0.202	3.798	4.688	14.879	3.770	0.140	0.140	0.865
0.003	0.011	2.058	2.646	8.188	2.184	0.045	0.043	0.390
0.364	0.676	4.880	7.274	20.777	5.344	0.278	0.279	1.165

For peer review only

BMJ Open: first published as 10.1136/bmjopen-2022-063051 on 8 November 2022. Downloaded from http://bmjopen.bmj.com/ on June 10, 2025 at Agence Bibliographique de l Enseignement Superieur (ABES) .
Protected by copyright, including for uses related to text and data mining, AI training, and similar technologies.

0.059	0.136	3.633	5.216	16.163	3.879	0.157	0.149	0.784
0.083	0.211	3.466	3.933	13.148	3.467	0.114	0.107	1.281
0.049	0.126	3.027	4.428	12.646	3.207	0.101	0.105	1.023
0.004	0.012	2.254	2.739	9.026	2.224	0.050	0.048	0.413
0.066	0.182	2.509	4.164	11.013	2.871	0.079	0.082	1.172
0.040	0.303	3.046	6.031	16.366	3.781	0.155	0.144	0.385
4.307	7.497	4.943	11.565	29.411	6.256	0.460	0.449	1.617
0.251	0.460	3.312	6.808	19.810	4.592	0.227	0.177	0.979
0.109	0.209	4.469	5.198	17.058	4.553	0.194	0.182	1.006
0.020	0.064	2.612	4.202	11.337	3.013	0.085	0.086	0.710
0.010	0.027	1.673	2.354	6.665	1.998	0.033	0.031	1.238
0.005	0.017	2.558	3.184	9.667	2.606	0.063	0.064	0.377
0.017	0.047	2.537	3.163	9.173	2.730	0.063	0.063	0.845
0.156	0.357	3.105	3.630	11.718	3.059	0.090	0.089	1.984
0.496	1.498	3.688	7.971	23.076	4.837	0.279	0.231	1.062
0.097	0.211	3.514	3.858	12.669	3.425	0.108	0.106	1.402
0.015	0.045	2.234	2.843	9.386	2.324	0.055	0.050	0.937
0.015	0.041	3.000	3.715	10.778	2.970	0.080	0.088	0.565
0.007	0.023	2.662	3.378	11.376	2.694	0.077	0.071	0.423
0.010	0.071	2.885	4.088	12.580	3.113	0.098	0.093	0.312
0.020	0.067	2.674	3.641	10.202	2.743	0.070	0.076	0.774
0.005	0.009	1.941	2.438	8.082	2.096	0.042	0.037	0.530
0.094	0.349	2.932	3.509	10.841	3.047	0.083	0.081	2.044
0.042	0.130	2.598	4.490	11.942	3.133	0.094	0.092	0.946
0.044	0.182	1.604	2.311	6.687	1.877	0.031	0.029	2.104
0.049	0.119	2.818	3.448	10.414	2.988	0.078	0.076	1.158
0.112	0.295	4.647	5.228	18.128	4.607	0.209	0.191	0.834
1.181	5.512	3.626	7.662	19.509	4.543	0.222	0.218	2.164
0.078	0.239	2.966	3.629	11.960	2.882	0.086	0.085	1.665
0.016	0.040	2.054	2.604	8.405	2.090	0.044	0.042	1.193
0.133	0.264	3.526	4.008	13.454	3.419	0.115	0.111	1.572
0.023	0.103	2.488	4.181	11.759	2.758	0.081	0.082	0.733
0.028	0.187	3.376	6.094	16.842	4.360	0.184	0.162	0.395
0.003	0.010	2.058	2.628	8.482	2.109	0.045	0.042	0.422
0.060	0.169	2.876	3.210	9.865	3.022	0.075	0.072	1.979
0.041	0.092	2.534	4.791	13.958	3.151	0.110	0.095	0.683
0.051	0.118	3.367	4.437	14.181	3.586	0.127	0.117	0.909
0.323	0.545	4.747	9.608	24.939	5.860	0.365	0.358	0.651
0.424	0.811	2.828	4.463	12.938	3.306	0.107	0.099	2.356
0.315	0.524	3.432	4.980	14.519	3.980	0.144	0.134	1.701
0.066	0.176	2.482	3.060	9.082	2.609	0.059	0.060	1.963
0.108	0.279	2.829	4.298	13.230	3.376	0.112	0.095	1.206
0.639	2.114	4.957	9.395	25.968	6.032	0.392	0.366	1.109
0.148	0.424	3.121	3.948	11.926	3.295	0.098	0.097	2.209
0.221	0.393	3.803	6.053	18.164	4.583	0.208	0.181	1.031
0.009	0.021	1.782	2.158	6.541	1.799	0.029	0.030	0.933
0.077	0.178	3.345	4.520	13.440	3.752	0.126	0.119	1.234
0.001	0.003	1.249	1.627	4.931	1.263	0.016	0.016	0.420
0.001	0.002	1.171	1.571	5.218	1.191	0.016	0.014	0.365
0.025	0.056	2.550	2.828	9.049	2.602	0.059	0.057	1.291

BMJ Open: first published as 10.1136/bmjopen-2022-063051 on 8 November 2022. Downloaded from http://bmjopen.bmj.com/ on June 10, 2025 at Agence Bibliographique de l Enseignement Superieur (ABES) .
Protected by copyright, including for uses related to text and data mining, AI training, and similar technologies.

0.003	0.008	1.614	2.232	6.529	1.706	0.028	0.028	0.544
0.004	0.008	2.024	2.328	7.829	1.956	0.038	0.037	0.595
0.152	0.463	3.752	6.083	20.202	4.746	0.240	0.179	0.764
0.110	0.280	3.307	5.198	14.592	3.553	0.130	0.135	1.248
0.074	0.206	2.337	3.921	10.721	2.726	0.073	0.072	1.265
0.054	0.145	3.253	4.288	12.309	3.606	0.111	0.110	0.924
0.130	0.248	3.443	4.427	13.709	3.601	0.123	0.120	1.325
0.020	0.057	2.337	2.977	8.842	2.448	0.054	0.055	1.207
0.875	1.999	5.504	11.272	31.139	6.996	0.545	0.487	0.882
0.025	0.094	2.229	5.284	13.469	2.867	0.097	0.093	0.481
0.033	0.056	2.807	3.647	10.997	2.972	0.082	0.080	0.984
0.058	0.183	3.309	4.297	13.094	3.291	0.108	0.112	1.192
0.230	0.762	4.694	6.020	17.946	5.054	0.227	0.222	1.171
0.006	0.021	2.550	3.222	9.787	2.806	0.069	0.065	0.377
0.008	0.022	2.539	3.357	10.019	2.758	0.069	0.067	0.526
0.006	0.012	1.792	2.444	7.653	2.150	0.041	0.034	0.834
0.051	0.155	2.582	3.108	9.392	2.699	0.063	0.063	1.671
0.027	0.052	2.791	3.230	9.826	2.820	0.069	0.071	1.005
0.078	0.135	3.086	3.614	10.669	3.209	0.086	0.088	1.562
0.018	0.041	2.968	3.431	10.338	2.993	0.077	0.080	0.871
0.025	0.041	2.996	3.439	10.693	3.209	0.086	0.081	0.826
0.080	0.247	3.390	4.303	13.330	3.390	0.113	0.115	1.321
0.006	0.011	1.980	2.183	6.667	2.038	0.034	0.034	0.957
0.013	0.024	1.860	2.600	7.731	1.939	0.037	0.038	0.960
0.057	0.177	1.771	2.520	7.349	2.020	0.037	0.035	1.909
0.034	0.101	2.142	2.834	8.480	2.306	0.049	0.048	1.758
0.030	0.104	2.525	3.927	10.784	2.783	0.075	0.078	0.972
0.031	0.079	2.552	3.426	10.614	2.776	0.074	0.069	0.998
0.058	0.230	2.391	2.810	8.625	2.316	0.050	0.053	1.969
0.019	0.039	3.067	3.601	11.501	3.064	0.088	0.087	0.793
0.036	0.108	0.981	1.591	4.414	1.106	0.012	0.012	2.888
0.043	0.091	3.448	4.293	13.109	3.606	0.118	0.116	0.848
0.027	0.068	2.188	3.205	9.355	2.372	0.055	0.055	1.086
0.204	0.441	4.669	5.375	16.745	4.748	0.199	0.197	1.128
0.145	0.259	2.815	3.184	10.027	2.889	0.072	0.070	2.243
0.079	0.196	3.412	3.903	11.686	3.419	0.100	0.105	1.424
1.014	2.041	6.801	10.575	28.975	7.694	0.557	0.565	1.066
0.016	0.073	1.988	2.577	7.813	2.160	0.042	0.040	1.274
0.022	0.082	2.507	3.337	10.511	2.750	0.072	0.066	0.695
0.056	0.146	3.141	3.432	11.178	3.152	0.088	0.085	1.217
0.034	0.085	2.409	3.774	10.852	2.821	0.077	0.071	0.845
0.026	0.050	2.316	2.781	8.572	2.264	0.049	0.051	1.334
0.040	0.098	2.113	2.553	7.909	2.222	0.044	0.042	1.627
0.014	0.067	1.016	1.949	4.922	1.111	0.014	0.016	1.743
0.071	0.245	2.801	3.116	10.051	2.771	0.070	0.069	2.029
0.005	0.014	1.964	2.682	8.337	2.070	0.043	0.041	0.565
0.056	0.155	3.187	3.553	11.772	3.139	0.092	0.089	1.483

For peer review only

BMJ Open: first published as 10.1136/bmjopen-2022-063051 on 8 November 2022. Downloaded from http://bmjopen.bmj.com/ on June 10, 2025 at Agence Bibliographique de l Enseignement Superieur (ABES) .
Protected by copyright, including for uses related to text and data mining, AI training, and similar technologies.

aspect ratic	bottleneck	bulge locat	nonspericit	aneurysm v	aneurysm s	undulation	ellipticity ir	mean of m
eAR	BF	BL	NSI	AVSV	AASA	UI	EI	MAA
-	-	-	-	-	-	-	-	mm^-1
1.625	1.471	0.153	0.270	0.485	0.671	0.079	0.240	0.318
2.417	2.012	0.364	0.370	0.285	0.545	0.277	0.271	0.254
1.534	1.000	0.052	0.311	0.311	0.529	0.101	0.282	0.322
1.811	1.836	0.626	0.278	0.370	0.567	0.077	0.255	0.302
1.739	1.358	0.340	0.270	0.390	0.580	0.023	0.264	0.325
0.657	1.101	0.202	0.249	0.549	0.709	0.034	0.237	0.322
2.499	2.064	0.491	0.257	0.555	0.721	0.045	0.234	0.090
1.115	1.117	0.351	0.254	0.478	0.650	0.043	0.240	0.324
0.821	1.004	0.019	0.258	0.555	0.723	0.037	0.247	0.308
1.490	1.649	0.475	0.279	0.407	0.605	0.046	0.267	0.354
1.441	1.113	0.499	0.236	0.639	0.770	0.018	0.231	0.239
2.401	2.536	0.414	0.304	0.261	0.465	0.077	0.284	0.259
1.644	1.768	0.543	0.249	0.431	0.603	0.027	0.240	0.216
0.531	1.148	0.113	0.299	0.285	0.491	0.079	0.275	0.356
0.805	1.000	0.010	0.291	0.460	0.667	0.039	0.276	0.401
2.082	1.729	0.453	0.261	0.396	0.579	0.073	0.245	0.185
0.798	1.000	0.031	0.289	0.441	0.647	0.037	0.277	0.666
2.164	1.847	0.528	0.267	0.459	0.644	0.047	0.251	0.163
1.052	1.172	0.466	0.239	0.628	0.766	0.017	0.233	0.524
1.452	1.214	0.464	0.260	0.454	0.633	0.029	0.251	0.389
1.513	1.531	0.674	0.275	0.390	0.584	0.074	0.252	0.292
1.214	1.180	0.285	0.266	0.562	0.737	0.054	0.248	0.315
1.924	1.583	0.324	0.243	0.494	0.655	0.022	0.235	0.179
0.997	1.153	0.390	0.278	0.354	0.550	0.034	0.266	0.283
1.402	1.454	0.443	0.226	0.748	0.845	0.016	0.220	0.200
0.802	0.986	0.424	0.286	0.396	0.600	0.079	0.259	0.239
0.701	0.998	0.026	0.297	0.377	0.589	0.080	0.272	0.357
0.874	0.993	0.153	0.232	0.680	0.799	0.016	0.226	0.132
1.016	1.204	0.520	0.299	0.349	0.561	0.112	0.264	0.321
0.985	1.417	0.453	0.271	0.385	0.577	0.053	0.253	0.303
1.330	1.958	0.536	0.354	0.188	0.404	0.204	0.300	0.317
2.226	1.674	0.290	0.322	0.275	0.496	0.119	0.276	0.176
1.023	1.178	0.492	0.254	0.522	0.690	0.024	0.245	0.337
0.787	1.281	0.383	0.279	0.344	0.540	0.066	0.257	0.354
1.444	1.163	0.261	0.307	0.277	0.486	0.099	0.278	0.371
0.897	1.049	0.432	0.258	0.539	0.709	0.039	0.243	0.499
1.353	1.145	0.347	0.266	0.404	0.591	0.042	0.253	0.325
0.998	1.361	0.313	0.263	0.473	0.654	0.055	0.246	0.271
1.134	1.112	0.234	0.247	0.595	0.746	0.033	0.231	0.128
1.358	1.027	0.320	0.288	0.400	0.605	0.087	0.256	0.284
0.780	1.024	0.204	0.259	0.578	0.743	0.032	0.248	0.335
2.421	1.532	0.475	0.270	0.351	0.541	0.036	0.259	0.193
3.215	1.713	0.478	0.224	0.662	0.777	0.012	0.220	0.088
1.163	1.378	0.409	0.268	0.413	0.601	0.055	0.254	0.274
1.594	2.251	0.194	0.327	0.241	0.456	0.136	0.277	0.212
1.202	1.308	0.446	0.255	0.413	0.591	0.032	0.242	0.336
2.428	1.802	0.503	0.242	0.588	0.734	0.027	0.232	0.135

For peer review only

BMJ Open: first published as 10.1136/bmjopen-2022-063051 on 8 November 2022. Downloaded from http://bmjopen.bmj.com/ on June 10, 2025 at Agence Bibliographique de l Enseignement Superieur (ABES) . Protected by copyright, including for uses related to text and data mining, AI training, and similar technologies.

1.036	0.977	0.145	0.297	0.405	0.618	0.109	0.264	0.331
1.215	1.183	0.417	0.254	0.499	0.669	0.022	0.244	0.258
0.651	1.059	0.327	0.319	0.256	0.470	0.037	0.304	0.154
0.920	1.169	0.349	0.271	0.352	0.543	0.052	0.257	0.345
0.581	1.000	0.015	0.318	0.415	0.647	0.050	0.301	0.368
1.233	1.019	0.561	0.280	0.437	0.635	0.069	0.258	0.435
0.527	1.000	0.154	0.309	0.456	0.680	0.067	0.284	0.343
2.223	1.872	0.519	0.236	0.528	0.679	0.019	0.229	0.169
1.037	1.000	0.024	0.329	0.323	0.556	0.099	0.287	0.313
0.555	1.091	0.219	0.279	0.399	0.596	0.047	0.265	0.413
3.305	1.703	0.484	0.262	0.382	0.566	0.041	0.252	0.142
1.927	2.168	0.604	0.306	0.347	0.565	0.145	0.256	0.232
1.149	1.205	0.410	0.246	0.503	0.666	0.026	0.237	0.314
0.890	1.187	0.333	0.238	0.559	0.706	0.019	0.231	0.494
1.757	2.633	0.381	0.268	0.380	0.569	0.049	0.251	0.223
1.063	1.000	0.054	0.332	0.264	0.489	0.126	0.292	0.373
0.666	0.999	0.185	0.282	0.488	0.685	0.059	0.262	0.302
0.626	1.000	0.072	0.336	0.313	0.550	0.102	0.301	0.437
0.698	1.278	0.503	0.299	0.383	0.597	0.104	0.257	0.391
1.850	1.899	0.554	0.259	0.479	0.656	0.059	0.239	0.432
1.374	2.359	0.431	0.279	0.312	0.506	0.047	0.264	0.285
0.700	1.000	0.077	0.267	0.568	0.742	0.027	0.255	0.443
1.534	1.155	0.439	0.242	0.569	0.719	0.027	0.233	0.261
0.590	0.998	0.009	0.309	0.405	0.630	0.084	0.281	0.578
0.653	1.067	0.304	0.284	0.437	0.638	0.025	0.274	0.355
1.043	1.303	0.312	0.347	0.290	0.533	0.202	0.281	0.330
1.137	1.351	0.350	0.262	0.379	0.563	0.031	0.253	0.321
1.279	1.434	0.449	0.258	0.453	0.630	0.051	0.244	0.176
0.850	0.997	0.026	0.264	0.531	0.708	0.044	0.248	0.397
2.714	1.699	0.589	0.288	0.251	0.443	0.067	0.270	0.220
1.361	1.480	0.572	0.244	0.470	0.635	0.018	0.238	0.367
1.509	1.147	0.305	0.255	0.420	0.597	0.025	0.247	0.326
2.705	2.766	0.544	0.245	0.488	0.652	0.027	0.235	0.119
1.056	1.184	0.275	0.268	0.505	0.688	0.068	0.237	0.167
0.951	0.962	0.134	0.271	0.346	0.537	0.041	0.258	0.334
0.957	1.203	0.325	0.298	0.388	0.602	0.103	0.263	0.331
0.547	0.970	0.043	0.307	0.353	0.572	0.072	0.283	0.258
2.558	2.061	0.539	0.335	0.221	0.436	0.163	0.293	0.213
0.738	0.964	0.338	0.238	0.616	0.754	0.029	0.228	0.320
1.018	0.996	0.078	0.276	0.444	0.639	0.063	0.252	0.293
1.601	1.728	0.463	0.272	0.366	0.558	0.059	0.250	0.157
0.902	0.999	0.139	0.280	0.526	0.718	0.069	0.254	0.354
2.623	1.546	0.263	0.339	0.185	0.389	0.152	0.296	0.310
0.398	0.991	0.076	0.300	0.349	0.562	0.070	0.277	0.298
0.561	1.013	0.325	0.291	0.396	0.605	0.081	0.264	0.374
1.690	1.350	0.455	0.324	0.203	0.405	0.088	0.304	0.462
1.328	1.691	0.552	0.279	0.413	0.610	0.078	0.251	0.273
1.649	1.000	0.110	0.263	0.403	0.588	0.033	0.255	0.148
0.979	1.218	0.257	0.267	0.457	0.642	0.070	0.248	0.296
1.853	1.713	0.549	0.256	0.488	0.661	0.045	0.239	0.181

BMJ Open: first published as 10.1136/bmjopen-2022-063051 on 8 November 2022. Downloaded from http://bmjopen.bmj.com/ on June 10, 2025 at Agence Bibliographique de l Enseignement Superieur (ABES) . Protected by copyright, including for uses related to text and data mining, AI training, and similar technologies.

2.281	1.444	0.689	0.298	0.324	0.534	0.091	0.270	0.297
3.872	1.683	0.422	0.260	0.511	0.685	0.052	0.231	0.073
0.694	1.000	0.050	0.295	0.436	0.647	0.057	0.271	0.532
1.031	1.009	0.069	0.257	0.417	0.597	0.009	0.255	0.456
0.485	1.000	0.001	0.301	0.407	0.623	0.018	0.296	0.593
1.480	1.156	0.560	0.275	0.478	0.669	0.091	0.246	0.152
1.377	1.384	0.467	0.247	0.545	0.704	0.039	0.232	0.241
0.875	0.965	0.010	0.278	0.346	0.542	0.053	0.260	0.393
0.689	1.096	0.434	0.238	0.511	0.666	0.017	0.232	0.406
0.765	0.994	0.048	0.262	0.556	0.727	0.021	0.253	0.494
1.398	1.116	0.237	0.278	0.416	0.613	0.051	0.261	0.401
0.661	0.999	0.114	0.313	0.276	0.490	0.059	0.295	0.631
0.860	1.185	0.206	0.270	0.375	0.565	0.042	0.255	0.565
1.009	0.969	0.008	0.325	0.315	0.545	0.115	0.294	0.283
0.998	1.142	0.263	0.277	0.406	0.602	0.047	0.259	0.353
1.456	1.326	0.441	0.227	0.614	0.742	0.012	0.222	0.274
0.952	1.314	0.224	0.280	0.395	0.593	0.070	0.253	0.198
1.590	1.708	0.279	0.336	0.343	0.586	0.158	0.260	0.163
1.980	1.982	0.453	0.229	0.559	0.699	0.010	0.226	0.088
1.291	1.403	0.357	0.271	0.343	0.533	0.037	0.258	0.286
0.730	1.334	0.118	0.365	0.283	0.538	0.170	0.299	0.230
0.375	1.000	0.059	0.449	0.195	0.484	0.115	0.409	0.320
0.924	1.092	0.359	0.251	0.584	0.740	0.016	0.244	0.268
2.164	1.461	0.559	0.277	0.342	0.538	0.060	0.263	0.453
0.864	1.229	0.217	0.241	0.495	0.654	0.016	0.236	0.243
1.259	2.051	0.108	0.277	0.285	0.476	0.041	0.263	0.182
0.767	1.023	0.225	0.293	0.487	0.695	0.054	0.271	0.483
2.097	2.949	0.546	0.395	0.229	0.491	0.282	0.285	0.215
0.796	1.018	0.284	0.285	0.471	0.672	0.044	0.267	0.482
0.613	1.000	0.040	0.335	0.390	0.637	0.134	0.277	0.535
1.273	1.147	0.315	0.288	0.328	0.530	0.064	0.268	0.354
1.722	1.509	0.519	0.283	0.401	0.602	0.072	0.256	0.303
2.094	1.054	0.310	0.272	0.512	0.698	0.064	0.230	0.254
0.503	1.009	0.204	0.303	0.218	0.413	0.069	0.288	0.174
2.034	1.750	0.499	0.327	0.273	0.496	0.148	0.275	0.304
1.712	1.261	0.377	0.364	0.247	0.492	0.205	0.283	0.281
1.711	1.227	0.332	0.334	0.285	0.516	0.172	0.271	0.255
0.827	1.121	0.175	0.298	0.379	0.592	0.071	0.272	0.346
2.496	2.359	0.471	0.236	0.555	0.702	0.021	0.229	0.137
2.173	1.152	0.520	0.280	0.296	0.489	0.061	0.260	0.138
1.053	1.060	0.327	0.241	0.584	0.730	0.029	0.230	0.197
1.015	1.152	0.472	0.264	0.475	0.657	0.052	0.243	0.184
1.953	1.081	0.491	0.267	0.382	0.570	0.046	0.258	0.206
1.232	1.346	0.387	0.231	0.633	0.761	0.013	0.227	0.245
0.624	0.994	0.101	0.300	0.390	0.606	0.056	0.281	0.278
1.404	1.529	0.477	0.289	0.388	0.594	0.095	0.258	0.401
0.669	1.000	0.086	0.317	0.389	0.619	0.083	0.295	0.974
1.076	1.550	0.450	0.282	0.363	0.562	0.090	0.253	0.328
0.472	0.969	0.129	0.365	0.268	0.520	0.154	0.315	0.791
1.586	1.369	0.274	0.262	0.507	0.684	0.060	0.238	0.198

BMJ Open: first published as 10.1136/bmjopen-2022-063051 on 8 November 2022. Downloaded from http://bmjopen.bmj.com/ on June 10, 2025 at Agence Bibliographique de l Enseignement Superieur (ABES) . Protected by copyright, including for uses related to text and data mining, AI training, and similar technologies.

1.054	1.201	0.355	0.310	0.384	0.608	0.117	0.267	0.349
1.453	1.452	0.652	0.279	0.363	0.561	0.078	0.254	0.339
1.412	1.316	0.338	0.345	0.316	0.563	0.180	0.278	0.418
0.509	0.985	0.000	0.415	0.237	0.520	0.241	0.341	0.717
1.700	1.489	0.626	0.290	0.329	0.532	0.091	0.265	0.359
0.615	1.352	0.249	0.387	0.104	0.287	0.215	0.329	0.418
2.990	1.941	0.524	0.242	0.556	0.709	0.032	0.227	0.092
1.452	1.358	0.550	0.269	0.507	0.691	0.070	0.243	0.237
1.149	1.250	0.248	0.317	0.447	0.680	0.142	0.259	0.296
0.990	1.009	0.242	0.339	0.281	0.514	0.113	0.296	0.459
1.459	1.117	0.411	0.319	0.310	0.533	0.146	0.276	0.646
0.461	0.915	0.154	0.420	0.217	0.495	0.213	0.349	0.588
0.979	1.289	0.449	0.293	0.344	0.552	0.055	0.274	0.566
2.355	1.916	0.548	0.264	0.415	0.599	0.051	0.247	0.269
1.750	1.650	0.095	0.378	0.242	0.495	0.270	0.279	0.226
1.580	1.845	0.205	0.313	0.394	0.622	0.141	0.263	0.347
1.146	1.285	0.421	0.284	0.318	0.516	0.080	0.254	0.594
0.706	1.000	0.010	0.303	0.334	0.548	0.075	0.282	0.538
0.530	1.000	0.157	0.402	0.233	0.503	0.195	0.355	0.507
0.410	1.061	0.241	0.443	0.113	0.333	0.239	0.370	0.537
1.027	1.194	0.485	0.299	0.280	0.485	0.078	0.273	0.501
0.617	1.045	0.099	0.340	0.394	0.647	0.200	0.262	0.841
2.354	1.474	0.312	0.305	0.248	0.451	0.079	0.280	0.315
1.355	1.113	0.287	0.305	0.291	0.501	0.098	0.269	0.398
2.590	2.710	0.626	0.371	0.190	0.417	0.218	0.305	0.462
1.336	1.605	0.479	0.265	0.392	0.579	0.050	0.246	0.397
0.946	1.511	0.221	0.295	0.336	0.544	0.118	0.249	0.289
3.649	1.959	0.320	0.326	0.199	0.401	0.074	0.305	0.151
2.097	1.414	0.346	0.366	0.243	0.487	0.261	0.285	0.355
1.486	1.127	0.438	0.271	0.360	0.551	0.091	0.247	0.546
1.842	1.648	0.293	0.274	0.465	0.656	0.076	0.247	0.279
1.112	0.957	0.276	0.323	0.186	0.382	0.159	0.290	0.471
0.552	0.987	0.043	0.396	0.123	0.326	0.180	0.344	0.392
0.526	0.996	0.113	0.357	0.279	0.527	0.180	0.317	0.764
2.102	1.299	0.521	0.280	0.343	0.540	0.042	0.268	0.364
1.039	1.074	0.564	0.284	0.403	0.605	0.100	0.246	0.419
1.125	1.149	0.251	0.288	0.390	0.595	0.102	0.251	0.378
1.068	1.010	0.476	0.279	0.533	0.725	0.101	0.237	0.207
3.180	2.032	0.487	0.236	0.514	0.666	0.017	0.229	0.207
2.128	1.947	0.420	0.240	0.584	0.730	0.029	0.230	0.211
2.303	1.525	0.379	0.275	0.350	0.544	0.072	0.252	0.354
1.536	1.691	0.692	0.313	0.333	0.554	0.138	0.256	0.331
1.728	1.239	0.351	0.339	0.242	0.466	0.201	0.274	0.189
2.647	1.653	0.685	0.319	0.299	0.522	0.142	0.279	0.284
1.362	1.469	0.396	0.257	0.529	0.699	0.059	0.233	0.244
1.119	1.538	0.595	0.288	0.384	0.589	0.086	0.261	0.685
1.487	1.206	0.279	0.306	0.371	0.590	0.138	0.259	0.331
0.542	0.946	0.453	0.346	0.283	0.523	0.186	0.289	1.245
0.481	0.962	0.216	0.379	0.260	0.520	0.222	0.310	1.290
1.403	1.314	0.236	0.291	0.404	0.612	0.096	0.258	0.498

For peer review only

BMJ Open: first published as 10.1136/bmjopen-2022-063051 on 8 November 2022. Downloaded from http://bmjopen.bmj.com/ on June 10, 2025 at Agence Bibliographique de l Enseignement Superieur (ABES) .
Protected by copyright, including for uses related to text and data mining, AI training, and similar technologies.

0.711	0.977	0.072	0.350	0.270	0.510	0.175	0.286	0.960
0.708	0.998	0.033	0.322	0.406	0.642	0.142	0.283	0.778
0.980	1.519	0.420	0.333	0.277	0.506	0.154	0.261	0.273
1.826	1.137	0.564	0.281	0.356	0.554	0.090	0.257	0.286
1.820	1.472	0.417	0.290	0.323	0.526	0.097	0.255	0.339
1.099	1.472	0.213	0.286	0.359	0.562	0.041	0.272	0.360
1.629	1.712	0.402	0.277	0.472	0.665	0.101	0.240	0.288
1.468	1.378	0.359	0.288	0.330	0.533	0.071	0.266	0.513
1.421	1.272	0.704	0.270	0.405	0.595	0.075	0.243	0.158
0.887	1.004	0.010	0.354	0.222	0.450	0.172	0.290	0.503
1.207	1.141	0.506	0.268	0.543	0.721	0.073	0.241	0.427
1.556	1.359	0.236	0.324	0.270	0.490	0.155	0.284	0.360
1.395	1.551	0.291	0.282	0.286	0.480	0.051	0.264	0.222
0.432	0.970	0.141	0.391	0.247	0.513	0.180	0.323	0.548
0.640	1.000	0.066	0.355	0.317	0.572	0.129	0.310	0.553
0.948	0.993	0.061	0.298	0.422	0.637	0.094	0.267	0.685
1.924	1.521	0.592	0.274	0.314	0.505	0.048	0.261	0.385
1.151	1.409	0.443	0.276	0.489	0.680	0.078	0.251	0.443
1.759	1.666	0.358	0.272	0.542	0.725	0.062	0.245	0.330
0.999	1.000	0.060	0.308	0.387	0.610	0.109	0.270	0.463
0.886	1.166	0.485	0.265	0.569	0.741	0.067	0.240	0.439
1.677	1.400	0.378	0.369	0.242	0.489	0.251	0.278	0.358
1.025	1.064	0.274	0.260	0.532	0.704	0.026	0.252	0.717
1.287	1.313	0.633	0.284	0.481	0.681	0.112	0.248	0.603
2.382	2.568	0.604	0.321	0.273	0.492	0.156	0.268	0.404
2.160	1.506	0.348	0.320	0.298	0.521	0.102	0.286	0.439
1.372	1.184	0.514	0.395	0.198	0.446	0.325	0.294	0.524
1.231	1.411	0.288	0.294	0.349	0.557	0.099	0.256	0.453
2.389	1.586	0.667	0.295	0.232	0.425	0.075	0.276	0.374
0.932	0.994	0.365	0.305	0.434	0.655	0.102	0.272	0.483
4.155	2.651	0.700	0.325	0.284	0.507	0.137	0.272	0.473
1.009	1.166	0.421	0.266	0.454	0.639	0.044	0.252	0.377
1.468	1.390	0.440	0.274	0.372	0.565	0.063	0.254	0.475
1.277	1.687	0.423	0.265	0.432	0.618	0.063	0.242	0.231
2.472	2.341	0.557	0.254	0.537	0.702	0.046	0.239	0.274
1.625	1.394	0.333	0.295	0.358	0.568	0.111	0.263	0.329
1.466	1.326	0.386	0.250	0.478	0.647	0.037	0.235	0.142
1.520	1.268	0.547	0.363	0.169	0.381	0.221	0.303	0.600
0.843	1.420	0.333	0.352	0.220	0.447	0.171	0.290	0.536
1.325	1.726	0.471	0.302	0.340	0.554	0.113	0.265	0.381
1.130	1.404	0.483	0.289	0.371	0.576	0.088	0.261	0.405
1.639	1.526	0.331	0.261	0.497	0.674	0.048	0.244	0.474
1.870	2.178	0.437	0.320	0.344	0.573	0.168	0.262	0.442
3.059	1.575	0.476	0.309	0.176	0.361	0.142	0.289	0.651
2.282	1.516	0.635	0.300	0.269	0.472	0.077	0.275	0.360
0.732	0.995	0.012	0.324	0.313	0.541	0.148	0.286	0.680
1.679	1.311	0.233	0.310	0.313	0.530	0.136	0.269	0.383

BMJ Open: first published as 10.1136/bmjopen-2022-063051 on 8 November 2022. Downloaded from http://bmjopen.bmj.com/ on June 10, 2025 at Agence Bibliographique de l Enseignement Superieur (ABES) . Protected by copyright, including for uses related to text and data mining, AI training, and similar technologies.

mean of ma	standard de	high mean cu	L2-norm of	mean of Ga	mean of ma	standard de	high Gaussia	L2-norm of
absMAA	MSD	HMC	MLN	GAA	absGAA	GSD	HGC	GLN
mm^-1	mm^-1	%	-	mm^-2	mm^-2	mm^-2	%	-
0.370	0.303	27.483	0.329	0.069	0.227	0.376	170.270	2.699
0.328	0.307	99.650	0.491	0.034	0.179	0.308	561.209	5.898
0.382	0.330	39.608	0.316	0.048	0.220	0.383	193.206	2.283
0.343	0.255	35.989	0.317	0.050	0.192	0.287	202.369	2.361
0.337	0.247	25.724	0.306	0.081	0.152	0.244	111.783	1.818
0.348	0.234	10.601	0.264	0.090	0.155	0.217	56.300	1.293
0.140	0.155	68.740	0.506	0.006	0.030	0.072	337.335	7.205
0.379	0.315	27.518	0.311	0.080	0.199	0.306	125.715	1.876
0.325	0.237	-4.035	0.233	0.076	0.159	0.256	38.871	1.205
0.376	0.331	22.618	0.325	0.092	0.203	0.412	115.984	2.393
0.248	0.178	7.167	0.294	0.047	0.083	0.136	54.474	1.768
0.294	0.242	65.689	0.374	0.041	0.130	0.235	310.560	3.334
0.232	0.170	32.321	0.326	0.042	0.071	0.102	131.248	1.942
0.380	0.249	39.230	0.262	0.102	0.203	0.260	172.089	1.276
0.404	0.211	-2.756	0.215	0.132	0.193	0.229	12.202	0.746
0.215	0.197	46.687	0.382	0.024	0.082	0.158	281.687	4.003
0.671	0.414	-0.486	0.222	0.361	0.563	0.758	23.583	0.845
0.199	0.192	44.389	0.398	0.020	0.063	0.127	232.352	4.009
0.543	0.286	2.134	0.252	0.241	0.363	0.400	28.454	1.043
0.399	0.190	13.360	0.256	0.120	0.191	0.207	54.113	1.056
0.307	0.212	21.546	0.290	0.053	0.152	0.204	138.982	1.721
0.340	0.239	10.459	0.284	0.081	0.165	0.226	74.818	1.560
0.203	0.158	28.289	0.329	0.028	0.056	0.096	122.201	2.377
0.315	0.227	33.131	0.287	0.073	0.131	0.186	133.613	1.570
0.216	0.119	3.469	0.271	0.036	0.056	0.064	27.970	1.247
0.271	0.231	16.426	0.271	0.038	0.130	0.217	140.469	1.842
0.382	0.264	-3.851	0.197	0.096	0.246	0.282	55.765	0.735
0.140	0.088	2.641	0.257	0.016	0.025	0.033	36.799	1.203
0.387	0.372	50.037	0.365	0.077	0.284	0.468	327.761	3.296
0.333	0.246	41.619	0.324	0.085	0.154	0.209	177.817	1.951
0.354	0.270	84.214	0.364	0.055	0.217	0.303	487.876	2.950
0.237	0.244	86.955	0.450	0.019	0.087	0.200	441.938	5.629
0.371	0.235	13.847	0.266	0.100	0.161	0.201	51.703	1.185
0.439	0.399	46.462	0.326	0.087	0.306	0.492	240.832	2.349
0.407	0.281	37.388	0.281	0.076	0.231	0.343	163.135	1.613
0.570	0.384	4.723	0.241	0.184	0.475	0.580	60.221	1.122
0.362	0.272	20.362	0.280	0.081	0.167	0.275	85.294	1.573
0.308	0.246	27.931	0.317	0.060	0.144	0.226	147.719	2.208
0.164	0.148	40.176	0.378	0.015	0.033	0.059	142.546	2.862
0.343	0.312	37.421	0.341	0.048	0.213	0.351	242.425	2.908
0.387	0.269	3.259	0.237	0.098	0.204	0.253	45.488	1.042
0.226	0.209	46.111	0.364	0.027	0.073	0.137	206.103	2.868
0.096	0.068	19.469	0.339	0.007	0.012	0.020	92.486	2.471
0.289	0.212	30.106	0.314	0.061	0.121	0.182	145.513	1.983
0.281	0.269	107.395	0.461	0.030	0.133	0.249	629.400	5.743
0.393	0.319	32.247	0.311	0.093	0.194	0.294	119.328	1.750
0.165	0.153	31.289	0.381	0.015	0.037	0.066	136.383	2.960

For peer review only

BMJ Open: first published as 10.1136/bmjopen-2022-063051 on 8 November 2022. Downloaded from http://bmjopen.bmj.com/ on June 10, 2025 at Agence Bibliographique de l Enseignement Superieur (ABES) .
Protected by copyright, including for uses related to text and data mining, AI training, and similar technologies.

0.350	0.247	13.398	0.258	0.070	0.203	0.269	112.222	1.370
0.287	0.208	15.684	0.280	0.052	0.102	0.226	66.441	2.078
0.182	0.175	57.716	0.334	0.022	0.042	0.081	218.754	2.151
0.356	0.234	30.075	0.275	0.096	0.198	0.247	164.159	1.450
0.388	0.259	-7.566	0.195	0.122	0.195	0.277	10.566	0.715
0.460	0.300	6.766	0.251	0.122	0.315	0.390	69.545	1.155
0.407	0.329	-3.969	0.208	0.118	0.246	0.302	36.806	0.780
0.203	0.182	35.467	0.372	0.023	0.063	0.105	179.517	3.037
0.419	0.407	48.732	0.337	0.078	0.257	0.381	224.679	2.102
0.473	0.333	13.718	0.224	0.139	0.309	0.393	78.607	0.935
0.161	0.146	47.887	0.385	0.015	0.043	0.081	264.046	3.689
0.278	0.232	61.744	0.390	0.035	0.115	0.193	289.460	3.489
0.343	0.232	18.223	0.283	0.082	0.158	0.233	88.126	1.628
0.516	0.267	7.079	0.243	0.221	0.329	0.340	41.759	0.958
0.275	0.261	54.542	0.398	0.039	0.108	0.207	242.212	3.573
0.402	0.312	34.161	0.275	0.096	0.248	0.417	176.386	1.726
0.327	0.269	1.580	0.244	0.071	0.179	0.283	72.216	1.339
0.523	0.441	13.316	0.229	0.147	0.443	0.626	107.707	1.104
0.491	0.422	46.646	0.329	0.120	0.372	0.524	231.396	2.211
0.484	0.309	19.917	0.289	0.080	0.373	0.597	129.208	2.242
0.318	0.236	50.879	0.336	0.061	0.135	0.240	202.896	2.567
0.463	0.263	1.081	0.234	0.180	0.269	0.319	28.479	0.951
0.298	0.229	19.650	0.310	0.057	0.120	0.208	94.046	2.157
0.601	0.450	-12.547	0.189	0.274	0.589	0.757	24.710	0.673
0.368	0.232	16.362	0.257	0.120	0.161	0.209	60.852	1.110
0.385	0.324	48.503	0.340	0.063	0.256	0.413	281.276	2.831
0.340	0.253	36.700	0.321	0.085	0.162	0.290	161.584	2.334
0.205	0.197	40.081	0.374	0.025	0.068	0.150	216.724	3.849
0.437	0.302	3.354	0.240	0.136	0.240	0.328	34.409	1.029
0.234	0.160	59.080	0.336	0.034	0.082	0.108	276.784	2.173
0.374	0.216	17.165	0.279	0.114	0.175	0.261	71.811	1.539
0.356	0.235	21.604	0.277	0.073	0.173	0.277	101.693	1.713
0.163	0.184	59.477	0.479	0.013	0.047	0.138	347.994	8.316
0.268	0.333	43.610	0.421	0.021	0.093	0.193	166.645	3.114
0.398	0.341	33.368	0.288	0.094	0.204	0.327	128.610	1.558
0.415	0.393	32.874	0.323	0.084	0.229	0.342	134.917	1.756
0.320	0.293	-0.625	0.200	0.038	0.168	0.269	62.166	0.895
0.255	0.212	83.131	0.388	0.023	0.103	0.163	433.185	3.457
0.379	0.308	14.760	0.291	0.088	0.207	0.331	89.730	1.849
0.395	0.322	15.166	0.254	0.043	0.241	0.361	105.098	1.550
0.201	0.181	48.023	0.352	0.012	0.064	0.109	248.305	2.981
0.392	0.291	1.273	0.245	0.094	0.233	0.293	55.595	1.109
0.368	0.321	93.888	0.400	0.051	0.203	0.379	462.490	3.849
0.350	0.276	20.654	0.231	0.081	0.163	0.223	93.445	0.961
0.428	0.351	7.344	0.228	0.100	0.274	0.369	72.784	0.947
0.478	0.292	47.932	0.282	0.105	0.283	0.429	171.297	1.482
0.348	0.308	47.938	0.367	0.054	0.186	0.289	236.237	2.935
0.167	0.145	30.251	0.322	0.010	0.043	0.078	162.837	2.388
0.343	0.294	34.369	0.325	0.075	0.203	0.309	211.068	2.415
0.234	0.207	30.349	0.335	0.016	0.074	0.146	129.073	2.742

BMJ Open: first published as 10.1136/bmjopen-2022-063051 on 8 November 2022. Downloaded from http://bmjopen.bmj.com/ on June 10, 2025 at Agence Bibliographique de l Enseignement Superieur (ABES) .
Protected by copyright, including for uses related to text and data mining, AI training, and similar technologies.

0.310	0.203	40.308	0.321	0.062	0.127	0.156	158.831	1.680
0.134	0.159	116.852	0.652	0.004	0.032	0.070	729.119	12.129
0.582	0.368	1.515	0.213	0.245	0.414	0.448	25.923	0.694
0.456	0.212	15.229	0.243	0.171	0.207	0.272	32.309	0.940
0.596	0.330	-4.095	0.194	0.295	0.427	0.550	10.610	0.637
0.198	0.195	35.769	0.362	0.010	0.071	0.132	235.187	3.551
0.287	0.219	20.911	0.302	0.047	0.113	0.167	100.239	1.872
0.442	0.314	19.405	0.241	0.102	0.267	0.354	94.929	1.064
0.422	0.250	13.919	0.250	0.164	0.215	0.238	56.828	1.001
0.523	0.306	4.891	0.240	0.221	0.313	0.342	26.158	0.871
0.462	0.355	30.353	0.311	0.127	0.265	0.410	111.064	1.816
0.694	0.535	9.189	0.210	0.239	0.801	1.159	98.527	0.957
0.632	0.437	20.122	0.248	0.262	0.507	0.657	83.067	1.073
0.287	0.214	18.435	0.266	0.052	0.111	0.229	88.334	1.656
0.384	0.290	31.078	0.302	0.114	0.181	0.260	109.950	1.561
0.289	0.180	12.421	0.289	0.069	0.095	0.137	43.848	1.499
0.240	0.200	49.804	0.341	0.036	0.079	0.118	206.468	2.274
0.240	0.234	97.060	0.481	0.018	0.087	0.128	487.833	4.638
0.095	0.071	28.605	0.350	0.007	0.012	0.023	123.417	2.849
0.302	0.200	35.247	0.296	0.068	0.112	0.147	124.830	1.462
0.324	0.338	121.985	0.512	0.040	0.148	0.249	593.122	4.969
0.334	0.280	-5.348	0.180	0.085	0.189	0.332	52.250	0.772
0.271	0.137	11.424	0.266	0.071	0.080	0.092	34.642	1.143
0.472	0.278	31.700	0.294	0.131	0.275	0.419	114.179	1.681
0.246	0.119	19.664	0.260	0.058	0.064	0.064	51.720	1.000
0.233	0.223	89.689	0.436	0.028	0.080	0.135	433.125	3.965
0.534	0.370	0.416	0.228	0.195	0.369	0.501	30.857	0.949
0.312	0.312	151.925	0.593	0.026	0.159	0.256	935.858	7.911
0.526	0.357	6.666	0.243	0.197	0.375	0.483	54.078	1.073
0.559	0.295	4.862	0.210	0.250	0.355	0.369	25.014	0.660
0.363	0.233	26.305	0.276	0.093	0.198	0.265	140.458	1.494
0.359	0.305	48.969	0.371	0.077	0.185	0.285	219.141	2.764
0.335	0.338	54.332	0.440	0.050	0.171	0.468	262.402	6.402
0.199	0.168	69.450	0.300	0.016	0.056	0.091	303.266	1.787
0.363	0.302	68.165	0.377	0.052	0.219	0.295	369.005	2.910
0.349	0.311	83.616	0.408	0.044	0.209	0.311	478.957	3.737
0.334	0.316	73.015	0.394	0.042	0.195	0.284	424.433	3.396
0.377	0.293	17.496	0.259	0.093	0.191	0.292	85.111	1.259
0.154	0.123	31.337	0.360	0.016	0.033	0.058	137.452	2.922
0.155	0.120	44.422	0.320	0.010	0.037	0.061	224.235	2.390
0.227	0.165	11.027	0.270	0.029	0.076	0.109	80.816	1.565
0.255	0.255	33.511	0.334	0.026	0.107	0.171	194.240	2.452
0.209	0.129	20.799	0.280	0.026	0.060	0.102	100.045	1.762
0.253	0.159	10.847	0.290	0.056	0.080	0.103	53.801	1.446
0.317	0.254	9.439	0.232	0.058	0.141	0.240	68.197	1.174
0.436	0.318	35.395	0.324	0.115	0.280	0.420	170.562	2.199
0.974	0.334	4.159	0.204	0.852	0.945	0.784	8.047	0.571
0.372	0.298	35.316	0.314	0.074	0.231	0.414	206.100	2.662
0.791	0.300	8.528	0.188	0.627	0.663	0.529	24.912	0.511
0.225	0.170	22.277	0.313	0.034	0.068	0.114	101.540	2.151

BMJ Open: first published as 10.1136/bmjopen-2022-063051 on 8 November 2022. Downloaded from http://bmjopen.bmj.com/ on June 10, 2025 at Agence Bibliographique de l Enseignement Superieur (ABES) .
Protected by copyright, including for uses related to text and data mining, AI training, and similar technologies.

0.395	0.337	26.292	0.304	0.106	0.215	0.343	119.503	1.779
0.345	0.208	27.427	0.291	0.095	0.150	0.229	104.142	1.671
0.481	0.370	49.783	0.340	0.141	0.339	0.471	228.326	2.284
0.717	0.172	0.717	0.165	0.476	0.494	0.292	-2.452	0.350
0.360	0.183	26.541	0.277	0.083	0.154	0.221	89.651	1.407
0.420	0.192	75.210	0.252	0.135	0.181	0.207	215.113	0.927
0.114	0.110	38.262	0.407	0.008	0.019	0.049	180.146	5.047
0.242	0.132	15.827	0.287	0.046	0.076	0.105	73.711	1.611
0.363	0.333	33.399	0.348	0.076	0.189	0.303	155.409	2.388
0.545	0.457	35.031	0.288	0.193	0.368	0.588	125.531	1.531
0.664	0.437	23.027	0.275	0.240	0.730	0.921	150.513	1.489
0.589	0.286	-5.813	0.161	0.347	0.429	0.381	9.752	0.395
0.568	0.184	26.758	0.252	0.283	0.309	0.258	53.829	0.861
0.297	0.218	30.931	0.323	0.053	0.124	0.194	140.585	2.194
0.290	0.329	105.626	0.537	0.032	0.148	0.425	646.131	9.678
0.393	0.341	45.084	0.379	0.096	0.269	0.401	266.984	3.148
0.594	0.180	30.718	0.252	0.316	0.331	0.285	60.140	0.880
0.569	0.351	21.800	0.248	0.239	0.421	1.604	92.936	3.043
0.523	0.311	-7.988	0.163	0.232	0.306	0.414	-5.200	0.449
0.543	0.371	39.201	0.218	0.241	0.362	0.570	137.911	0.872
0.546	0.364	37.232	0.277	0.195	0.408	0.621	157.810	1.634
0.873	0.447	13.886	0.235	0.691	0.832	0.948	41.574	0.896
0.341	0.238	48.851	0.314	0.055	0.157	0.237	200.304	1.940
0.440	0.311	38.254	0.292	0.125	0.259	0.359	156.080	1.601
0.524	0.447	84.399	0.402	0.138	0.440	0.790	445.200	3.938
0.431	0.279	31.785	0.299	0.136	0.222	0.294	107.420	1.554
0.362	0.304	49.502	0.326	0.067	0.191	0.295	224.935	2.304
0.165	0.136	80.958	0.391	0.015	0.035	0.074	323.417	3.489
0.391	0.288	50.280	0.329	0.069	0.237	0.307	251.364	2.052
0.551	0.257	16.638	0.248	0.216	0.402	0.423	80.139	1.007
0.322	0.285	28.080	0.346	0.058	0.168	0.298	165.452	2.882
0.482	0.297	40.044	0.252	0.141	0.354	0.464	199.146	1.251
0.407	0.307	44.513	0.228	0.099	0.252	0.444	217.488	1.200
0.767	0.275	3.142	0.177	0.594	0.632	0.378	14.077	0.420
0.364	0.139	24.614	0.263	0.095	0.133	0.144	56.210	0.992
0.425	0.219	19.227	0.263	0.137	0.223	0.314	75.266	1.328
0.403	0.274	22.733	0.279	0.113	0.232	0.333	114.462	1.583
0.264	0.252	33.935	0.365	0.031	0.116	0.252	198.855	3.979
0.223	0.159	28.928	0.341	0.039	0.065	0.143	118.067	3.175
0.256	0.244	28.024	0.377	0.031	0.105	0.236	163.323	4.077
0.381	0.243	32.272	0.299	0.085	0.197	0.259	138.150	1.661
0.385	0.313	55.871	0.369	0.082	0.234	0.360	283.973	3.034
0.241	0.245	92.100	0.448	0.020	0.098	0.167	521.985	4.429
0.308	0.213	43.675	0.325	0.043	0.134	0.208	190.504	2.243
0.276	0.227	25.543	0.336	0.051	0.108	0.209	122.525	2.754
0.703	0.413	20.526	0.276	0.370	0.689	0.789	102.406	1.304
0.387	0.315	34.960	0.321	0.076	0.237	0.340	188.784	2.155
1.246	0.507	5.409	0.190	1.456	1.771	1.521	26.783	0.528
1.290	0.436	2.759	0.174	1.617	1.792	1.226	13.602	0.418
0.520	0.377	23.268	0.304	0.197	0.380	0.577	113.641	1.815

For peer review only

BMJ Open: first published as 10.1136/bmjopen-2022-063051 on 8 November 2022. Downloaded from http://bmjopen.bmj.com/ on June 10, 2025 at Agence Bibliographique de l Enseignement Superieur (ABES) .
Protected by copyright, including for uses related to text and data mining, AI training, and similar technologies.

0.978	0.554	22.089	0.237	0.888	1.297	1.236	102.055	0.872
0.793	0.359	-1.413	0.201	0.561	0.741	0.666	14.568	0.599
0.371	0.370	78.107	0.406	0.058	0.229	0.371	427.990	3.659
0.320	0.265	29.756	0.313	0.050	0.157	0.273	158.021	2.246
0.414	0.326	51.809	0.338	0.073	0.248	0.370	232.553	2.444
0.395	0.282	28.826	0.291	0.104	0.216	0.310	129.108	1.660
0.349	0.308	36.082	0.359	0.061	0.192	0.311	192.483	2.890
0.566	0.434	35.500	0.307	0.218	0.438	0.681	150.907	1.871
0.201	0.237	57.108	0.454	0.011	0.091	0.499	454.480	15.975
0.572	0.377	61.654	0.298	0.184	0.483	0.553	285.505	1.644
0.450	0.243	6.697	0.256	0.150	0.274	0.309	54.358	1.170
0.423	0.363	49.203	0.329	0.083	0.279	0.447	246.705	2.375
0.270	0.257	52.916	0.353	0.041	0.090	0.158	189.102	2.229
0.677	0.576	15.981	0.220	0.295	0.543	0.734	59.595	0.760
0.615	0.430	6.457	0.213	0.291	0.469	0.609	40.678	0.786
0.717	0.438	1.433	0.223	0.383	0.619	0.769	23.782	0.812
0.394	0.224	31.241	0.284	0.101	0.197	0.275	118.561	1.495
0.501	0.363	15.854	0.284	0.148	0.372	0.510	98.952	1.638
0.416	0.481	32.256	0.425	-0.035	0.396	3.326	301.410	22.151
0.517	0.364	10.600	0.245	0.156	0.394	0.477	79.837	1.090
0.474	0.330	1.492	0.255	0.155	0.349	0.439	60.040	1.264
0.443	0.394	72.470	0.383	0.091	0.325	0.686	393.159	4.508
0.717	0.244	-0.307	0.223	0.459	0.548	0.439	5.803	0.691
0.631	0.386	13.614	0.279	0.315	0.503	0.598	63.297	1.292
0.436	0.294	51.879	0.336	0.092	0.240	0.339	190.884	1.993
0.492	0.408	42.402	0.337	0.126	0.340	0.542	184.095	2.209
0.552	0.458	60.888	0.351	0.111	0.581	0.852	393.852	2.740
0.518	0.409	38.234	0.316	0.150	0.401	0.663	185.284	2.293
0.418	0.324	58.963	0.335	0.073	0.282	0.490	307.733	2.848
0.529	0.450	11.413	0.276	0.194	0.421	0.745	86.600	1.692
0.609	0.623	80.026	0.459	0.130	0.591	1.244	415.731	5.422
0.409	0.258	14.050	0.259	0.115	0.203	0.303	57.781	1.302
0.498	0.281	25.777	0.277	0.205	0.274	0.301	75.337	1.155
0.297	0.299	40.100	0.372	0.042	0.133	0.260	195.973	3.215
0.297	0.221	17.446	0.320	0.050	0.129	0.218	100.845	2.327
0.380	0.315	37.038	0.330	0.069	0.253	0.385	228.068	2.567
0.171	0.152	34.278	0.350	0.015	0.043	0.100	163.667	3.608
0.611	0.415	58.447	0.307	0.181	0.614	0.818	313.327	1.864
0.594	0.462	60.049	0.326	0.204	0.578	0.816	319.459	2.242
0.424	0.366	38.583	0.340	0.107	0.296	0.508	215.801	2.702
0.486	0.372	32.390	0.297	0.110	0.312	0.450	131.456	1.699
0.513	0.295	16.990	0.278	0.186	0.333	0.424	73.202	1.443
0.511	0.407	46.090	0.352	0.083	0.447	0.953	264.583	4.138
0.653	0.286	64.988	0.297	0.187	0.566	0.711	260.920	1.612
0.397	0.269	54.190	0.324	0.089	0.203	0.300	205.775	2.049
0.742	0.476	10.353	0.216	0.421	0.637	0.722	40.798	0.712
0.478	0.451	59.272	0.379	0.099	0.390	0.685	332.115	3.557

BMJ Open: first published as 10.1136/bmjopen-2022-063051 on 8 November 2022. Downloaded from http://bmjopen.bmj.com/ on June 10, 2025 at Agence Bibliographique de l Enseignement Superieur (ABES) . Protected by copyright, including for uses related to text and data mining, AI training, and similar technologies.

Gaussian curvature

For peer review only

BMJ Open: first published as 10.1136/bmjopen-2022-063051 on 8 November 2022. Downloaded from http://bmjopen.bmj.com/ on June 10, 2025 at Agence Bibliographique de l Enseignement Superieur (ABES) .
Protected by copyright, including for uses related to text and data mining, AI training, and similar technologies.

STROBE Statement—Checklist of items that should be included in reports of ***cohort studies***

	Item No	Recommendation	Page No
Title and abstract	1	(*a*) Indicate the study's design with a commonly used term in the title or the abstract	1
		(*b*) Provide in the abstract an informative and balanced summary of what was done and what was found	2
Introduction			
Background/rationale	2	Explain the scientific background and rationale for the investigation being reported	3
Objectives	3	State specific objectives, including any prespecified hypotheses	3-4
Methods			
Study design	4	Present key elements of study design early in the paper	5-8
Setting	5	Describe the setting, locations, and relevant dates, including periods of recruitment, exposure, follow-up, and data collection	n.a.
Participants	6	(*a*) Give the eligibility criteria, and the sources and methods of selection of participants. Describe methods of follow-up (*b*) For matched studies, give matching criteria and number of exposed and unexposed	n.a.
Variables	7	Clearly define all outcomes, exposures, predictors, potential confounders, and effect modifiers. Give diagnostic criteria, if applicable	6-8
Data sources/ measurement	8*	For each variable of interest, give sources of data and details of methods of assessment (measurement). Describe comparability of assessment methods if there is more than one group	5
Bias	9	Describe any efforts to address potential sources of bias	13
Study size	10	Explain how the study size was arrived at	5
Quantitative variables	11	Explain how quantitative variables were handled in the analyses. If applicable, describe which groupings were chosen and why	6-7
Statistical methods	12	(*a*) Describe all statistical methods, including those used to control for confounding	8
		(*b*) Describe any methods used to examine subgroups and interactions	8
		(*c*) Explain how missing data were addressed	n.a.
		(*d*) If applicable, explain how loss to follow-up was addressed	n.a.
		(*e*) Describe any sensitivity analyses	5-8
Results			
Participants	13*	(a) Report numbers of individuals at each stage of study—eg numbers potentially eligible, examined for eligibility, confirmed eligible, included in the study, completing follow-up, and analysed	5
		(b) Give reasons for non-participation at each stage	n.a.
		(c) Consider use of a flow diagram	n.a.
Descriptive data	14*	(a) Give characteristics of study participants (eg demographic, clinical, social) and information on exposures and potential confounders	n.a.
		(b) Indicate number of participants with missing data for each variable of interest	n.a.
		(c) Summarise follow-up time (eg, average and total amount)	n.a.
Outcome data	15*	Report numbers of outcome events or summary measures over time	n.a.

For peer review only - http://bmjopen.bmj.com/site/about/guidelines.xhtml

For peer review only

Enseignement Superieur (ABES) .
Protected by copyright, including for uses related to text and data mining, AI training, and similar technologies.

Main results	16	(*a*) Give unadjusted estimates and, if applicable, confounder-adjusted estimates and their precision (eg, 95% confidence interval). Make clear which confounders were adjusted for and why they were included	9-10
		(*b*) Report category boundaries when continuous variables were categorized	n.a.
		(*c*) If relevant, consider translating estimates of relative risk into absolute risk for a meaningful time period	n.a.
Other analyses	17	Report other analyses done—eg analyses of subgroups and interactions, and sensitivity analyses	9-10
Discussion			
Key results	18	Summarise key results with reference to study objectives	11
Limitations	19	Discuss limitations of the study, taking into account sources of potential bias or imprecision. Discuss both direction and magnitude of any potential bias	13
Interpretation	20	Give a cautious overall interpretation of results considering objectives, limitations, multiplicity of analyses, results from similar studies, and other relevant evidence	13
Generalisability	21	Discuss the generalisability (external validity) of the study results	11-12
Other information			
Funding	22	Give the source of funding and the role of the funders for the present study and, if applicable, for the original study on which the present article is based	14

*Give information separately for exposed and unexposed groups.

Note: An Explanation and Elaboration article discusses each checklist item and gives methodological background and published examples of transparent reporting. The STROBE checklist is best used in conjunction with this article (freely available on the Web sites of PLoS Medicine at http://www.plosmedicine.org/, Annals of Internal Medicine at http://www.annals.org/, and Epidemiology at http://www.epidem.com/). Information on the STROBE Initiative is available at http://www.strobe-statement.org.

For peer review only

Enseignement Superieur (ABES) .
Protected by copyright, including for uses related to text and data mining, AI training, and similar technologies.